Locomotion Performance of Autonomous Mobile Robot on Rough Terrain for Outdoor Survey

屋外調査用自律移動型ロボットの不整地移動性能

February 2018

Katsuaki TANAKA
田中　克明

Locomotion Performance of Autonomous Mobile Robot on Rough Terrain for Outdoor Survey

屋外調査用自律移動型ロボットの不整地移動性能

February 2018

Waseda University
Graduate School of Advanced Science and Engineering,
Department of Advanced Science and Engineering,
Research on Physics and Applied Physics B

Katsuaki TANAKA

田中　克明

Abstract

Interest in field robots has been increasing since the radiation accident at the Fukushima nuclear plant due to the Great East Japan Earthquake in 2011. Field robots play a very important role as a means to protect human safety and discover new things. Mobile robots used for monitoring increase understanding of the environment and ecosystem to ensure better protection. Mobile robots are expected to solve problems of conventional monitoring methods such as monitoring posts, manual transport, bio-logging, and monitoring cars by reducing human labor costs and improving human safety and flexibility through microscopic monitoring.

The locomotion performance is one of the most important research subjects for mobile robots. Previous studies have focused on moving on rough terrain, and such robots are effective for a given target area and purpose. However, almost all of the robots with a high locomotion performance have many actuators to cope with complex environments. This leads to a complex robot design and high-power consumption. These factors reduce maintainability and increase control complexity. In addition, many studies on controlling mobile robots use geometry sensors such as cameras and lasers in order to recognize obstacles and know the robot's position. This also leads to high computational cost and power consumption. In order to overcome these problems, the author focused on locomotion with a minimum number of actuators and autonomous movement using only simple sensors.

The objective of this study was to design a mobile robot platform with a high locomotion performance on rough terrain that has a simple design and low power consumption as a first step towards developing a large-scale and long-term monitoring system. The author proposes a method for a simple design and low power consumption by reducing the number of actuators and proposes a novel mechanical and control design to realize a high locomotion performance. In order to realize these concepts, the author set two design requirements: locomotion performance on rough terrain with a minimum number of actuators and outdoor navigation by simple sensors. Compared to other unmanned ground vehicle-type robots, the proposed robot is effective for long-term operation with reduced energy consumption and improved maintainability. The simple design can greatly reduce the unit cost, which can help with realizing the production of multiple robots for large-scale monitoring.

Chapter 2 introduces novel mechanical designs that help increase the locomotion performance with simplicity and low power consumption. Three important elements for designing a target robot are introduced: the locomotion mechanism, wheel shapes, and a shell shape. A novel locomotion mechanism using a driving mechanism that can drive multiple axes at once is introduced first. Then two novel wheel models are presented that can adapt to locomotion on

rough terrain: an elliptic leg and notched wheel. Finally, a novel shell shape of the robot is introduced that can also contribute to a high locomotion performance, especially in areas thick with tall grasses.

Chapter 3 introduces a novel control design to increase the locomotion performance with simplicity and low power consumption. Three important elements of autonomous control design are introduced: environmental recognition, motion control, and navigation. A novel method of estimating surface conditions is presented to recognize the environment, and the possibility of acquiring details on the mobile environment with only internal sensors is discussed. A novel motion control design based on the subsumption architecture proposed by Rodney Brooks is then presented to realize autonomous control using only simple sensors. A navigation method is presented at the end of the chapter for efficient movement to get to the destination. Novel methods of generating a cost map and the selected path planning method are described as parts of the navigation method.

Chapter 4 introduces some application examples using the developed mobile robot. Experiments were conducted in various environments, and the elemental technologies introduced in Chapters 2 and 3 were used in combination. Monitoring in an urban park was conducted with the objective of image acquisition, and the camera on a smartphone with an omnidirectional lens was used to take pictures. Monitoring in a pasture was conducted with the objective of monitoring the radiation level. A Geiger counter was used for measurement. Monitoring in a forest was conducted with the objective of measuring geometric data. A laser range finder system was used. Another example application was tunnel and ceiling inspection. This example was in response to new demands originating from the small size and light weight of the robot.

Chapter 5 presents the overall discussion. The effect and validity of the proposed methods are discussed from the viewpoint of monitoring and locomotion performance. Then, the originality and impact of the proposed methods are considered. The main features of this proposal are described: the mechanism using only two motors and the control using only internal sensors. Finally, the limitations of the proposal are described: the limit of utilizing static mechanics as a model, the limit at which the energy efficiency is not optimized depending on the application, and the limit of the application range.

Chapter 6 describes the conclusions based on this proposal and details of plans for future studies.

To increase the locomotion performance of an autonomous mobile robot for monitoring on uneven terrain, this thesis proposes a novel mechanical design that uses only two actuators and a novel control method that uses only internal sensors based on the concept of a simple design and low power consumption. The effectiveness and validity of the methods were evaluated through verification experiments and application demonstrations.

The results showed that the mechanical shape of the part where the robot contacts the outside world is important, and a new wheel shape and casing shape are proposed. The importance of recognizing the surface with internal sensors is described, and methods of motion control that can adapt to the real environment and path planning using locomotion data are proposed. Examples of various applications using robots developed on the basis of these designs are presented, and their practicality and potential application are discussed and demonstrated.

The significance of the thesis is that it not only proposes a novel design to increase the locomotion performance but also describes the effects by introducing a generalized model and analysis from experimental data. Such descriptions will contribute to the design of other mobile robots to adapt to the target environment and help with selecting design parameters. The proposed design is simple and has low power consumption, which will contribute to reducing the manufacturing cost and the long-term goal of a monitoring system using multiple robots.

The results of this study can contribute to the further popularization of robots used outdoors and are expected to become the basic technology for future robot development owing to their generality and high potential applicability. Further developments based on this study will involve establishing a novel method of environmental monitoring. The study contributes not only to robotics but also to developments in the fields of environment and ecology. This can lead to great strides towards building a society where human being coexist with nature in the future.

Acknowledgement

This study was conducted at the Waseda Research Institute for Science and Engineering, the Humanoid Robotics Institute, and the Waseda University's Future Robotics Organization. This research is supported by the Consolidated Research Institute for Advanced Science and Medical Care, Waseda University (ASMeW), SolidWorks K.K., STMicroelectronics K.K., Leading Graduate Program in Science and Engineering, Waseda University from MEXT, Japan and Research Fellowships for Young Scientists, Japan Society for the Promotion of Science.

First of all, I would like to gratefully thank my supervisor Prof. Atsuo Takanishi. Over the last seven years, including bachelor's and master's degrees, his significantly important comments and suggestions on my research gave me great awareness and extremely abundant experiences. It was due to his guidance and kindness that I was able to gain many opportunities and experiences to challenge so far.

I would also like to thank my examiners, Prof. Toru Asahi, Prof. Massimiliano Zecca, Prof. Hiroyuki Ishii, and Dr. Hideki Kondo, for providing me accurate and helpful comments on my presentation and thesis. Prof. Toru Asahi gave me many opportunities for experiences through the Leading Graduate Program in Science and Engineering, Waseda Univesity and the Waseda EDGE program. I feel that these experiences will become very important in future life. Prof. Massimiliano Zecca gave me important advice in my research and it became an important role in constructing the thesis. Prof. Hiroyuki Ishii gave important advice in deciding the direction of research as a boss of my research group. Achievements and success of the research are under his great contribution. Dr. Hideki Kondo gave a lot of advice on how to think and how to summarize my thesis as a senior in the laboratory.

I would also like to thank my collaborative researcher, Prof. Hiroshi Okochi and the members in the laboratory. Thanks to them it has become possible to realize experiments in Fukushima. I would also like to thank the provider of experiment environment, Prof. Takemoto and the members at The University of Tokyo Tanishi Forest. Thanks to them it has become possible to conduct outdoor tests many times. I would also like to Prof. Ishii and his family for providing me an experimental environment in the forest. Thanks to them it has become possible to conduct experiments in a harsher environment

I would also like to thank interns and laboratory host institutions and researchers, Prof, Paolo Dario and Prof. Cesare Stefanini, and the members in Prof. Cesare Stefanini's laboratory in The BioRobotics Institute of Scuola Superiore Sant'Anna, Italy, as a practicum at the overseas research institution for three months in 2016, and Mr. Takeshi Hakamada and the members in isapce inc.

as a company internship for 14 months from 2016 to 2018,

I would like to thank Prof. Kenji Hashimoto, Prof. Aiman Omer, Dr. Sarah Consentino, Dr. Takuya Otani, Dr. Martim Brandao, Dr. Salvatore Sessa, Dr. Tatsuhiro Kishi, Dr. Gabriele Trovato, Dr. Mattuieu Destephe, Dr. Nobutsuna Endo, Dr. Klaus Petersen, Dr. Zhuohua Lin, and Dr. Yohaon Noh, for their valuable comments on my research. I would also like to thank the researchers and graduate and undergraduate students belonging to “Environmental Monitoring” group, Prof. Yusuke Sugahara, Prof. Satoshi Okabayashi, Prof. Qing Shi, Mr. Shinichi Kinoshita, Mr. Eric Mossor, Mr. Hikaru Sugita, Mr. Yusaku Miura, Mr. Yuya Okamoto, Mr. Daisuke Kuroiwa, Ms. Junko Mitsuzuka, Mr. Daiki Endo, Mr. Wu Cheng Wei, Mr. Sho Inoue, Mr, Hiroya Yokoyama, Ms. Thingting Zhong, Mr. Kazuki Kida, Mr. Hiroshi Kojima, Ms. Nu Nu Win, and Ko Matsuhiro, Mr. Claudio Protano, Mr. Arjun Narang, Mr. Maxime Nicolas, Mr. Florian Mercier, and Mr. Ahmed Ibrahim. The everyday discussion on their research contents and chats with them have made my life as a doctoral student all the more enjoyable. I am also thankful to the other Takanishi Laboratory members and community members that I belong such as Leading Graduate Program, Waseda University and young researchers in Global Robot Academia, Waseda University for their comments their encouragement, and their interest in my research.

I would like to thank the secretaries in Takanishi Laboratory and the all staff related to the Leading Graduate Program in Science and engineering, Waseda Univesity, Waseda EDGE program, Research Fellowships for Young Scientists, Japan Society for the Promotion of Science for their continued research support.

I would also like to especially thank my friends and family for their enriching my life. I am able to have a great time during student life.

Tokyo, February 2018

Katsuaki Tanaka

Table of contents

Chapter 1: Introduction

1.1 Chapter introduction

This thesis proposes methods of improving the locomotion performance of the small mobile robot on uneven terrain for outdoor survey. This study is a first step in developing the large-scale and long-term monitoring system using multiple mobile robots, and the author introduces technical elements that are considered necessary for constructing the system.

This chapter introduces the background of this study in order to show the importance of the study from the viewpoint of social demands and clarify the purpose of the study in order to show the detail about the direction and aim of the study. After that, the chapter introduces the conventional studies and state-of-arts of related studies from the viewpoint of application as monitoring devices and the elemental technology of mobile robots on rough terrain. Finally, the chapter shows a composition of this thesis in order to make it easier for readers to understand the flow and contents of this thesis.

1.2 Background of this study

1.2.1 Demands for field robot

The interest in field robot has been increasing since the radiation accident at Fukushima Nuclear Plant due to the Great East Japan Earthquake in 2011. In recent years, the field robot is expected to be useful tool in various places. Regarding the damage situation and the measures taken by the government during the Great East Japan Earthquake, the summary report is established by the Cabinet Office [1.1]. Regarding accidents at the Fukushima nuclear power plant, Investigation Committee on the Accident at the Fukushima Nuclear Power Station summarizes the survey report [1.2].

The future demands of the filed robot also can be read from materials published by government. Fig. 1.1 shows current Estimates of Market Size of the Robot Industry in Japan. The robot market in 2035 is expected to reach 9.7 trillion yen according to the market research of future robot industry reported by New Energy and Industrial Technology Development Organization (NEDO) and Ministry of Economy, Trade and Industry in 2012 [1.3]. In addition to this, NEDO announces the Robot White Paper in 2014 from viewpoint to revitalizing the robot business, and it covers two fields, service robot and field robot, which will expand the market size in the future [1.4].

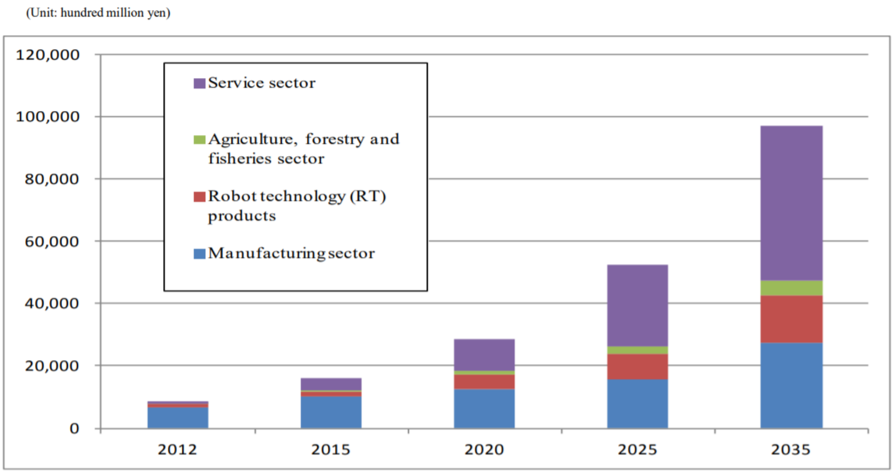

Figure 1.1 Current Estimates of Market Size of the Robot Industry in Japan.
(This figure was taken from the New Energy and Industrial Technology Development Organization)

Field robot play a very important role as a means to protect the safety of people's lives and to discover something new. For example, disaster robots contribute in discovering and rescuing people in disaster areas, environmental monitoring robots contribute to protecting the environment, space exploration robots contribute greatly to discovery in unknown fields.

Several field robots have a locomotion mechanism and work while moving outdoors. The type of work that a robot can play can be increased by having the function of locomotion. On the other hand, the locomotion mechanism complicates the structure and control of the robot, and this can increase a price of the robot. For this reason, recently, robots that have limited the number of driving mechanism including a locomotion mechanism for reducing the price have been marketed as products.

1.2.2 Demands for monitoring

In the wake of the Great East Japan Great Earthquake of 2011, Japan suffers from a variety of natural disasters such as landslides and eruptions, and in recent years' demand for monitoring has been increasing form the viewpoints of forecasting disasters, grasping the situation and ecosystem investigation. These social demands are summarized below.

1.2.2.1 Environmental monitoring

Natural destruction can be cited as one of the parts of the “shadow” behind the remarkable development of science and technology. In recent years, many people have come to recognize this as an environmental problem, since surveys on the influences of the destruction have been actively conducted.

Originally human beings have used natural environment since long time ago and have been trying to coexist with nature. Using nature put a burden naturally, but none of it has stayed within the scope of natural self-healing. However, as the population has increased at the same time as the development of civilization, the burden on nature begins to increase, and it has been said that the burden dramatically increased as a result of the industrial revolution centered on Europe in the 18th and 19th centuries.

Humans began to recognize such problems widely as environmental problems triggered by publication of “Spring of Silence” in 1962 [1.5] that picked up environmental pollution, and until now, problems such as acid rain, ozone holes, abnormal weather and global warming have been taken up as a serious problem. Today, environmental problems, especially global environmental issues are positioned as one of the major international issues along with poverty and conflict.

In order to think again about symbiosis between people and nature, it is necessary to understand environmental problems correctly and to find an effective solution method. The importance of symbiosis with nature has made it necessary to engage in the active protection of nature [1.6] by monitoring the impact of our activities on the environment and imposing controls.

Environmental protection has indeed become an important international issue that has been discussed in several forums [1.7,8]. This has led to increase monitoring of the environment [1.9] in the bid to properly understand the underlying problems and proffer effective solutions. However, environmental monitoring involves some conflict [1.10]. For example, the introduction of a human being weighing 60 kg to an environment imposes a tremendous burden on nature [1.11]. This raises the need for other monitoring methods that do not involve human beings.

1.2.2.2 Monitoring wild animals

Recently, the influence of these environmental problems on living organisms has become remarkable, and it has become visible in a visible form. For example, the problem of destruction of ecosystem due to disorder of food chain, increase of endangered species, problem of animal damage.

Damage by wild animals has become serious problem, there are a lot of reports in terms of crops damage or encounter of human and wild animals. Information on damage caused by animal damage in Japan is compiled by the Ministry of Agriculture, Forestry and Fisheries' anti-beast damage counter [1.12]. According to the government, annual damage amount is around 20 billion yen in Japan, and this amount is still large for a party. Fig. 1.2 shows amount of crop damage caused by wild bird beasts. More than half are found to be damage by deer and wild boar, and countermeasures against these wild animals are expected.

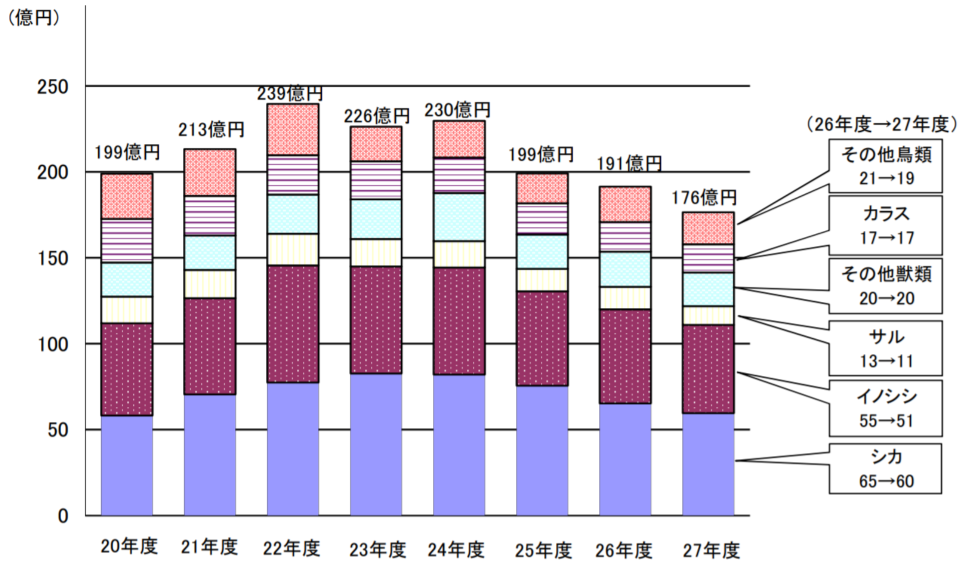

Figure 1.2 Changes in amount of crop damage caused by wild bird beasts
(This figure was taken from the Ministry of Agriculture, Forestry and Fisheries)

Encounter of human and wild animals is also a problem. Damages that serious injuries are reported are encountered with large wild animals such as bears. The distance between human and wild animals is getting closer due to the declining habitat area due to deforestation. Fig. 1.3 shows a picture of wild bear. This picture was taken near seminar house of Waseda University in Karuizawa, Japan by trail camera of my monitoring team. This place is about 30 [m] away from the accommodation.

Figure 1.3 Wild bear near seminar house of Waseda University in Karuizawa, Japan

Fig. 1.4 also shows wild animals near residential area in Chiba, Japan. Fig. 1.4 (a) is taken near the accommodation. Fig. 1.4 (b) is also taken near residential areas.

(a) A monkey near the accommodation fence (b) Raccoon crashed into a car

Figure 1.4 Wild animals near residential areas in Chiba, Japan

Deer-train collisions is reported as a one of the serious problems between human and animals in [1.13,14]. In the U.S.A., the problem of deer-vehicle collision also has been reported [1.15].

In recent years, local governments in each district have established an anti-animal damage team and various countermeasures have been taken, but the amount of damage still remains high. In terms of countermeasures against beast damage, in addition to taking time and effort, chemical safety and ethical problems are involved, and it is difficult to solve it at present.

Improving habitat or managing the number of individuals is required for preventing these problems. Therefore, it is necessary to know the ecological system of living animals and the situation of living well and to take appropriate measures. For that purpose, there is a demand for behavioral investigation of animals as an extension of environmental monitoring. Also, not only the approach from a passive standpoint of monitoring, but also a system construction as a mechanism to drive away animals and guide them to correct behavior is required.

Monitoring feedback is considered to be effective way to control the number of individuals. Fig. 1.5 shows a monitoring feedback control chart for controlling the number of individuals. The ecosystem can be controlled by improving animal habitat environment or protecting animals from extinction or extermination vermin. In order to realize this animal control, the effective monitoring is required.

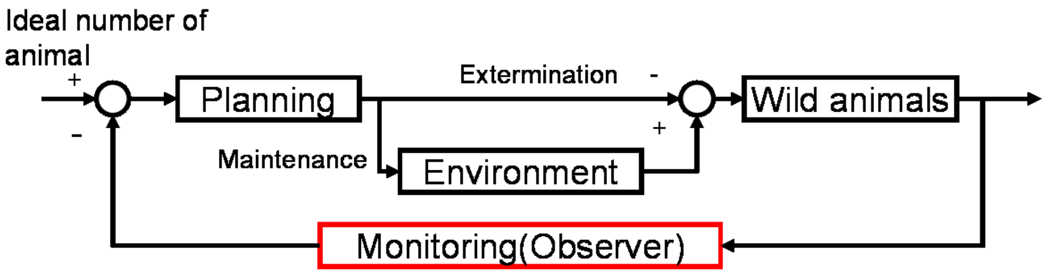

Figure 1.5 Monitoring feedback for controlling the number of individuals

1.2.2.3 Monitoring in a disaster site

Japan's landscape originally suffered from natural disasters and there are many disasters such as earthquakes, typhoons, volcanoes. There is a demand for environmental monitoring that continuously measures the environment for a long time as a method of approach on how to anticipate disasters especially when observing the situation at the site of a natural disaster where secondary disasters are likely to occur in the future. Documents related to these disasters are updated annually by the Cabinet Office as disaster prevention white papers along with disaster countermeasures [1.16].

In Fukushima Prefecture where the accident of radiation pollution leakage at Fukushima Nuclear Power Plant occurred at the 2011 Great East Japan Earthquake, there were voices worrying about changes in ecosystems of animals and plants exposed to high radiation doses, but observations within difficult-to-go areas is difficult, and even as of the present of 2014, there are not many surveys on ecosystems. As a part of disaster reconstruction, it is easily assumed that investigations of ecosystems within the off limits will be conducted in the future, and environmental monitoring is required as a system to acquire various environmental indicators at that time.

1.2.2.4 Inspection of infrastructure

There are many buildings such as tunnels and bridges to build infrastructure. Tunnels and bridges are one of the most important transportation infrastructures in Japan. However, most of the tunnels have been over 30 years since construction, the risk of collapse accident is becoming obvious. A lot of road bridges and tunnels are built in the period of high economic growth around the Tokyo Olympics in 1964, and the percentage of these buildings are becoming 50 years old in 2030 according to the Ministry of Land, Infrastructure, Transport and Tourism (MLIT) of Japan, [1.17]. The maintenance and management of these road stock become issues in Japan, therefore, the inspection robots are expected to support these tasks.

Collapse of Sasago tunnel in 2012 [1.18] is one of the most famous accident and 9 people have died in the accident. After that, the Japanese government discussed the way of inspection and the Ministry of Land, Infrastructure and Transport is considering the use of robots.

1.2.3 Conventional methods of monitoring

Conventional monitoring methods can roughly be divided into fixed type and mobile type, and can be divided into the following four methods from the difference of moving media.

1.2.3.1 Fixed type: Monitoring post

Monitoring post is useful to monitor macroscopically. Fig. 1.6 is a Fukushima prefecture radioactivity measurement map conducted in Fukushima Prefecture [1.19]. This map discloses macroscopic measurement results based on information on airborne radiation dose from each measurement point. The observation point is mainly limited to private houses and roads, but it shows rough numerical values together with other surrounding data.

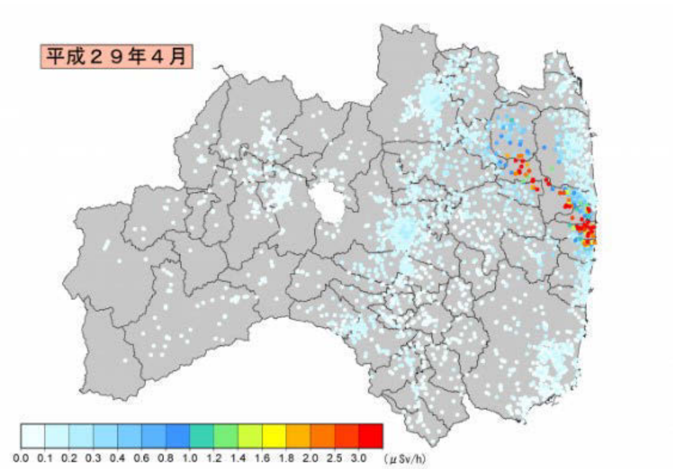

Figure 1.6 Fukushima prefecture radioactivity measurement map
(This figure was taken from the Fukushima Prefecture's web site)

Fig. 1.7 shows an example of a monitoring post used as fixed-point observation. These pictures were taken in Namie Town in Fukushima where is prohibited to enter due to high radiation level. The monitoring post for measuring radiation level and the other monitoring posts such as instrument screen for thermometers are set in this area.


(a) Monitoring post (Radiation level) (b) Monitoring post (Temperature and humidity)
Figure 1.7 Monitoring post in Namie Town, Fukushima, Japan

There are various types of monitoring posts, and monitoring of atmospheric pollutants such as radiation dose, PM 2.5, CO_2, NO_X, SO_X and the like has been actively carried out recently from the monitoring of temperature and humidity.

An advantage of such an observation is that a wider range of data can be obtained, and continuous observation can be made for a long period of time. As a method of observation, fixed point observation is mainly used, and it is fixed type and it is easy to supply power to the equipment, so it is suitable for long term observation. Another advantage of observation with monitoring post is that observation is safe. Once the device was set up, user can basically measure without human's hands. This can greatly reduce the risk of endangering human.

The biggest disadvantage of fixed-point observation is that the observation area is limited because the measuring instrument cannot move, and flexible monitoring cannot be performed. Some of observation data show a large difference in observation data only by measuring about 1 - 10 [m] in place. For example, there is a report that the radiation dose is stored in rain water and locally accumulated in places where forest ponds and puddles are likely to form (there are hot spots). Only fixed-point observation in units of 1 [km], it is extremely difficult to obtain such local data and more micro observation is necessary.

1.2.3.2 Mobile type: Hand carried sensor

Portable monitoring sensors are suitable for micro observation because they are a way for people to carry measuring instruments. It is basically possible to observe the range where people can enter, and it is also possible to monitor relatively difficult sites such as mountainous areas. For example, forest resource monitoring survey is conducted in Shizuoka prefecture [1.20]. In the area as shown in the figure, it is difficult to intrude a large-sized device and it is difficult to move, so portable monitoring sensors are effective.

A disadvantage of the portable monitoring sensor is that there is a problem in safety because it is necessary for a person to directly enter the observation area. Since it is necessary for human beings to carry each device, the risk that the observer puts the risk at risk extremely high. For this reason, flexible measurements can be made, but it is difficult to measure in areas where disasters or secondary disasters can be predicted or in areas requiring long-term measurements.

Moreover, it can be considered that enormous cost will be incurred when conducting a large-scale investigation. It takes time and effort to investigate, and labor costs are expected to be enormous, so it is not suitable for long term observation.

1.2.3.3 Mobile type: Biologging

Bio logging monitors the movement of animals by embedding a sensor in a part of an animal or attaching a device such as a collar to an animal. In this method, the experimenter attaches ultra-compact data logger on animals, and sometimes radio wave transmitter and small camera are also attached.

It is possible to grasp the ecosystem of the target animal by attaching it to the target animal. It can be used for investigating the behavior of animals. It is also possible to monitor the environment where it is difficult for humans to enter in. Wild animals are easier to move the natural environment than humans, and the possibility of monitoring of areas where observation was difficult is improved.

However, flexible observation is difficult with the method based on bio logging, and it is difficult to obtain data at a target location. Moreover, the burden on the animals is large, and it is accompanied by hardships when attaching the sensors. The size and weight of the sensors are limited so as not to give a large burden to creature, the weight is required to be within 3-5 % of animal’s weight.

1.2.3.4 Mobile type: Monitoring car

Recently, observation with a monitoring car has also been carried out, and it is active in various situations. Fig. 1.8 shows a measurement map of airborne radiation level using a monitoring car by Fukushima Prefectural Government. This figure is published on the website of Fukushima prefecture [1.21]. It can be measured more precisely than by fixed point observation and is characterized by its ability to facilitate a wider range of monitoring than using portable monitoring sensors.

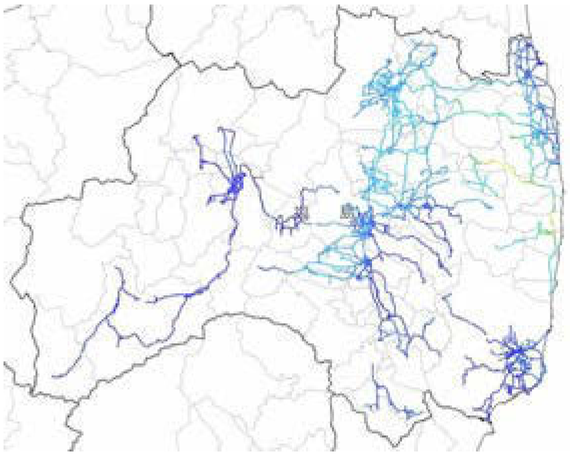

Figure 1.8 Measuring radiation level by monitoring car

Observation by monitoring car is located between fixed point observation and observation using portable monitoring sensor and it is an observation method which neutralizes the merit and demerit of each other. However, this method still requires human hands and there is a problem that the observation area is restricted to residential streets and roads where cars can travel, and safety and flexibility are lacking.

1.2.4 Motivation

As a research subject, it is difficult to build a large-scale monitoring system that the author envisioned. The demand for monitoring and the conventional methods are describe in previous sections. Conventional methods can be used for a specific survey, it is necessary to develop further devices in order to carry out detailed monitoring over a large-scale and long-term.

Figure 1.9 shows a huge monitoring system of the future envisioned by the author. The author thinks that it can be useful for human life by acquiring data in every place and handling those data in one large cloud. These data will be a clue that human beings to know the environment. This is one of the ways human beings preserve the environment and ecosystems, and it becomes a material to quickly detect and control abnormity such as disasters. This is a major effort toward harmonious coexistence between humans and nature and there is no doubt that it is one of the important tasks for human beings to survive for a long time.

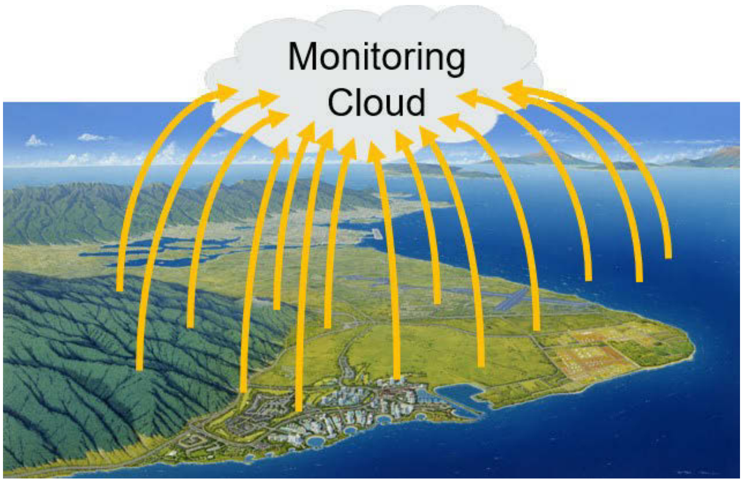

Figure 1.9 A huge monitoring system of the future envisioned by the author

Robots have the potential to be a means to solve the problems of conventional monitoring methods and to construct a huge monitoring system. Table 1.1 shows the positioning of the environmental monitoring robot. The author is aiming to propose a monitoring method that is safer and more mobile (more flexible) than the conventional methods. It is not necessary for a human to take the trouble to go to the observation point if mobile robots can be used.

Table 1.1 Conventional methods of monitoring

	Trace by human	Biologging	Spot sensor	This study Mobile robot with sensor
Human labor	Working all the time	Finding animals and installation	Only at installation	Only at installation
Safety for human	Needed to stay in the danger area	Needed to enter in the danger area	Needed to enter in the danger area	Not needed to enter in the danger area
Flexibility	Freely change measurement points	Rely heavily on animal behavior	Unable to measure except the fixed place	Freely change measurement points

1.3 Purpose of this study

The purpose of this study is to develop new devices for constructing a huge monitoring system. The goal is to build a system with a high self - autonomy that cannot be handled by human beings as much as possible. If such a system is constructed, human beings will be able to live more abundantly

As an approach to achieve the purpose, the author focused on device's mobility. Mobility of devices is considered to be an important factor for detailed and large-scale monitoring. As the device moves, the range that can be observed with one measuring instrument is significantly expanded. If multiple mobile devices can be used, huge observation is also possible. In addition to this, the burden on the experimenter can be greatly reduced by performing this automatic mobility.

Robot technology is required for the mobile to operate automatically. Information on the moving environment is acquired by the sensor, the situation is calculated by the calculator, and the motion of the actuator is generated. These series of flows are necessary for the movement of the device, which is exactly the same as the element of the robot. Regarding the movement of the robot, a lot of studies have been conducted in the field of mobile robots.

In this study, the author aims to develop a further technology of mobile robots and develop a mobile robot adapts in the monitoring system.

1.4 Related studies

1.4.1 Monitoring robot

1.4.1.1 Classification of monitoring robot

Regarding existing environmental monitoring robots, they are summarized in Robotics for Environmental Monitoring of IEEE robotics & automation magazine published in 2012 [1.22]. This article, written by M. Dunbabin and L. Marques, is also categorized on the technology and capabilities of environmental monitoring robots. According to this article, the environmental monitoring robot is roughly classified into three according to target environments, one is underwater monitoring (Marine), one is air monitoring (Aerial), and ground monitoring (Ground). Table 1.2 shows the number of studies publish as academic papers on monitoring fields

Table 1.2 The number of research relating to environmental robotics

	Marine	Aerial	Ground
Small scale (< 10,000 [m^2])	12	7	5
Medium scale (10,000 [m^2] <, < 1 [km^2])	13	11	4
Large scale (1 [km^2] <)	23	6	1

1.4.1.2 Marine monitoring

Autonomous Surface Vehicle (ASV) and Autonomous Underwater Vehicle (AUV) are used for marine monitoring. Although more than 70 % of the earth is covered by water, human has only explored less than 5 %. Monitoring using a robot is necessary because it is difficult for humans to dive in the ocean for a long time and to monitor. Since there is no big obstacle in the water, it is possible to stabilize the position of the robot by using buoyancy and it is possible to perform a wide range of monitoring over a long period of time. The types of study are classified according to the scale of monitoring by [1.22], from [1.23] to [1.29] are classified in small scale monitoring that area is under 10,000 [m^2], from [1.29] to [1.42] are classified in medium scale monitoring that area is over 10,000 [m^2] and under 1 [km^2], and from [1.43] to [1.64] are classified in large scale monitoring that area is over 1 [km^2].

1.4.1.3 Aerial monitoring

Unmanned aerial vehicles (UAV) are used for airborne monitoring. Since it is difficult for humans to monitor overhead in the first place, monitoring using a robot is necessary. There is no big obstacle in the air, so you can move fast. Therefore, it is effective when quick monitoring at the time of the disaster becomes necessary. Also, because it is possible to observe on the ground from the sky, it is possible to acquire a wide range of information at one time. However, in order to maintain the position of the robot in the air, it is difficult to operate for a long time because sufficient energy against gravity is required. Attempting to install a large capacity battery to obtain a lot of energy leads to heavy weight and further energy consumption. In operation, consideration of energy is important. The types of study are classified according to the scale of monitoring by [1.21], from [1.65] to [1.71] are classified in small scale monitoring, from [1.72] to [1.82] are classified in medium scale monitoring, and from [1.83] to [1.89] are classified in large scale monitoring.

1.4.1.4 Ground monitoring

Unmanned ground vehicles (UGV) require monitoring in various places such as monitoring on a volcano, monitoring at a disaster site, monitoring landslides, monitoring ecosystems, and so on. Since humans basically operate on the ground, the demand for monitoring on the ground is high accordingly. However, since human mobility is high, most monitoring performed by a robot is currently made by humans. At the moment, there are many reasons to use such as substitution to protect the safety of human beings, without human trouble. In the future, development of a robot that transcends human mobility is necessary. Monitoring on the ground has more obstacles than underwater or in the air, and it is difficult to move. Therefore, it is difficult to conduct wide-ranging monitoring. From the viewpoint of energy, the ground support the weight of the robot, so it consumes less energy, but since the surrounding environment changes dramatically on the ground compared to underwater and air, the acquisition of energy become difficult. The types of study are classified according to the scale of monitoring by [1.21], from [1.90] to [1.94] are classified in small scale monitoring, from [1.95] to [1.98] are classified in medium scale monitoring, and [1.99] are classified in large scale monitoring.

According to a survey by Matthew Dunbabin and Lino Marques, mobile monitoring robots exceeding 1 [km^2] are currently only large robots working in the desert. There is no example that realizes monitoring in such environments where obstacles such as forests are abundant.

1.4.2 Mechanical design of mobile robot on rough terrain

A lot of previous studies conducted on the mechanical design of a mobile robot on rough terrain.

According to the handbook of robotics published in Japan [1.100], locomotion mechanisms of mobile robot moving on the surface can be roughly divided into 4 main types; leg, tracked, wheel and trunk.

According to the review article [1.101] that is summarizing the locomotion system for ground mobile robot in unstructured environments, the locomotion mechanism can be divided into three main categories; leg, tracked, and wheel. It also states that there are other hybrid robots.

To sum up the information of these documents, there are roughly three representative mechanisms; leg, tracked and wheel, for the locomotion mechanism of the robot, and there are various other types such as a hybrid type and code type as shown in Fig. 1.10.

Figure 1.10 Classification of locomotion mechanism of mobile robot on the surface

1.4.2.1 Leg type

A robot having a locomotion mechanism of four legs or more has been developed for rough terrain movement. Quadruped robot and hexapod are popular and most of them are referring to the movement of animals and insects.

Quadruped robots are well summarized in [1.102], a lot of robots and its perception progress are introduced in this paper. The walk patterns of animals were studied in developing the quadruped robot [1.103-105]. Bigdog [1.106-108] that was developed by Boston Dynamics is a most famous robot as a quadruped robot, and this robot can move in the tough environment with balancing its posture. TITAN [1.109-116] is also famous robot that was developed in Japan since

1976.

Hexapod robots that locomotion mechanism has six legs are introduced in [1.117]. The mechanism and control for hexapod robot is introduced in [1.118]. According to summary paper [1.118], hexapods can be divided into two groups; rectangular and hexagonal in terms of the legged position mounted to the body. Rectangular hexapods have two pairs of three legs on two sides. Hexagonal hexapods have six legs that are mounted on a round or hexagonal body. There are a lot of hexapods sold as a toy.

A legged robot can have high moving performance capable of handling rough terrain, however, autonomous movement is difficult due to its complexity of mechanism and control. High power consumption has also become one of the problem to develop a robot for long-term and large-scale monitoring.

1.4.2.2 Tracked type

A robot having a tracked mechanism is suitable for moving on uneven and soft terrains. There is can be classified into two according to the number and layout of the tracks [1.101].

The non-actuated track type of robot has a simple mechanism in a tracked type. Nanokhod [1.119] is an example of this type. The non-actuated track type can move well on uneven surfaces with simple control, but the climbing step ability is not so high.

The actuated track type of robot is considered as leg-track hybrid robot and have a high capacity to handle with high obstacles. Quince [1.120,121] is a famous as a robot actually used at a disaster site. It is developed for the purpose of rescue activities, and can move on rubble and move stairs. High locomotion performance is realized by controlling sub tracks attached to the side of the main left and right of the tracks.

A tracked type robot has a slight mechanism of complication. Although control is easy with a non-actuated track type, it is not suitable for rough terrain movement, such as forests because of its low ability to climb the step. The movement performance is high in the actuated track type, but autonomous movement is difficult due to its complexity of mechanism and control as similar to the leg type. Furthermore, fibers such as grass may be entangled with the belt in environments such as forests, so it is considered not suitable for use in target applications.

1.4.2.3 Wheel type

A robot having wheels is considered to be the lowest power consumption mechanism and it is easy to control from the simplicity of design. Most of the cars used in the world are wheel-shaped, characterized by their stability and speed.

Many planetary exploration robots adopt the mechanism of the wheel. SR2 rover [1.122], Micro5 rover [1.123], SOLERO [1.124] are CRAB II [1.125] have been developed as a planetary exploration robot. Locomotion performance of some of these rovers is evaluated in [1.126].

Although the mechanism of the wheel is useful when moving on a well-maintained road surface, it is not suitable for use on uneven grounds because the step climbing performance is low. According to the calculation formula in described in [1.127], the wheeled robot could not climb up step over the height of the wheel's radius. Assuming the actual environment, the ability to climb the step becomes less than half of it.

Studies using link structures and suspensions have been made as an approach to improve these mobility properties. Sojourner, the first autonomous Mars exploration vehicle in NASA Jet Propulsion Laboratory (JPL), has a suspension mechanism called a rocker bogey [1.128,129]. The rover could climb obstacles such as rocks at a height 1.5 times the diameter of the wheel. This is realized by using a complicated link mechanism and a large number of actuators, and a total of 10 motors was used for the moving system [1.130]. Rocky 7 that is also developed at JPL is also have rocker bogey [1.131]. Analysis of control of vehicles equipped with suspensions with active joint structure is well done by Iagnemma et al [1.132].

As regards to an approach to increasing the locomotion performance by proposing a special wheel shape, a lot of wheel shapes are proposed to suit the target environment. Loper used Tri-Lobe wheel that three small wheels mounted to a central hub [1.133]. CLOVER used special wheel like gear and used in a volcanic environment [1.134]. These mechanisms are useful in each environment, but these wheels mechanisms have not well maintained using mechanical model and not meet our target environment. Spoke type wheel is well known as simple wheel and a lot of studies are focused on its climbing steps performance and its stability [1.135,136]. However, almost of these studies have not mentioned the way for satisfying both these climbing abilities.

1.4.2.4 Cord type

Snake robots composed of a large number of joints connected in series. Studies on the mechanism and control of a cord-like function body called Active Cord Mechanism (ACM), which works by changing the shape with such a configuration [1.137]. Hirose has been studied as a pioneer of research on the mechanism of this type of moving body [1.138].

Since the cord type robot can be designed to have a small cross-sectional area with respect to the traveling direction, it has the advantage that it can enter the narrowed portion. However, many actuators are required to realize complicated motion, which complicates the mechanical and control design.

1.4.3 Control design of mobile robot outdoors

A lot of previous studies conducted on control design of a mobile robot on rough terrain. Among them, I introduce two studies similar to this study.

1.4.3.1 SLAM

Simultaneous localization and mapping (SLAM) is one of the famous technology to solve the computational problem of creating an unknown environment map and simultaneously grasping the position of the robot. This problem is known as chicken-and-egg problem, and many solutions have been proposed. Tutorials for learning the SLAM technology are also published [1.139,140].

In SLAM methods, almost of the previous works were conducted by using cameras and lasers for knowing own position and grasping the detailed information on the surrounding terrain. These methods are so powerful and useful to control the robot, especially in a simple environment with less obstacles such as indoors. However, these methods are largely depending on the environmental situation and it is so difficult to use it in a grassy area and using in every weather condition because of the noise problem. There are still a lot of technical problems that must be solved using this method for a long time in a particularly complicated environment outdoors.

In this study, the self-position of the robot is estimated based on the information of GNNS using the map in the world coordinate system already constructed, and the detailed information of the terrain is updated in the map. Similar acts have been done in terms of collecting and updating a large amount of information on the map, but it does not address the fundamental computational problem of SLAM.

1.4.3.2 Multirobot systems

As a method of operating multiple robots, swarm and multi-agent system have been studied.

(a) Swarm

Swarm robotics is an approach of cooperation of robot system that consists of multiple simple mobile robots. Swarm makes robots collective action by interaction between the robot group and the surrounding environments. It is based on group intelligence inspired by observation results of social insects.

The complex tasks can be realized by acting as a group and sometimes the performance of the large number of robots contribute to the robustness and flexibility of the system.

Swarm technology is a technique to move as a group as seen in behavior of insects, and in many cases, studies in which one robot separately plays a role are treated as a multiagent system as described later.

(b) Multi-agent system

The multi-agent system is consisting of multiple agents and each agent can perform tasks separately, not as a group that gathers in one place.

In study of agents, each agent needs to work according to the environment so that the agent must be able to recognize the environmental information. The agent also has to decide on his own actions to take. The algorithm of that decision ranges is wide from simple to complex.

The multi-agent system is more likely to collaborate evolutions rather than individual evolution while general agents' study focuses on how to evolve ourselves and become an agent more suitable for the problem. The simpler the behavioral logic of each agent, the more flexible the system. Conversely, the more complex the behavioral logic of each agent, the better the pursuit of optimality, but it will be a system that cannot deal with the unexpected problems.

The most interesting point of this kind of learning system is sometimes unpredicted group behavior of agents may be autonomously formed. There are times when we take actions beyond the creation of human beings, and in that sense, it may feel that the robot has surpassed human thought.

My long-term goal of the monitoring system follows the concept of this multi-agent system, and development of the system is positioned as an extension of this study.

1.5 Objective of this study

1.5.1 Setting the theme

As introduced in the previous section, many monitoring robots have been developed. However, there are few cases where a large-scale monitoring can be realized in a robot moving on the ground. This is caused by a lot of obstacles that prevent the robot's movement on the ground unlike underwater and aerial. It is particularly difficult to move in the natural environment where development of human beings has not done such as forests. However, cases in which investigation in these areas is increasing as demand for environmental and ecosystem monitoring. Therefore, the author focused on the development of devices that can move in these natural environments and thought about building a monitoring system using terrestrial mobile robots.

Fig. 1.11 shows a long-term goal image of the monitoring system. The author plans to introduce multiple robots into forest area, and these robots will monitor cooperatively. Each robot moves autonomously around the energy charge station, and the robot come back to the station when the battery level became low like a Roomba [1.141-147]. The monitoring data are uploaded to the cloud server and the users such as citizens and farmers can get the data by accessing to the server and downloading it. The operator can also access to the robot though the network and control the robot directly in emergency case.

The most challenging task of developing this system for the robot is to move on rough terrain. There are a lot of obstacles in forest area such as grasses and fallen tree. The robot is required to have high locomotion performance in moving such a tough environment. Therefore, the author tries to develop a platform of mobile robot that can move on such an environment.

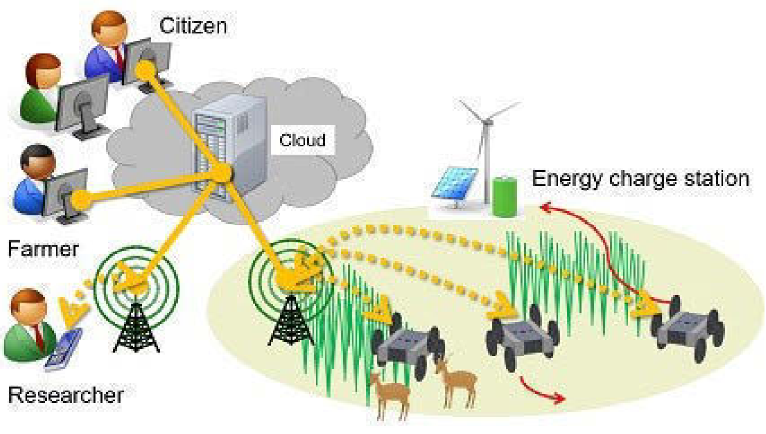

Figure 1.11 A long-term goal of monitoring system

1.5.2 Design concepts for robot locomotion

The author made concepts of design for developing a new robot that cane used for long-term and large-scale monitoring.

Three design concepts; simple design, high locomotion performance, and low power consumption are decided for developing the robot. Simple design is required as much as possible for reducing cost and easy maintenance. High locomotion performance is required so as to cope with obstacles outdoors for moving on rough terrain. Low power consumption is required as much as possible for long term operation and environmental friendly.

Two design requirements are set as follows in order to meet these concepts.

(a) Locomotion performance on rough terrain by minimum number of actuators

By reducing the number of actuators, it is possible to greatly simplify the mechanical design and control design of the robot and it also leads to reduction of power consumption. It is a challenge to have high locomotion performance because it becomes difficult to cope with complicated environments when the number of actuators is small.

(b) Outdoor navigation by simple sensors

By controlling the robot with simple sensors, it is also possible to greatly simplify the mechanical design and control design of the robot and it is able to reduction of power consumption. It is also a challenge to have high locomotion performance because it becomes difficult to cope with complicated environments when not using a high-performance sensor.

1.5.3 Approach

As an approach to robot development, the author considered the position of the study compared with conventional studies. Table 1.3 shows a difference between conventional studies and this study. PhamtomX [1.148-153], Quince [1.120,121], ACM-R3 [1.154-160], and CERES [1.161] are introduced as examples of a typical mobile robot. Generally, robots with high locomotion performance have many actuators and use high-performed sensors to cope with complicated uneven surfaces. However, there are problems that the number of actuators and high-performed sensors complicate the robot's design and increases the power consumption. On the other hand, the design of a robot using less actuators and simple sensors makes the robot's design simple and power consumption can be suppressed, but locomotion performance becomes a problem and it leads difficult to use in rough terrain.

Table 1.3 Difference between conventional studies and this study

	Phantom X	Quince	ACM-R3	CERES	This study WAMOT
Locomotion type	Leg	Tracked	Grassland	Wheel	Special wheel
Target area	Forest	Volcano	Grassland	Artificial road	Forest
Navigation	Remote control	Remote control	Remote control	Remote control	Auto control with internal sensor
Number of actuators	16	6	20	4	2
Design	Complex (Control timing is required)	Complex (Control timing is required)	Complex (Control timing is required)	Simple (Control timing is not required)	Simple (Control timing is not required)
Locomotion performance	High (Able to move on rough terrain)	High (Able to move on rough terrain)	High (Able to move on rough terrain)	Low (Unable to move on rough terrain)	High (Able to move on rough terrain)
Power consumption	High (100W/kg)	Medium (30W/kg)	Medium (15W/kg)	Low (0.5W/kg)	Low (Under 5W/kg)

Therefore, in this study, design simplification and power consumption reduction are realizing by limiting the number of actuators of the robot to two, that is considered to be the minimum required number of movement and using the internal sensors that is considered to be simple sensors. And, high locomotion performance is realized by proposing novel mechanical and control designs.

1.5.4 Objective

The objective of this study is to design a platform of mobile robot that have a high locomotion performance on rough terrain with simple and low power consumption. In order to achieve its objective, the author approached from two perspectives, mechanical design and control design. Fig. 1.12 shows elemental technologies for increasing locomotion performance of mobile robots.

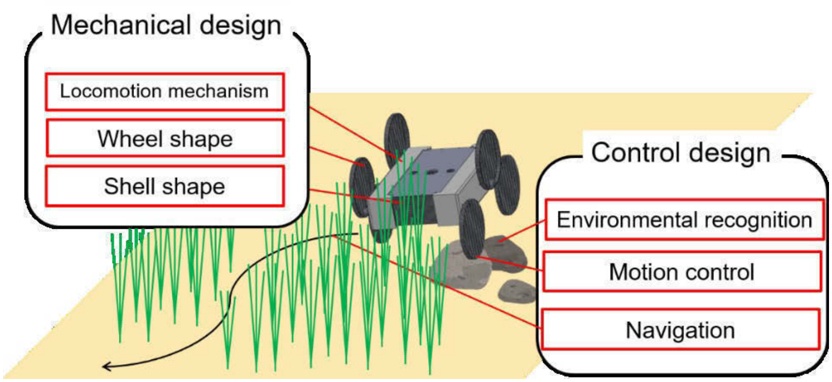

Figure 1.12 Elemental technologies for increasing locomotion performance

1.5.4.1 Mechanical design

Three factors were examined as a method of approaching the objective from a hardware perspective as follows.

(a) Locomotion mechanism

The design of the driving part has a great influence on the movement of the robot. In this study, it was aimed at simplifying the design and reducing energy consumption by minimizing the number of actuators required to move the robot.

(b) Wheel shape

The shape of the wheel also greatly affects the locomotion performance of the robot. The robot exchanges the forces at the point where the wheel and the surface contact each other. From this point the robot gains a large frictional force and replaces it with the propulsive force in the movement.

(c) Shell shape

In a complicated moving environment outdoors, the shape of the shell can also be a factor influencing the locomotion performance. There is a possibility that the robot receives a large resistance from the point of contact between the obstacle and the shell, and how to reduce the magnitude of the resistance value is important.

1.5.4.2 Control design

Three factors were examined as a method of approaching the objective from a software perspective as follows.

(a) Environmental recognition

The condition of the surface has a great influence on the movement of the robot. By recognizing the condition of the surface by the robot, the adaptive motion according to the environment can be realized and it leads to improvement of locomotion performance.

(b) Motion control

Motion control of robot is one of the factors directly related to the locomotion performance of the robot. It is very important for the robot how to decide the next motion and perform optimal motion from environmental information.

(c) Navigation

Improving the moving efficiency of the robot in the whole operation leads to the improvement of the locomotion performance. By analyzing information on a wide range of environments, the trajectory generation of the robot can be realized.

1.6 Composition of this thesis

Fig. 1.13 shows the composition of this thesis. This thesis is composed of two main parts: development and application. In the development part, chapters 2 and 3 describe the details of each element of the methods to increase the locomotion performance of the robot. The development part is separated into mechanical and control design. The theoretical interpretation of the elements constituting the robot is described, and the results of verification experiments are presented. In the application part, chapter 4 introduces applications as practical examples and explains the experimental conditions with the sensor for monitoring. Chapter 5 discusses the proposed methods, and Chapter 6 summarizes the conclusion and future works.

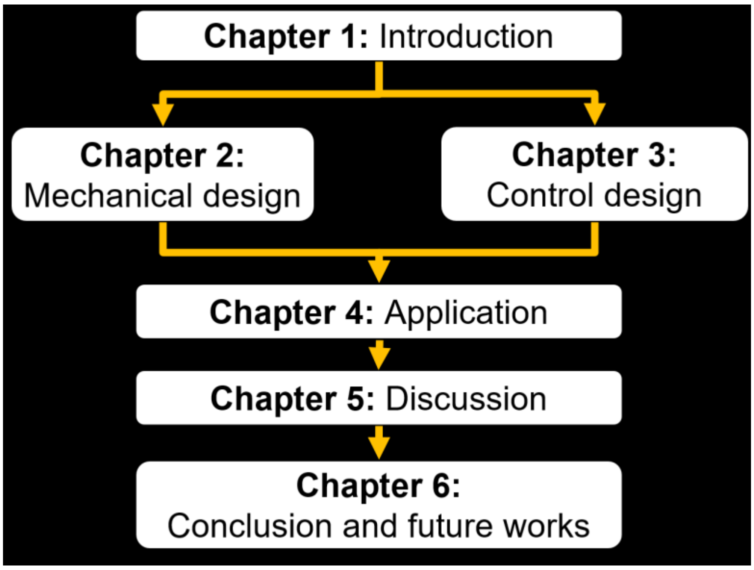

Figure 1.13 Composition of this thesis

Chapter 2: Mechanical design

2.1 Chapter introduction

The mechanical design of the robot is described in this chapter. The mechanical design is one of the most important factors of having a high locomotion performance of the mobile robot. The design has a great influence on the locomotive itself and the ability to cope with rough terrain such as climbing steps and slopes largely changes.

The objective of this chapter is to describe methods of increasing the locomotion performance of a mobile robot from a hardware perspective and to verify its effect. The motion is modeled and expressed by mathematical expression to understand the effect, and the theory is verified by simulation and experiment using developed robots.

This chapter shows the requirements and an overall design of the robot and describes detail designs of novel wheels and a shell shape. Required specification and the overall design are decided to use in outdoor environments and the detailed shapes of the wheels and the shell are modeled and designed to increase locomotion performance according to various target environments. Novel wheel models; elliptic leg and notched wheel, are also proposed for generalizing the shape and calculating the performance.

The author uses figures and sentences by referring the author's published papers in this chapter [2.1-9].

2.2 Requirements

2.2.1 Target field survey

A field survey was conducted for deciding the hardware requirements of a mobile robot. The abstract of the field survey is described as follows:

2.2.1.1 Condition

Date: 4th June 2012

Place: Forest in Tokorozawa campus, Waseda University

Weather: Sunny

2.2.1.2 Results

(a) Uneven surface condition

A lot of uneven shape were existing caused by small stone or upsurge of soil. In the survey, almost of the height difference of uneven terrain was within 30 [mm]. Therefore, I decide such a surface as ordinary surface and the other surfaces are regards as obstacles.

(b) Obstacles

A lot of obstacles such as tall grasses and fallen trees were existing in forest. In the survey, almost of all the height of fallen trees were under 100[mm], sometimes over 200[mm] obstacles were existing. 200[mm] seems to be so tough for the small mobile robot to climb. Therefore, I decided the maximum height of the climbing step of the robot to 100 [mm] as one of the hardware requirements.

2.2.2 Required specification

Based on the field survey, requirements of robots to be developed are determined and summarized in Table 2.1.

Table 2.1 Specification sheet (1/2)

D/W	Major item	Sub item	Requirement	Supplement
D	Overall	Operation	Able to move in outdoor environment	Grass land, forest, sand
D			Able to sense the surrounding environment	
W			Able to move autonomously	
W			Able to operate for a long term	Half a year
W			Able to operate in a large scale	$60\text{x}10^4$ [m^2]
D			Able to adapt to the natural environment	Direct sunlight, rain, winds, snow
D	Mechanical design	Mechanism	Basic movement is possible	Forward, backward, turning
D			Able to move on rough terrain	Stable movement on uneven road surface of less than 50 mm, climbing step of 100 mm
W			Dustproof and waterproof	
D			Mechanism that is hard to move to an immovable state	
W			Able to move even if the robot become falling state	
D			Simple design	Minimize degrees of freedom
D		Shape	Compact design	For moving between trees
D		Weight	Light	So as not to break even to fall, reducing environmental burden
W		Material	Light weight	Variety of plastics, using aluminum for metal parts
D			Well strength	
W			Strong in natural environment	Direct sunlight, rain, winds, snow, temperature (-30°~90°)
D			Suitable for processing	Accurate enough to accommodate dimensional tolerances, a screw hole can be opened
W		Assembly	Easy to assemble	Reducing the number of parts, minimizing the number of screws
W		Other	Well maintenance	Modular structure, Reducing the types of parts

Table 2.1 Specification sheet (2/2)

D	Electrical system	Power supply	Mounting the power to the robot	Battery
W			Obtaining the power on its own	
D			Do not short-circuit	Waterproofing of electrical system
W		Sensors	Using small sensors	
W			Using sensors with low power consumption	
W			Minimizing the number of actuators	
D			The maximum load on the actuator should below the maximum continuous torque	
W			Making the size as small as possible	
W			Make the output as small as possible	
W		Communications	Using a general-purpose wireless communication method	4G/LTE, Wifi
W			Using wires inside of the robot	

2.3 Overall design

2.3.1 Inspired by insect locomotion

The locomotion mechanism of the robot is often developed with reference to the movement of the creatures such as animals and insects. Animals and insects make a motion so as to create multiple points in contact with the surface to support their weight in a stable. In general, it is known that when a mobile robot is walking horizontally on a horizontal plane, the robot does not fall over if the projected point of center of mass exists inside the supporting polygon formed by connecting support points between the legs and the surface. Therefore, many mobile robots try to use multiple legs locomotion for realizing stable locomotion.

However, observing the behavior of multiple legged insects with more than 6 legs noticed the regularity of movement. Fig. 2.1 shows examples of regular motion of centipedes and cockroaches. These insects allow stable movement by creating triangular supporting polygons at points contacting the surface. In the next phase, this triangle transitions as if it changed symmetrically, and insects make a triangle all the time by making these triangles repeatedly.

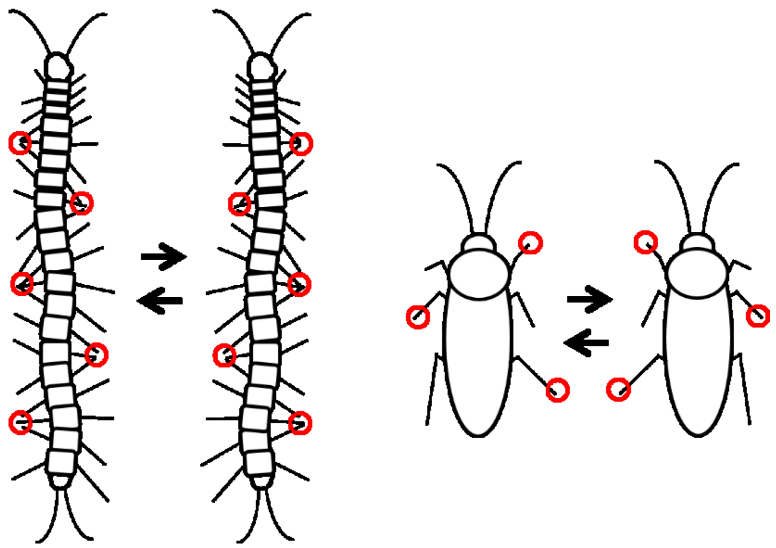

(a) Centipede (b) Cockroaches

Figure 2.1 Regular pattern of multiple legs

The author thought that the movement of multiple legs can be realized with even by limiting the number of actuators and at least two degrees of freedom are required for movement on a two-dimensional plane. Therefore, the author decided to use only two motors for locomotion.

2.3.2 Two-motor locomotion mechanism

Two motor mechanism that drives multiple shafts is proposed so as to reduce the number of the actuators. Fig. 2.2 shows an overview of proposed two-motor mechanism design. Timing belts and pulleys are used for driving multiple axis with one motor and it can drive up to six shafts with two motors in total.

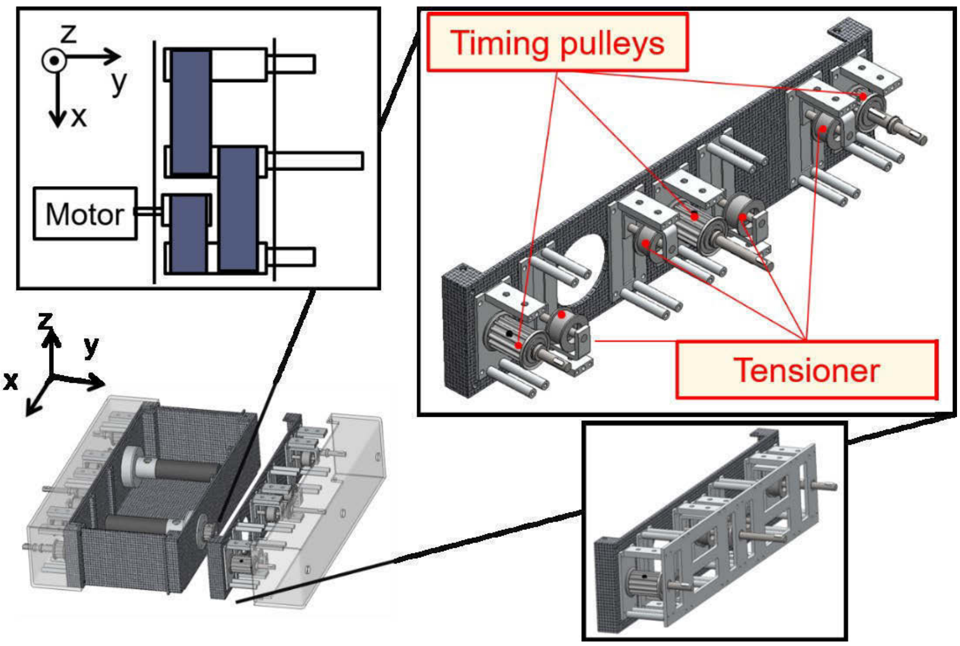

Figure 2.2 Two-motor mechanism

Timing belts and pulleys can transmit the motor power into multiple pairs of left and right side of shafts. It is necessary to output a value exceeding the total value of the required torque applied to all the shafts connected by the timing belt with one motor. The maximum value coincides with the value for operating the robot with one motor, although this value also depends on the relationship between the robot and the surface. In other words, it is possible to move the rough terrain with only two motors with the output that power can move the robot with one motor. On the other hands, when a motor is used for each shaft, the maximum required power of each motor also become the same value of using two motors. In short, the required power for each motor of the robot moving on rough terrain does not change even if the number of motors is increased. In other words, it is necessary to use a motor with the same output when a motor is provided for each axis, and this becomes disadvantageous in terms of weight, power consumption.

Table 2.2 shows effectiveness of two motor mechanism. Two-motor mechanism can reduce the width of the robot because the position of the two motors can be shifted, and the width of the robot is determined to be about the length of one motor. On the other hands, the width of the six-motor mechanism become long because the positions of the left and right motors overlap. The six-motor mechanism have disadvantages even from the perspective of weight even if considering the other parts such as belts and pulleys and the product cost is also increasing according to the number of motors. Considering the power consumption under the same operation, it is thought that the power consumption of six-motor mechanism become higher than that of two-motor mechanism as the reason for the increase in the no-load current of the motor increases as the number of motors increases. In terms of control, the control flexibility of the two-motor mechanism become lower, but this can reduce the control complexity. Since it is possible to produce a certain high locomotion performance by contriving the phase of the special wheel added to the shaft, flexibility of control is compromised, and priority is given to ease of control.

Table 2.2 Effectiveness of two motor mechanism

	Two-motor mechanism	Six-motor mechanism
Size	Small (W250)	Large (W400)
Weight	Light (2kg)	Heavy (3kg)
Cost	Low ($3k)	High ($6k)
Power consumption under the same operation	Low	High ($4I_0$ higher) *I_0 is a no-load current
Control flexibility	Low	High
Control complexity	Low (Easy)	High (Difficult)

Fig. 2.3 shows the phase of each axis. The rotations of the legs are respectively identified as θ_{r1}, θ_{r2}, θ_{r3}, θ_{l1}, θ_{l2}, and θ_{l3}, and are defined as follows, where θ_0 is the phase difference between the right and left wheels:

$$\theta_{l1} = \theta_{l2} = \theta_{l3} = \omega_l t \tag{2.1}$$

$$\theta_{r1} = \theta_{r2} = \theta_{r3} = \omega_r t + \theta_0 \tag{2.2}$$

Figure 2.3 The phase of each axis

2.3.3 Selection of locomotion mechanism

Representative locomotion mechanisms are compared to selecting the mechanism. According to the Handbooks of Robotics [2.10], there are three main locomotion mechanisms of mobile robots. Wheel, tracked, and one DOF leg mechanism are compared in terms of design concepts.

Table 2.3 shows a comparison of locomotion mechanism. The author compares these locomotion mechanisms by observing the state of each representative robot introduced in Chapter 1 and referring to similar comparison in [2.11]. Tracked mechanism has a high locomotion mechanism, but the design is complicated, and this leads the cost high and maintenance difficult. Addition to this, the complicated design can tangle fibers such as grass and it does not work well in target environment such as a forest. Therefore, locomotion mechanism was considered with reference to the mechanism of wheels and legs which is a simple design.

In comparison of locomotion performance between leg and wheel mechanism, it is characterized from one another in climbing slope ability and climbing step ability. In addition to this, one DOF leg mechanism has disadvantages in terms of power consumption, it is caused by unstable movement due to the shape of the leg. Therefore, the author proposed a locomotion mechanism that changes the shapes to be intermediate between the wheels and the legs.

Fig. 2.4 shows simple models of each locomotion mechanism. Elliptic leg is designed as a mechanism that changed the shape of the leg. By making the legs round, the time to stably contact with the surface becomes long, and the movement of the robot in the vertical direction can be reduced. This can make power consumption low and climbing slopes ability high; it will be a design that fits the concept.

Notched wheel is designed as a mechanism that changed the shape of the wheel. By making notched parts into a circle, climbing step ability that will improve.

Table 2.3 Comparison of locomotion mechanism

		Wheel	Tracked	One DOF leg	Elliptic leg	Notched wheel
Simple design	Cost	Low	High	Low	Low	Low
	Maintenance ability	Easy	Difficult	Easy	Easy	Easy
High locomotion performance	Climbing slopes	High	High	Low	High	High
	Climbing steps	Low	High	High	High	High
Low power consumption	Energy efficiency	High	Low	Low	High	High
	Required torque	Low	High	High	Low	Low

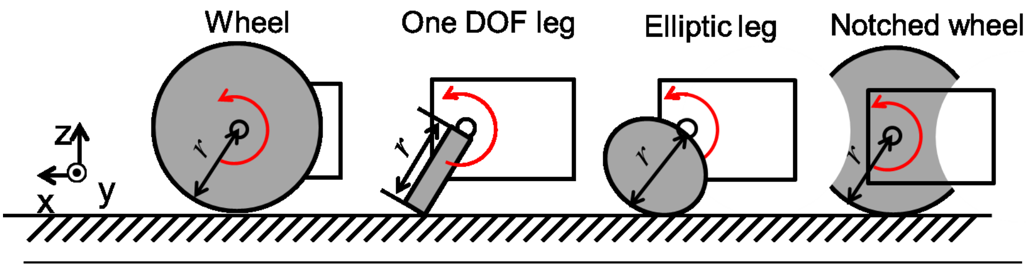

Figure 2.4 Simple models of each locomotion mechanism

2.3.4 Other designs

2.3.4.1 Symmetry

Symmetry design is used for designing the robot (Fig. 2.5). The robot is synchronized of three dimensions; x-direction: front and back, y-direction: left and right, and z-direction: top and down. The symmetry of x-direction makes the robot control easy. The same control can be applied when moving forward or backward. The symmetry of y-direction makes the control of the robot stable. Since it is symmetrical, the project point of center of mass is positioned at the center of the robot, and the stability and straightness of movement are improved. The symmetry of z-direction makes the control of the robot robust. The robot can operate in the same way as the original state, even when the robot falls over while moving.

Symmetry also makes the robot design simple. This leads the number of the kind of the parts low. Since it becomes to construct a robot by using a plurality of parts of the same kind, it is possible to reduce kinds of parts. This contributes to drastically reducing manufacturing costs and also reduces the number of parts when managing spare parts.

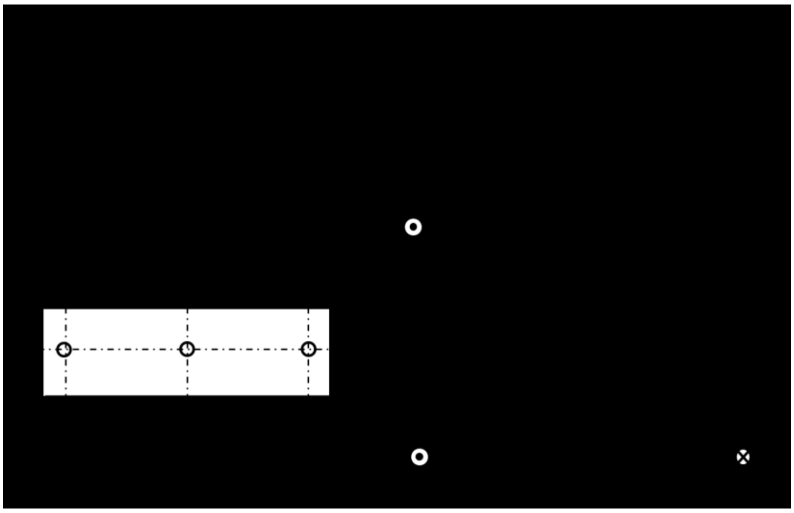

Figure 2.5 Symmetrical design

2.3.4.2 Waterproof

The design of the robot is waterproof so as to be able to operate the robot in all weather conditions. The robot is desired to have IP55 level of waterproof for operating in rainy condition. The electrical parts of the robot are located in the shell and the box is closed using waterproofing parts.

Fig. 2.6 shows the waterproofing design of the shell of the robot. The gasket and crank cable are used in the covering of the shell. O-ring and oil seal are used in the bearing box to prevent the water entering from the motor axis.

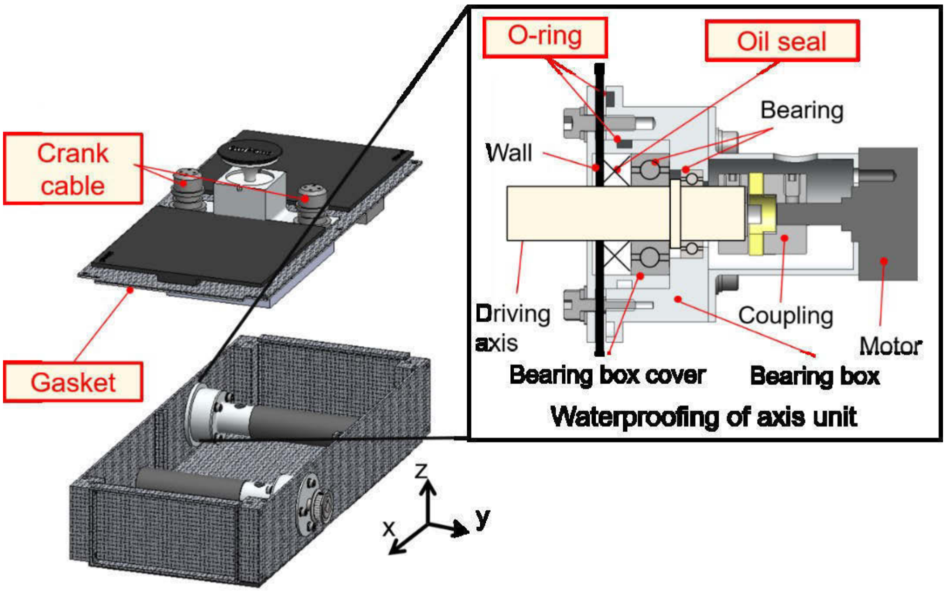

Figure 2.6 Waterproofing

2.4 Elliptic leg

2.4.1 Locomotion mechanism

An elliptic leg model is proposed so as to realize the stable locomotion and have high locomotion performance. The six legs are attached so as to be the center of the wheel were shifted from the center of the shafts. In addition, the middle parts of the legs are attached so as to be shifted by 180 degrees phase difference for increasing the area of the supporting polygon.

Fig. 2.7 shows the locomotion mechanism of the robot using elliptic legs. Locomotion mechanism of elliptic legs is simpler compared to a similar locomotion mechanism presented by R-Hex Research [2.12] that robot has six motors for locomotion. The legs of each of the three pairs of left and right are connected by a timing belt and rotate at the same speed. The rotations of the legs are respectively identified as θ_{l1}, θ_{l2}, θ_{l3}, θ_{r1}, θ_{r2}, and θ_{r3}, and are defined as follows:

$$\theta_{l1} = \theta_{l3} = \omega_l t, \quad \theta_{l2} = \omega_l t + \pi \tag{2.3}$$

$$\theta_{r1} = \theta_{r3} = \omega_r t + \theta_0, \quad \theta_{r2} = \omega_r t + \pi + \theta_0 \tag{2.4}$$

where ω_l and ω_r, are angular velocity of the left and right motor, θ_0 is a phase difference of the left and right.

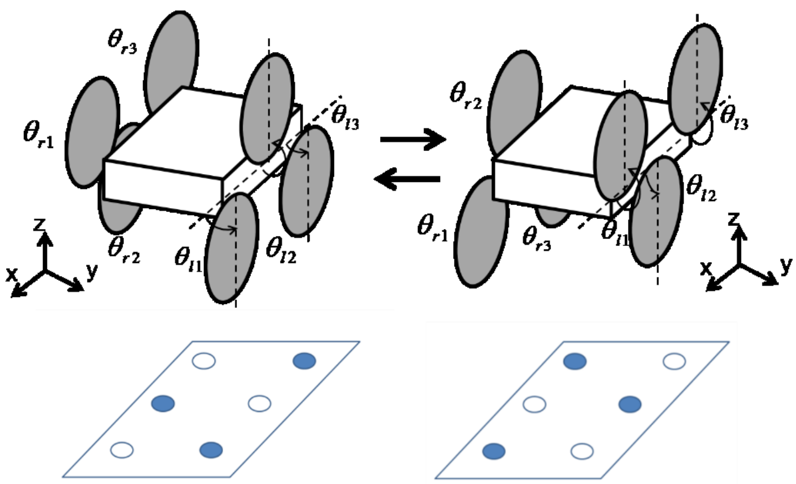

Figure 2.7 Locomotion mechanism of the robot using elliptic legs

This movement is like a swinging the wheel, a part of the wheel comes into contact with an obstacle and the robot try to climb the step by its friction. Therefore, the performance of climbing step is remarkably improved as compared with ordinary wheels. Even when moving on a flat surface, especially when the left and right phases differ by 180 degrees, stable locomotion becomes possible.

Fig. 2.8 shows a comparison between elliptic leg model and R-hex model. Elliptic legs can make the rotational speed of every legs constant because the range of the angle of the leg when the surface and the leg are in contact is wide. On the other hand, since that of R-Hex legs is small, robot would rub the belly. Therefore, the robot has to rotate the legs first during the time when legs don't contact the surface; R-Hex legs have to change the rotational speed for stable locomotion.

The moving mechanism of the ellipse legs is also characterized in that does not depend on the direction of movement. The characteristics of the front and rear symmetrical design of the robot are utilized as it is, and the movement of the robot does not change by the movement in the back and forth direction. On the other hand, since that of R-Hex legs is not front-back symmetric, it is necessary to change the control according to the moving direction.

These characteristics of elliptic legs make the control easier and contribute to realize autonomous locomotion on rough terrain.

More information on R-hex is described in [2.13-39].

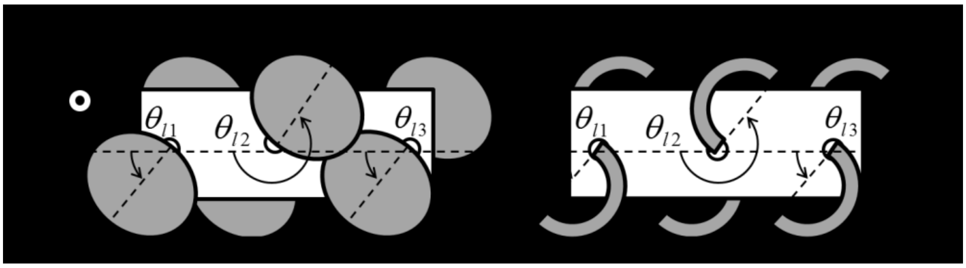

(a) When $\theta_{l1} = \pi/4$

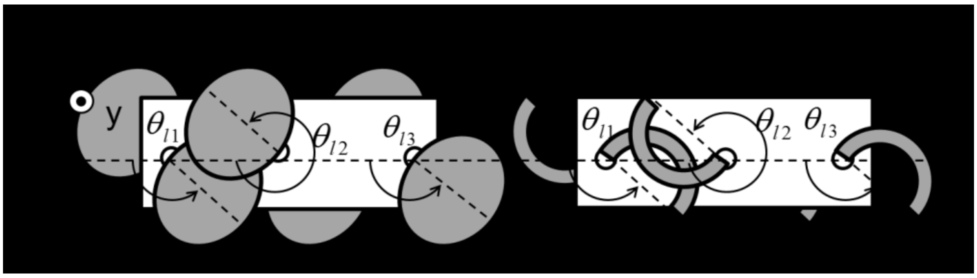

(b) When $\theta_{l1} = 3\pi/4$

Figure 2.8 Comparison between elliptic leg model and R-hex model

2.4.2 Optimizing the shape

It is necessary to consider the detail shape of the legs because the power consumption of driving parts significantly depends on the properties of the legs. Fig. 2.9 shows an elliptic leg model and Table 2.4 explain each parameter. This model is proposed for optimizing the power consumption during moving flat surface.

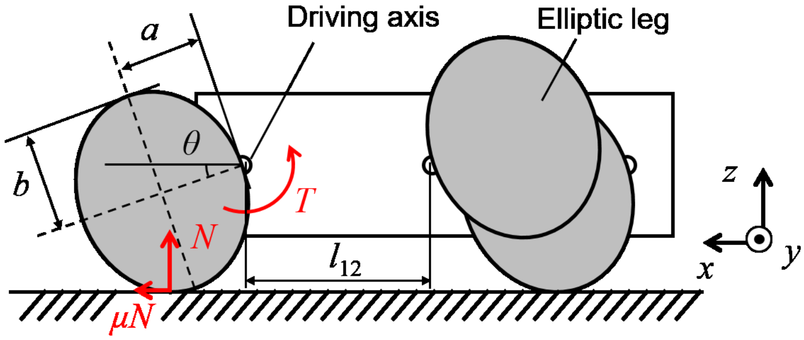

Figure 2.9 Elliptic leg model

Table 2.4 Explanation of each parameter in Fig. 2.8

Parameter	Explanation
a	Semi-major axis
b	Semi-minor axis
l_{12}	Distance between axis 1 and 2
θ	Phase of the leg
μ	Friction coefficient
T	Required torque
M	Mass of the robot
g	Gravity
N	Normal force

The semi-major axis a represents the step-climbing ability, which I set to the maximum value to avoid interference with the hardware. The semi-minor axis, b also has a range because of hardware limited, b is from $0.5a$ to $1.5a$.

The required torque for each leg position θ is given by this calculation.

$$T = \frac{Mga}{\sin(\varphi)}\sqrt{1+\frac{C+D^2}{C+D}+2\sqrt{\frac{C}{C+D}}}\cdot\sin(\theta+\varphi+\arctan(C\frac{\sqrt{\frac{1}{C+D}}}{1+\sqrt{\frac{C}{C+D}}})) \quad (2.5)$$

where

$\varphi = \arctan(1/\mu), \quad C = \tan^2(\theta), \quad D = (b/a)^2$

Fig. 2.10 shows the relationship between the required torque and the semi-minor axis b in a condition that friction coefficient is 0.2. The applied friction coefficient is the estimated average value for real fields.

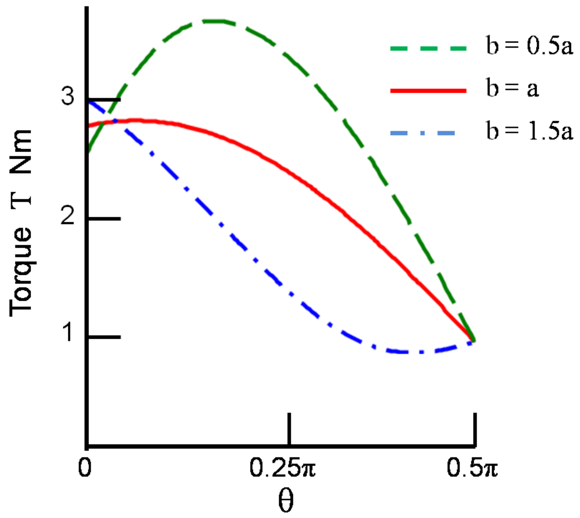

Figure 2.10 Simulation on required torque using elliptic leg

The advantage of this model is that it can easily simulate the energy consumption and generalize any other leg similar to a circle or stick by changing the shape.

2.4.3 Implementation

The original leg that combined a circle and two lines were fabricated so as to touch the surface to form a shape similar to the elliptic model as shown in Fig. 2.11. This shape was devised due to the problem of modeling and the convenience of attachment to the shaft.

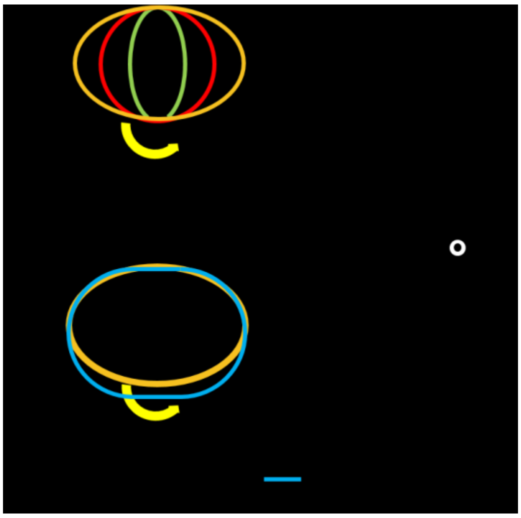

Figure 2.11 Implemented leg

Fig. 2.12 shows a fabricated robot based on the elliptical leg model and Table 2.5 shows specifications of the robot. The robot is called Waseda Animal Monitoring robOT (WAMOT). Fig. 2.12 (a) shows a robot fabricated using polyoxymethylene (POM) material. This is made by cutting POM which is one of called engineering plastic. It is a very lightweight model as it is a feature that elliptical legs are hollow. However, in outdoor use, there are cases where branches are tangled and stacked. Fig. 2.12 (b) shows a robot fabricated using carbon fiber reinforced plastics (CFRP) material. Since CFRP is extremely hard and lightweight, it is attracting attention as a material substituting for aluminum. Unlike the POM model, elliptical legs of this model are not hollow and suitable for outdoor use.

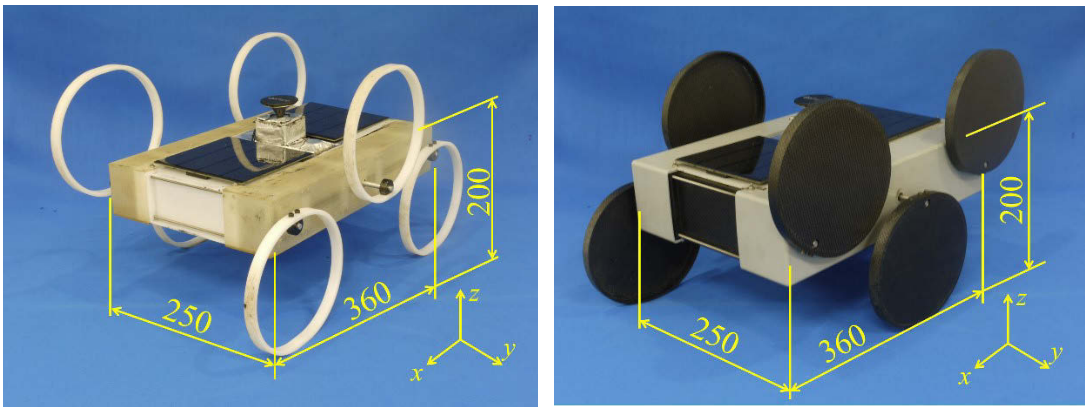

(a) Fabricated using POM material (b) Fabricated using CFRP

Figure 2.12 Overview of Waseda Animal Monitoring robOT (WAMOT) with elliptic leg. These robots were fabricated under the cooperation of NiKKi Fron Co., Ltd.

Table 2.5 Specification of the robot

(a) POM

Items			Value
Size	Width	mm	250
	Length	mm	360
	Height	mm	200
Weight		kg	3.2
Velocity		m/min	10
Capacity of battery		Wh	26.4
Updime		h	3
Wattage of motor		W	11x2

(b) CFRP

Items			Value
Size	Width	mm	250
	Length	mm	360
	Height	mm	200
Weight		kg	5.0
Velocity		m/min	10
Capacity of battery		Wh	47.7
Updime		h	4
Wattage of motor		W	15x2

2.4.4 Verification

The performance of WAMOT was evaluated by testing its climbing slope and step abilities and implementing it on real fields.

2.4.4.1 Performance test: Climbing slope

The climbing slope ability was measured by the following method:

(a) A slope was prepared of inclinations ranging from 3 to 21 [deg] in steps of 3 [deg] (see Fig. 2.13).

(b) WAMOT was made to climb a length of 1 [m] forward from a stationary position on each slope.

(c) For successful climbs of each slope out of five trials confirmed the ability of the robot to climb it.

Based on the above procedure, it was found that WAMOT could climb a slope with an inclination as much as 18 [deg].

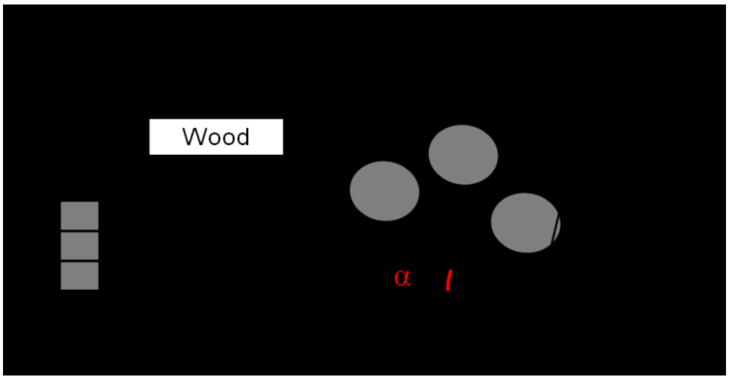

Figure 2.13 climbing slope test

2.4.4.2 Performance test: Climbing step

The climbing step ability was measured by the following method.

(a) A Step with heights was prepared ranging from 20 to 200[mm] in steps of 20[mm] (see Fig. 2.14).

(b) WAMOT was operated forward toward a step from a distance of 250[mm] at maximum speed.

(c) Four successful climbing of a step out of five trials confirmed the ability of the robot to climb the step.

Based on the above procedure, it was confirmed that WAMOT could climb a step as high as 180[mm].

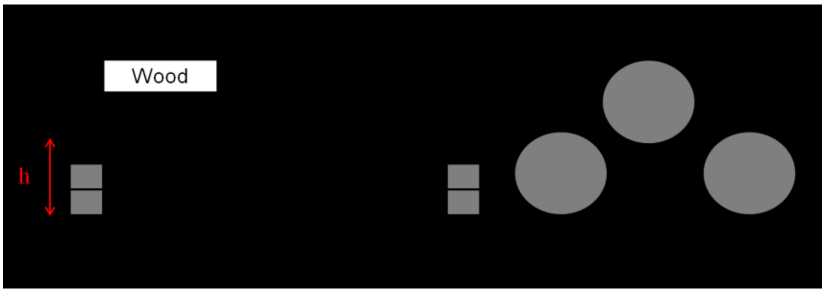

Figure 2.14 Climbing step test

2.4.4.3 Demonstration experiment

The author experimentally implemented WAMOT in the artificial ecosystem of the Toyama Park in Tokyo, which the author considered to be a comparatively easy terrain, to verify the performance of the robot. The motion pattern of the robot was programmed into the motor control board. The robot was to repeatedly operate in the active mode for 5[min] followed by the rest mode for 15[min] under actual operating conditions. In the active mode, it was to repeatedly execute a motion comprising 40[s] forward movement, stopping for 5[s], 10[s] backward movement, and stopping for another 5[s]. This motion pattern is useful for avoiding obstacles such as trees. The robot could move on easy terrain without any problems.

The author also tested the robot in the natural ecosystem of the mountain forest on Mount Fuji in Shizuoka (Fig. 2.15), which the author considered to be a comparatively difficult terrain. The motion pattern of the robot was also programmed into the motor control board. The robot was to repeatedly operate in the active mode for 3[min] followed by the rest mode for 27[min] under actual operating conditions. In the active mode, it was to repeatedly execute a motion comprising 60[s] of forward movement, stopping for 5[s], backward movement for 10[s], and stopping for another 5[s] stop. The robot could move on difficult terrain. However, sometimes robot became stuck in a small bamboo. It is noteworthy that the robot was not flooded by the rain that fell during the experiment.


Figure 2.15 Experiment in the mountain forest

Fig. 2.16 shows the WAMOT (CFRP ver.) on rough terrain in forest. Since the legs are not hollow, it was confirmed that the risk of getting tangled with twigs was reduced.

Figure 2.16 WAMOT on rough terrain in forest

Fig. 2.17 shows the WAMOT on snow covered surface. It was confirmed that the robot can move if it is on a relatively hard snow such as a ski resort. On a very soft snow like a new snow, it is thought that the robot become an immoveable condition because robot's legs dig a hole in the ground and the robot's casing comes into contact with the ground. In order to cope with such a surface, it is considered necessary to increase the width of the leg and lower the ground pressure between the robot and the ground.

Figure 2.17 WAMOT on snow covered surface

Fig. 2.18 shows the WAMOT on sand surface with sea water in seaside. Since the robot is waterproof, it was confirmed that it can move also on the coast. Since the weight of the robot is smaller than the buoyancy, in the sea the robot does not move the ocean floor but floats on the sea surface. Also, it was confirmed that the robot is turned over by the waves. Design considering the relation between the weight of the robot and buoyancy, and higher waterproof performance is required when used for survey near the seabed.

Figure 2.18 WAMOT on sand surface with sea water in seaside

2.4.5 Discussion

The proposed locomotion mechanism using elliptic legs seems be effective for coping with complex environment such as forest. The robot could move outdoors and its slope and step climbing capabilities met the requirements. However, sometimes the robot could not move in the mountain forest because its being stuck in obstacles like bamboos was not envisaged. The shape of the robot is expected to improve to solve this problem.

The behavior of the robot was different for θ_0, which is the phase difference between the equations of the right and left legs. When θ_0 was close to π, the locomotion of the robot was stable and without significant inclination in its posture. This is useful for flatland locomotion and low energy consumption. When θ_0 was close to zero, the locomotion of the robot was unstable and with a significant inclination in its posture. This is, however, useful for climbing high steps and inclining the robot when charging the battery.

2.5 Notched wheel

2.5.1 Approach to make a notched wheel model

The model using four wheels is used for designing a notched wheel model. In a study of elliptic leg model, ease of falling on a slope of a six-legged robot was confirmed. The area of the supporting polygon decreases when the wheel or leg at the center contacts the surface, and the robot becomes unstable. Fig. 2.19 shows a relationship between the projected point of the center of mass and supporting polygon using elliptic legs. From Phase 2 to Phase 3, the robot becomes unstable because it is supported by the three rear legs, making it easy to fall backwards.

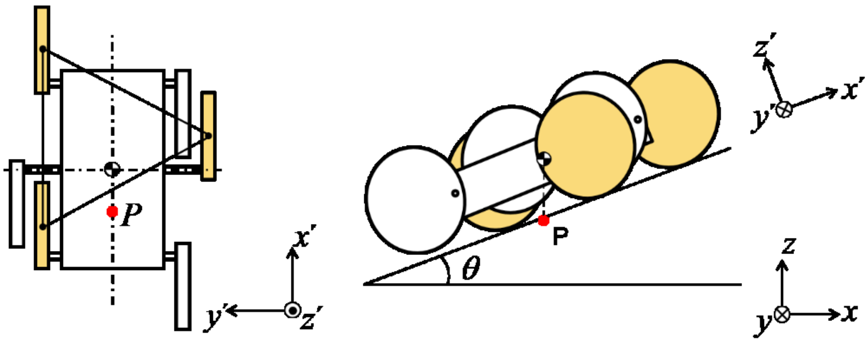

(a) Phase 1

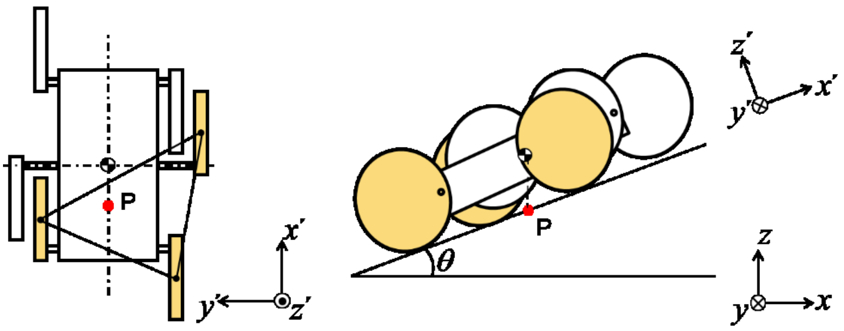

(b) Phase 2

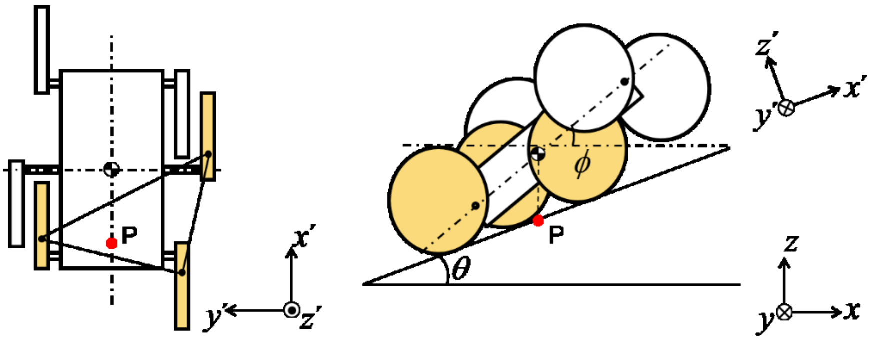

(c) Phase 3

Figure 2.19 The relationship between the projected point of the center of mass and supporting polygon using elliptic legs. P is a projected point of the center of mass.

Four wheels increase the supporting polygon, and the robot becomes stable. Fig. 2.20 shows a relationship between the projected point of the center of mass and supporting polygon using four wheels. Unlike elliptical legs, stable locomotion is possible with only four wheels if the wheels are close to a circle, and it will also stabilize on climbing a slope.

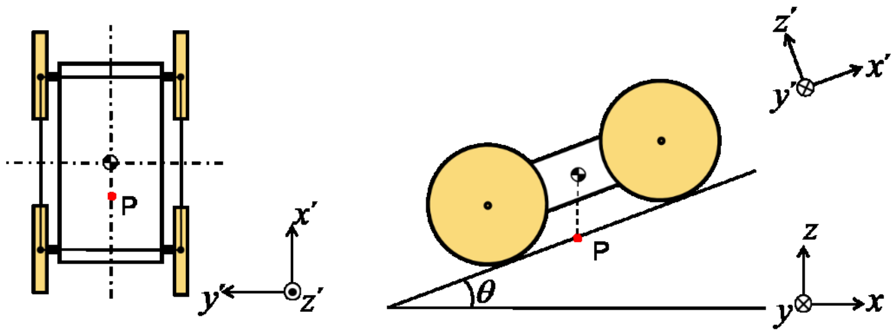

Figure 2.20 The relationship between the projected point of the center of the mass and supporting polygon using four wheels. P is a projected point of the center of mass.

The locomotion performance in rough terrain is able to increase by changing the shape of the wheel. In previous research, a lot of wheel shapes have been proposed to suit the target environment. Loper used Tri-Lobe wheel that three small wheels mounted to a central hub [2.40]. CLOVER used special wheel like gear and used in a volcanic environment [2.41]. These mechanisms are useful in each environment, but these wheels' mechanisms have not well maintained using mechanical model and not meet our target environment. Spoke type wheel is well known as simple wheel and a lot of studies are focused on its climbing steps performance and its stability [2.42]. However, almost of these studies have not mentioned the way for satisfying both these climbing abilities and generalized the shape using a model.

2.5.2 A study of climbing a step

The wheel shape is greatly affected to the climbing a step. Comparison of three types in terms of climbing step ability is introduced in this section. In general, the robot cannot get high friction to the ground outdoors, the model assumes a situation where sufficient friction with obstacles cannot be obtained in the arc portion of the wheel.

Fig. 2.21 (a) shows a climbing a step of a circle type wheel and Table 2.6 explain each parameter. The maximum height potential of the climbing a step (H_{max}) is calculated as follows;

$$H_{\max} = r \tag{2.6}$$

This is a value that can be geometrically maximized, and it actually varies depending on the influence of friction.

Fig. 2.21 (b) and (c) show a climbing a step of spoken and notched type. Since there is a prong hook on the wheel, the robot can climb a step higher than its own height of the wheel shaft. However, H_{max} can be a little small at spoke type because prong hooks also lower the height of the forward axis ($h_{e,f}$). H_{max} at spoke type is as follows;

$$H_{\max} = r(\cos\frac{\theta}{2} + \sin\frac{\theta}{2}) \tag{2.7}$$

When the circular part is touched to the surface during the robot climbing at notch type, H_{max} become larger.

$$H_{\max} = r(1 + \sin\frac{\theta}{2}) \tag{2.8}$$

(a) Circle type (b) Spoke type (c) Notch type

Figure 2.21 Comparison of three types in climbing step ability. (First phase)

Table 2.6 Explanation of each parameter in Fig. 2.20

Parameter	Explanation
R	Radius of the wheel
θ	Notch angle of the wheel
l_{13}	Distance between axis 1 and 3
$h_{e,f}$	Height of the forward shaft
H	Height of the step
H_{max}	Maximum height potential of the climbing a step

Considering to the robot climb up to the last, it is conditional that it does not flip over before the rear wheel can climb. Fig. 2.22 shows the final phase of climbing a step of each wheel shape and Table 2.7 explains a newly appearing parameter. The effective length between the shaft of the rear wheel and the contact point to the step (l_e) should be shorter than that of between the rear shaft and the center of mass (l_g).

On the condition that the center of mass is located the center of the robot, the robot can finish climbing a step when the H meet the following formula.

$$\sqrt{r^2-(H-h_{e,b})^2} < \frac{l_{13}}{2}\cos(\arctan(\frac{H}{l_{13}})) \tag{2.9}$$

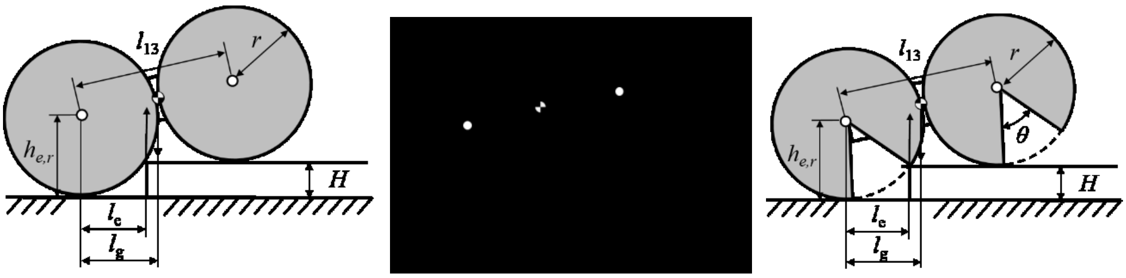

(a) Circle type (b) Spoke type (c) Notch type

Figure 2.22 Comparison of three types in climbing step ability. (Final phase)

Table 2.7 Explanation of each parameter in Fig. 2.21

Parameter	Explanation
l_e	Effective length between the shaft of the rear wheel and the contact point to the step
l_g	Length between the rear shaft and the center of the mass
$h_{e,r}$	Height of the rear shaft

2.5.3 A study of climbing a slope

The wheel shape is also greatly affected to the climbing a slope. Comparison of three types in climbing slope ability is introduced in this section. The model assumes situation that the robot climbs at so slow speed that the effect of acceleration can be neglected.

Fig. 2.23 (a) shows a climbing a slope of circle type wheel. In general, circle type has high climbing ability. The maximum angle of the climbing a step ϕ_{max} is calculated as follows;

$$\phi_{\max} = \arctan(\frac{l_{13}}{2r}) \tag{2.10}$$

Fig. 2.23 (b) and (c) show a climbing the slope of spoke and notch type. There is prong hook on the wheel, l_e should be shorter than l_g. The maximum angle of the climbing a step ϕ_{max} is calculated as follows;

$$\phi_{\max} = \arctan(\frac{\frac{l_{13}}{2} - r\sin\frac{\theta}{2}}{r\cos\frac{\theta}{2}}) \tag{2.11}$$

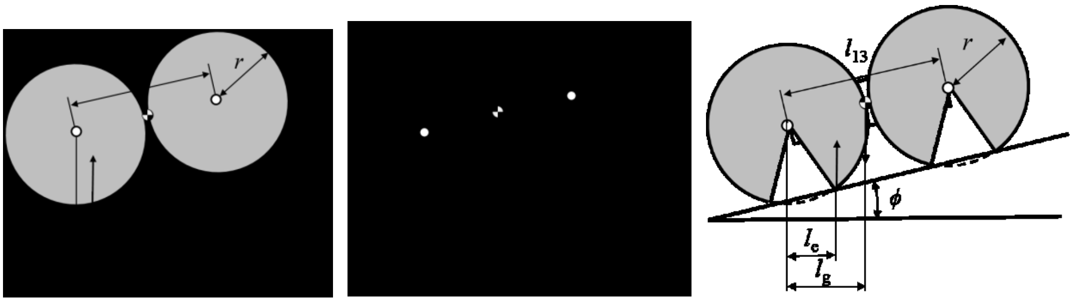

(a)Circle type (b) Spoke type (c) Notch type

Figure 2.23 Comparison of three types of wheel in climbing slope ability

2.5.4 A study on number of notches

The number of notches is also important for designing the wheel. A lot of notches would reduce the time the robot climbs over the step. However, climbing step ability become low when the angle of the notch is not considered well. Angle range is better to calculated so as not to lower the climbing ability. Therefore, the condition is considered so that the circle part of the wheel should touch to the surface when the notch part of wheel can catch a step.

When considering the influence of the number of notches, the situations are classified into four cases as shown in Fig. 2.24.

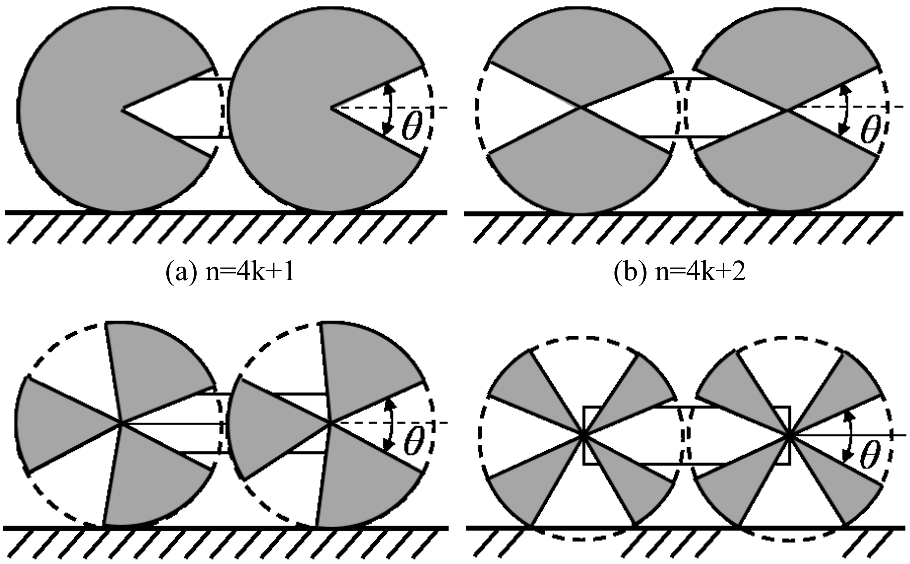

(a) n=4k+1 (b) n=4k+2

(c) n=4k+3 (d) n=4k+4

Figure 2.24 Four cases of the number of notches

Table 2.8 shows the conditional expression of the notched angle for the arc portion of the wheel to touch the surface when the robot catches the step in each case. Fig. 2.25 shows a result of optimal number of notches. After all, only odd or twice the odd number of notches can be candidate of optimal number. The twice one is considered well in terms of reducing the time the robot climb over a step, therefore, twice the odd number of notches become an optimal number of notches in each notched angle. For example, when the angle of the notch is decided to be $\pi/2$, the best number of notches become 2.

Table 2.8 Angle range in each case.

Pattern	n=4k+1	n=4k+2	n=4k+3	n=4k+4
Angle range	$0 < \theta < \frac{\pi}{n}$	$0 < \theta < \frac{2\pi}{n}$	$0 < \theta < \frac{\pi}{n}$	Any angle is not suitable

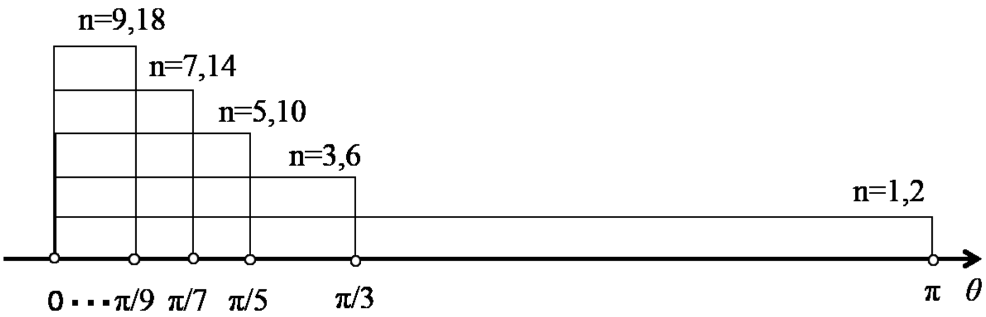

Figure 2.25 Optimal number of notches

2.5.5 A study of the edge shape of the notch

The edge shape of the notch is also affected to the climbing step ability. Fig. 2.26 shows comparison between standard and rounded edge shape design. Rounded edge shape reduced the length of the effective radius (r_e) and effective notch angle (θ_e). This reduces the climbing step ability and increase the climbing slope ability.

The climbing step ability and the climbing slope ability are changed to the following formula by changing shape.

$$H_{\max} = r_e(1+\sin\frac{\theta_e}{2}) \tag{2.12}$$

$$\phi_{\max} = \arctan(\frac{\frac{l_{13}}{2} - r_e \sin\frac{\theta_e}{2}}{r_e \cos\frac{\theta_e}{2}}) \tag{2.13}$$

The robot can finish climbing a step when the H meets the following formula.

$$\sqrt{{r_e}^2 - (H - h_{e,b})^2} < \frac{l_{13}}{2}\cos(\arctan(\frac{H}{l_{13}})) \tag{2.14}$$

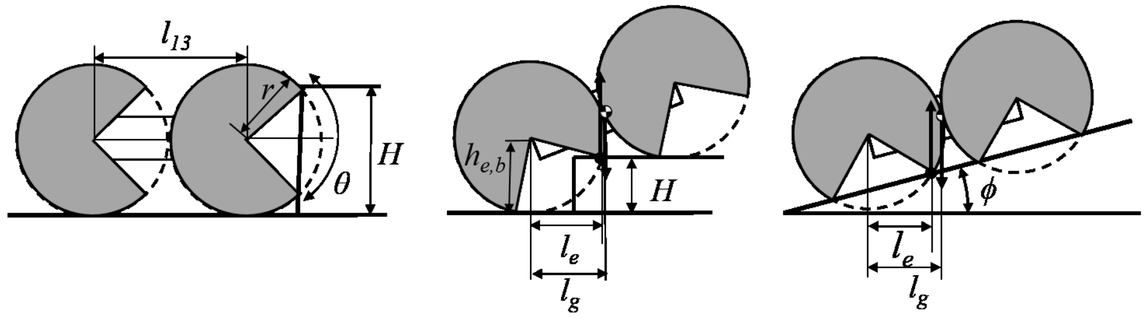

(a) Standard shape

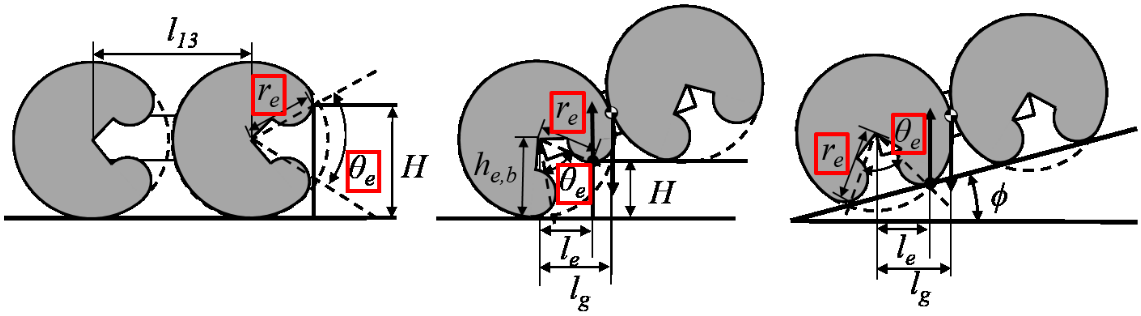

(b) Rounded shape

Figure 2.26 Comparison between standard and rounded edge shape design

In contrast, arc-shaped notch does not reduce the maximum height potential of the climbing a step of the robot. Fig. 2.27 shows comparison between standard and arc-shaped edge shape design. This type of notched also increases the finishing climb step ability because arc-shaped can shorten l_e.

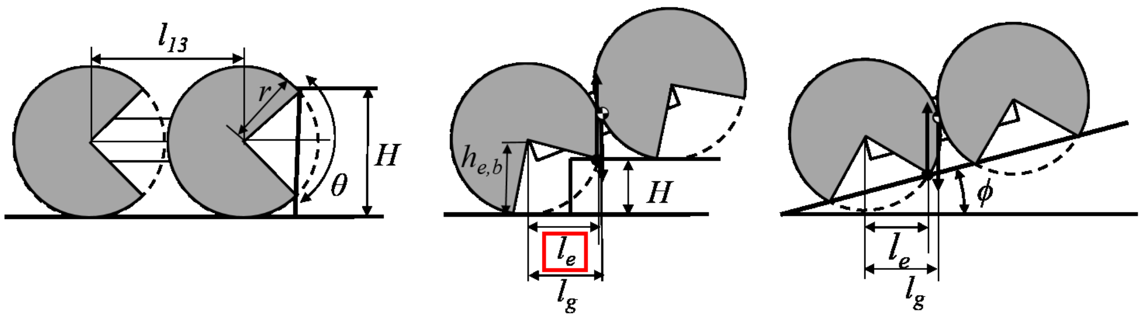

(a) Standard shape

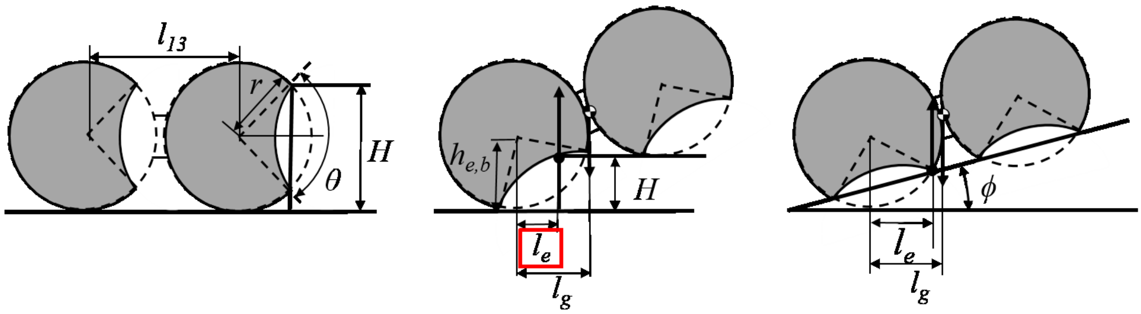

(b) Arc-shape

Figure 2.27 Comparison between standard and arc-shaped edge shape design

2.5.6 A study of the phase difference between left and right wheels

The phase difference between left and right wheels affects the climbing slope ability. The shape of stability margin changed depending on the phase difference. Fig. 2.28 shows stability margin of the robot in two different condition. Fig. 2.28 (a) is when the phases of the left and right wheels are the same and Fig. 2.28 (b) is when the right side of the wheels are π/2 different from left side wheels. When the phases of the left and right wheels are the same, the distance between the center of the robot and the edge of the stability margin (l_d) is calculated as follow;

$$l_d = \frac{l_{13}}{2} - r\sin\frac{\theta}{2} \tag{2.15}$$

When the right side of the wheels are π/2 different from left side wheels, the stability margin shift to backward, and l_d become longer than that of no phase difference. This can make the climbing slope ability high. l_d when the right side of the wheels is π/2 different from left side wheels is calculated as follows;

$$l_d = \frac{l_{13}}{2} - \frac{r}{2}\sin\frac{\theta}{2} \tag{2.16}$$

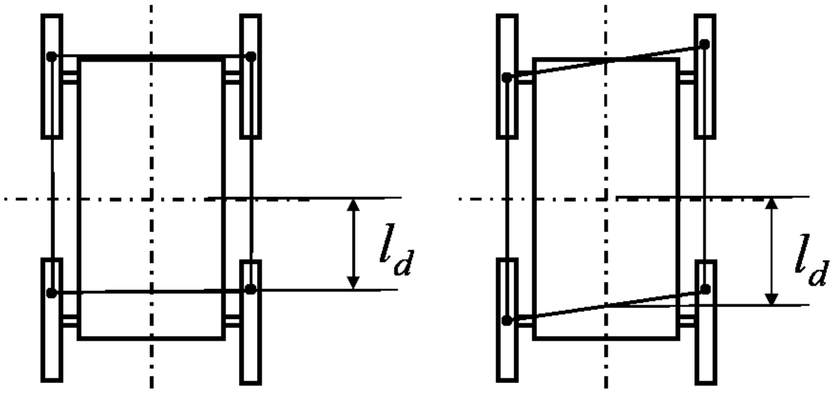

(a) Normal condition (b) Different phase condition

Figure 2.28 Stability margin of the robot

Fig. 2.29 shows height of the center of mass of the robot in two different condition. In a normal condition, the height of the center of mass (h_d) is calculated as follow;

$$h_d = r\cos\frac{\theta}{2} \tag{2.17}$$

In a different phase condition, h_d become shorter than that of no phase difference, this is also a positive effect for increasing the climbing slope ability. h_d when the right side of the wheels is π/2 different from left side wheels is calculated as follows;

$$h_d = \frac{r}{2}(1+\cos\frac{\theta}{2}) \tag{2.18}$$

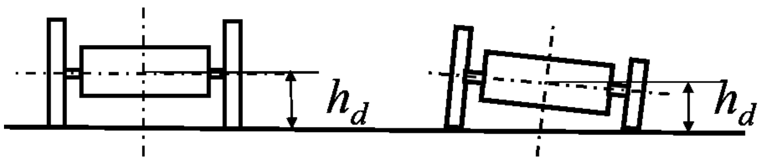

(b) Normal condition (b) Different phase condition

Figure 2.29 Height of the center of mass of the robot

Thus, ϕ_{max} when the right side of the wheels is π/2 different from left side wheels is calculated as follows;

$$\phi_{max} = \arctan\left(\frac{l_{13} - r\sin\frac{\theta}{2}}{r(1+\cos\frac{\theta}{2})}\right) \tag{2.19}$$

2.5.7 Implementation

Fig. 2.30 shows a fabricated robot based on the notched wheel model and Table 2.9 shows specifications of the robot. The material of notched wheel is made by ABS and the wheels are attached to the same shaft as the elliptical leg via connecting parts. The length of the middle part of shaft is shortened so that it does not go out in the four wheels' case, thought it extended outward in the six-leg's case. That is, the inner drive mechanism using timing belt is same as the elliptic leg mechanism.

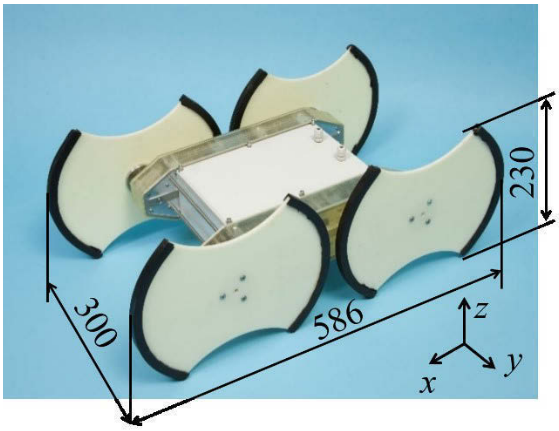

Figure 2.30 Overview of WAMOT with notched wheel

Table 2.9 Specification of the robot

Items			Value
Size	Width	mm	300
	Length	mm	586
	Height	mm	230
Weight		kg	5.0
Velocity		m/min	10
Capacity of battery		Wh	47.7
Uptime		h	4
Wattage of motor		W	15x2

2.5.8 Verification

2.5.8.1 Comparison with various wheel shapes

Dynamics simulation on v-rep was conducted to verify the validity of the proposed model. For adapting to the WAMOT, the size (l_{13}=300 [mm], r=140 [mm], θ=86°) was set. The notched angle was decided for the purpose of making spoke type when the number of notches is four.

Climbing a step ability test was conducted in steps of 5 [mm]. To prevent the situation that the robot climbs up using a high frictional force, the friction rate (μ=0.4) was set between the wheel and the surface. In this test, it was successful when it succeeds even once by moving the robot from a distance of a variety of obstacles. This is because a different phenomenon was confirmed when experimenting at different distances due to the friction. Table 2. 10 shows the simulation results. The maximum height of the steps when the front wheel climbed is shown in the upper column of simulation, and the result of the maximum height of the steps when the rear wheel climbed is shown with brackets in the lower column of simulation.

Climbing slopes ability test was also conducted in steps of 1°. In this test, it was successful when the robot climbs up 2 [m] of the slope. The results are also shown in Table 2.10.

Table 2.10 Dynamic simulation results of comparison with various wheel shape

Wheel type		Wheel	Standard	Standard	Standard	Standard	Rounded edge	Arc-shaped notch
Image								
Number of notches		0	4	3	2	2	2	2
Climbing steps ability	Theoretical	140	198	232	235	235	210	235
	Simulation	140 (25)	205 (125)	230 (170)	235 (125)	235 (115)	210 (180)	235 (180)
Climbing slopes ability	Theoretical	47	28	28	28	28	35	28
	Simulation	45	27	26	27	26	34	28

2.5.8.2 Comparison with a phase difference of left and right wheels

The objective of the experiment was to verify the effectiveness of the proposed method. The climbing slope and step abilities were compared using dynamic simulation among six types of the phase differences.

Table 2.11 shows dynamic simulation results of comparison with a phase difference of left and right wheels.

Table 2.11 Dynamic simulation results of comparison with a phase difference of left and right wheels

Phase type		A	B	C	D	E	F
Condition	L1	0	0	0	0	0	0
	L3	0	π/2	0	π/2	π/2	0
	R1	0	0	π/2	π/2	0	π/2
	R3	0	0	0	0	π/2	π/2
Climbing ability	Slope deg	30	37	28	36	28	38
	Step mm	185	160	160	160	140	160

From this experiment, it was confirmed that the robot when the right side of the wheels are π/2 different from left side wheels (F) has the highest climbing slopes ability and no phase difference (A) has the highest climbing steps ability.

2.5.8.3 Performance verification

The objective of the experiment was to measure the climbing performance of the robot and comparing to the simulation results. The condition that the right side of the wheels are π/2 different from left side wheels was set in the climbing slope test and the no phase difference condition was set in the climbing step test. 2 [m] plate was prepared as a slope and a step which is covered with high frictional sheets. The speed of the robot was set to slow, wheels rotated at about 3 [rpm], so as not to affect the climbing performance.

Table 2.12 shows the results of the experiment.

Table 2.12 The climbing steps and slopes ability test

		Simulation	WAMOT
Climbing slope ability	deg	38	36
Climbing step ability	mm	185	180

2.5.8.4 Demonstration experiment outdoors

The objective of the experiment was to confirm the climbing performance outdoors. The robot moved in the condition that the right side of the wheels is π/2 different from left side wheels. The speed of the robot is also set to 3 [rpm] so as not to affect the climbing performance. Fig. 2.31 shows the state of the experiment on the bank in riverside area. WAMOT could climb up 29 [deg] bank in riverside area, although there were a lot of grass and reeds are existing. This is because the phase difference stabilized the locomotion.

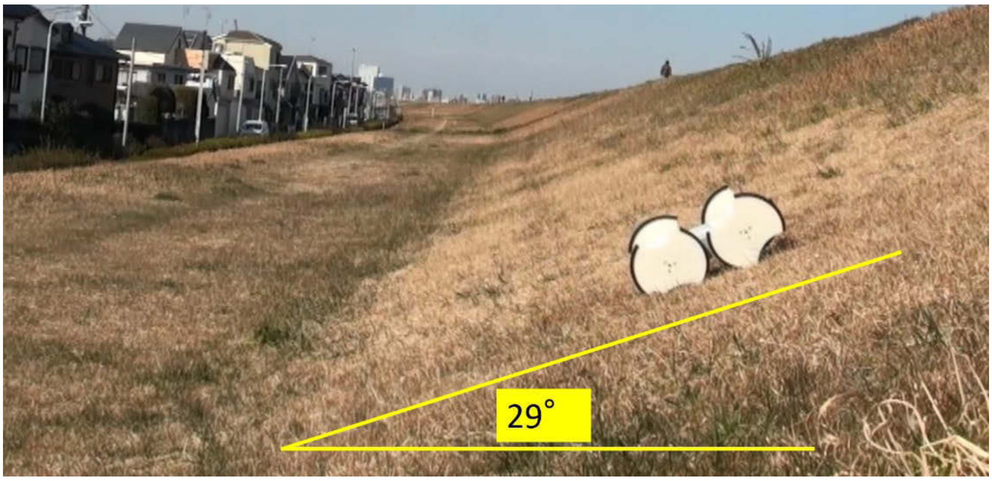

Figure 2.31 Demonstration experiment on the bank in riverside area

2.5.9 Discussion

Climbing slope and step abilities of mobile robots can be estimated by using the proposed model. The theoretical value is very similar to dynamic simulation value. This shows that we can estimate the climbing ability easily by using proposed calculation formula. The wheel shape can be easily selected and designed to meet the required specifications of the target environment.

It seems that the two parameters r_e and θ_e are important for considering the design of the wheel. These parameters greatly affect the climbing ability of the steps and slopes. Arc-shaped notch design is most effective shape because not only it does not reduce the maximum potential height of the climbing steps of the robot but also increase the finishing climb steps ability. Arc-shaped notch type can get more high ability by changing the notch angle, although it seems inferior to rounded edge shape in terms of climbing slope ability at a glance.

This model is significant not only useful for wheel type of mobile robot, but this model also can apply to the other mobile robot such as crawler and legged type. Many mobile robots can use this model by only considering contacting point on the ground.

The phase difference of the robot affects the climbing performance of the robot by simulation experiment. Type F has the highest climbing slopes ability. This is because two reasons. One is that the rear wheels were always being different phase so that l_d was also being long. The other reason is that the h_d was always being short when the robot came to flip motion. These two conditions were generated stable when the phase is type F. Type A has the highest climbing steps ability. This is because the robot was stable without rotating in the roll direction.

It is effective to make two locomotion mode; climbing slope mode and climbing steps mode by just rotating π/2 of one side of the wheels and changing the phase difference. It is desirable to change the phase automatically according to the situation to the surface condition.

2.6 Shell shape

2.6.1 Approach to cope with grass field

Passing through tall grass is difficult for land-based mobile robots. Most conventional mobile robots cannot pass through grass fields taller than their own height. The common approach for coping with such a field is to change the robot's route when it meets such obstacles to avoid getting stuck [2.43-45]. However, extra time is needed for the robot to arrive at the destination and detecting grass can be difficult. If the robot cannot operate in a tall grass field, the field cannot be monitored.

There are three possible solutions for a robot to pass through a field with tall grasses: cutting [2.46-48], bending [2.49], or slipping between grasses [2.50]. Cutting the grass requires a cutting mechanism and a high level of power consumption. Energy efficiency is key to realizing long-term continuous operation for autonomous mobile robots. Thus, these methods are not suited to our purpose of environmental monitoring. Moreover, they can hurt the natural environment, which is counter to our goal to protect the environment. Bending the grass usually uses arms with multiple actuators to cope with several obstacles. However, these methods need a high level of power consumption to remove obstacles, and the control is complicated because of the large number of actuators. This makes the robot heavy and difficult to maintain, which is also not suitable for monitoring. Slipping between grasses may be an effective method for realizing a light weight and minimizing the number of actuators. However, the size of the robot needs to be very small. Most robots that can be mounted with monitoring sensors are not small enough to slip between grasses. In short, a robot with monitoring sensors that provides a high locomotive performance in a tall grass field with only a small number of actuators has not yet been achieved.

2.6.2 Modeling of the immobile condition

The immobile condition was investigated for WAMOT where the robot is in contact with obstacles. The condition was analyzed how the robot can be improved by using a fault-tree method. It was confirmed that contact with tall grasses is the most frequent cause of immobility because the robot bounces off or partially rides over the grass. Fig. 2.32 shows a model of bouncing and lifting. The elastic force of the grass affects the robot as a reaction force in both the x and z directions. The robot cannot move owing to these reaction forces. The main cause is considered to be the low amount of power available to bend the grass and the large reaction force from the bent grass. Therefore, I thought that the robot could avoid immobility by generating a stronger grass bending force and spreading the force in the *y* direction in order to decrease the density of the grass remaining in front of the robot.

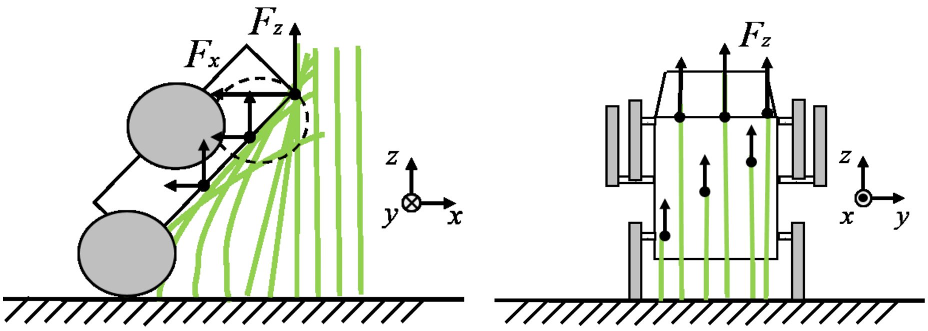

(a) Side view (b) Front view

Figure 2.32 Modeling of bouncing and lifting.

2.6.3 Inspiration from Icebreaker

In order to spread the reaction force in the *y* direction, the way of changing the robot's shape is proposed to avoid adding actuators. WAMOT sometimes moves up and down in the *z* direction when moving forward, which is similar to the behavior of an icebreaker. Especially when the phase difference between left and right legs of WAMOT is close to 0, the robot moves up and down in the pitch direction as shown in Fig. 2.33. This behavior is an effective approach for passing through tall grass, although it is inefficient for flat surfaces such as a cement road. Therefore, I referenced the icebreaker mechanism and shape as a model.

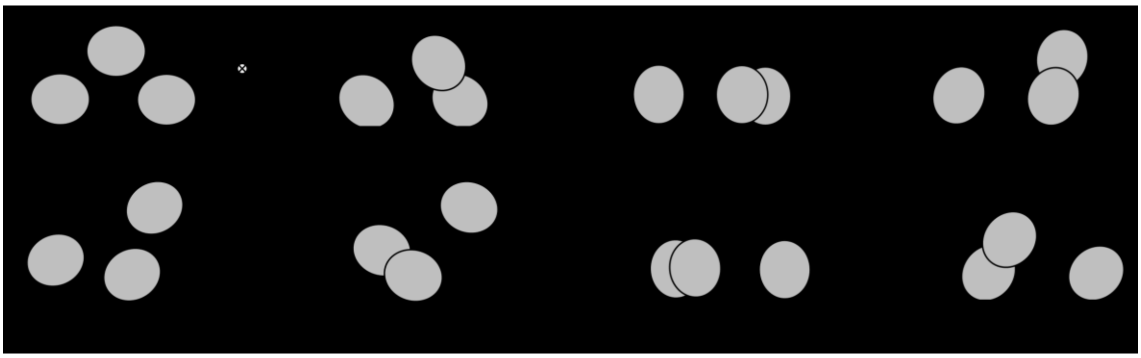

Figure 2.33 Locomotion behavior when the phase difference between left and right legs is 0

Fig. 2.34 shows motion behavior model of an icebreaker and WAMOT and Table 2.13 shows parameters of each model. In the touching phase (phase I) in Fig 2.32 (a), the icebreaker touches an ice plate and exerts a force on the plate. The icebreaker then receives a reaction force from the plate that lifts it up because the reaction force F_z is generated along with the reaction force F_x. Therefore, the center of the mass lifts up, and the icebreaker mounts the plate. This behavior is called ramming, and Vinogradov concluded that this potential energy is generated from the kinetic energy of the icebreaker [2.51,52].

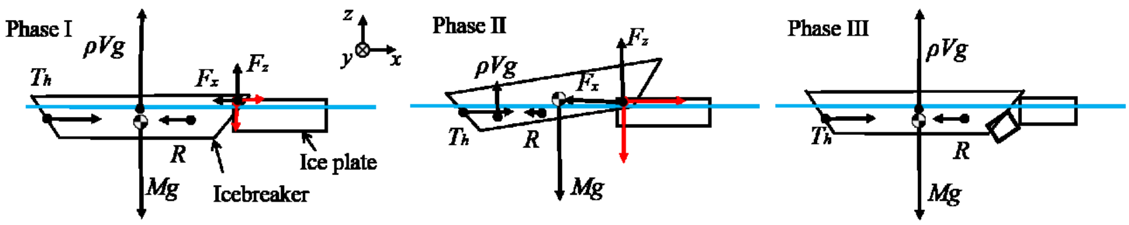

(a) Locomotion mechanism of icebreaker

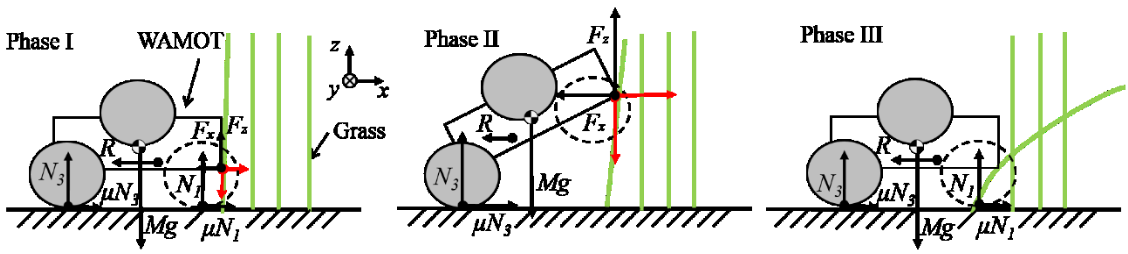

(b) Locomotion mechanism of WAMOT

Figure 2.34 Similarity of the motion behavior between an icebreaker and WAMOT

Table 2.13 Explanation of each parameter in Fig. 2.32

Model of icebreaker		Model of WAMOT	
Parameter	Explanation	Parameter	Explanation
F_x	Reaction force from ice plate in x direction	F_x	Reaction force from grass in x direction
F_z	Reaction force from ice plate in z direction	F_z	Reaction force from grass in z direction
T_h	Thrust by screw	μN_1, μN_3	Thrust by elliptic legs
R	Resistance from broken ice	R	Resistance from broken grass
M	Mass of the ship	M	Mass of the robot
ρVg	Buoyancy from the sea	N_1, N_3	Normal force

In the touching and mounting phases (phases I and II), the reaction force from the plate is as follows:

$$F_x = T_h - R - Ma_x \tag{2.20}$$

$$F_z = Mg - \rho Vg + Ma_z \tag{2.21}$$

where a_x and a_y are the acceleration of the icebreaker.

In the mounting phase, F_x and F_z increase because the buoyancy of the icebreaker decreases, along with the force in the *x* direction of acceleration of the icebreaker and the resistance from the water. When the plate no longer supports the force from the icebreaker, F_z affects the momentum that divides the plate, and the plate breaks in breaking phase (phase III).

Fig 2.34 (b) shows the locomotion mechanism of WAMOT. The behavior of WAMOT is very similar to that of icebreaker. In the touching phase (phase I), WAMOT touches the tall grass and exerts a force; this produces a reaction force from the grass. This reaction force lifts up WAMOT, and F_x affects the momentum to push the grass. When the grass no longer supports the force from WAMOT, the grass is bent in bending phase (phase III).

In the touching and mounting phases (phases I and II), the reaction force from the grass is as follows:

$$F_x = \mu N_3 - R - Ma_x \tag{2.22}$$

$$F_z = Mg - (N_1 + N_3) + Ma_z \tag{2.23}$$

where a_x and a_y are the acceleration of the WAMOT.

Equations (2.22) and (2.23) are very similar to (2.20) and (2.21). Therefore, the icebreaker model was used as a basis for designing the robot shell.

2.6.4 Effect of the robot’s shape

Changing the shape of WAMOT into the ship shape has two benefits. First benefit is that the moment to bend the grass increase because the contact point between the grass and robot is raised. Fig. 2.35 shows a comparison of WAMOT models between without and with the outer covering and Table 2.14 shows parameters of each model. These models use wheels instead of elliptic legs for the reason to simplify the calculation.

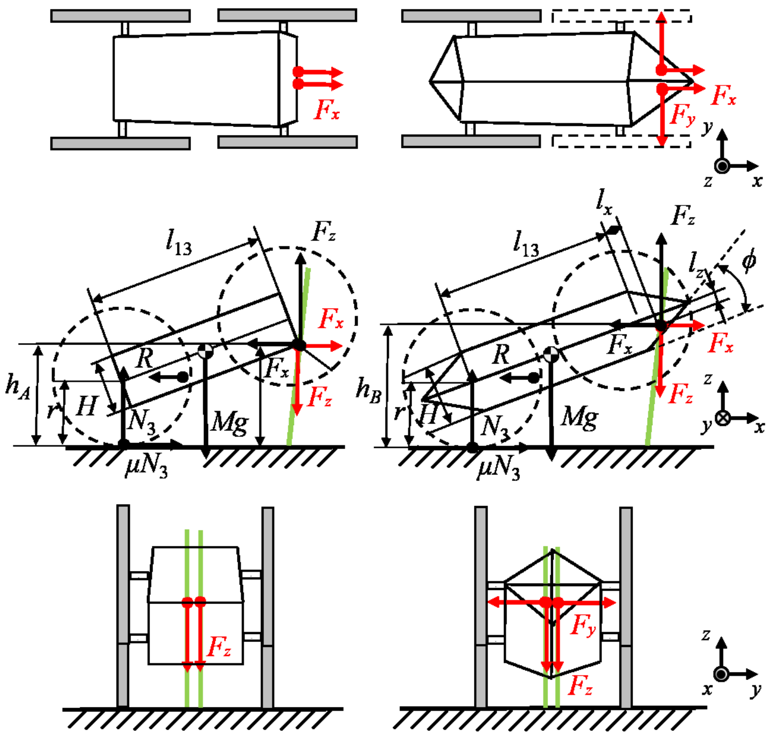

(a) WAMOT without outer covering (b) WAMOT with outer covering

Figure 2.35 Comparison of WAMOT models

Table 2.14 Explanation of each parameter in Fig. 2.34

Parameter	Explanation
F_y	Reaction force from grass in y direction
h_A	Height of contact point with grass in the without outer covering condition
h_B	Height of contact point with grass in the with outer covering condition
r	Radius of wheels
H	Height of the shell of the robot
l_{13}	Distance between the front and rear axis
l_x	Distance between the contact point and the front surface of the robot in x direction
l_y	Distance between the contact point and the front surface of the robot in y direction
ϕ	Inclination angle of the bow

Assuming that both robots are inclined at the same angle, the position of the contact point is calculated as follows:

$$h_A = l_{13}\sin\phi + r - \frac{H}{2}\cos\phi \tag{2.24}$$

$$h_B = (l_{13} + l_x)\sin\phi + r - l_z\cos\phi \tag{2.25}$$

The bending moment around the grassroots is greater when an outer covering is attached to the robot because h_A is longer than h_B.

Another benefit is that F_y is generated in the direction perpendicular to the reaction force F_x. According to Runeberg [2.53] and Shimansky [2.54], the reaction force is in the direction normal to the surface. Fig. 2.36 shows an image of divided reaction force.

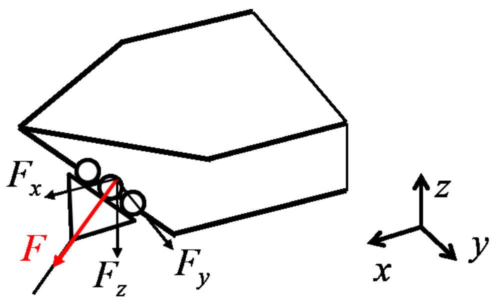

Figure 2.36 Image of divided reaction force

The divided reaction forces F_x, F_y, F_z are related as follows:

$$F_x : F_y : F_z = \tan\alpha : 1 : \tan\beta \tag{2.26}$$

$$\tan\alpha = \tan\beta \cdot \tan\phi \tag{2.27}$$

where α is the opening angle of the bow, β is the opening angle of the rib line. These parameters are shown in Fig. 2.37.

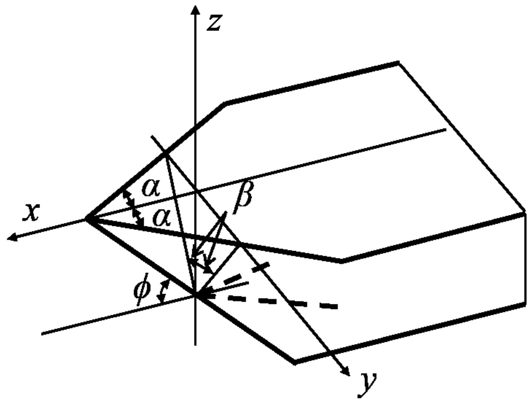

Figure 2.37 Important parameters on the ship

According to equation in (2.26), the force received by the grass from the robot with an outer covering is 1/sinα greater than that of the robot without an outer covering. Therefore, assuming that the reaction force F_x is the same, the moment used by the robot with an outer covering (M_A) to bend the grass is greater than that used by the robot without the outer covering (M_B) as follows:

$$\frac{M_B}{M_A} = \frac{(L + l_x)\sin\varphi + r - l_z \cos\varphi}{\sin\alpha(L\sin\varphi + r - \frac{H}{2}\cos\varphi)} \tag{2.28}$$

In addition to this, the density of the grass remaining in front of the robot decreases after the grass is bent in the y direction. Therefore, the resistance from the bent grass is reduced, which allows the robot to move in the x direction more smoothly.

2.6.5 Effect of the elliptic legs

Fig. 2.38 compares the wheels and elliptic leg mechanism. Either mechanism eventually will be in the same posture and produce the same force. However, when the robot use elliptic legs, the robot can easily reach the final state without using the grass; the front of the robot is lifted by only the influence of the locomotion mechanism.

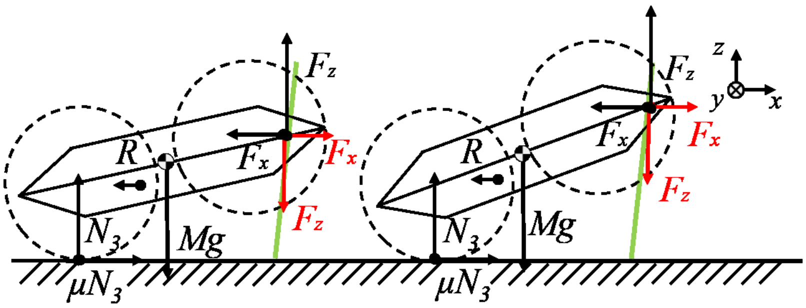

(a) Wheel mechanism

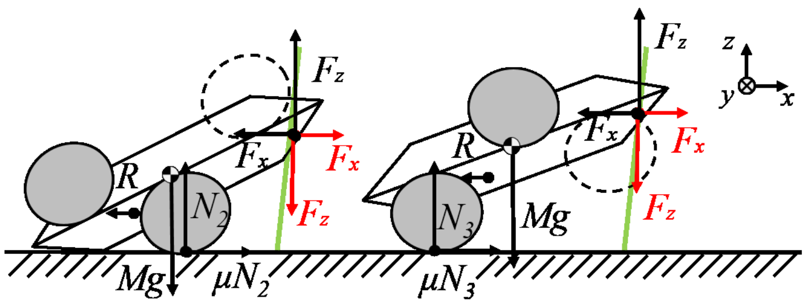

(b) Elliptic leg mechanism

Figure 2.38 Comparison between wheel mechanism and elliptic leg mechanism of WAMOT

This ability is effective when a robot moves on a high-slip surface such as sand and fallen leaves because the robot may not generate enough thrust with the small coefficient of friction to the surface. When the robot cannot get enough thrust, it cannot lift up; the moment used by the robot to bend the grass becomes small. However, the elliptic leg mechanism guarantees a large moment against the grass.

2.6.6 Design of the outer covering of the robot

The design theory of icebreaker was referenced for designing the outer shape of the robot. We utilized the parameters of the hull covering coefficient proposed by Shimansky [2.55] According to Shimansky, the icebreaking coefficient η_1 and ice cutting coefficient η_2 are defined as follows;

$$\eta_1 = \frac{F_z}{F_x} \propto \frac{1}{\tan\phi} \tag{2.29}$$

$$\eta_2 = \frac{F_y}{F_x} \propto \frac{1}{\tan\beta \tan\phi} \tag{2.30}$$

The large values of η_1 and η_2 are effective to increase locomotive performance of icebreakers. Therefore, locomotive performance of icebreaker can be improved by decreasing ϕ and β.

Three outer shapes in Fig. 2.39 was designed by referring icebreakers. These outer shapes were implemented on WAMOT, as an outer cover, using a 3D printer (CONNEX 500, RGD525). The parameters of these covers are determined, as shown in Table 2.15, to satisfy the requirements as shown below.

(a) The width of WAMOT with the cover should be same as that of WAMOT without it.
(b) ϕ should be 25 [deg], which is common in icebreakers.
(c) β should be minimized without interferences to other mechanical structures of WAMOT.

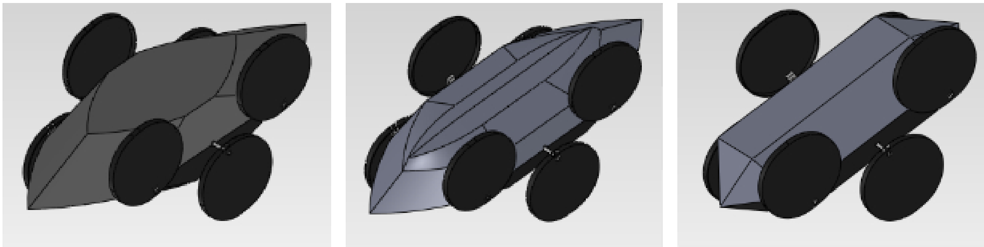

(a) Spoon bow (b) Clipper bow (c) Simplified clipper bow

Figure 2.39 Design of outer covering

Table 2.15 Parameters of outer covering

Parameters	Spoon bow covering	Clipper bow covering	Simplified clipper bow covering
2	100	90	100
2β	135	152	152
ϕ	25	25	25

The reaction forces on the outer covers from tall grasses was measured when WAMOT passed over them. The experiment was conducted under two different conditions, θ=0[deg] and θ=20 [deg], for each outer cover. The method of the experiment was shown in below.

1. Prepare the artificial bamboo grasses, and place it on clay (γ=20[deg]).
2. Attach each outer cover on the carriage.
3. Pull the carriage at the same speed to pass over the artificial bamboo grasses.
4. Measure the horizontal reaction force F_x and the vertical reaction force F_z.

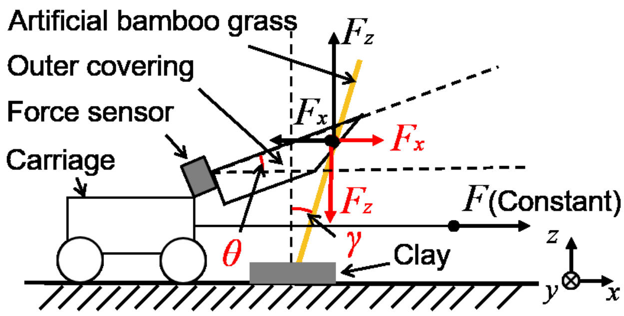

Figure 2.39 Experimental condition

Fig. 2.40 shows the results of the experiments. The average reaction force from artificial bamboo F_x and F_z is smallest at the covering is clipper bow shape.

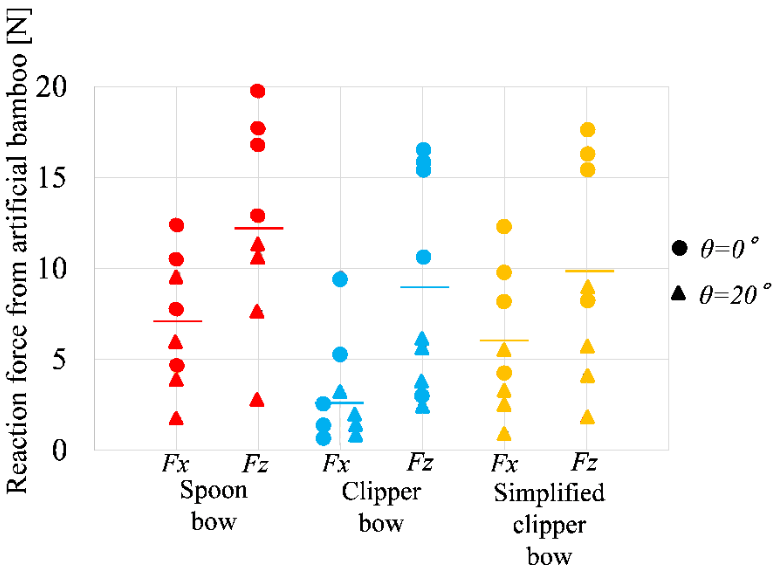

Figure 2.40 Results of reaction force

Finally, the outer covering was designed to attach to WAMOT by referencing the representative clipper bow shape of the icebreaker. Fig. 2.41 shows a design of the outer covering.

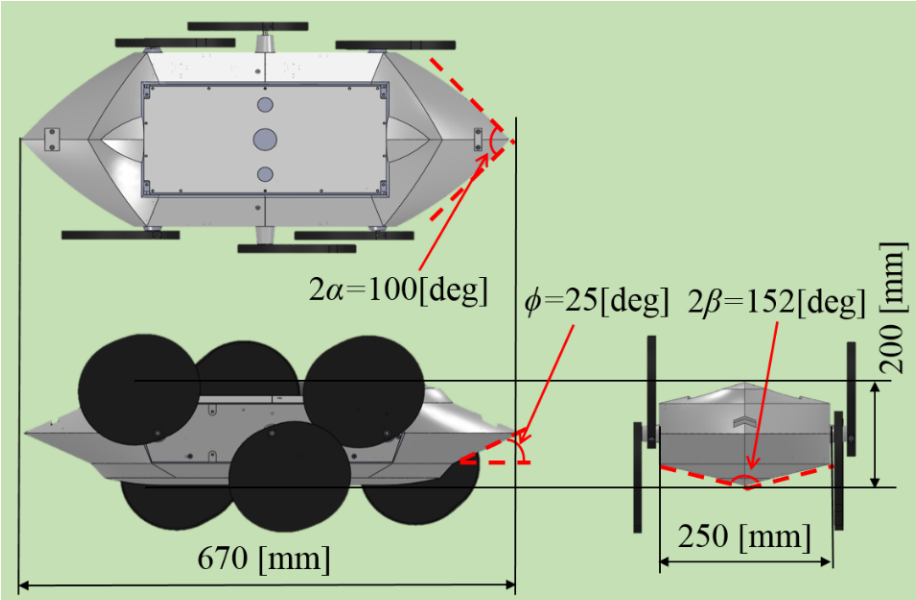

Figure 2.41 Design of the outer covering for WAMOT.

2.6.7 Implementation

The outer covering was attached to WAMOT, and the robot is called "Grassbreaker." Fig. 2.42 shows an overview of "Grassbreaker" and Table 2.16 shows specifications. The mechanism and mounted motors were the same as those of WAMOT. The tapers were also attached to the rotating shaft to prevent entanglement with grass. The grass that catches in the shaft is moved outside, and the grass is pushed outside the robot when the ellipse leg is rotating to the backside of the robot.

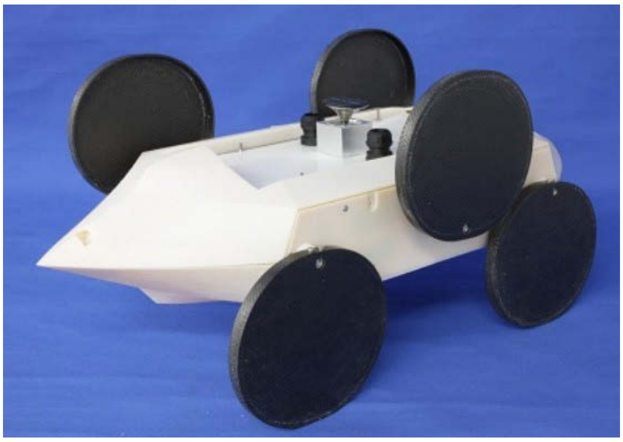

Figure 2.42 Overview of "Grassbreaker"; WAMOT with an attached outer covering.

Table 2.16 Specification of the robot

Items		Value
Size	Width mm	300
	Length mm	670
	Height mm	200
Weight kg		5.5
Velocity m/min		10
Capacity of battery Wh		47.7
Updime h		4
Wattage of motor W		15x2

2.6.8 Simulation and experiment

2.6.8.1 Simulation

The objective of the experiment was to verify the validity of the model of the "Grassbreaker". The model was verified through a kinetics simulation. Four types of mobile robots (Table 2.17) were prepared and determined which model could generate large forces against the grass.

Table 2.17 Characteristics of four types

	A	B (WAMOT)	C	D (Grassbreaker)
Shape	Cube	Cube	Ship	Ship
Mechanism	Wheel	Elliptic leg	Wheel	Elliptic leg

Fig. 2.43 shows the simulation conditions. Two 500 [mm] sticks were prepared as artificial grass with spring elements as a replacement for tall grass. The grass bends around the root in contact with the ground when it receives a force from the robot but tries to return to its original position. The grasses were arranged offset from the center of the robot by 50 mm in the y direction. These grasses were set to be inclined in proportion to the magnitude of the moment caused by the received force. Therefore, the author can determine the magnitude of the forces received by the grass from the robot by measuring the inclination of the grass:

$$\theta_x = f(F_x) \tag{2.29}$$

$$\theta_y = f(F_y) \tag{2.30}$$

where θ_x is the angle between the z axis and the vector projecting the grass on a y–z plane and θ_y is the angle between the z axis and the vector projecting the grass on a z–x plane (Fig. 10).

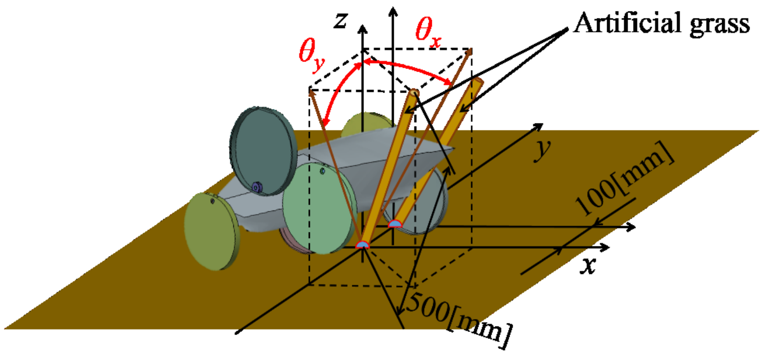

Figure 2.43 Simulation condition: Type D is shown on this figure

The robot was in contact with the grass before moving and tried to topple without run-up. The robots tried to continue forward while being pulled back from the grasses. Six trials were performed while changing the coefficient of friction in increments of 0.1 and measured the angle for 10 [s] at intervals of 25 [ms] in each trial.

Fig. 2.44 (a) shows the result of inclining the artificial grass in the x direction. The points daubed with diagonal lines represent the maximum inclination angle, and the points daubed all over show the average inclination angle. The average inclinations of the ship type (C and D) were larger than those of the cube type (A and B). The maximum inclination of type B was as large as that of the ship type. The elliptic legs allowed a large force to be generated instantaneously.

Fig. 2.44 (b) shows the result of inclining the artificial grass in the y direction. The average inclinations of the ship type (C and D) were as large as those in the x direction, while those of the cube type (A and B) were almost zero. This inclination increased the entire inclination of the grass. The maximum inclination of type D seemed larger than that of type C, although the average inclinations were almost the same. The elliptic legs again caused a large force to be generated instantaneously.

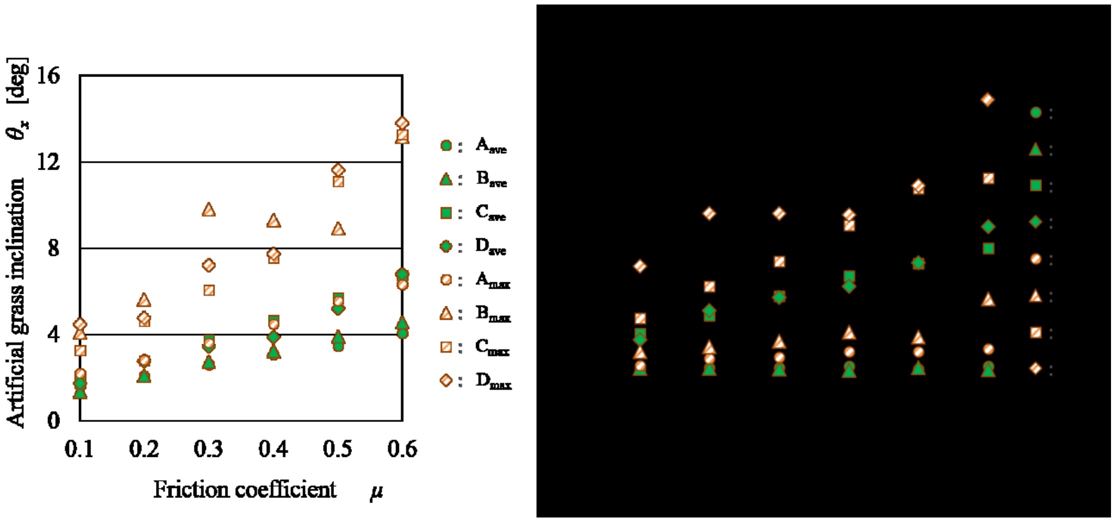

(a) *x* direction (b) *y* direction

Figure 2.44 Simulation result of artificial grass inclination

2.6.8.2 Demonstration experiment

The objective of the demonstration experiment was to verify the effectiveness of Grassbreaker. An experiment was carried out at a riverside area in Japan where many reeds that were 1–1.5 [m] tall were growing. A particular flat area was chosen and operated the robot at random points. The location was changed for each trial because each location was deformed after the robot moved over it. It was tested whether or not Grassbreaker and WAMOT could move 1.5 [m] forward in each area. In order to make the robots' weights equal, an equivalent weight to the outer covering was added to WAMOT. The locomotion time was measured for a robot to pass 150 [cm] forward. The robot was assumed to be immovable when the robot could not reach in 120 [s], and the travel distance was measured. The robot motion pattern was repeated only forwards for 120 [s] with the maximum power that the motors could generate.

Table 2.18 presents the experimental results. WAMOT could not move 1.5 m forward in 120 [s] in every six conditions. The reeds prevented the robot from moving forward with reaction forces in both the *x* and *z* directions. The robot would flip or become immobile with no more torque generated that could overcome the reaction force in the *x* direction. In the Grassbreaker test, although the robot could not move 1.5 [m] forward in 120 [s] in the first and fourth trials, the robot successfully moved forward two-thirds of the time. The two failures were caused by entangled reeds in the leg axis of the robot, and the robot became immobile with no more torque generated to overcome these tangled forces. Fig. 2.45 compares the average speeds of WAMOT and Grassbreaker. A t-test was performed to investigate the significant differences between the average speeds of WAMOT and Grassbreaker. The experimental results confirmed significant differences ($p < 0.05$) between the average speeds of WAMOT and Grassbreaker. Thus, it was concluded that the robot shape affects movement in a real tall grass environment such as reed beds.

Table 2.18 RESULTS OF DEMONSTRATION EXPERIMENT

Trial	WAMOT		Grassbreaker	
	Operating time [s]	Distance [cm]	Operating time [s]	Distance [cm]
1st	120	80	120	120
2nd	120	100	72	150
3rd	120	130	51	150
4th	120	50	120	50
5th	120	60	36	150
6th	120	90	39	150

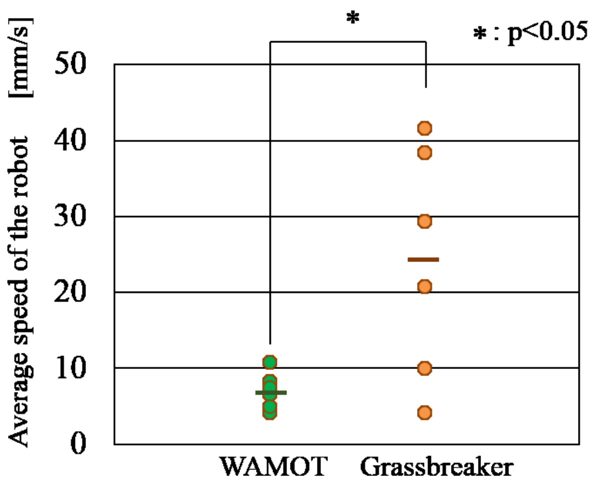

Figure 2.45 Average speeds of WAMOT and Grassbreaker.

2.6.9 Discussion

The robot shape helped increase the locomotion performance on a grass field. The simulation confirmed that the ship shape generates a larger force than cube shape. A larger force F_y is generated by the ship shape. F_x also becomes larger. This cases a large total moment to be generated against the grass. Therefore, the robot can move forward smoothly with an effective shape. It was confirmed this phenomenon in a demonstration experiment. The results showed that altering the robot shape is also a valid approach in a real environment. This presents a novel approach to increasing a robot locomotion. Until now, the design of the robot's cover has only focused on safety when the robot is in contact with humans. However, this method means that a cover is also useful for improving the locomotive performance and can lead to practical improvements for both indoor and outdoor movements. This method is significant not only because it fills a gap in terms of locomotive performance but also because it can reduce the number of actuators. This can reduce the cost and energy consumption and make it easy to maintain and control the robot. This is suited to our plan to monitor the environment by using multiple robots.

The pitching behavior of the elliptic mechanism leads to a high level of locomotive performance. The robot uses its own weight as an effective method to push through tall grass. By lifting the housing, the robot amplifies its momentum and push through the grass with a stronger force while slipping on a high-slip surface. The simulation confirmed that the elliptic mechanism generates a larger instantaneous force than the wheel mechanism. The maximum values of F_x and F_y were larger for the cube and ship shapes, respectively, with the elliptic leg type than with the wheel type. This instantaneous force may break the grass and make a path for the robot to move forward. This mechanism should be applicable for the robot to pass over other soft obstacles. In addition, previous studies proved that, by using a tiny mobile robot, the rolling behavior may also increase the locomotion performance. The effect of changing the robot posture, not only pitching behavior but also rolling behavior on the locomotion performance, is remarkable and may be useful to the motion control of the robot.

Optimization of the robot design such as detail parameters of the robot shape might be more effective to increase locomotion performance, although this paper only suggests the effectiveness of changing the robot shape. Also, analysis of the relationship between the specifications of the robot such as speed and the properties of grass might be more effective. However, there are some limitations in the proposed model because the grass model is so simple that this cannot describe the resistance from broken grass as well as an icebreaker model does. Detailed model might more contribute to increase the locomotion performance of the robot because the resistance is considered to be largely affected in real environment. This may also help in predicting the required energy to travel over grass fields.

Chapter 3: Control design

3.1 Chapter introduction

The control design of the robot is described in this chapter. The control design is one of the most important factors of having a high locomotion performance of the mobile robot. The design has a great influence on the locomotive itself and the ability to avoid obstacles and toward the destination.

The objective of this chapter is to describe methods of increasing the locomotion performance of a mobile robot from a software perspective and to verify its effect. The motion is modeled and expressed by mathematical expression to understand the effect, and the theory is verified by experiment using developed robots.

This chapter describes the control architecture of mobile robots for their autonomy in complex environments. For the autonomous navigation, the robot needs to sense the environment for understanding the condition, controlling their motion for adapting the environment, planning their path route for reaching the target area more efficiently and strategically. In this chapter, the author explains the control method of each element and show some experimental data using the method.

The author uses figures and sentences by referring the author's published papers in this chapter [3.1-8].

3.2 System design

3.2.1 Motivation for control design

Since various surfaces and obstacles are existing outdoors, how to deal with these by robot movement becomes important. A lot of studies have been conducted to control the mobile robot outdoors. However, there is a problem that the control design becomes complicated and the power consumption increases when considering incorporating complicated control. A lot of conventional methods use geometry sensors such as cameras and laser for controlling the robot, but these methods are not suitable for long-term use because it is difficult to cope with environmental changes and weather changes. For realizing long-term operation, a simple and robust control method is required.

The number of neurons is being considered to affect the complexity of the control upon reference to the control organisms Since mammals such as humans have a large number of neurons, a complicated processing can be performed, and information necessary for movement can be instantly judged. On the other hands, it is conceivable that insects such as a dung bean (see Fig. 3.1) with few neurons judge the situation from simple information and move.

Figure 3.1 Dung bean

Dung bean is acquiring surrounding information by tactile while they have a slight vision, they behave very simple such as moving to the right and left each time hitting the wall. When a dung bean gets in contact with an obstacle ahead, it takes an action to move in the right direction (Fig. 3.2). And, when the dung beetle comes in contact with the next obstacle, it moves in the opposite direction to the left.

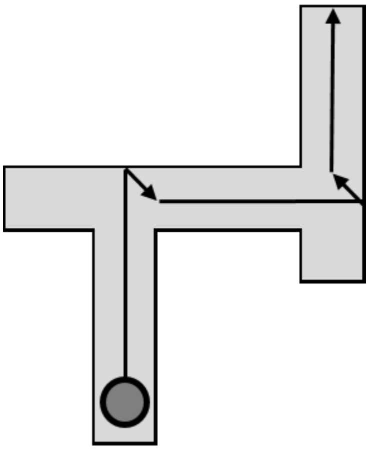

Figure 3.2 Alternative behavior of dung bean

This behavior seems so simple, but the dung bean could move in various environments. The author thought that simple task can be conducted inside of the robot and the complex tasks can be conducted outside the robot. Fig. 3.3 shows a concept of control design. By the robot having only a simple function, the design of the control becomes simple, and the energy consumption of the robot itself can be reduced. In addition, robust control that is hard to rely on the environment becomes possible.

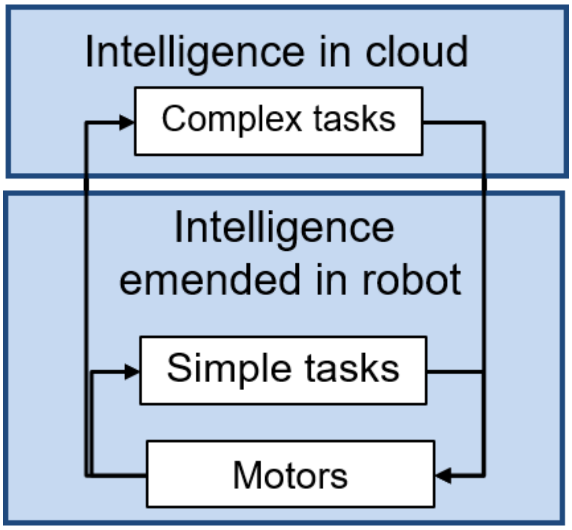

Figure 3.3 Consept design of control

3.2.2 System overall design

The control system is required for operating long-term outdoors, so it is desirable to use sensors that are less susceptible to external environment. And, it is also necessary to construct a system with low power consumption so that the robot can operate for a long time even a little. In addition, since it will be operated with multiple robots in the future, it is expected to reduce the product cost of each robot. Therefore, simple sensors are selected for controlling the robot and the control architecture is built to suit the purpose of reducing the respective calculation processing.

The control processing system is divided into two main parts. Simple processing is conducted in the processors on the robot and complex processing is conducted in the processors on a server that is located outside the robot. The calculation cost of the robot can be reduced by sending the locomotion data to an external server and making is calculating on the server.

Fig. 3.4 shows the overview image of the long-term goal of monitoring system using mobile robots. Each robot moves autonomously by recognizing the surface condition and controlling the motion. The locomotion data and monitoring data are uploaded to the server, and the locomotion data are analyzed for generating an optimal path plan for navigating the robot to the destination.

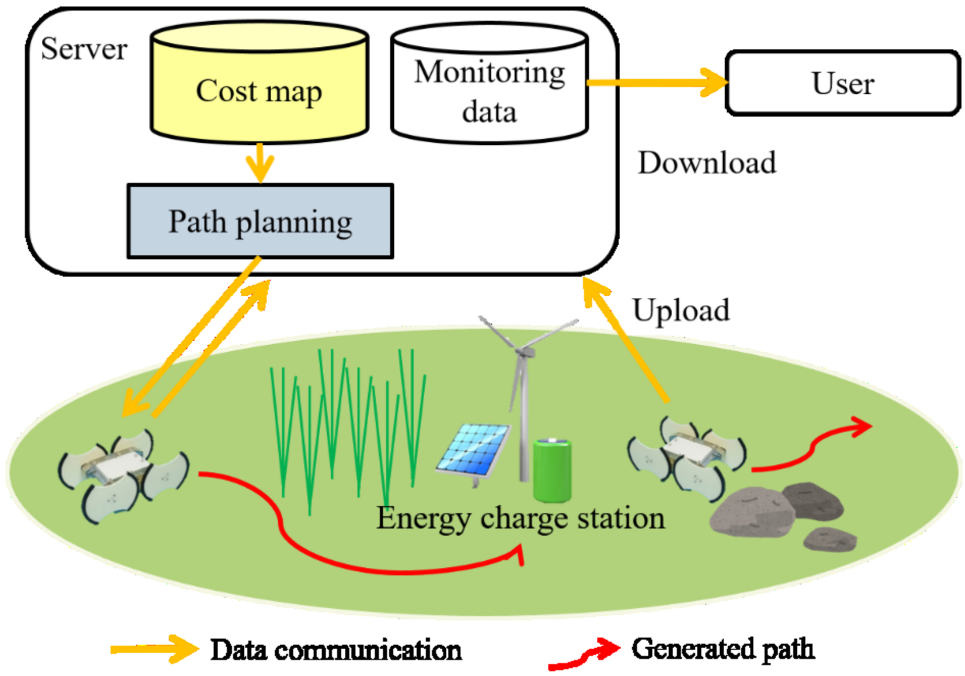

Figure 3.4 Long-term goal of our monitoring system.

3.2.3 Selecting simple sensors and processors

Sensors are selected for controlling the mobile robot. The sensor is used to know the information of the outside world when the robot moves, and it is also used to know the situation of the movement of the robot.

A lot of studies on sensor's processing have been conducted for many years. The robot recognizes various situations from the information obtained by the sensors and determines the next motion of the robot. With the remarkable development of science and technology in recent years, sensors and processors for mounting on robots are becoming smaller and higher performance, and many modules that can be mounted on small robots are sold.

A lot of mobile robots use geometry sensors such as range finders (LRF) [3.9] and cameras [3.10] for recognizing the surface environment. These sensors are effective to understand the shape of the terrain environment precisely so that the robot can recognize their positional relationship with surrounding obstacles and avoid the obstacles. In the methods using the laser range finder, open source such as using point cloud has been recently provided and many researchers easily can use it, thought complicated calculation processing is required and development cost is required. The methods using the camera also be available by using open source code in middleware such as Robot Operating System (ROS). However, in a complex outdoor environment, there are few robust methods to cope with environmental changes. Therefore, the author tried to install internal sensors on an autonomous mobile robot as sensors less susceptible to environmental changes and lower power consumption.

Table 3.1 shows sensor system comparison. Internal sensors have a lot of advantages in terms of power consumption, computational cost, product cost, weather effects, and difficulty in outdoor use. However, the accuracy of environmental recognition becomes low compared to the method using geometry sensor.

Table 3.1 Sensor system comparison

	Internal sensors	Geometry sensors
Power consumption	Low	High
Computational cost	Low	High
Product cost	Low	High
Weather effects	Low	High
Difficulty in outdoor use	Easy	Difficult
Accuracy of environment recognition	Low	High

Since the environmental recognition becomes lower, it is necessary to combine various algorithms to construct a control that can cope with a complicated environment. The author considered the robot to have high moving performance by combining various simple sensors.

Fig. 3.5 shows a system overview of developed robot. By giving the robot internal functions such as surface estimator and motion control, the robot can move while recognizing the surface condition. And, the cost generation and path planner which are computationally expensive, are located on the server for reducing the computational load on the robot.

Environment data measured by the robot are uploaded to the cloud storage via a smartphone. By using the existing cloud storage, it is advantageous that multiple users can easily access the environmental data at the same time, and it is not necessary to manage the server individually.

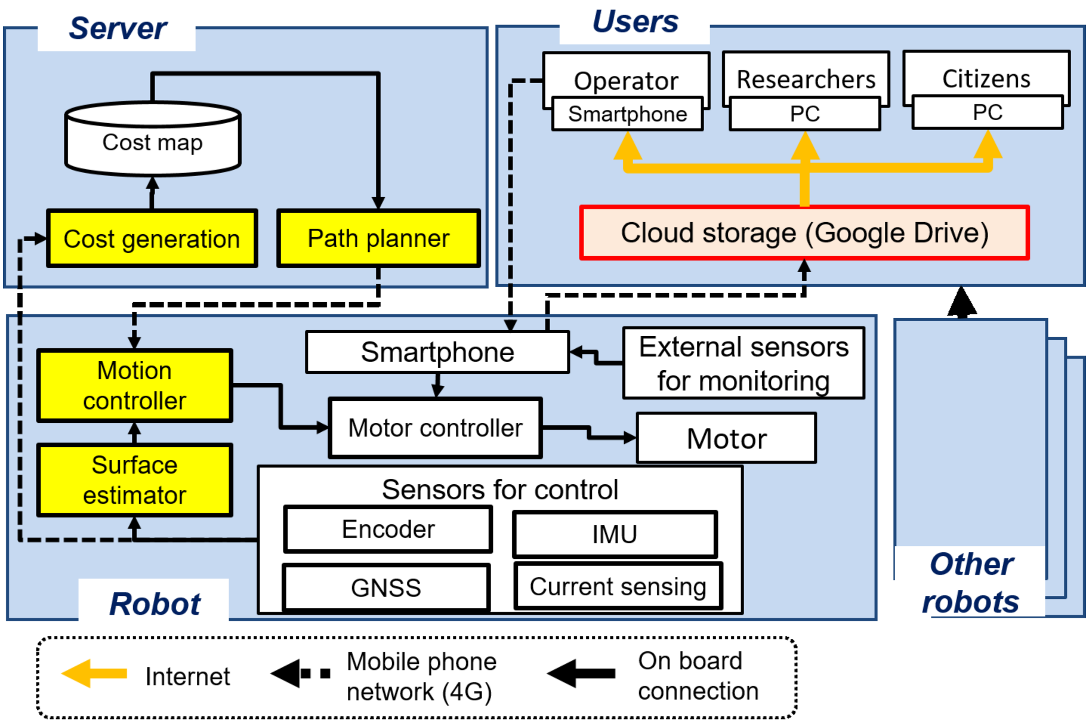

Figure 3.5 System overview

3.3 Environmental recognition

3.3.1 Section introduction

Environment recognition is one of the most important topics to enable a mobile robot to move on rough terrain. In a highly uncertain natural environment, the acquisition of information about its surroundings is the key to allow a robot to pass through them. A robot can recognize an obstacle and generate a way past it by navigation and localization using this information. By using this effective method, the robot can move under difficult conditions such as a natural environment.

Several studies have been conducted on environment recognition using laser range finders or cameras [3.9-12]. By using this tool, a robot can recognize its own position or surroundings using some calculations such as simultaneous localization and mapping (SLAM). This method is very popular and effective at avoiding dangerous areas that can recognize visually. However, the robot cannot recognize other dangerous areas such as swamps where robots can become immovable because of the slipperiness or softness of the surface, which the robot cannot detect using visual information.

Surface conditions can affect the locomotion performance of mobile robots. For example, a robot can slip on a slippery surface such as sand or ice [3.13,14]. Since the travel distance of the robot changes on such a surface, localization becomes difficult using a calculation of wheel rotational speed. The hardness of a surface also affects the posture of robots such as humanoid robots [3.15]. The robot has to consider such problems with soft surfaces. Unevenness also affects the stability of a robot [3.16]. A tiny mobile robot can easily turn over on an uneven surface. On such a surface, a mobile robot should slow down to avoid an immovable condition. Recognizing the surface condition in greater detail that can be acquired from visual information will allow a robot to avoid an immovable condition or change its control to suit the surface condition.

The objective of the current work is to design a model for estimating the surface condition using a tiny mobile robot.

3.3.2 Estimating surface condition

3.3.2.1 Classification of surface

The important parameter of road condition is considered. According to the Handbook of robotics [3.17] published in Japan, the environment for robot can be roughly divided into four categories: Space, gas, liquid, and solid. Fig. 3.6 shows a major classification of mobile environment of robot. The road surface condition handled in this research is called a solid surface at the boundary between gas and solid.

[redacted]

Figure 3.6 A major classification of mobile environment of robot

Fig. 3.7 shows the classification of solid surface. According to the robot engineering handbook, the solid surface can be further classified. The target fields of this research are classified as ground and floor, since the robot moves under the condition that it is subject to surface constraints on two dimensions and the robot does not move on the wall and ceiling surface. Especially the environment such as the forest is uneven and there is no geometric regularity. Therefore, it is positioned as an irregular surface.

[redacted]

Figure 3.7 Classification of solid surface

This classification classifies the situation of the surface geometrically, and it is thought that irregularities are one important factor in the target environment. For example, it is difficult for a robot with a small wheel radius to move on a gravel surface with large irregularities such as a riverbed where stones are spread, though it is possible to move on a surface paved with concrete with little unevenness. It is difficult for a large-sized robot such as biped robots to balance well and walk stable on the uneven condition. Therefore, unevenness of the surface is determined as the one of the important parameters of surface.

Considering the mechanical model of the robot and the surface, force exchanges at this boundary surface because the locomotion mechanism of the robot and the surface are in contact with each other. The robot receives a reaction force from the surface and it can be divided into a normal force in the vertical direction and a friction in the horizontal direction. Mechanical property of material of two contacting objects has a great influence on the movement of the robot after the contacting.

Regarding the friction, the friction coefficient is determined by the compatibility between the locomotion mechanism and the surface. When the surface changes, the coefficient of friction changes accordingly. Friction is very important as an element for generating a driving force in the mobile robot. The magnitude of the coefficient of friction affects whether or not the robot slides on the surface and gives a great change to the locomotion performance. Therefore, the slipperiness of the surface is determined as the one of the important parameters of surface.

Regarding the normal force from the surface, deformation of materials gives a big factor. For example, when a biped walking robot travels on a soft road surface, the force received from the ground changes and the balance is lost. In the case of a small mobile robot, the locomotion performance also changes depending on the hardness of the surface. Therefore, the hardness of the surface is determined as the one of the important parameters of surface.

Fig. 3.8 shows important factors on rough terrain. These three parameters are also used in research on biped robot locomotion [3.18] and have studied.

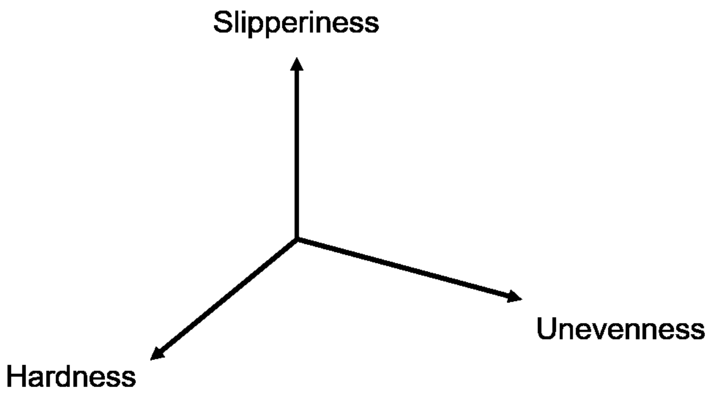

Figure 3.8 Important factors on rough terrain

Slipperiness has been thoroughly investigated in terra-mechanics [3.19,21], where mechanical analyses have been performed on the mutual relationships between wheels and soil. Yoshida and Nagatani in Tohoku University conducted a study on the slipperiness and applied the results to the Mars rover wheel as a planetary exploration robot [3.22]. Their surface model was effective for a mobile robot. However, other surface condition parameters such as hardness and unevenness have not been effectively considered in this field.

Kang et al. proposed softness for determining surface hardness conditions. She formulated an algorithm for controlling a humanoid robot on a multitude of surface patterns [3.23]. In this research, force sensors were used to recognize the softness of the surface. However, this method cannot be applied to small mobile robots because the size of the force sensor is too large. Hasimoto et al. used WS-5 (Waseda Shoes - No.5) to overcome an uneven surface, but solutions in hardware does not fit for tiny mobile robots because the relative size ratio of the uneven surface and robots is different.

In short, a method to measure the degree of roughness and hardness of the surface using a small robot has not been established. Therefore, the authors examined the possibility of estimating these two parameters using the internal sensor.

3.3.2.2 Hardness of surface

Hardness is one of the most important parameters of a surface. Control becomes difficult on a soft surface for a humanoid robot, and the impact becomes large on a hard surface when a robot falls. Recognizing hardness may make it possible to prevent getting stuck in a swamp or could be used to classify an environment.

Kang measured this parameter using 6-axis force sensors on the foot of a humanoid robot and measured the reaction force from the surface [3.18]. However, a small mobile robot like WAMOT cannot use this method because of the size limitation. Therefore, another method is desired to determine the hardness of a surface.

The motor current was focused, which is related to the reaction force. When the reaction force become high, the motor current also becomes higher. In particular, WAMOT behaves with a pitting motion at regular intervals during the coordinated phase mode, and WAMOT receives a large reaction force from the surface when the robot taps the surface.

Fig. 3.9 shows the simple model used for the hardness estimation. The Kelvin–Voigt model is used for representing the hardness of the surface, it can be represented by a spring and damper in parallel.

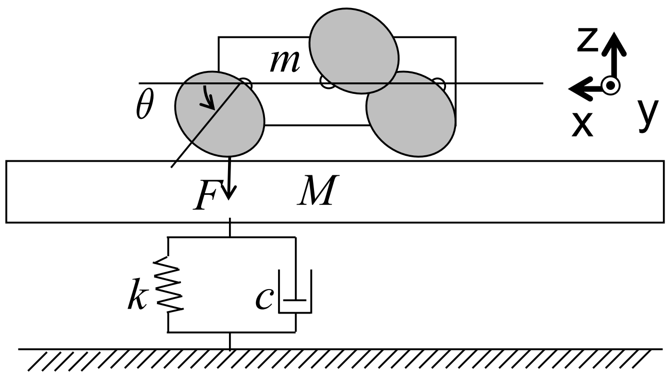

Figure 3.9 Model used for hardness estimation

Assuming that the surface has mass, the motion equation of the surface is expressed by the following.

$$F = M\ddot{z} + c\dot{z} + kz \tag{3.1}$$

where F is the force from the robot, M is the mass of the surface, and z is the displacement of the surface in the vertical direction, c is a viscosity coefficient, and k is elastic coefficient.

Fig. 3.10 shows a torque applied to the front side motor when the elastic coefficient is changed. The simple simulation is conducted using hardness model and the tendency of torque during robot movement is examined. In this simulation, elliptic legs are used and the phase difference between the left and right motors is set to be 0. One master motor is controlled by speed control and the other slave motor is controlled by position control with reference to the master motor.

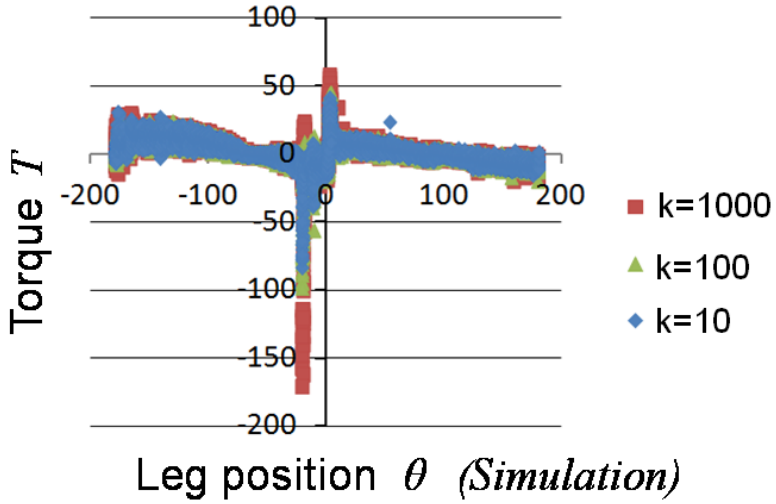

Figure 3.10 Torque applied to the motor when the elastic coefficient is changed

Around the locomotion phase is -25 [deg], the torque takes a large negative value, and takes the local maximum value immediately after that. It can be seen from the graph that this local maximum value takes a larger value than the torque curve due to the shape of the ellipse, while the author does not know the reason for this large negative value in simulation. In this phase, the front leg is struck against the floor from the state where the robot is greatly inclined in the pitch direction. The sudden force from this ground is applied in the direction opposite to the direction of rotation of the leg and temporarily works to stop the rotation of the legs. Since the master motor is controlled by peed control, the robot tries to rotate the leg at a constant speed. In order to withstand the sudden force and maintain the speed, the motor controller is considered to temporarily flow a large current. It is considered that this current increase as the impact increases; the hardness of the road surface can be measured if the current can be measured.

Fig. 3.11 shows the motor current of WAMOT during the coordinated phase mode between phase π and 2π when the robot moves across the flat floor of the laboratory. At the moment of the robot taps the surface, the current peaks. The reaction force of the robot changes when the elastic coefficient and viscosity coefficient values change because the mechanical energy of the system becomes smaller as a result of the damping. Assuming the force from the robot does not change when the surface hardness changes, this change is largely depending of the elastic coefficient and viscosity coefficient values.

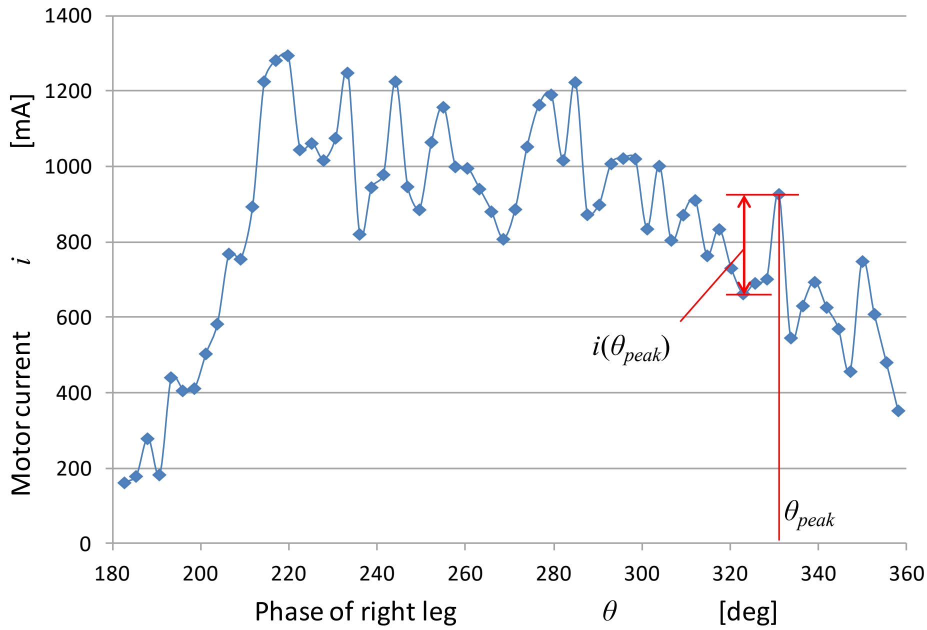

Figure 3.11 Current of motor in coordinated phase mode

Based on the value of the maximum current for the motor controller (i_{max}), the hardness is determined as follows using the percentage of the peak.

$$H = \frac{i(\theta_{peak})}{i_{\max}} \tag{3.2}$$

The current peak is defined as the maximum difference between the local minimum value and local maximum value. Fig. 3.11 also shows the point where current peak and how to measure the current peak value of this point.

3.2.2.3 Unevenness of surface

Unevenness is also one of the most important parameters of a surface. Control become difficult on uneven surfaces for any robot. Especially for small mobile robots like WAMOT, the robot can easily turn over and become immovable because even small steps become relatively large obstacles. Recognizing unevenness may make it possible to prevent a robot from overturning on uneven terrain and could be used to classify an environment.

Almost all of the previous studies used robot posture only for instantaneous control. It is also important to prevent an immovable condition. Recognizing the surface condition would make it possible to select the optimal motion pattern.

Since the unevenness of the surface affects the instability of the robot, the robot measures its inclination degree per unit of time. WAMOT become stable during the leg phase from 0 to π in a flat area. Fig. 3.12 shows the model for the unevenness estimation.

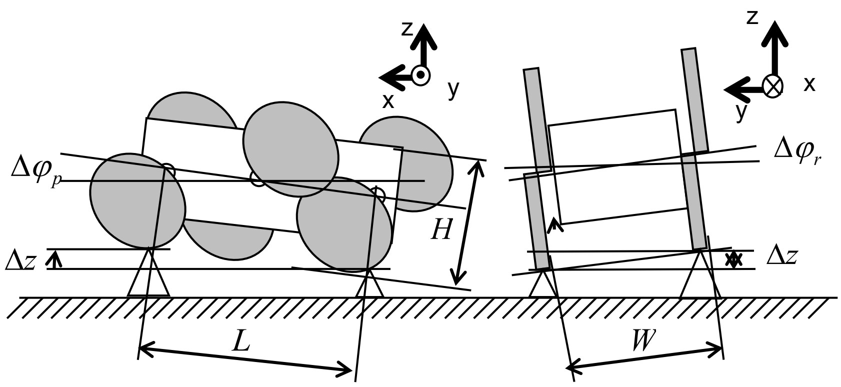

Figure 3.12 Model used for unevenness estimation

In the coordinated phase mode or opposite phase mode, the unevenness is determined based on the inclination degree of the robot. The unevenness is determined as follows.

$$U = \frac{\int_0^{\pi} (L \,|\sin\varphi_p(\theta)| + W \,|\sin\varphi_r(\theta)|)d\theta}{\pi\sqrt{L^2 + W^2 + H^2}} \tag{3.3}$$

where, L is the length the robot, W is the width of the robot, H is the height of the robot, φ_p is the pitch angle of rotation, and φ_r is the roll angle of rotation.

3.3.3 Verification

3.3.3.1 Validity of model

The objective of this experiment was to verify the validity of the model of the surface condition. The hardness and unevenness formula were used to measure the surface condition parameter in five places: the flat floor of the laboratory, urethane sponge, cement ground, uneven terrain of an urban park, and grassland in the urban park. The robot moved on each surface for 30 [s] in the coordinated phase mode, and 10 trials were performed on each surface.

Fig. 3.13 (a) shows the estimated hardness, and Fig. 3.13 (b) shows the estimated unevenness of each surface. The bar chart shows the average hardness, as well as the maximum and minimum values from the 10 trials. A t-test was done to investigate the significant difference for each surface, and bonferroni correction was used to counteract the problem of multiple comparisons.

In terms of the hardness, significant differences between the flat floor in the laboratory and the urethane sponge and between the urethane sponge and the cement ground are shown. However, there is no significant difference between the other surfaces, especially outdoors.

In terms of unevenness, significant differences between the grassland in the urban park and three of the other surfaces (the flat floor in the laboratory, urethane sponge, and cement ground) are shown. Unfortunately, there is no significant difference between the uneven terrain and the other surfaces because of insufficient data. This is because there were many flat portions in the uneven terrain of the urban park, and the robot was parallel to the ground for several seconds when it climbed over a step.

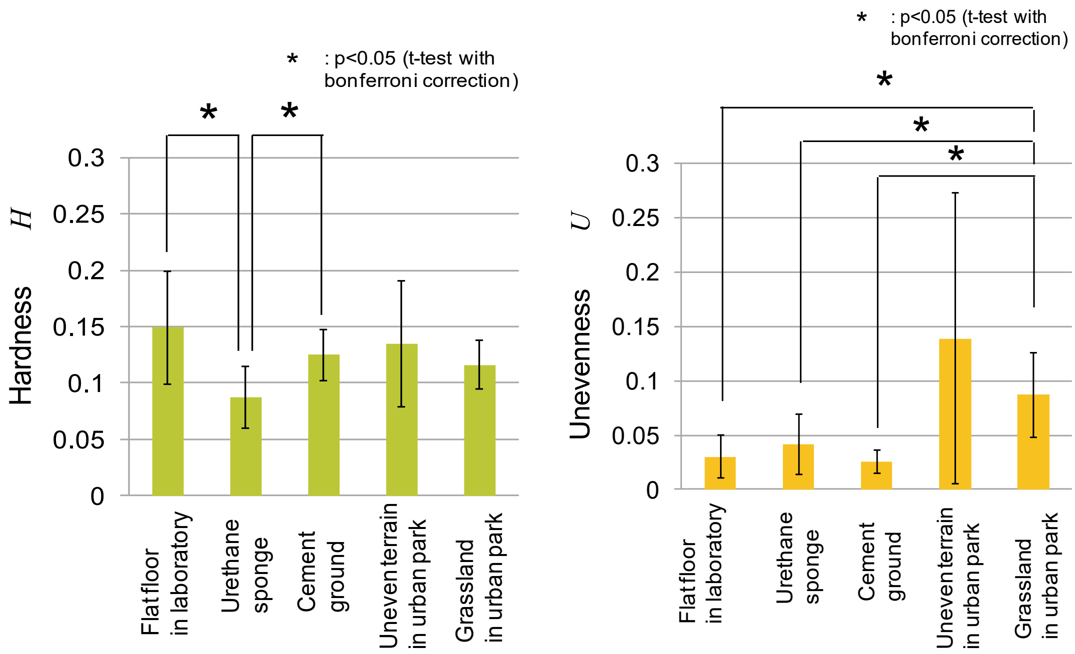

(a) Estimated hardness (b) Estimated unevenness

Figure 3.13 Hardness and unevenness of variety of surfaces

3.3.3.2 Demonstration experiment

The objective of this experiment was to control the robot motion using the proposed model. Two demonstration experiments were conducted in the laboratory.

The first experiment was to determine whether the robot could avoid a soft surface for preventing an immovable condition like being stuck in a swamp. A hard surface made of wood and a soft surface made of urethane sponge were prepared. The robot moved on the hard surface for 1 [m], which allows it to measure the hardness one time. It then entered the area with the soft surface. On the soft surface, the robot could move for 2 [m] and measured the hardness three times. The threshold of hardness was set at 0.08, which was the average hardness of the urethane, and did not overlap the hard surface. When the hardness was below the threshold, the robot was programmed to move backward to avoid the soft surface.

Success was defined as the case where the robot successfully moved backward during its movement on the soft surface. When the robot crossed the soft surface or turned back on a hard surface, the case was determined to be unsuccessful. 10 trials were conducted using two patterns: without and with the surface estimation program.

Fig. 3.14 shows the appearance of the experiment with surface estimation program. Whereas the success rate was 0% without the program, it was 80% with the program. Two failures were caused by the robot passing across the soft surface.

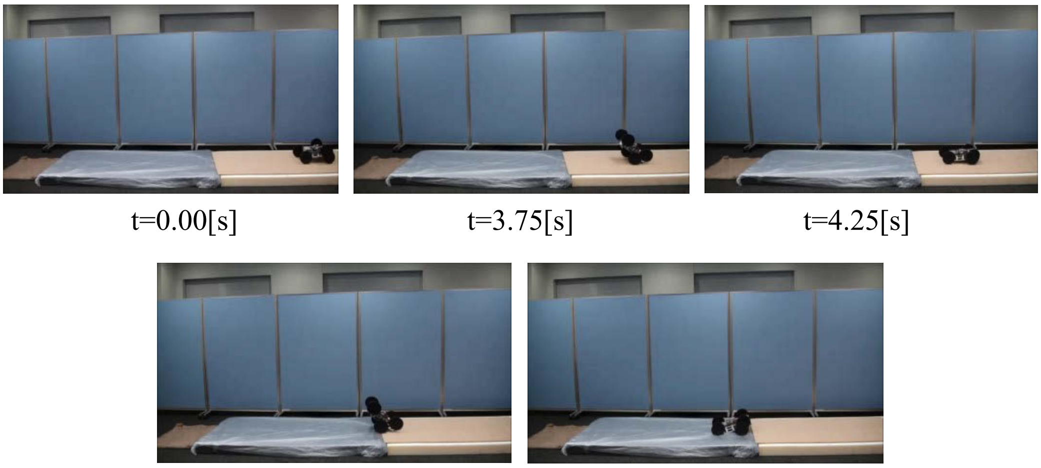

t=0.00[s] t=3.75[s] t=4.25[s]

t=8.75[s] t=9.25[s]

Figure 3.14 Demonstration experiment 1 (With program)

The second experiment was conducted to determine whether the robot could climb over large obstacles. A 1 × 2 [m^2] obstacle area was created by stacking numerous 2-L water bottles. To prevent the robot from slipping on these bottles, the bottles were covered with cloth to form a hill. The top of this hill was about 220 [mm] high, and the robot could not climb this hill in the opposite phase mode at high speed.

The robot's movements were compared between with and without the program. The robot started in the opposite phase mode at high speed. With the program, the robot was programmed to change to the coordinated phase mode and low speed when it recognized uneven terrain, which tended to allow it to climb better than in the opposite phase mode at high speed.

Success was defined as the case where the robot successfully climbed the obstacle. A case where the robot turned over or became stuck and could not pass through in 1 [min] was determined to be unsuccessful. 10 trials were conducted using two patterns: without and with the surface estimation program.

Fig. 3.15 (a) shows the appearance of the experiment without the surface estimation program and Fig. 3.15 (b) shows with the surface estimation program. Whereas the success rate was 0% without the program because of the turnover problem, it was 80% with the program. Two failures were caused by the robot turning over even though it recognized the high unevenness.

t=0.00[s] t=4.00[s] t=7.00[s]

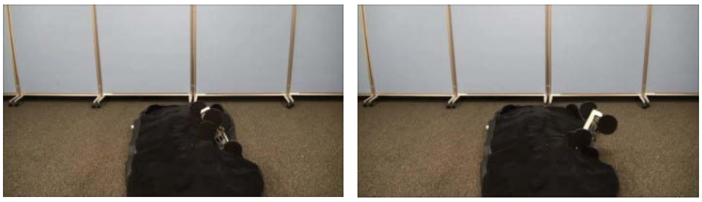

t=9.00[s] t=9.80[s]

(a) Without program

t=0.00[s] t=4.00[s] t=6.00[s]

t=7.00[s] t=10.00[s] t=12.00[s]



t=15.00[s] t=19.00[s] t=25.00[s]

t=30.00[s]

(b) With program

Figure 3.15 Demonstration experiment 2 (With program)

3.3.4 Discussion

The hardness estimation of a surface using sensor data was successful at differentiating between a soft surface like urethane and a hard surface like cement ground. Recognizing these differences is difficult for small mobile robots using the previous study methods. Using this method, the robot could avoid an immovable condition because of soft ground like a swamp, which has not been effectively considered in previous research. However, this method does not work well outdoors. There are two possible factors. One is because the robot posture is not parallel to the ground, which affects the robot's current and changes the peak point of the phase. The other is due to hardware factors. The author used a belt to transmit the force from the motor to a leg and a gear to increase the torque by 690 times, which reduced the instantaneous force. Because of this, the peak current became weak. Therefore, the peak current was not significantly different from the noise. To solve this problem, the robot should use a lower gear rate motor, and the motor should be directly connected to the leg.

The estimation of the unevenness of the surface using sensor data was successful at differentiating between an uneven surface like the grassland in an urban park and other flat areas. This method was useful for selecting the robot speed or motion pattern. Until now, robot posture has only been used instantaneously to prevent turnovers, and not for selecting robot control parameters. Introducing the surface condition idea contributes to a new way of thinking about robot control. More consideration needs to be given to the measured range of unevenness because no significant difference was found between the uneven terrain in an urban park and other surfaces.

The unevenness should be determined using more data such as the average of three rotations. Although this algorithm makes the difference clearer than before, it is not appropriate for instantaneous risk aversion. To use the surface condition estimation more effectively, it is required to use this parameter combined with instantaneous robot control.

This method is significant in terms of proposing a new approach for recognizing environment. Information from cameras or laser range finders, which is conventional ways to recognize environment, is tough to recognize the surface condition. This method can provide more detail environmental information to the robot, it can become a clue for overcoming complicated field. This method is also significant not only because it fills gaps in the previous research, but also because it does not require any special sensors such as a laser range finder and does not consume a large quantity of energy. Therefore, it achieves a core objective of our environmental monitoring system using multiple mobile robot.

3.4 Motion control

3.4.1 Section introduction

Motion control is also one of the most important topics to enable a mobile robot to move on rough terrain. For the autonomous movement of the robot, it is necessary to decide the next action by using the information which recognized the surface condition.

As explained by the concept of the control design, control method using internal sensors is studied. In order to cope with complex environments, the structure of the Subsumption Architecture [3.24] is used. The concept of architecture is that it can exert advanced functions by combining it even if the capability of each function is low. By using this concept, simple sensors can be used for each sensor, and a control algorithm that can operate even in complicated environments can be constructed

Conventional control algorithms using Subsumption Architecture such as [3.25,26] are only focused on the control for obstacle avoidance and path planning. However, when considering the actual operation of the robot outdoors, it may become immovable due to the influence of obstacles, and it is necessary to consider these problems.

The author proposes an autonomous motion control algorithm by focusing on solving a problem that the robot becomes immovable condition such as stacking and flipping occurring in the real environment.

3.4.2 Autonomous motion control algorithm

An effective autonomous motion control algorithm is composed by combining multiple sensors using the concept of Subsumption Architecture. Fig. 3.16 is a conceptual diagram of the developed autonomous motion control algorithm.

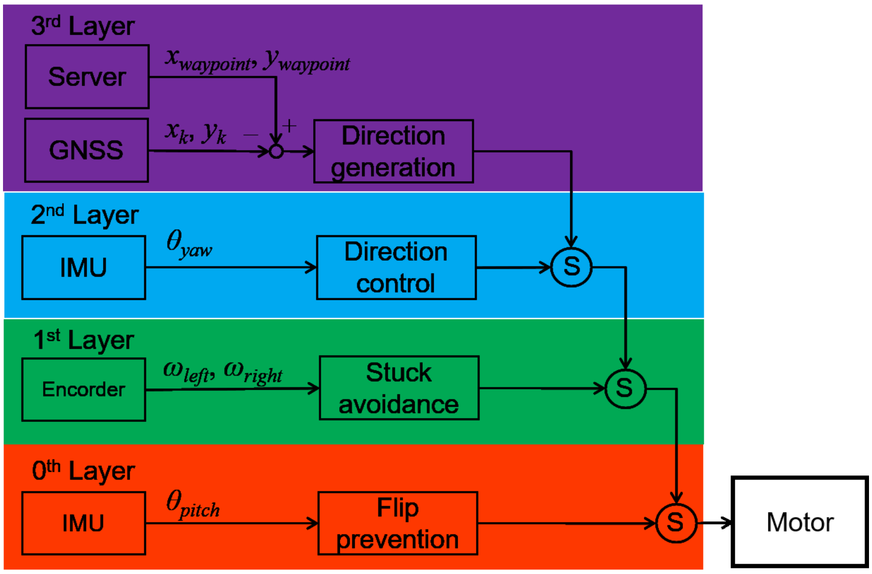

Figure 3.16 Conceptual diagram of autonomous motion control algorithm

At lower layers, flip prevention and stuck avoidance programs are performed, and the robot avoids immovable conditions. These layers are arranged in the most fundamental part of the control and are preferentially processed. At higher layers, direction generation and direction control programs are performed for navigating the robot to the destination.

Only the minimum necessary elements are embedded for these controls. Even if communication with the server is interrupted, the robot can continue to move automatically to the given destination. However, since these basic movements cannot move efficiently, further calculations are required for efficient movement. This will be explained in the next section.

3.4.2.1 0th layer: Flip prevention

For the flip-prevention program, the robot measures its pitch angle θ_{pitch} every 20 [ms] (Figure 3.17).

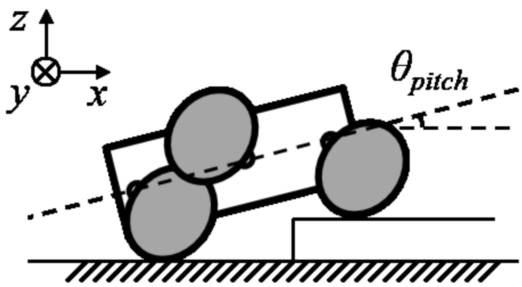

Figure 3.17 A situation where the robot is likely to flip

$$\theta_{pitch} = \arctan(\frac{G_x}{G_z}) \tag{3.4}$$

where G_x, G_z are acceleration in x, z direction.

When the housing of the robot is inclined up or down by more than 30°, the robot backs up and attempts to avoid this situation. Fig. 3.18 shows the flip prevention program.

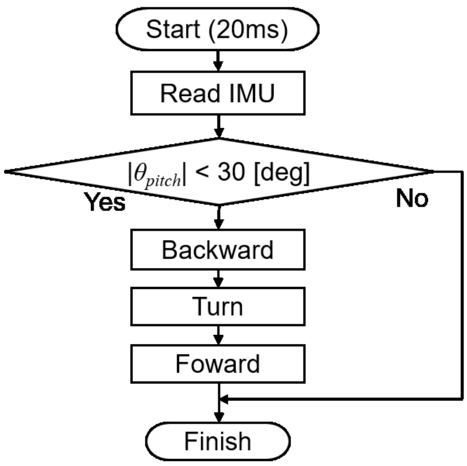

Figure 3.18 Flip prevention program

3.4.2.2 1st layer: Stuck avoidance

In the stack avoidance program, the robot measures the motor's rotational speeds ω every 20 [ms].

When the rotational speed falls below 1 [rpm] in any 200 [ms] period, the robot again backs up in an attempt to avoid this situation. The robot can avoid becoming disabled by implementing this program. Fig. 3.19 shows the stuck avoidance program.

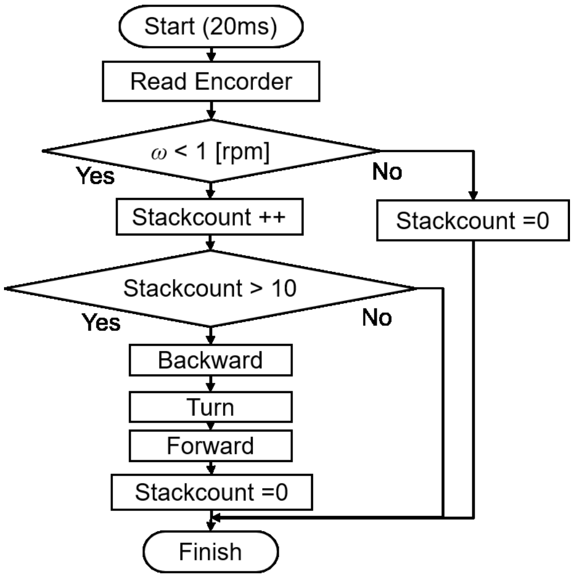

Figure 3.19 Stack avoidance program

3.4.2.3 2nd layer: Direction control

The robot moves while correcting its heading by calculating its heading θ_{yaw} and the direction to the via point θ_{dir} until the distance to the next waypoint d become certain distance. These angles and distances were determined based on data determined from preliminary experiments in the target area. Fig. 3.20 shows the relationship between parameters and robot.

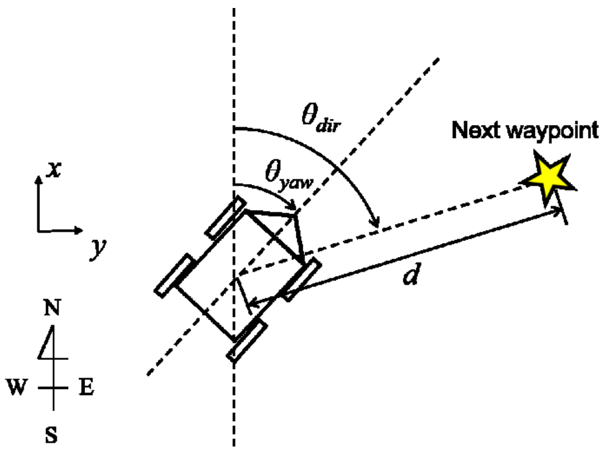

Figure 3.20 Relationship between parameters and robot

The direction to the via point θ_{dir} is calculated as follows;

$$\theta_{dir} = \arctan(\frac{X}{Y}) \tag{3.5}$$

$$X = (x_1 - x_2) \cdot \frac{a \cdot \cos(\frac{y_1 + y_2}{2})}{\sqrt{1 - e^2 \cdot \sin^2(\frac{y_1 + y_2}{2})}} \tag{3.6}$$

$$Y = (y_1 - y_2) \cdot \frac{a(1 - e^2)}{\sqrt[\frac{3}{2}]{1 - e^2 \cdot \sin^2(\frac{y_1 + y_2}{2})}} \tag{3.7}$$

where x_1 and y_1 are the longitude and latitude of the via point and x_2 and y_2 are the longitude and latitude of the robot point, respectively; a is the equatorial radius, and e is the major eccentricity.

Fig. 3.21 shows the directional control program. In the turning control, feedback control by θ_{yaw} is not used. Forward and turning time is fixed. This is based on an experimental knowledge that the noise taking on the IMU while the robot operates is taken into consideration and the risk being immovable condition can be reduced by using rough control rather than the delicate control outdoors.

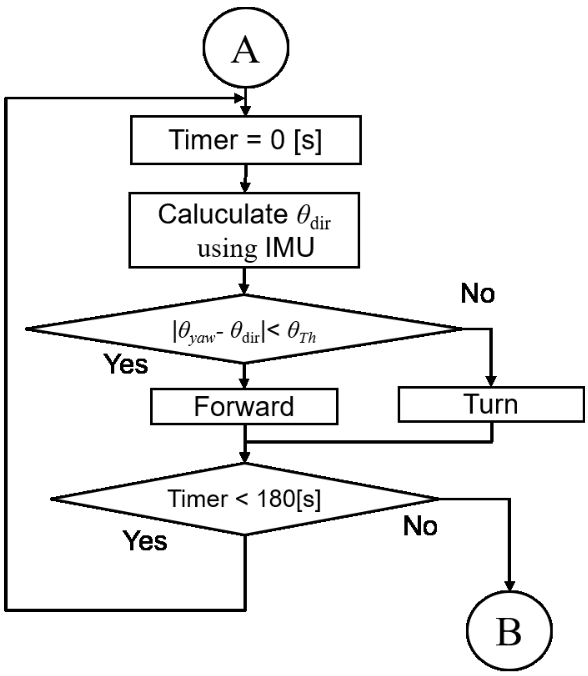

Figure 3.21 Directinal control program

In addition, the IMU is equipped with a geomagnetic sensor and an acceleration sensor. By integrating these sensor information, it is calculated so as to enable accurate direction control even if the posture changes. The relational expression for deriving the direction θ_{yaw} is shown below.

$$\tan\varphi = \frac{-G_y}{G_y \sin\theta + G_z \cos\theta} \tag{3.8}$$

$$\tan\theta_{yaw} = \frac{B_z \sin\theta - B_y \cos\theta}{B_x \cos\theta + B_y \sin\varphi \sin\theta + B_z \sin\varphi \cos\theta} \tag{3.9}$$

where G_x, G_y, G_z are acceleration in x, y, z direction, B_x, B_y, B_z are geomagnetism in x, y, z axis direction, θ is the polar angle in a spherical coordinate system and φ is azimuth angle in the spherical coordinate system.

3.4.2.4 3rd layer: Direction generation

The robot estimates its own position using GNSS and moves toward each waypoint. The robot calculates the relationship between the robot and waypoints and decide the next motion. The robot decides whether it has reached the waypoints when it enters an area with a radius of 6 [m] from the waypoints. This threshold is considered the accuracy of GPS that was used in experiment in natural forest in Shizuoka, and it is better to use even smaller values when using better GNSS.

The distance to the waypoint d is calculated as follows;

$$d = \sqrt{X^2 + Y^2} \tag{3.10}$$

Fig. 3.22 shows a flowchart of direction generation program. The robot moves while changing the waypoint one after another until it reaches the goal.

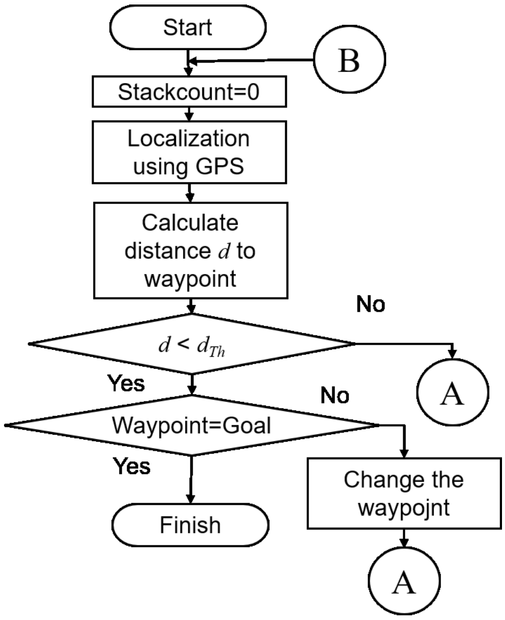

Figure 3.22 Direction generation program

3.4.3 Verification

3.4.3.1 Performance test in mock forest

The objective of the experiment was to confirm the performance of the proposed motion control in a mock forest. The experiment was conducted in the Tanashi forest in Japan (Fig. 3.23), where many trees exist, and the field size as 14x14 [m^2] are divided into 48 grids (each grid size is 2x2 [m^2]). In this experiment, GNSS (EVK-7P, ublox) was implemented on WAMOT as a position sensor.

Figure 3.23 Tanashi Forest (The University of Tokyo)

GNSS data of each grid were transmitted to the robot before the operation, and it was confirmed whether or not the robot could move. The path route was decided according to a sequence map and WAMOT starts from grid 0 and moves until the 48th grid. Fig. 3.24 shows a locomotive sequence map.

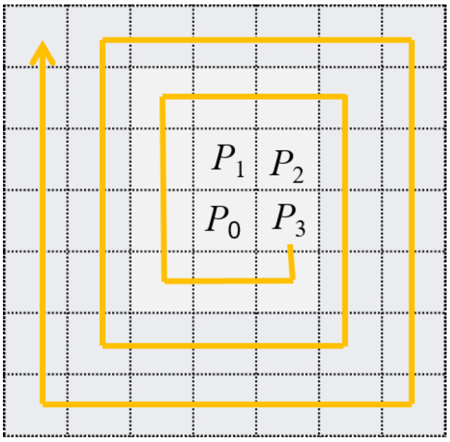

Figure 3.24 Locomotive sequence map. P_0 is the starting grid that was assumed to be the charging station.

Fig. 3.25 shows the WAMOT during the control test. Sensors for motion control and notched wheel are mounted on the robot.

Figure 3.25 WAMOT during the control test in mock forest in Tokyo

Fig. 3.26 shows the trajectory of the robot from GNSS data. The robot sequentially passed through the given 48 points and moved in total for 67 [min].

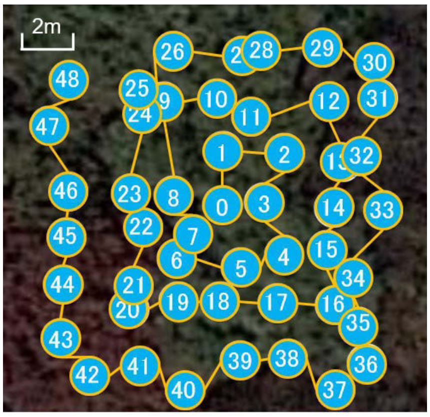

Figure 3.26 Trajectory of the robot from GNSS data.

3.4.3.2 Performance test in natural forest

The performance test was also conducted in natural forest. The experiment was conducted in the natural forest on Mount Fuji in Shizuoka, Japan, where many trees, grasses and slopes are existing. The field size as 60x100 [m^2] are divided into 60 grids (each grid size is 10x10 [m^2]). In this experiment, GPS (GMS6-CR6, CanMore Electronics) was implemented on WAMOT as a position sensor. The position data of two waypoints on the path were also transmitted to the robot before the operation.

Fig. 3.27 shows the WAMOT during the control test. Sensors for motion control and notched wheel are mounted on the robot.

Figure 3.27 WAMOT during the control test in Mt. Fuji in Shizuoka

The robot was operated autonomously using proposed motion control algorithms. The trajectory of the robot is shown in Fig. 3.27. The robot moved 50 [m] on rough terrain and could reach to the goal in 21 [min] thought the environment was very complicated and robots have avoided obstacles many times.

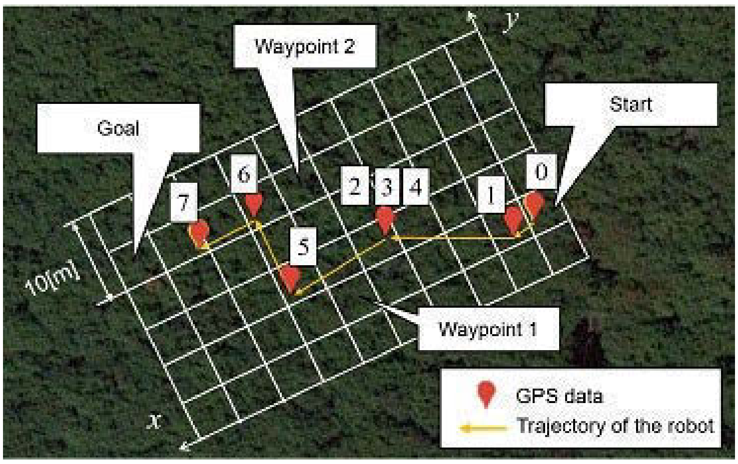

Figure 3.27 Trajectory of the robot

3.4.4 Discussion

The robot was able to move through a complicated environment using the internal sensor. And, it was confirmed that it can move with almost the same control in two different environments. In the method proposed this time, it is almost unnecessary to adjust the parameters according to the environment, although it is necessary to adjust the sensor processing and threshold value every time depending on the environment, weather and time in the method using cameras and lasers. Also, the robot operated normally even in complex environments like forests using the proposed control algorithm although obstacles such as bamboo become noise of the sensor, and it is conceivable that the robot malfunctions when using the external sensors. This is basically due to the fact that the sensor is arranged inside the robot and it is a method of estimating the external situation from the situation inside the robot. It is very robust in that control does not rely on external environmental changes.

The proposed method has versatility and can be applied to many other robots. Since the proposed control utilizes only a small size and low power consumption sensor, it can also be used with a small robot. In addition, the sensors used in this control algorithm are only the sensors used by ordinary robots. Therefore, it is easy to purchase at low cost as a general-purpose product, and algorithms for sensor processing are also available as open sources.

Mechanical design has greatly influenced the simplification of control design. Since only two motors are able to move steadily with rough terrain, it is not necessary to control the detailed posture of the robot or control the movement. In addition, the symmetry of the mechanical design also contributes to the simplification of the control algorithm, it is not necessary to control the robot in accordance with the direction and situation. This is a synergistic effect between mechanical design and control design, and the concept of design aiming at simple design is greatly contributing to this effect.

The limitation of the proposed motion control is that it is difficult to move efficiently because position accuracy is poor. Also, unlike cameras and lasers, it is not possible to obtain unknown surface data, and it also affects the reduction of the movement efficiency. In the case where there are obstacles that should not be scratched, it is difficult to adapt control using only the internal sensor.

3.5 Path planning

3.5.1 Section introduction

Effective path planning is required for autonomous mobile robots in extreme environment such as a forest area. Complex terrain and a lot of obstacles are existing in a natural forest environment. Even when human beings pass such environments, they will find a route that is easy to follow by eye and then move.

Previous studies have proposed path planning methods using the Voronoi diagram [3.27] and the potential method [3.28]. Some method evaluates the load required for robot movement as costs for generating the optimal route using geometrical information [3.29]. These methods are basically avoiding obstacles, and useful in a simple environment with less obstacles such as indoors. However, conventional methods don't match to the complex environment such as natural forest area because the movable areas are limited, and it becomes impossible to observe a wide range when trying to avoid all the obstacles. In addition, the time and the energy consumption to the destination may increase due to the possibility to be a detour path that. The robot can displace obstacles and move in areas with relatively low vegetation. The path is expected to be generated considering passing over the grassy area.

The objective of this section was to design an effective path planning in forest area. Cost map was focused to select an effective path. Two ways of generating the cost map and the experiment using the map were introduced in this section.

3.5.2 Cost map generation

3.5.2.1 Cost map

Autonomous navigation is one of the most important mobile robot issue; this technology allows the robots to arrive at the goal point without human interruption. W. Ali et al. proposed a classification based tree detection method using Valmet 830 Forwarder that can detect the tree by image processing using a mounted camera [3.30]. P. Fleischmann et al. proposed an image-based segmentation method using a John Deere XUV 855D Gator that can detect obstacles using mounted stereo-cameras to make a clear path [3.31]. D. Wooden presented perception and navigation algorithms using BigDog that can generate an optimal path by using a cost map generated by a laser scanner and a stereo vision camera [3.32].

Cost map generation is useful in generating an optimal path for the robot. Specifically, grid-based cost map generation is frequently used for navigating mobile robots because this method makes it easy to comprehend and grasp the situation visually.

A. Kelly et al., represented the world as a two-dimensional horizontal grid surrounding the robot with mapping sensor data, in order to generate the location of obstacles as a cost map [3.33] [3.34]. This method enables Crusher that was developed for the UGCV-Perceptor Integration (UPI) program to operate in a complex environment. J. Alberts reported the experimental results of operating a mobile robot in the forest using a modified Learning Applied to Ground Robotics (LAGR) system developed at Carnegie Mellon [3.35]. This system also uses cost maps and enables the robot to navigate autonomously. Most of the cost values of these cost map generations are calculated accurately using geometric information collected by the camera or laser.

Conventional methods using geometric information are largely depending on surrounding environments outdoors, long-term use is difficult due to the weather effect. The threshold of sensor processing largely depends on the weather, and must take into consideration amount of solar radiation, the effect of raindrops, and dirty lenses due to mud. These methods are especially difficult to implement in small mobile robots because sensor processing, such as image processing, becomes too difficult. A lot of noise is captured on the sensor that makes data processing difficult. The robot is small compared to the obstacles in the forest, which makes it pick up noise from things such as grass and sand dust. Furthermore, the posture of the robot becomes unstable, which makes processing difficult. In order to solve this problem, the author tried to use the internal robot sensors for cost map generation.

S. Martin, et al., have proposed to create a large-scale cost map from vehicle experience [3.36] [3.37]. Remotely operated vehicle experiences are stored and try to make a cost map using the data. The concept of these studies is similar to my concept, but the vehicle has to remotely controlled as a first step because of the hardware limitation. And, with this method, it is difficult to distinguish whether an area not passing through is an obstacle or just not passed. For further automation, technologies are required for robots to automatically record costs even in unknown environments and create the cost map.

3.5.2.2 Approach to generate a cost map

A grid map is created by dividing the observation area into small square grids, and the loads of movement for the robot are saved as a cost in each grid. The optimal path can be generated using such a cost map.

The cost is based on moving distance, and the longer the travel distance consumes more energy consumption. In addition to this, it is considered effective to add the height difference of the topography and grass vegetation in forest area. The robot needs a large torque when the robot climbs up a hill or climbs a step, and accordingly it consumes more energy. It is known that much energy is consumed even when the robot moves in the grassy area.

For example, the results of preliminary experiments are shown in Fig. 3.28. This experiment was conducted by comparing the energy consumption through going straight 3 [m] on general asphalt, hard sandy ground, such as a park, and 0.2-0.5 [m] a tall grassy area. The robot specifications are almost the same as the robot used in the verification experiment, but the maximum output of the motor and weight of the robot is slightly different. From this experiment, it was found that the energy consumption is greatly dependent on the environment.

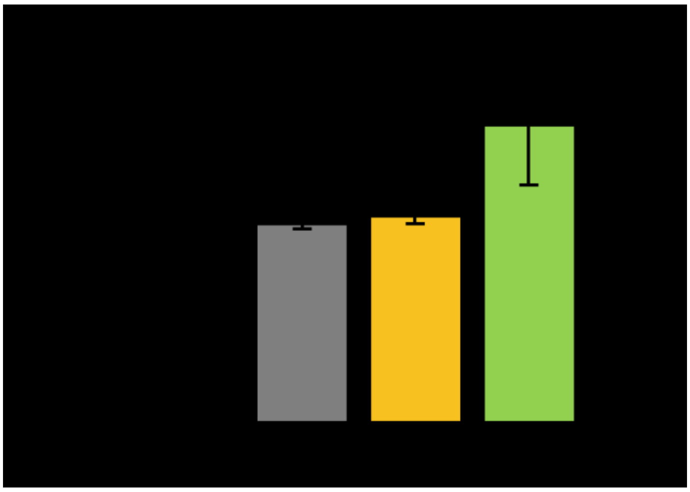

Figure 3.28 Comparison of the energy consumption to go straight 3 [m] as a preliminary experiment.

Fig. 3.29 shows the relationship between the number of activated program and travel distance in motion control test in natural forest in Shizuoka. It seems that there is a negative correlation between the two, although it is not clear due to the influence of GPS accuracy. From these experiences, the author thought that the movement data of the robot could be used as a cost.

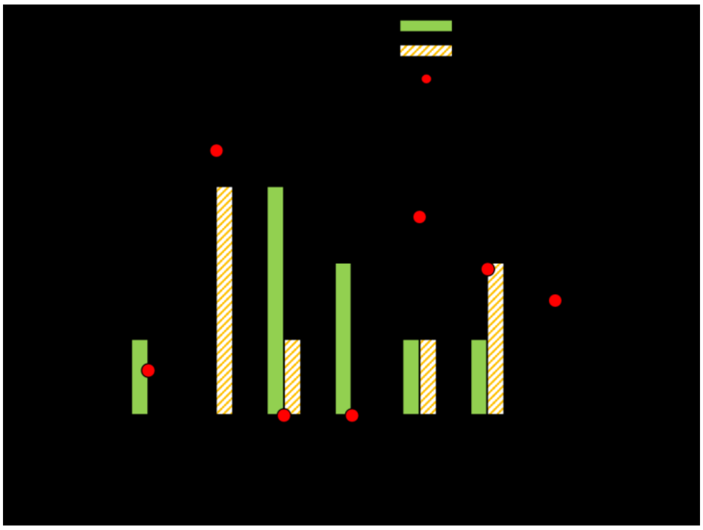

Figure 3.29 Relationship between the number of activated program and travel distance in motion control test in natural forest in Shizuoka

However, it is difficult for a robot to move for the first time in a complicated environment called a forest. When assuming actual operation, it is considered that there are many cases where humans enter the target environment to place the robot once. For this reason, a method is examined that estimating the movement cost of the robot based on the information that humans measured the environment before the operation. In addition, a method of autonomously moving robot itself in an unknown environment and collecting information on costs is also examined.

3.5.2.3 Cost map generation by human

A way that humans to directly investigate the environment and determine the cost is one of the methods of generating cost map. Human vision is so excellent that they can easily understand the environment.

A path planning algorithm to calculate the cost to the destination was developed based on the cost map. The cost on each grid was calculated using following formula.

$$C_{k,k+1} = w_d D_{k,k+1} + w_h (H_{k+1} - H_k) + w_v \sqrt{(x_{k+1} - x_k)^2 + (y_{k+1} - y_k)^2} \tag{3.11}$$

where $C_{k,k+1}$ is the cost of the robot from gird k to k+1, $D_{k,k+1}$ is the vegetation degree between grid k to k+1, H_k is the height of terrain at grid k, w_d, w_h, and w_v is the weight of each cost, and x_k and y_k is the position of the robot in k grid.

Fig. 3.30 shows the vegetation degree of each environment. Vegetation degree was divided into six stages based on grass height and density. An environment where the grass does not grow at all is assumed to be 0 (Fig. 3.30 (a)), and an environment where the robot cannot move at all because of the high grass density is regarded as 1.0 (Fig. 3.30 (f)). In the environment between them, the degree of vegetation was gradually divided as shown in Fig. 3.30 (b) to Fig. 3.30 (e). The height of the environment is also divided into six stages and distributed the highest place in the target environment as 1 and the lowest place as 0. The path to plan changes when the weight of each cost is changed. This is because that the mobility of the robot is different according to its characteristics.

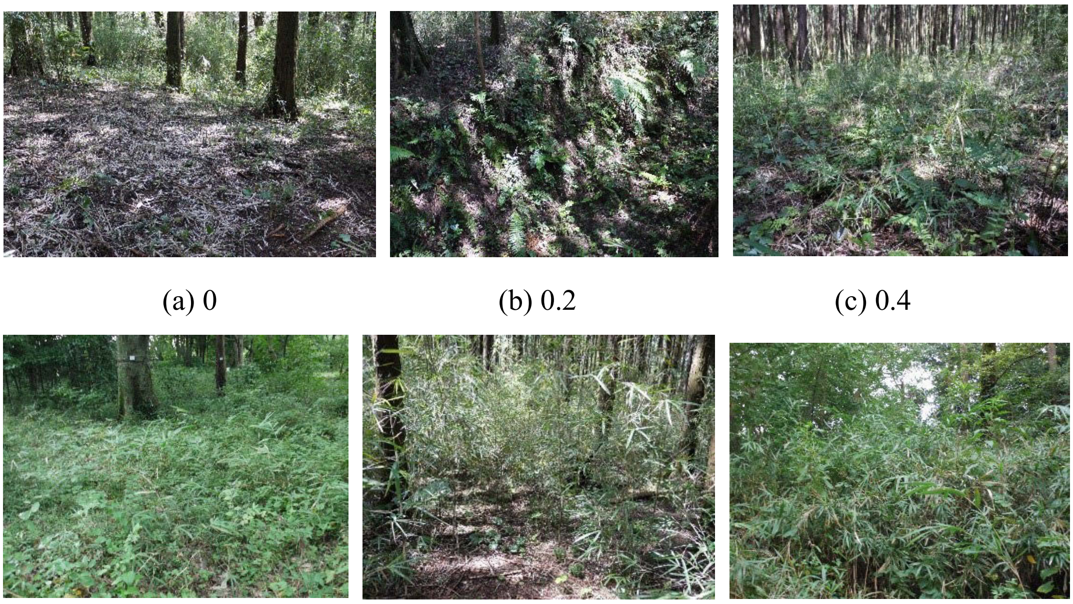

(a) 0 (b) 0.2 (c) 0.4

(d) 0.6 (e) 0.8 (f) 1.0

Figure 3.30 Vegetation degree of each environment

3.5.2.4 Cost map generation by robot

A way to use the environmental information the robot moved is also one of the methods of generating cost map. Fig. 3.31 shows the flow of the generation and use of the cost map. The uploaded locomotion data from the robot is used by a two-path planner on the server and the cost map is stored in the database. The server switches the path planner according to the situation. When the robot is moving to explore unknown environments, the server uses the path planner for exploration in an unknown area to generate the cost map. When the robot moves in known areas such as returning to the starting grid, the server uses the path planner for navigation and the path is calculated using the cost map.

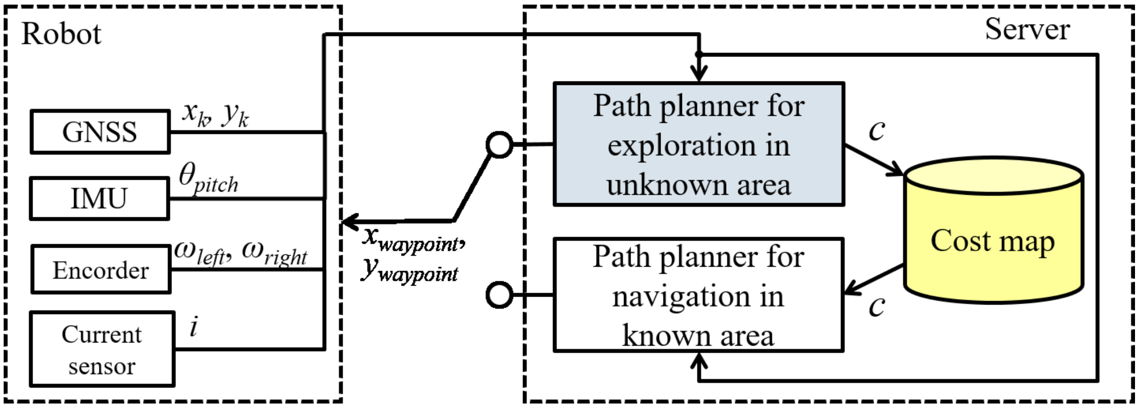

Figure 3.31 Flowchart of generation and use of cost map.

Cost values of each grid are calculated based on locomotive data gathered through an internal sensor on the mobile robot. The cost value is calculated using the energy consumption during movement and the risk of immovable conditions. Cost values are expressed based on the actual motor power calculated from the motor current value and the added risk converted into the same physical quantity as motor power by using maximum values of the motor power. The energy consumption per unit of time was used because the total energy consumption takes into account the time it takes to reach the destination due to GNSS error. Cost value c is calculated as follows:

$$c = \frac{p_{ave}}{P_{\max}} + (1 - \frac{p_{ave}}{P_{\max}}) \cdot (\frac{1}{2} + \frac{n_{f+s} - K}{2\sqrt{1 + (n_{f+s} - K)^2}}) \tag{3.12}$$

where pave is the average power of the motor to the path the of the grid, P_{max} is the max power of the motor driver, n_{f+s} is the number of flip preventions and stack avoidances programmed in the grid, and K is the safety ratio.

The cost value becomes dimensionless by dividing by the maximum value of the possible current, and it is represented by a number between 0 and 1. Fig. 3.32 shows the relation between cost value and the number of flip preventions and stuck avoidances in the grid. The latter part of the cost value function uses a sigmoid function that is an S-shaped curve [3.38]. It is known based on the trend of previous experiments that there is a high possibility that there is a large obstacle when the number of flip preventions and stack avoidances exceeds a certain number, but there is not much of a chance when this number is small. The cost map can be changed by changing this coefficient, although we normally choose the average number of times as a coefficient. When the robot is operated in a relatively simple environment such as an artificially created park, this value will be set low so as to be able to operate with safety as a priority. On the other hand, when the robot is operated in a complex environment such as a natural forest without much human interaction, this value will be set high in order to grasp the magnitude of energy consumption in tall grass.

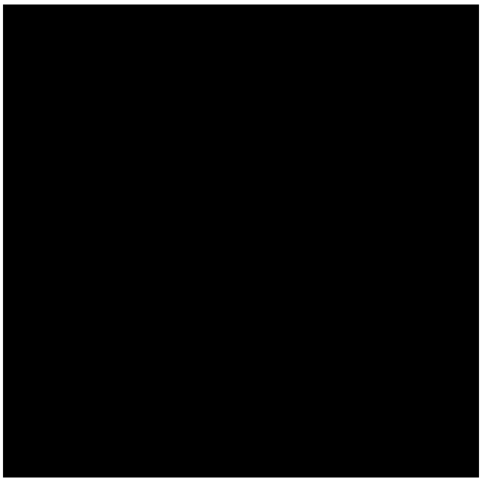

Figure 3.32 Relationship between cost value and number of flip preventions and stack avoidances in the grid.

Considering a complex environment, such as a steep slope, the cost within one grid is better to have eight dimensions in order to take account for all the possible directions of movement to next grids. Fig. 3.33 shows eight dimensional cost's vectors. Eight cost data are stored as vectors in one grid. By incorporating the concept of direction into cost, it is expected to be used in a more complicated environment.

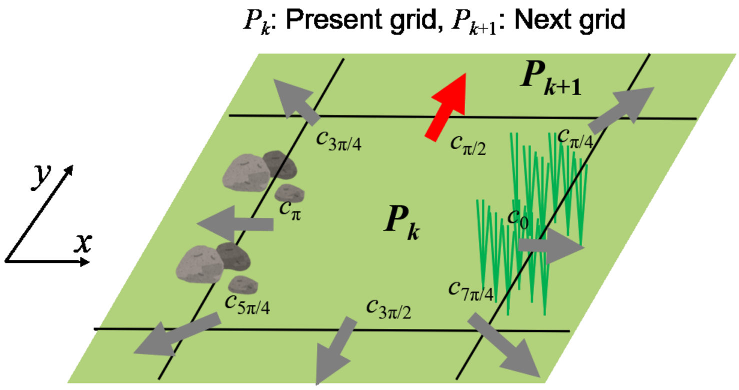

Figure 3.33 Eight dimensional cost's vectors

3.5.3 Path planning for navigation

Path planning for navigation generates the optimal path for the target grid by using a generated cost map. The author plans to use this when the robot returns to the energy charge station for long-term monitoring.

A* algorithm [3.39] is used for selecting the best path from the starting grid to goal grid. The optimal path is generated in order to minimize the total cost. The waypoint grid, which becomes each corner of the path, is calculated and the grid number is transmitted to the robot for navigation. Motion control of the robot operates it autonomously to the target destination based on this data.

A* algorithm was used to determine the optimal path route for reducing the calculation cost. In the A* algorithm, the entire cost to the destination $f(s)$ is expressed by the following equation using the total movement costs to the certain point S and the expected cost $h(s)$ from the point S to the destination.

$$f(s) = g(s) + h(s) \tag{3.13}$$

$$g(s) = \sum_{k=0}^{s} C_{k,k+1} \tag{3.14}$$

$$h(s) = \sqrt{(x_g - x_s)^2 + (y_g - y_s)^2} \tag{3.15}$$

where x_g and y_g is the position of goal point and x_s and y_s is the position of point S.

Fig. 3.34 shows shows the procedure of calculating the route when using the A * algorithm.

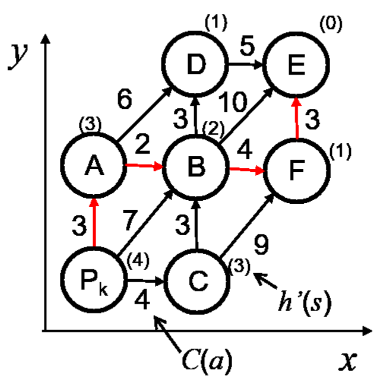

Step	Open list	Close list
1	P_k(4)	
2	A(6), B(9), C(7)	P_k(4)
3	B(9), C(7), B(7), D(10)	P_k(0), A(6)
4	B(7), D(10), B(9), F(14)	P_k(0), A(3), C(7)
5	D(10), F(14), D(9), E(15), F(10)	P_k(0), A(3), C(4), B(7)
6	E(15), F(10), E(13)	P_k(0), A(3), C(4), B(5), D(9)
7	E(13), E(12)	P_k(0), A(3), C(4), B(5), D(8), F(10)
8	E(12)	P_k(0), A(3), C(4), B(5), D(8), F(9), E(12)

Figure 3.34 Procedure of A* algorithm

The optimal path route is determined so that the cost $f(s)$ is minimized, and the grid, which becomes each turning angle of the path becomes the waypoints. The position data of waypoints are transmitted from the host PC to the robot, and the robot is programmed to go to the destination through each waypoint.

3.5.4 Verification

3.5.4.1 Generating the cost map by human

In order to verify a validity of the path planning and motion control of the robot, the experiment was conducted in natural forest. The robot was operated in the forest near Mt. Fuji where a lot of obstacles such as trees and tall grasses are exiting. 50x30 [m^2] area was divided into 60 grids.

The author measured the target field by human and decide the height of the terrain and vegetation degree of each grid and the cost map of the target environment was generated on the server. Fig. 3.35 shows the results of measurements of each cost.

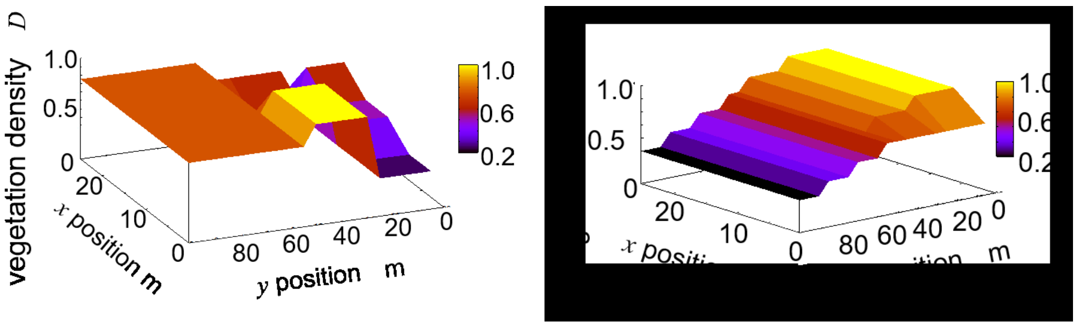

(a) Vegetation degree (b) Height of terrain

Figure 3.35 Costs on each grid

3.5.4.2 Path planning using cost map by human

The objective of this experiment was to verify the validity of the cost map generated by human. The optimal path route was generated by using the proposed method. The weight of each cost was set with the same weight. The waypoint on the path was also calculated according to the optimal path, and the position data of this waypoint are sent to the robot. In experimental environment, two waypoints were decided according to the optimal path and sent to the robot (Fig. 3.36).

The robot was operated autonomously using proposed motion control algorithms. The robot was not able to move over 20 [m] without the path planning in this environment, the proposed path planning is effective in such an environment.

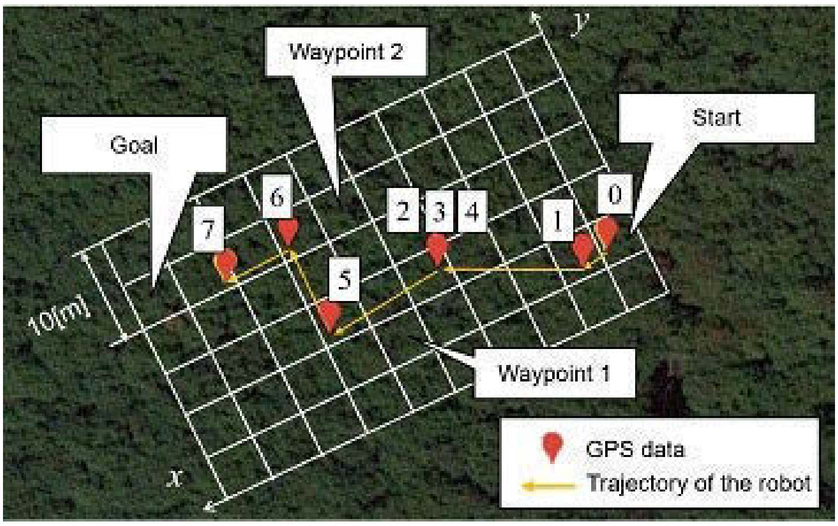

Figure 3.36 Trajectory of the robot

3.5.4.3 Generating the cost map by robot

The objective of the experiment was to confirm whether a cost map can be generated in a natural environment. The experiment was conducted in the Tanashi forest in Japan, where many trees exist. 14x14 [m2] area was divided into 48 grids (each grid size is 2x2 [m2]). WAMOT starts from grid 0 and moves until the 48th grid. Cost value is calculated for each grid. The safety rate of the cost value function is set to the average number of flip preventions and stuck avoidances.

The robot moved on the map with a good degree of accuracy and confirmed that the data was acquired correctly. The total operating time was 67 [min] and the energy consumption from the starting grid to the 48th grid was calculated as 77 [KJ]. The safety rate of the cost value was 1.07. Fig. 3.37 shows the generated cost map. The results of the generated cost map (Fig. 3.37 (c)) are calculated using the average power of the motor to the grid (Fig. 3.37 (a)) and the number of flip preventions and stuck avoidance program in the grid (Fig. 3.37 (b)). Comparing the calculated cost map with the actual environment, the places where the cost is more than 0.86 have some fallen trees that could have interfered with the robot’s movement. Almost all of the places where the cost is between 0.5 to 0.6 have a single tree and the robot avoided it with a flip prevention program.

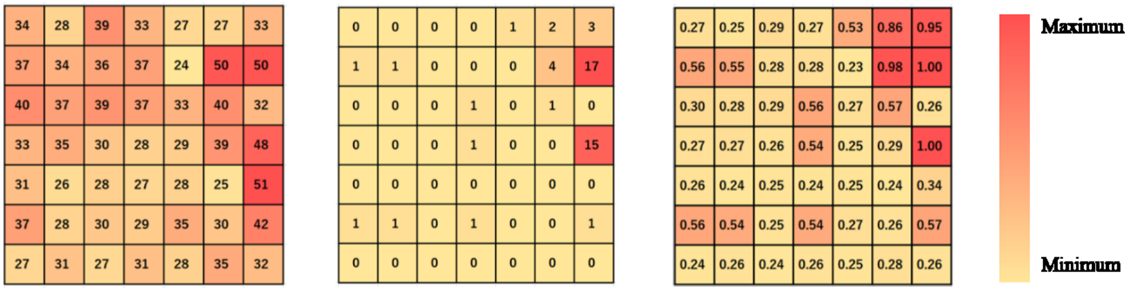

(a) Average power of motor to path the grid (Left)

(b) The number of flip preventions and stuck avoidance program in the grid (Center)

(c) Generated cost value of each grid (Right)

Figure 3.37 Experimental result of cost map generation.

3.5.4.4 Path planning using cost map

The objective of this experiment was to verify the validity of the cost map. The experiment was conducted using the cost map that was generated by a previous experiment. The start and goal grid were set so that high and low cost was mixed (Fig. 3.38). The robot moves from the starting grid to the goal grid under two conditions by using path planning with the cost map and without the cost map. The author was measured that the operating time, average current value, and number of flip preventions and stuck avoidances and calculated the energy consumption from the starting grid to the goal grid. The experiment was conducted seven times under each condition and the measured data were compared.

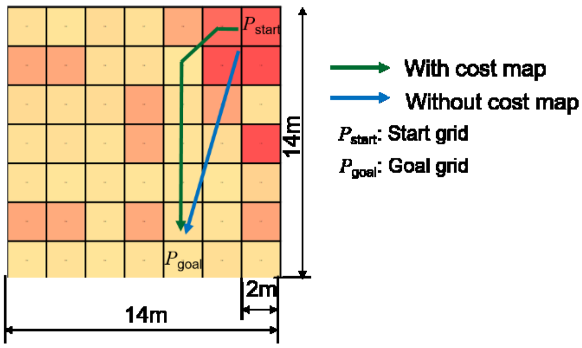

Figure 3.38 An experimental condition of path planning using cost map

Fig. 3.39 shows the results of the measured and calculated data. One of the data samples without the cost map was not added to the data because we assumed it was a failure not to reach the goal within 900 [s]. A T-test was conducted on each comparison. It was confirmed that any of the energy consumption, operating time, average power value, and number of flip prevention and stuck avoidances was reduced using the proposed method using cost map. The significant difference ($p<0.01$) of energy consumption between using path planning with the cost map and without the cost map was confirmed in this experiment. This is because the robot enters the high cost grid and takes a lot of energy until it gets out when the proposed method was not used. It was confirmed that the cost map acquired by the robot is effective for navigation.

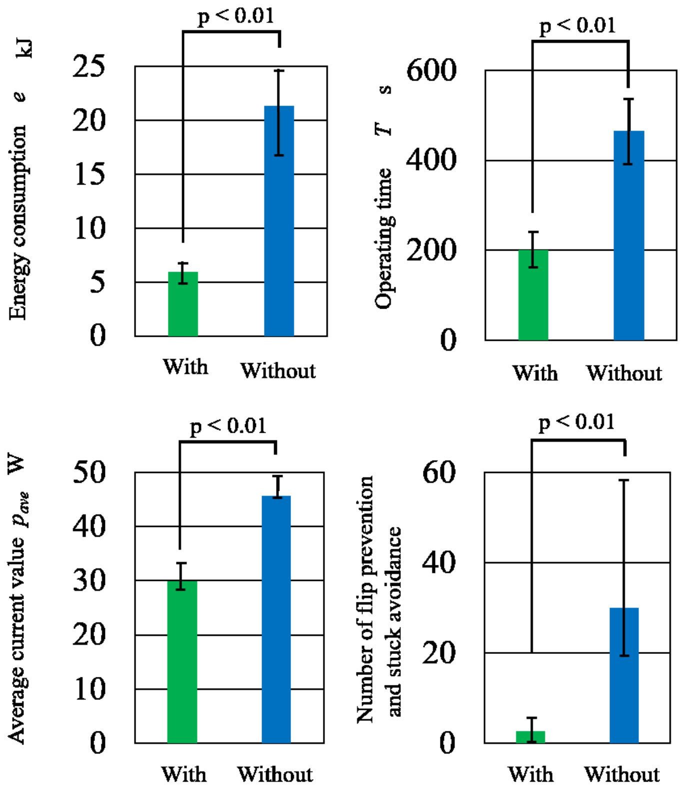

Figure 3.39 Results comparing energy consumption with and without the proposed method

3.5.5 Discussion

3.5.5.1 Cost generation by human

The generated path plan was effective for the robot to move in forest area. The robot could move in the target environment and reach to the goal. The author thinks that this has succeeded by adding a concept of vegetation to the cost, and the vegetation degree is very important for moving in the forest. The proposed method can be selected as the path route of the robot in places with low vegetation, whereas almost conventional methods avoid moving in the grass. This enables flexible mobility within the forest and allows monitoring of many environments.

Proposed path planning can be applied to various robots by changing the ratio of each weight of cost. For example, when using the robot with outer covering that was introduce in Chapter 2, it is considered effective to lower the weight of the vegetation degree. In the case where a large observation device is mounted on the robot, it is considered effective to increase the weight of the elevation of terrain because the center of gravity becomes high and the risk of falling is considered.

The grid size is better with more considered according to the accuracy of localization of the robot. In this experiment, 5x5 [m2] grid was created considering the accuracy of GPS, but it is necessary to reduce the size to about 2x2 [m2] in order to realize efficient movement in the forest. The accuracy of the GPS in the forest remarkably decreased and an error of about 10 [m] sometimes occurred. In the experiment, the average value of GPS data was used to improve the accuracy, but this would lengthen the operation time of the robot. These problems are thought to be largely eliminated by implementing highly accurate GNSS.

3.5.5.2 Cost generation by robot

The effectiveness of the proposed method was confirmed in the experiment. The generated cost map is helpful for planning the optimal path and is able to reduce the energy consumption. This shows that environmental recognition can only be performed by the experience using the internal sensor mounted on the robot. We believe that this result is significant for small mobile robots and is a big step in controlling the robot without using advanced external sensors. The significance of this method does not only address the weaknesses of tiny mobile robots, but also does not require high energy consumption and high product cost. This could be a major key in our goal of developing long-term monitoring systems using multiple robots.

Fig. 3.40 shows a relationship between energy consumption and number of flip prevention and stuck avoidances. In path planning using the cost map experiment, a large correlation (r=0.87) was confirmed between the energy consumption and the number of flip preventions and stuck avoidances. We understand that the risk was considered to be a major factor for determining the energy consumption in this environment and large obstacles such as trees are considered to be a major load in this experiment. This is because the test was performed in the winter and the environment did not contain much vegetation. The number of plants was so low that the areas without large obstacles were relatively easy to navigate. In order to verify further validation of the proposed method, now the author is collecting the experimental data in various conditions where energy consumption is likely to increase such as grasses and muddy area.

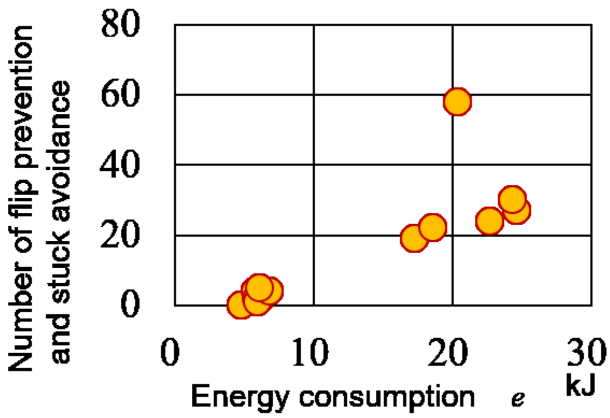

Figure 3.40 Relationship between energy consumption and number of flip prevention and stuck avoidances

The author thinks that we can roughly guess what type of environment the robot is in by analyzing all the acquired sensor data. For example, in the left central area of the experimental field, it was found that the average power of the motor was high, but the number of flip preventions and stuck avoidances was low. This area is thought to be a muddy or grassy road without large obstacles, which increased the energy consumption. This kind of estimation leads to high environmental recognition using a simple sensor. Furthermore, by storing it together with the geometrical data that can be acquired with high precision, the learning ability of the robot will improve drastically. There is a possibility that detailed environmental recognition can be done only using the internal sensor data if the learning database is large enough.

Chapter 4: Application

4.1 Chapter introduction

Some applications by using a developed mobile robot are introduced in this chapter. In field robot research, there is a high possibility that a different phenomenon from the theory assumed in the real environment occurs. This is because it is difficult to completely model the complicated outdoor environment and difficult to predict happenings. Therefore, it is important to repeat many experiments assuming actual operation and improve the robot so that it can be used in actual operation.

The objective of this chapter is to describe the methods and results of experiment of application example of robot. The system for obtaining the environmental information are developed and implemented in the operation system of the robot. In addition, the effectiveness of the application example of the robot was verified by experiments.

Mechanical and control elements that constitute the robot is described in chapter 2 and 3. In this chapter, the robot is operated by combining these elements for each application. In addition, measuring instruments and operating systems are developed according to each application. The author explains the systems and devices developed for applications and show experimental results using the developed robot.

The author uses figures and sentences by referring the author's published papers in this chapter [4.1-8].

4.2 Environmental monitoring

4.2.1 Section introduction

One of the most important factors to be considered in the development of an autonomous environmental monitoring system is its usability and convenience. Several studies have been conducted on the autonomous monitoring system and they were introduced in the summary paper [4.9]. An integration framework is described in [4.10]. This research allows the system to be extended in a way that is transparent to the sensor network. A group at the University of Southern California considered integrating technology, communications, and scientific exploration of aquatic ecosystems [4.11]. Although these systems have high performance, they are costly and complex, and cannot therefore be easy to use for another field researcher in the field. The next challenge in this research was a development remotely accessible operating software and a suitable electrical system for environmental monitoring.

In this section, the proposed system for environmental monitoring is described.

4.2.2 Monitoring plan

The objective of the monitoring was the measurement of environmental properties such as temperature, humidity, and radiation level [4.12], as well as Global Navigation Satellite System (GNSS) and image data for displaying the measurements on a monitoring map. Fig. 4.1 shows an image of a goal system for monitoring. Multiple robots were deployed in the field for cooperative environmental monitoring by using communication. Each robot was basically operated autonomously, and sometimes they were remote controlled by users in emergency case.

The robots uploaded the collected monitoring data to a server or sent them directly to users, who had the benefit of receiving the information remotely. Research institutes, university ecologist, zoologists, agricultural cooperatives, farmers, and local governments are considered as users. Monitoring data could be available for free by only accessing to the server.

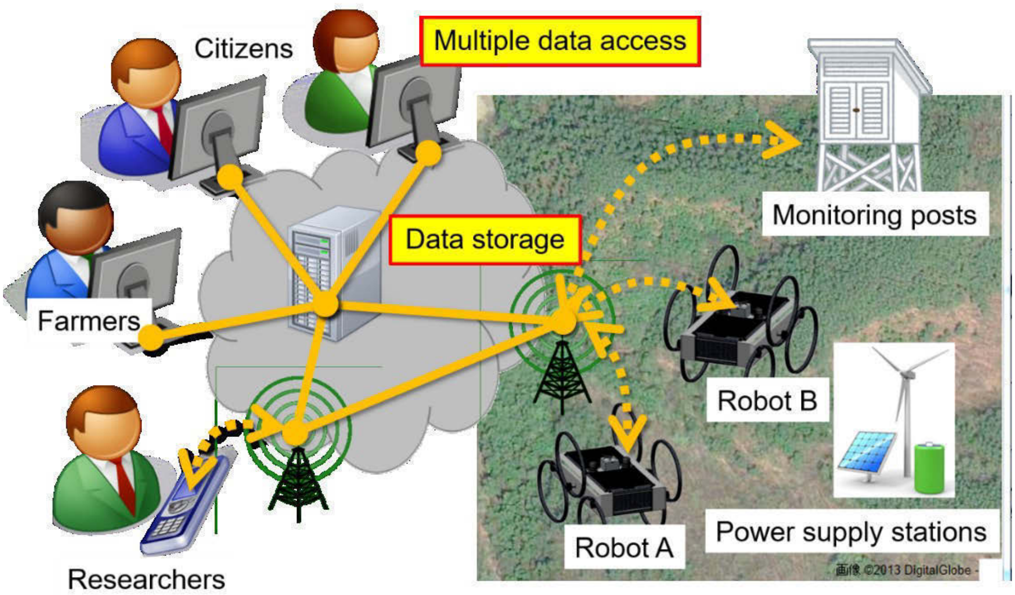

Figure 4.1 A goal system for monitoring

4.2.3 Operating software

Fig. 4.2 shows an operation software and electrical system for monitoring robot. The operating software for WAMOT comprised robots, a public cloud system, and users. The existing infrastructure was used in this software to reduce the capital expenditure and make it easy to use for users includes other field researchers. A smartphone was used as the communication tool, and a public cloud system (Google Drive) was used as the server. Various areas could thus be easily monitored without the development of a custom communication infrastructure or server. Multiple monitoring robots could also be directly operated, and several users could simultaneously access them.

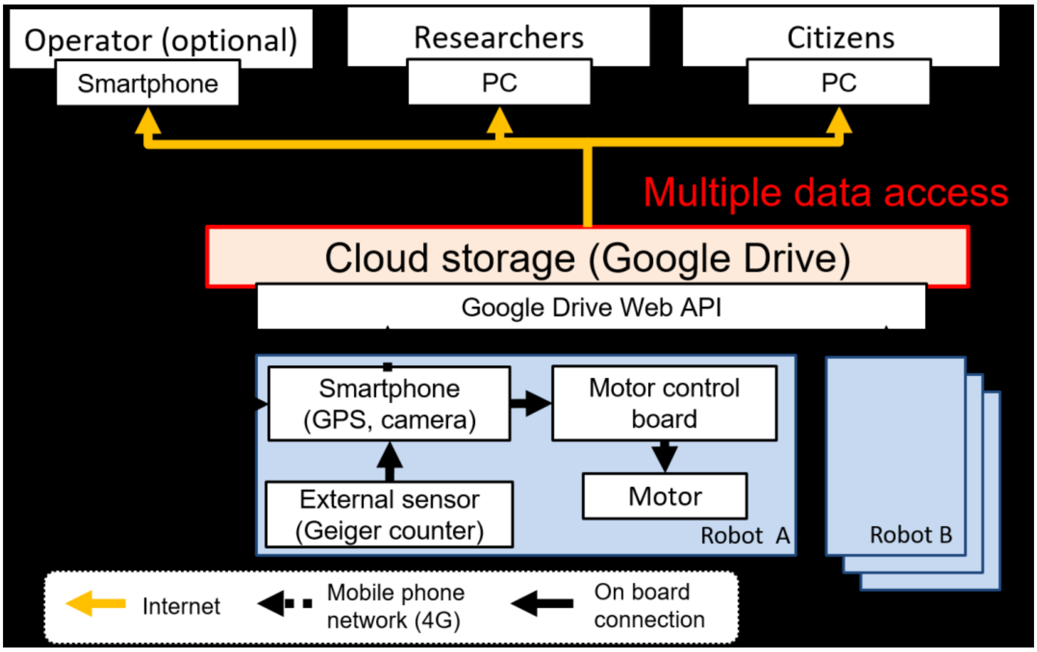

Figure 4.2 Operation software and electrical system for monitoring robot

4.2.3.1 Communication network

A mobile phone line (4G/LTE) was used as a communication network. The use of available mobile communication infrastructure and devices eliminates the need for a new communication system. Moreover, larger and more diverse areas could be monitored than when using other communication network such as Bluetooth. It also facilitates communication with the robot from another country. Users could access from foreign countries under the terms of the mobile phone line available.

4.2.3.2 Public cloud server

The public cloud system was used as a server for monitoring data storage. Server stored monitoring date, IP address belonged to smartphone mounted on the robot, GNSS data (Latitude and Longitude), battery level, other adding sensor data, and setting data that is set though application on the smartphone. These data were uploaded from smartphone and stored in spreadsheet on Google Drive. All users could get the data at the same time and share the data. Image data were also stored on Google Drive, user could monitor environmental appearance.

4.2.3.3 Android application

Android applications were developed for operating WAMOT. This application could be divided into two software; server interface and user interface.

Server interface was used on smartphone mounted on the robot. Fig. 4.3 (a) shows a sever interface of the developed application. In this interface, users could set the monitoring rate and resolution of the image.

It can be varied to control the energy consumption. The application can be used to switch the flight mode on/off. This also enables effective energy conservation because more energy is required for searching and networking in the non-flight mode [4.13]. The server only switches the flight mode on during the sensing.

The user interface was used for accessing robot directly. Fig. 4.3 (b) shows a user interface of the developed application. A user can also communicate directly with the robot via a personal smartphone, perform remote control, and obtain real time monitoring data from the display screen of the robot.

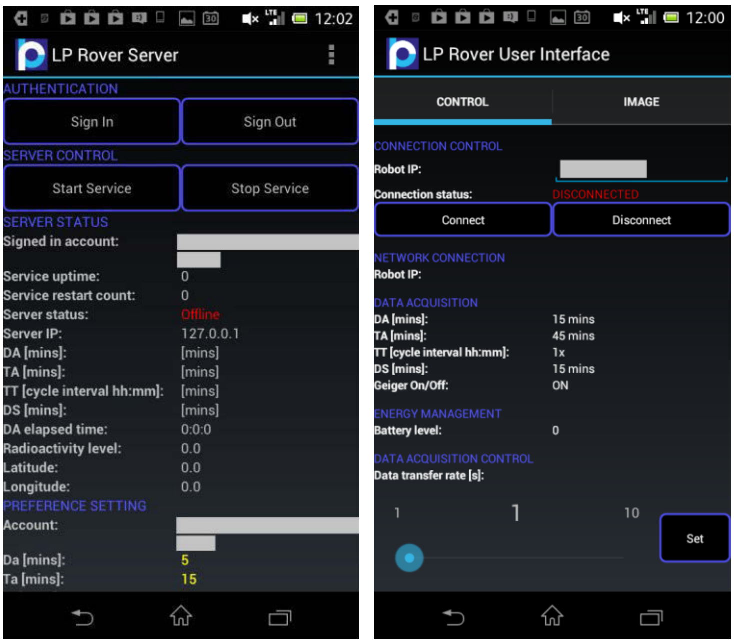

(a) Server interface (b) User interface

Figure 4.3 Developed application interface

User also could remote control the robot through this interface. Fig. 4.4 shows a user interface during the remote control. Image screen and 5 commands of operating robot; forward, backward, turn left, turn right, and stop, helped the user to remotely control the robot. This interface also was able to change the monitoring rate.

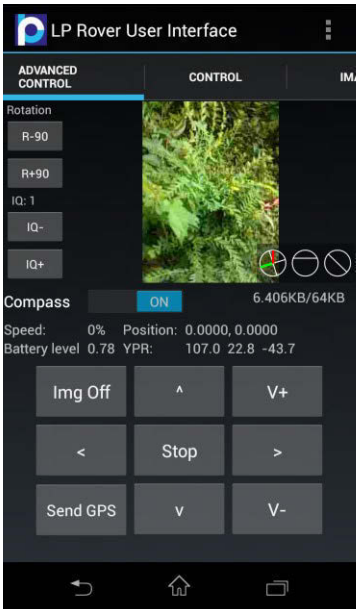

Figure 4.4 Remote control screen in user interface

Robot motion is programmed in motor control board. Fig. 4.5 shows a schedule of motion pattern. Motion pattern is set to suit the data acquisition. Monitoring data are acquired when the robot is stopped. Since, when the data is gathered during robot moving, the data might be incorrect because of vibration of the robot. The locomotion phase should not to be overlapped to the sensing phase.

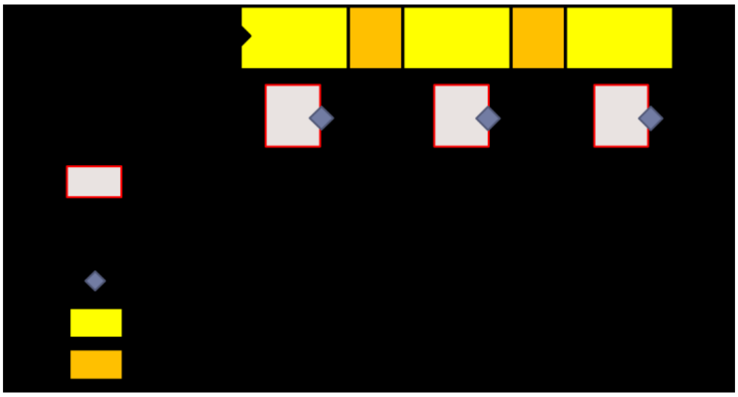

Figure 4.5 schedule of motion pattern

4.2.4 Monitoring module

4.2.4.1 Smartphone

The smartphone (Xperia SO-05D, Android 4.0) is used for communication between the robot and users. The robot uploads the monitoring data to the public server at set intervals and a user can obtain the data by accessing the server using an ID.

The use of a smartphone also enables gathering of data through its sensors and other external sensors. A smartphone sensor is sufficiently accurate and can be easily used for environmental monitoring.

There is some previous research about using a smartphone [4.14,15], however, these smartphones were only used as remote-control tools and robots do not mount the smartphone. This system use smartphone not only as a communication tool, but also as sensors.

4.2.4.2 Sensors

The sensing platform for monitoring consists of the two types of sensors: smartphone sensor and external sensor. The smartphone (Fig. 4.6 (a)) has a lot of sensors [4.16], Global Positioning

System (GPS) and a camera were used our electrical system. The GPS of the smartphone is used to determine the position of the robot, and it would also be used for navigation in the near future. The camera is used to monitor the surroundings and collect image data. The omnidirectional lens (Fig. 4.6 (b)) is used to enlarge the visual information about the field. A Geiger counter (Fig. 4.6 (c)), via microphone input as external sensor, was used to gather data on the radiation level. Such data has been in demand in Japan since the release of radioactive substances to the atmosphere from the Fukushima nuclear power plant.

(a) Smartphone (Xperia^{TM} AX SO-01E) (b) Omni directional lens (Go pano^{micro}) (c) Geiger counter (Pocket geiger type3)

Figure 4.6 Sensors for monitoring

4.2.5 Verification

The performance of the operating system of WAMOT was confirmed by demonstration experiment. Two kinds of experiments were done for confirming whether operating software and electrical system were working as expected.

4.2.5.1 Demonstration in a Natural Ecosystem

The operating software was tested in the natural ecosystem of the mountain forest on Mount Fuji in Shizuoka, which is considered to be a comparatively difficult terrain, to verify its performance in a real environment. In this experiment, the robot was not moving. The operating software was set to repeatedly operate in the sensing mode for 1 [min] followed by the non-sensing mode for 60 [min] under actual operating conditions. In the sensing mode, the robot monitored the environment and the data was collected once during each sensing mode. In the non-sensing mode, the server smartphone that was mounted on the robot switched the flight mode off for saving energy consumption.

The operating software had successfully continued to operate correctly for three days, though it was a rainy day and in a real environment. The total data were sixty and the collected data was uploaded to the Google drive. Fig. 4.7 shows the uploaded image data. From the brightness of the acquired image it is easy to see that the data was acquired for 3 days.

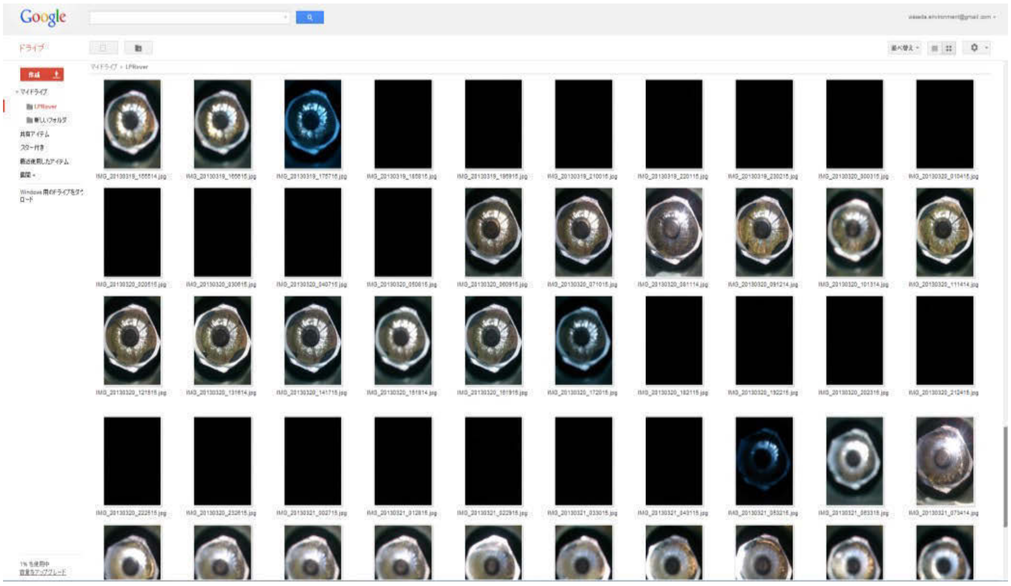

Figure 4.7 uploaded image data on Google Drive

Fig. 4.8 shows a monitoring map using the data acquired in the experiment. Using a system on the web on google makes it easy to create such a map.

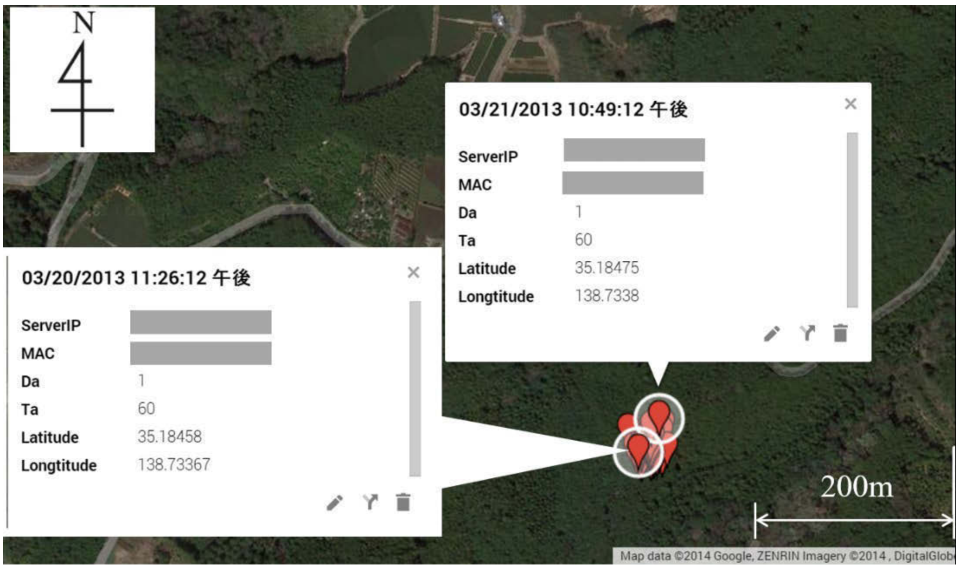

Figure 4.8 Monitoring map

4.2.5.2 Demonstration in an Artificial Ecosystem

WAMOT was experimentally operated in the artificial ecosystem of the Toyama Park in Tokyo, which is considered to be a comparatively easy terrain, to verify the electrical system performance of the robot. The motion pattern of the robot was programmed into the motor control board. The robot was to repeatedly operate in the active mode for 5 [min] followed by the rest mode for 15 [min] under actual operating conditions. The robot monitored the environment in the rest mode because monitoring in the active mode would be inaccurate owing to the presence of noise. This mode was set by the application in smartphone mounted on the robot. The monitoring data were collected once during each rest mode and uploaded to the Google drive.

The monitoring continued for two hours, during which time the electrical system operated correctly and the robot continually uploaded data for seven times. Fig. 4.9 shows the uploaded data, which were obtained by accessing the Google drive.

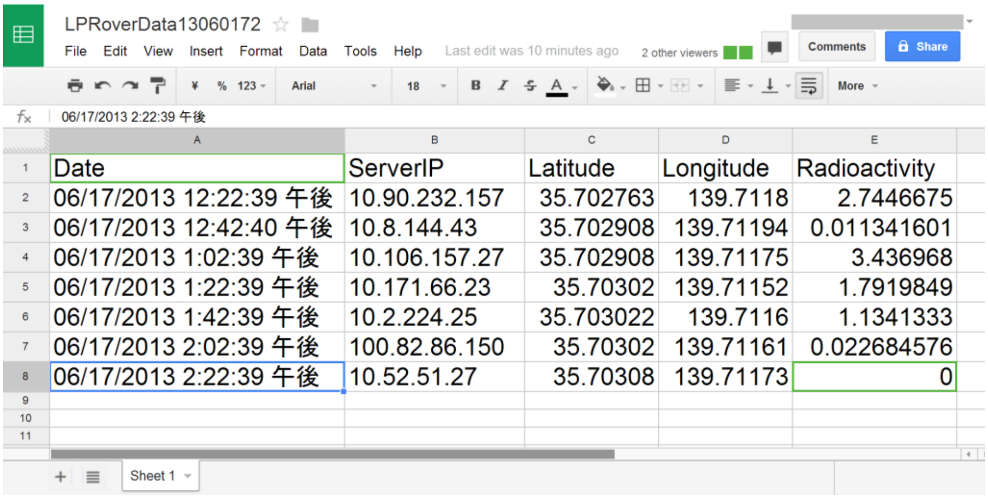

Date	ServerIP	Latitude	Longitude	Radioactivity
06/17/2013 12:22:39 午後	10.90.232.157	35.702763	139.7118	2.7446675
06/17/2013 12:42:40 午後	10.8.144.43	35.702908	139.71194	0.011341601
06/17/2013 1:02:39 午後	10.106.157.27	35.702908	139.71175	3.436968
06/17/2013 1:22:39 午後	10.171.66.23	35.70302	139.71152	1.7919849
06/17/2013 1:42:39 午後	10.2.224.25	35.703022	139.7116	1.1341333
06/17/2013 2:02:39 午後	100.82.86.150	35.70302	139.71161	0.022684576
06/17/2013 2:22:39 午後	10.52.51.27	35.70308	139.71173	0

Figure 4.9 Uploaded monitoring data on spreadsheet on Google drive. Japanese word "午後" means p.m.

Fig. 4.10 shows the image data extended by using software. The form of the uploaded image data was changed from a round shape to a square shape. Three people and one big tree can be seen from this image. Though these images are rough, user can monitor all directions.

Figure 4.10 Image data from demonstration experiment in an artificial ecosystem

Fig. 4.11 shows a trajectory of WAMOT during the experiment. This is also created using software on the web of google. By plotting the data measured in this manner on the map, it becomes possible to perceive the environment information sensuously.

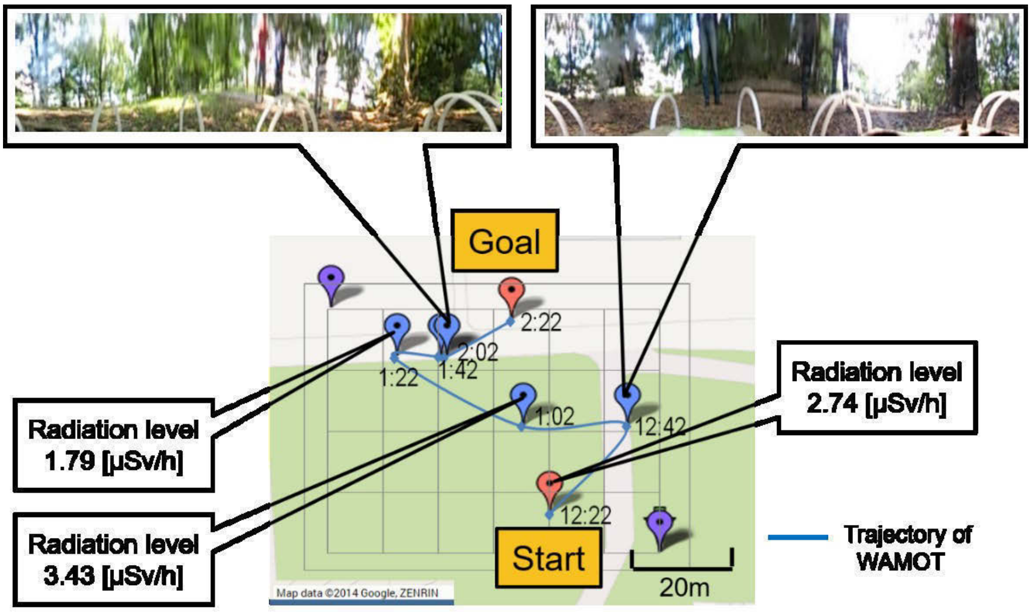

Figure 4.11 Trajectory of WAMOT: The robot starts from the starting point (12:22) and finish on goal point (2:22).

4.2.5.3 Demonstration in farmland

In order to confirm the usefulness of autonomous mobile environment monitoring robot and its operation system in agricultural work, the locomotion performance of the robot and measurement capability were evaluated on agricultural land.

In the experiments, a motion protocol was implemented to the robot and the robot alternately repeats movement for 4 [min] and stop for 6 [min]. In this motion protocol, the robot measures its position and the amount of radiation in the air while it is stopped and stores the measured data on Google Drive.

Experiments were conducted in pastures in Fukushima Prefecture. Fig. 4.12 shows an image of WAMOT in the experiment. The experiment was conducted 3 weeks after grass harvest. The height of grass at the time of the experiment was about 150 [mm] on average, about 500 [mm] at the maximum. In the experiment, position data of the goal point was set to 100 [m] ahead and the robot moved toward the goal. The target orientation in the motion control algorithm was parallel to a straight line connecting the start point and the end point.

Figure 4.12 WAMOT in farmland

Fig. 4.13 shows the trajectory of the robot created based on the measured self-position data. From this map, it can be seen that the robot could measure the environment through roughly the same route toward the target point. Since measurement points were not specified in this experiment, measurement points were confirmed slightly different in two trials.

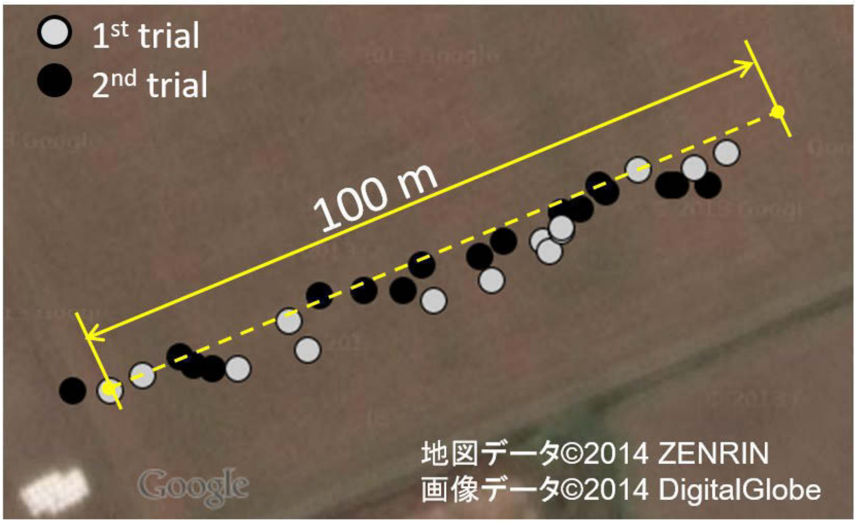

Figure 4.13 Trajectory from GPS data

Fig. 4.14 shows a map of radiation level that was made using the data measured by the robot. It is confirmed that the environment on the almost straight line can be measured in detail when the two-measurement data are combined. About 30 data can be acquired at intervals of 100 meters, therefore, it can be said that the measurement is made with an accuracy of about 3 [m] intervals.

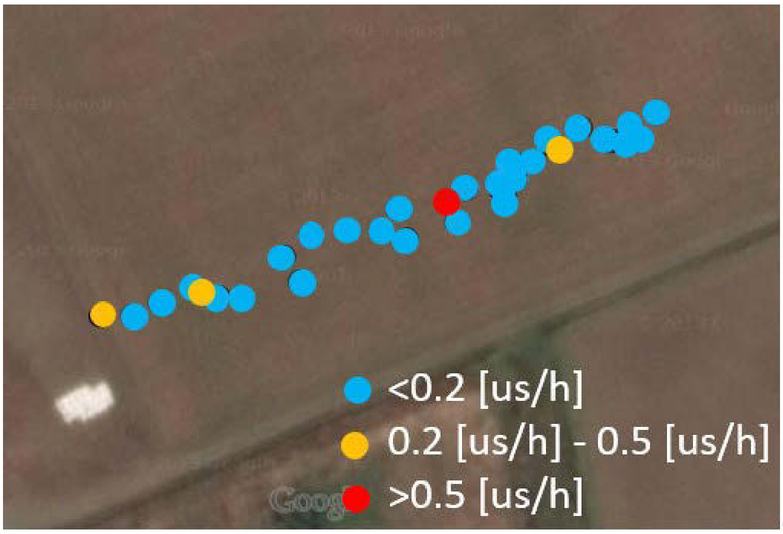

Figure 4.14 Map of radiation level. These data are acquired from the robot

Fig. 4.15 shows a locomotion distance of two trials. It is possible to read how the robot moves by using this graph. Although it looks almost the same as the whole operation, the gradient of the graph tends to become gentle a little in the second half compared to the first half. Especially at the point of 70 [m] to 90 [m], the inclination of the slope is the smallest. It was a gentle uphill slope of about 3 to 5 degrees in this interval, and this was considered that there was an influence on the movement of the robot.

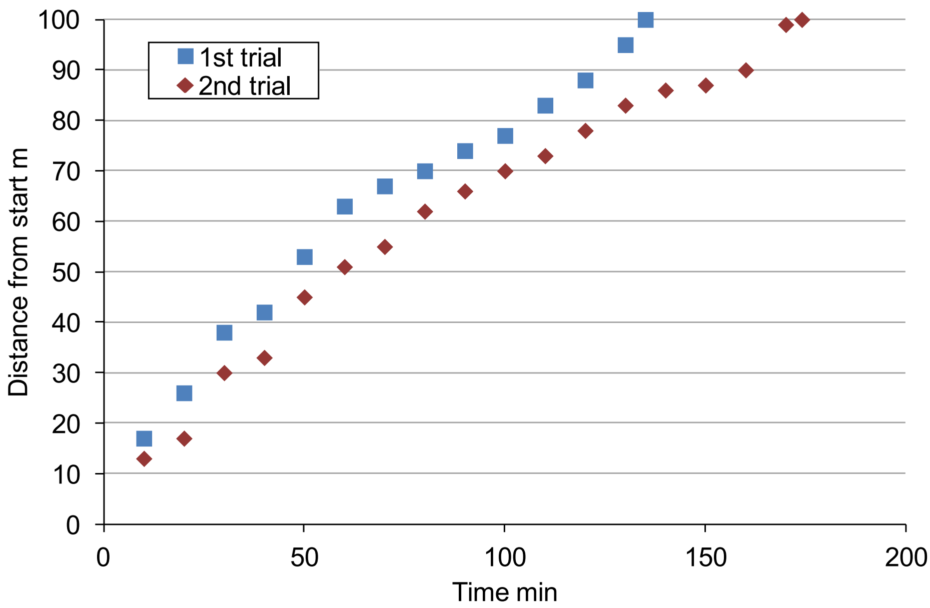

Figure 4.15 Locomotion distance

Fig. 4.16 shows a radiation level data on each point. The average radiation level was about 0.15 [μS/h]. There was only one data with a high radiation, but this is considered to be an error of the measuring instrument because similar data could not be observed in another nearby place.

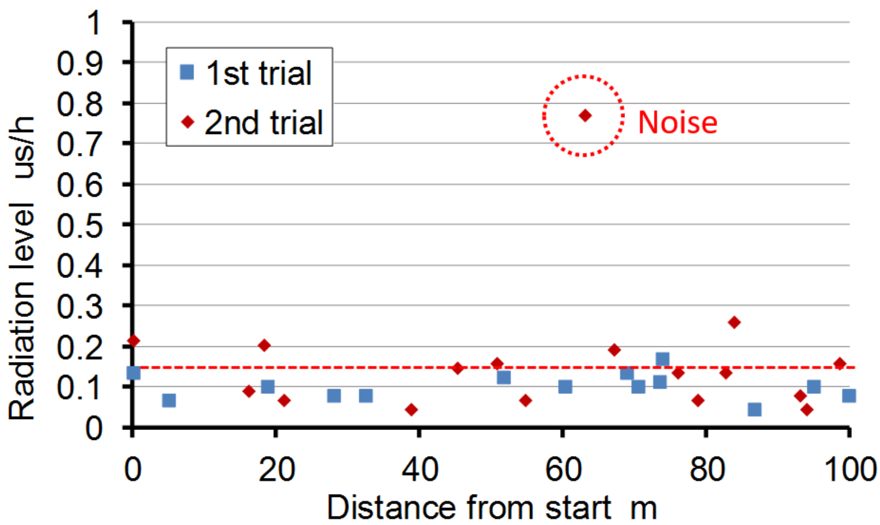

Figure 4.16 Radiation level measured by the robot

4.2.5.4 Testing remote operation

The objective of this experiment was to verify the practicality of remote control. The operability was examined in condition of large communication delay due to network connection.

The robot was prepared in Italy and remotely operated the robot using communication from Japan (Fig. 4.17). A Sim card for communication to be mounted on the robot were procured in Italy.

Figure 4.17 Communication distance of remote operation

Practicality of remote operation was examined by two kinds of experiments. The first experiment was conducted to verify whether the robot can get out of the narrow path when it enters. Fig. 4.18 shows an experimental condition of escape experiment from narrow space. The experimenters in Italy prepare the experiment environment as shown in the figure and the robot was put in the direction of the arrow to make the forward direction opposite to the narrow path. The experiment was conducted according to the experimental procedure as shown in Table 4.1. About the *L* of the narrow passage, three kinds of 400/600/800 are set. If it cannot pass within 5 [min], it is judged that the pass failed. Experimenters in Japan measure the time for getting out and ease of operation and communication status was evaluated.

The outline of the experiment was prepared to avoid different information depending on subjects, subjects understood the content by reading the outline before the experiment. In addition, the outline of the experiment describes the operation method of the robot, and the subject remote control the robot with only that information.

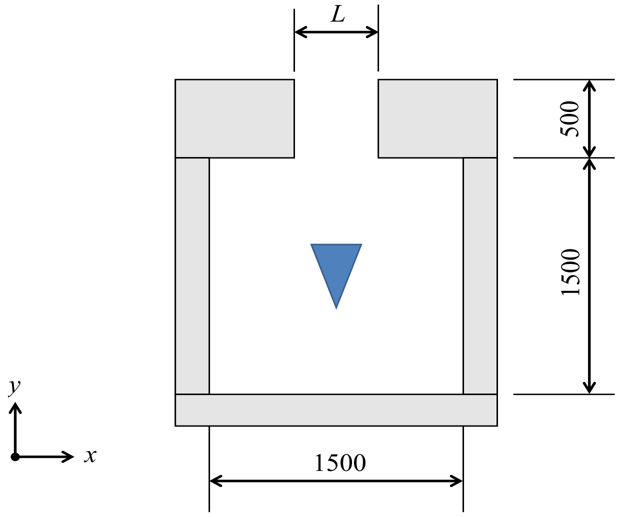

Figure 4.18 Experimental conditions of escape experiment from narrow space

Table 4.1 Experimental procedure of escape experiment from narrow space

No.	Place	Person	Contents
1	Italy	Experimenter	Cover on a robot's smartphone
2	Japan	Experimenter	Teach subjects an abstract of the experiment
3	Japan	Experimenter	Report completion of teaching to Italy
4	Italy	Experimenter	Remove the cover of the smartphone
5	Japan	Experimenter	Time measurement starts when confirming the removal
6	Japan	Subject	Remote control of robot
7	Japan	Subject	Report to the experimenter when it reaches the destination
8	Japan	Experimenter	Time measurement ends when reaching arrival report
9	Japan	Experimenter	Report goals to the experimenter in Italy
10	Italy	Experimenter	Determine success

The experiment was conducted until one subject succeeded three times, and a total of seven subjects conducted the tests. The data on each subject are listed in the Table 4.2.

Table 4.2 Experimental results

Subject No.	Number of experiments	Time [min : s]	Number of times communication was interrupted	Remarks
1	1	1:24	0	
	2	2:05	0	

	3	1:15	0	
2	1	1:47	0	
	2	1:1	0	
	3	2:45	0	
3	1	4:01	2	
	2	10:13	1	
	3	9:33	0	
4	1	1:59	0	
	2	1:18	0	
	3	-	0	Experimenter in Italy decided discontinuation because of the sign of robot overturning
	4	2:33	0	
5	1	-	0	Experimenter in Italy decided discontinuation because of the lack of preparation
	2	2:51	0	
	3	0:48	0	
	4	-	1	Experimenter in Japan decide discontinuation because of connection failed
	5	0:37	0	
6	1	1:18	0	
	2	2:33	0	
	3	1:22	0	
7	1	1:03	0	
	2	1:05	0	
	3	1:59	0	

Many subjects were able to achieve the mission, though it is assumed that there was a time lag in the operation of the robot. The time it took to achieve the mission heavily depended on the subject. And, it was confirmed that communication is sometimes stopped in operation for a long period of time exceeding 2 [min].

The second experiment was conducted to verify whether the robot could move a predetermined course. In the second experiment, the time was measured from the start to the goal. The judgment of whether or not it reached the goal, is made by the subject oneself based on the image of the smartphone. If the subject determines the goal in front of the goal, the distance from the goal to the robot is measured as an error.

Fig. 4.19 shows the experimental course. The length of the course is about 60 [m] and there are 2 corners. Cones of a marker were set up at the start point and the goal point, and the examinee remotely controlled while referring to it and the line on the road. The experiment was also conducted according to the experimental procedure as shown in Table 4.3.

The outline of the experiment was also prepared in this experiment, and the subject read the outline before the experiment.

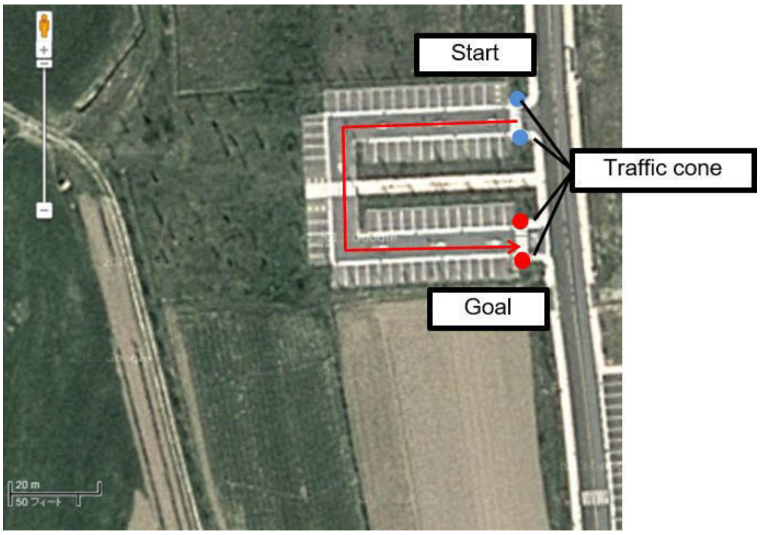

Figure 4.19 Experimental course

Table 4.3 Experimental procedure

No.	Place	Person	Contents
1	Japan	Experimenter	Teach subjects an abstract of the experiment
2	Italy	Experimenter	Prepare traffic cones
3	Italy	Experimenter	Place the robot at a starting position
4	Japan	Experimenter	Report completion of teaching to Italy
5	Italy	Experimenter	Report completion of preparing
6	Japan	Experimenter	Make a signal to start and time measurement starts
7	Japan	Subject	Remote control of robot
8	Japan	Experimenter	Record the number of times after confirming disconnection of communication
9	Japan	Subject	Reported to the experimenter when passing through narrow goal
10	Japan	Experimenter	Time measurement ends when reaching arrival report

11	Japan	Experimenter	Report goals to the experimenter in Italy
12	Italy	Experimenter	Determine success

In the experiment, only one subject was given a single chance, and a total of six subjects carried out the experiment. The data on each subject are listed in the Table 4.4.

Table 4.4 Experimental results

Subject No.	Number of experiments	Time [min : s]	Number of times communication was interrupted	Remarks
1	1	33:00	2	After passing through a 2nd corner and running backwards, timeout
2	1	27:00	5	After the 1st corner, the course out
3	1	30:20	14	Forced termination because of turning over
4	1	36:00	14	Mission Completed
5	1	32:00	27	The subject could see the goal cone, but could not complete it.
6	1	13:50	11	Forced termination because of course out

Many subjects could not achieve the mission. This is one of the reasons that the operation time is long, and the communication is interrupted many times. The robot was designed to continue the same operation up to the next command once the command was received. Assuming that communication is interrupted, it is necessary to change the specification to control to stop every time after operating for a certain period of time.

4.2.6 Discussion

4.2.6.1 Monitoring System

The robot continuously and autonomously uploaded monitoring data to the Google drive in the field, which confirmed the capability of the software for long-term environmental monitoring. The Google drive enabled easy monitoring and access of several users to the collected data. The GPS and image data were also sufficiently clear for monitoring purposes. Monitoring maps could be prepared from the collected data, which enables to easily understand the environment by users.

It was easy to share the data. Anyone with Google account will be able to view. Also, the acquired data is arranged on the spreadsheet, and it can be easily downloaded in the form of csv's files. Therefore, it was easy to download the file and analyze it on the local PC. In addition, by using the web software called Google My map, it is possible to display data of multiple transit points and their locations, and it was possible to easily create a monitoring map.

The developed system can be easily applied to existing monitoring devices and other outdoor mobile robots. This is considered to contribute greatly to building a huge monitoring network with multiple devices. In order to expand this system, the author thinks that it is necessary to define the type and standard of data to be uploaded.

The measurement height of the sensor may be a problem, although it is possible to grasp the trend of the radiation level with the relative value of the measured value even with using the developed robot. In Japan, the measurement height standard of airborne radiation is defined as 1 [m] to 1.2 [m] [4.17]. This is because the dose value may vary greatly depending on the measurement height. In order to satisfy this criterion, a mechanism such as an arm for measuring at a high place from a small robot is additionally required.

In farmland demonstration, the robot moved forward by 100 [m] at 135 [min] in the first trial and 174 [min] in the second trial. From these results, it is estimated that it is possible to measure with 3 robots for 10 hours and 5 robots for about 6 hours when measuring airborne radiation at 1 [ha] pasture at 10 [m] intervals.

When compared to the humanitarian work, though the overall measuring time becomes longer than human observation, the time for outdoor activity can be reduced by using the robot. Table 4.5 shows the time comparison between human work and robot. The overall measuring time and the outdoor activity time of human were estimated by the experiment in farmland. The experimenter was sunburned and consumed very much because of the strong sunlight. The author believes that even in such harsh environments the robot will become possible to work instead of humans.

Table 4.5 Time comparison between human work and robot

		Human (Estimated)	Robot
Overall measuring time	min	100	160
Outdoor activity time of human	min	100	10

4.2.6.2 Demonstrations

Some image data obtained in an artificial ecosystem demonstration were unclear because auto focus mode in smartphone did not work well. Auto focus on the smartphone usually tries to focus closed object in a mirror on omnidirectional lens, this leads to take unclear images because the images become clear only when camera focus on the whole of the lens. The camera on the smartphone should be used fixed focus mode during monitoring.

The average value of the radiation level varies greatly in the first trial and the second trial. This is because the value of 7.7×10^{-1} [μS / h] was measured once in the second trial, it seems that this value was due to trouble on the measuring instrument. If this value is removed, the average value of the radiation level of the second trial is 1.3×10^{-1} [μS / h], which is much closer to the measured value of the first trial. Therefore, in order to improve the usefulness of the proposed system, an algorithm for error avoidance would be necessary.

From the viewpoint of reducing the amount of data, the GUI on the user’s smartphone receives the data of photos every second. When the posture of the robot changes greatly as when mounting the elliptical leg, it may be difficult to operate, and the subjects in the experiment took a while to get used to handling of WAMOT. However, the subject could operate the robot without problems after the subjects understand the motion of the robot, since the robot has only basic motions and few operation commands.

4.3 Investigation of geometric information

4.3.1 Section introduction

Geometric information is expected as a method of obtaining information on the shape of the target object, because it is possible to acquire and express shape information far more precisely than measuring by human beings. If detailed shape data can be acquired, it is easy to know the size and characteristics of the object.

For example, according to an ecologist, the thickness of the tree becomes an important measurement parameter for the investigation of the circulation of carbon dioxide in the forest, because it is possible to estimate the height of a tree from the thickness of a tree, and it can be estimated how much carbon dioxide is absorbed by these data. The interval of trees in the forest also becomes important information, and it is easy to grasp the situation if 3-dimensional information can be acquired.

According to the experts on environmental studies, understanding the circulation of water in the forest is also considered important. It is because we can understand how pollutants circulate through forest and contribute to decontamination efficiency. In order to understand the circulation of water, information on the shape of the surface of the forest is effective. Therefore, three-dimensional information becomes useful.

Techniques for acquiring three-dimensional information are also required for inspection of infrastructure.

4.3.2 Inspection system

Fig. 4.20 shows an overview of inspection system. The three-dimensional geometrical sensor consists of a laser range finder （UTM-30LX-EW, HOKUYO）, a drive mechanism using DC motor, a single board PC, and wireless LAN module.

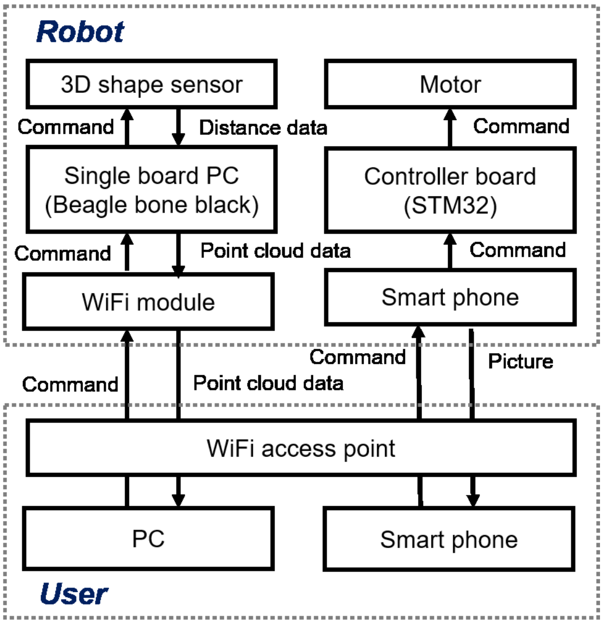

Figure 4.20 Overview of inspection system

The three-dimensional geometrical sensor realizes the measurement of the data by rotating the sensor that can measure distance information on a line more than 360° by the drive mechanism. The three-dimensional shape sensor performs measurement based on a command received from the remote operation interface via the wireless LAN module. Distance data measured by the sensor is converted to point group data by integration with angle data of the sensor drive mechanism. It takes about 30-60 [s] for one measurement. The measured data is transmitted to the remote operation interface via the wireless LAN module and rendered as a point cloud on the PC for drawing the three-dimensional shape data. The measurement range is 10 [m] from the robot and measurement accuracy is ± 30 [mm].

For wireless communication, a consumer's wireless LAN is selected from the view point that it is unnecessary to obtain a license, easy to obtain, maintain and operate. Table 4.6 shows specifications of selected wireless LAN. 2.4 GHz band is selected in terms of capable of long distance communication as a communication frequency and the smart phone on the robot and the android device as an operation interface are connected using IEEE 802.11 g.

Table 4.6 Specifications of selected wireless LAN

Access point	Product number		WAPM-APG300N
	Company		Buffalo
	Frequency band	GHz	2.4
	Power-supply voltage	V	100 (AC)

Antenna	Product number		WLE-HG-SEC
	Company		Buffalo
	Gain	dB	11.5
	Half value angle	deg	60
	Communication distance	m	1,000

The point cloud drawing software is installed on the PC for 3D data drawing, and it is possible to display the obtained 3D shape data as a point cloud. This technology uses the technology of the forest three-dimensional measuring device developed at the add-in laboratory [4.18,19].

Fig. 4.21 shows a three-dimensional geometrical sensor on WAMOT.

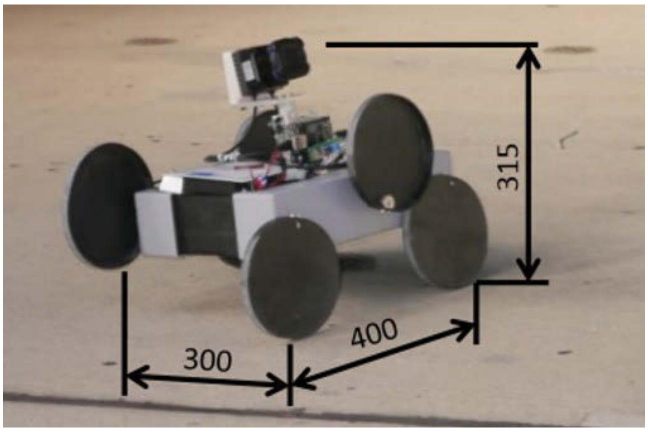

Figure 4.21 Three-dimensional geometrical sensor on WAMOT

4.3.3 Verification

The objective of the experiments was to verify the effectiveness of the investigation system. The three-dimensional geometrical sensor is mounted on the WAMOT and the robot gets the 3D geometrical information. The robot was tele-operated by operator for moving on rough terrain and the 3D sensor system is autonomously controlled by single board PC.

4.3.3.1 Investigation in tunnel

The experiment was conducted in Full-scale tunnel experiment facility in National Institute for Land and Infrastructure Management, Tsukuba, Ibaraki [4.20]. Fig. 4.22 shows inside of the tunnel.

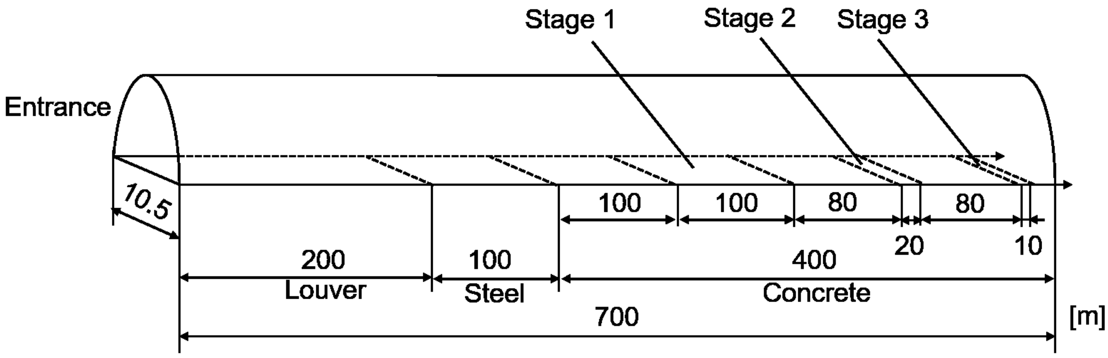

Figure 4.22 Inside the tunnel

The tunnel experiment facility has a real scale of tunnel (700 [m] long and 45.5 [m^2] in cross section), this is a large facility even from a global perspective. One of the wellheads was regarded as an entrance, and the other wellhead was shut off from the outside by a shutter as a termination. Inside the tunnel, obstacles were prepared imitating the site of the tunnel disaster. No obstacles were prepared from the entrance to the point of 400 [m]. Between the 400 [m] point and the 500 [m] point, metal obstructions imitating a vehicle were installed as stage 1. From the 580 [m] point to the 600 [m] point, simulated sand and H steel were laid on the surface, and unevenness and undulation were created as stage 2. Fig. 4.23 shows the image in stage 2. From 680 [m] point to 690 [m], a plate imitating a ceiling collapse was installed as stage 3.

Figure 4.23 Image of H steel and sand that was prepared in stage 2.

Fig. 4. 18 shows the image in stage 3. Large boards and wooden bars are prepared to mimic the state where the ceiling collapses making the movement of large machines difficult.

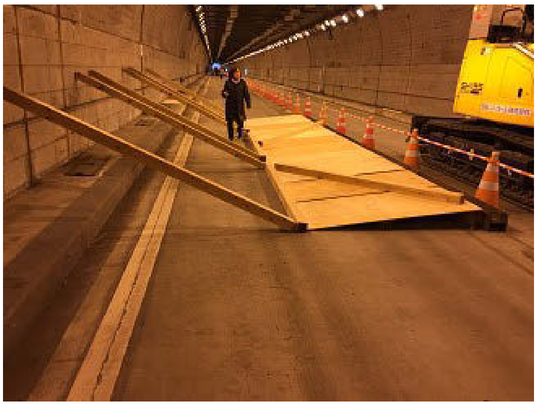

Figure 4.23 Image of a plate imitating a ceiling collapse in stage 3.

In the on-site verification project, each participant was asked to enter the tunnel with the robot from the entrance, gather information on the terminal, and return to the entrance. Each participant was given a holding time of 8 hours (9: 00-17: 00), during which time it was decided to carry out the above tasks and verify various functions of the robot system. In addition, installation and withdrawal were supposed to be done within the given time.

A command center near the tunnel entrance was set up at the beginning of the experiment. Fig. 4.24 shows the image of the command center. It took 45 [min] for three people to prepare the robot and set up a command center.

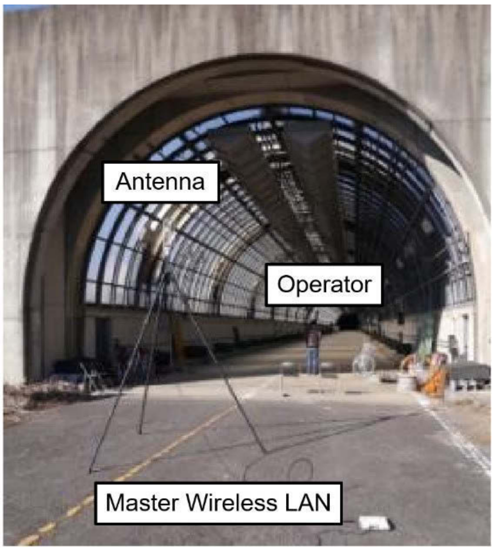

Figure 4.24 The command center near the tunnel entrance

After that, the three-dimensional shape measurement was evaluated in Stage 1 and the locomotion performance on rough terrain was evaluated in Stage 2.

The procedure of each trial execution is as follows.

1. Place the robot near the entrance
2. Robot enters tunnel by remote control
3. The experiment finished when the operator determines that forward movement is impossible
4. Measure the distance and the time of moving

The results are shown in Table 4.7 for two trials in which the robot entered the tunnel.

Table 4.7 Experimental results in tunnel

		1st trial	2nd trial
State with lighting		Yes	No
Distance of moving	m	505	255
Time of moving	min	180	67

Neither the first trial nor the second trial could reach the tunnel end. In the first trial, it was possible to pass stage 1 where obstacles were installed by remote control while taking a lot of time. Fig. 4.25 shows WAMOT in tunnel at stage 1.

Figure 4.25 WAMOT in tunnel (Stage 1)

However, in the vicinity of 505 [m], communication breakdown due to the attenuation of radio waves in wireless LAN became frequent, and the operator decided that further experiments were difficult. In the second trial, the remote operation became impossible due to insufficient lighting in the around 255 [m], and the operator decided that further experiments were difficult.

Fig. 4.26 shows three-dimensional shape data obtained by three-dimensional shape measurement in Stage 1.

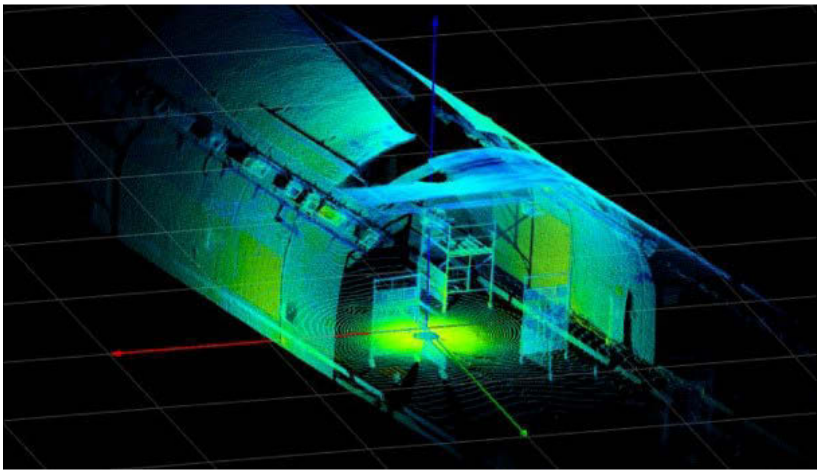

Figure 4.26 Three-dimensional shape data in tunnel (Stage 1)

In Stage 2, it was possible to move on the surface where sediment accumulated as same as moving on even surface and succeed to climb up H steel that height is 100 [mm].

In Stage 3, it was confirmed that it is possible to pass under the obstacle. Moreover, it was confirmed that the robot can move even on a board assuming the roof of the ceiling.

4.3.3.2 Investigation in forest

The experiment was conducted in the forest in Name Town, Fukushima where is prohibited to enter due to high radiation level. There is also a hypothesis that the raindrop radiation is moving due to the circulation of water, it is said that it accumulates in a lake or a pond and forms an area with high radiation level, so-called hot spot. Since the car can pass in a well-maintained environment such as a road, it is easy to measure the radiation level. However, in order to investigate the circulation of water, it is necessary to enter the mountain and forest and measure it. Since it is not possible to measure with a moving means such as a car, use of a robot is expected.

Fig. 4.27 shows the map of Name Town. This town is an area where a lot of radiation has been deposited due to the explosion of the Fukushima Daiichi Nuclear Power Plant during the Great East Japan Earthquake and access of many areas is restricted due to being dangerous.

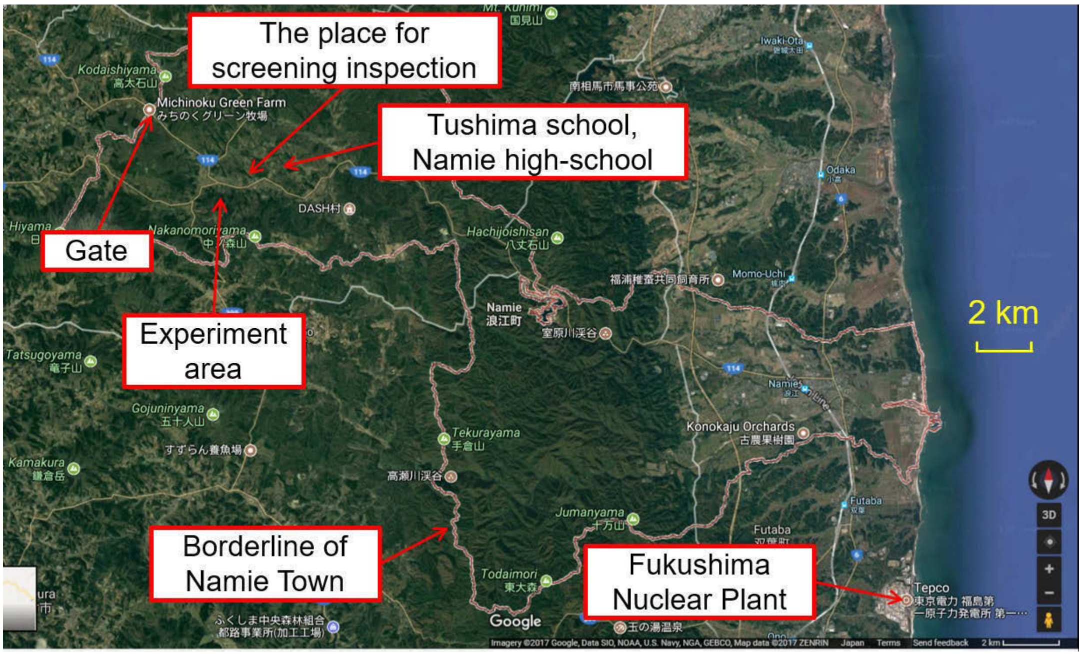

Figure 4.27 Namie Town map (Google map)

Fig. 4.28 shows the gate for entering into Namie Town. When invading a difficult-to-visit area, it is necessary to apply for a license to the government of Fukushima prefecture. In cooperation with the Okochi Laboratory [4.21] of the same university, these processes were carried out with necessary procedures. In the laboratory, it is investigated how radiation circulates in the forest by circulation of water [4.22-24].

(a) The state of the car lining at the gate (b) A state from the front of the gate

Figure 4.28 Gate for entering into Namie Town

Fig. 4.29 shows examination at a screening hall. After the experiment is finished, examination at a screening hall is conducted near the experiment site. In the case where a large amount of radiation is attached, a treatment for removing deposits is performed.

(a) Examination of radiation level in the car (b) Examination of radiation adhering to humans

Figure 4.29 Examination at a screening hall

Fig. 4.30 shows a protective clothing during the experiment. Experiments were conducted with clothing in protective clothing because radiation exposure during the experiment was feared. Hooded jackets and trousers, boots and masks, goggles were used, gloves were used when touching the soil and robot on the surface.

Figure 4.30 Protective clothing during the experiment

Fig. 4.31 shows command station in the car. User’s PC and Wifi access point was set in the station. The command station is located about 30-50 [m] away from the robot. The operator controls the robot near the station and get the environmental data after the robot being stopped.

Figure 4.31 The command station in the car

Fig. 4.32 shows three-dimensional shape data obtained by three-dimensional shape measurement in forest. These point cloud data can be visualized by using pcl_visualization library in The Point Cloud Library (PCL) [4.25], which is open to the public as open source. With this software, we can see 3D data from every direction. Data was acquired by the robot at 5 [m] intervals, and the acquired data was superimposed later by the technology of the joint research company.

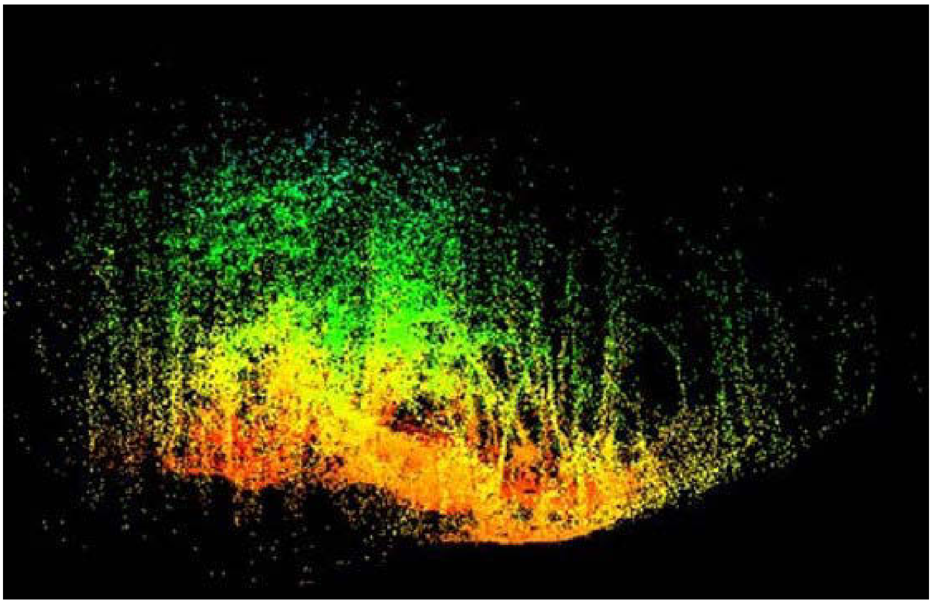

Figure 4.32 Three-dimensional shape data in forest

Since this system can record topographical information, it can be used to understand nature together with other acquired environmental information. The data were provided to the laboratory of the joint research and will be used for elucidation of the movement of radiation.

4.3.4 Discussion

4.3.4.1 Inspection system

The three-dimensional shape measurement sensor is a very powerful device for measuring the details of environmental information, and it is possible to acquire a large amount of data at once. 30-50[MB] data for each measurement point in 2 [min] that is quite faster than conventional measurement such as using Total Station (TS) by human. This has greatly contributed to miniaturization of electronic parts in recent calculation processing and improvement of data communication speeds. Also, thanks to the provision of a library called Point Cloud as open source, complicated processing can be easily handled.

The robot retained high locomotion performance capable of overcoming the steps of 100 [mm], thanks to the miniaturization of the three-dimensional measurement system, though it is conceivable that the position of the center of mass of the robot becomes high due to the attachment of the sensor and the movement performance would decrease. It is necessary to consider dustproof waterproof specification of the sensor towards the long-term operation outdoors.

The author believes that it will be possible to grasp cracks in the tunnel before the accident by using the three-dimensional monitoring system in this field even if the place is dangerous for human to enter in. It is necessary to verify how effective measurement accuracy is for practical use.

4.3.4.2 Demonstrations

It was confirmed that the locomotion performance of the robot is sufficiently usable although communication problems were confirmed in the demonstration in tunnel. Robots were developed for moving rough terrain such as forest and did not take into consideration rough terrain movement such as rubble, but due to its high mobility performance, it was confirmed that it can be used in such an environment.

Compared with other robots and construction machines that participated in the test, the size and weight of WAMOT were small and lightweight. Thanks to its compactness, it was confirmed that there are multiple places where it is easy to move in an environment difficult for large machines. On the contrary, there were environments in which large steps could only go with large machines or flying robots. The author thought that it is important to use various robots in each part of the specialty by considering the characteristics of each robot, and to use it flexibly in cooperation in the disaster area.

In demonstration in forest, the measurement was carried out in a relatively flat environment in the forest though many obstacles such as collapsed trees and branches existed. In such an environment, since the robot can move, the system can be used sufficiently. However, in forests there are many environments with steep slopes. In the case of a robot not equipped with an investigation sensor, it is possible to move by rolling down the slope, but such operation is difficult for a robot equipped with the investigation sensor. It is necessary to continue to study how to attach the sensor and how to move it while maintaining posture on the slope.

4.4 Inspection in the ceiling

4.4.1 Section introduction

Demands for using mobile robots for maintenance and inspection in the ceiling is increasing. There is a small space between the ceiling and the roof on the house. The space is used to arrange the infrastructure of the house by passing wiring such as a power supply cord, and to manage the temperature of the room by installing insulation materials.

Companies in all industries related to housing use this space in order to prepare the environment of the house. However, since the general ceiling plate is made up of thin plates with weak strength due to cost and supporting structure, it is difficult for humans to enter in. In addition to this, it is not possible to put large machine inside because of the narrow space. For that reason, infrastructure development is being carried out by the know-how of each company without human beings entering that space. However, the efficiency of these tasks is extremely poor, and improvements are being made by small machines.

Periodic inspection is also required. In recent years, there are many cases where wild animals live in the ceiling due to worsening habitat of wild animals. Residents are suffering from their noise and smells. In the undeveloped woodland near a populated area, there are many reports of damage caused by Paguma larvata [4.26]. In urban areas, damage by rats has been reported [4.27]. Small animals sometimes bite off the power cord. It is known that mites are infested in these small mammals, and risks of infections with animals as media are reported [4.28-31]. Therefore, there is a demand to check whether animals are lurking in the space in the ceiling. Although the robot proposed in this study has not been developed for the purpose of moving in the ceiling, it was judged that the point that the robot is small and lightweight and has the high locomotion ability was suitable for movement in the ceiling, and experiments for use were conducted.

4.4.2 Teleoperation system

A transmitter to be operated remotely is selected based on the advice from the employees of power companies involved in the operation of infrastructure equipment in the ceiling. Fig. 4.33 shows the transmitter used in teleoperation system.

Figure 4.33 Transmitter used in teleoperation system

Fig. 4.34 shows the teleoperation system. Small camera modules are used to give visual information from the robot to the operator. The robot is controlled by the transmitter, the user can control the moving direction and the speed of the robot.

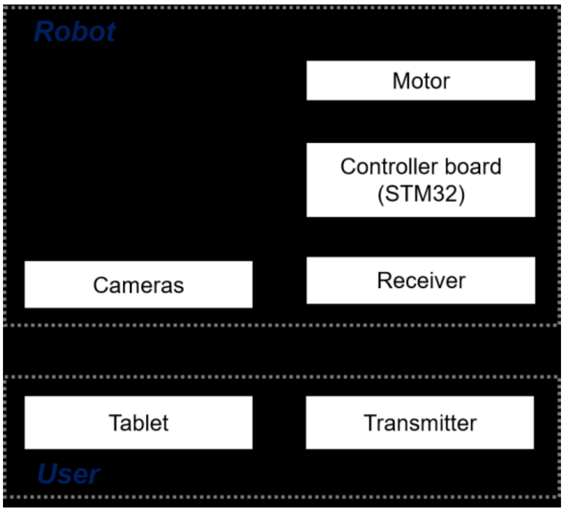

Figure 4.34 Tereoperation system

Fig. 4.35 shows cameras on WAMOT. The two cameras are mounted on the robot. A small camera (MCAMIR-WTF-HD) that can connect to the tablet via wireless Wi-Fi communication is implemented in front of the robot and another camera (HDR-AS300, Sony) that is waterproof is implemented behind the robot so that the movement of the robot can be seen from the back. Assuming an emergency, a stop switch is also provided.

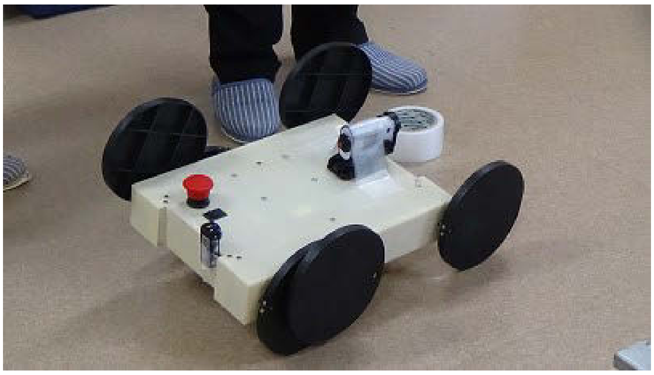

Figure 4.35 Cameras on WAMOT

The housing of the robot was molded by cutting the ABS toward the product, and the weight was further reduced to about 4 [kg] in total. The locomotion performance of the robot is the same as that of the case of POM and CFRP.

4.4.3 Verification

Experiments of the robot were carried out in two different environments, assuming the actual ceiling.

4.4.3.1 Experiments in test site

The experiment was conducted to verify whether the robot can move in an area with many obstacles assuming an actual ceiling. Fig. 4.36 shows an overall view of experimental equipment. In the experimental environment, there are many reinforcing bars, and there are many cables on which the electricity flows.

Figure 4.36 Overall view of experimental equipment

Fig. 4.37 shows the highest step in the experimental equipment. There is a reinforcing bar of about 100 mm, and if it contains the code above it will be about 160 mm high.

(a) Steps due to reinforcing bars and cables (b) Comparison of size with B6 size notebook

Figure 4.37 The highest step in the experimental equipment

Fig. 4.38 shows the places where multiple codes are arranged. In this place, there is a possibility that the robot may ride on the cord, and it may be considered that the robot becomes immovable conditioned.

Figure 4.38 Places where multiple codes are arranged

In the experiment, the experimenter confirmed whether the operator was able to remotely control the robot while observing the behavior of the robot directly and move the prepared course. It turned out that the robot could finish the prepared course by turning back repeatedly, although the moving direction of the robot was changed sometimes by the obstacles. Fig. 4.39 shows WAMOT climbing the step.

(a) Condition before the robot climb the step (b) Condition after the robot climb the step

Figure 4.39 WAMOT climbing the step

It was also experimented whether the robot could move by attaching a lightweight cable. Fig. 4.40 shows the attached cable into WAMOT. Basically, it was possible for the robot to operate at the same as in the state where the rope was not attached.

Figure 4.40 Attached cable into WAMOT

Fig. 4.41 shows the problems that have occurred that have occurred in experiments. When WAMOT rolls over, there is a possibility that it can return by rotating the leg and touching an obstacle in that state. However, it has been confirmed that it is difficult for the robot leg to be caught in the reinforcing bars like Fig. 4.41 (a) and return to the original state when entering between the reinforcing bars. In addition, when a robot copes with an obstacle, there is a possibility that the cable is entangled if there is a cable attached to the robot in the moving direction like Fig. 4.41 (b). It is necessary to further improve the shape of the wheel to avoid these situations and to consider the method of rescue when the robot becomes immovable.

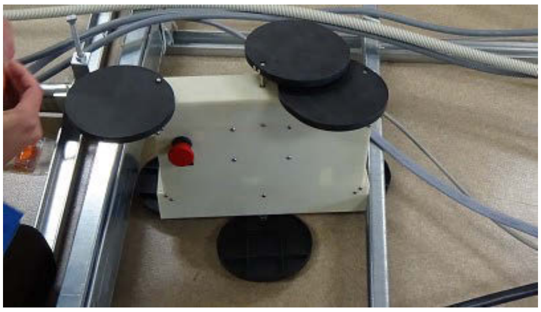

(a) State when the robot rolled over

(b) State where the code is entangled

Figure 4.41 Problems that have occurred that have occurred in the experiment

4.4.3.2 Experiments on the actual ceiling

Experiments were conducted to verify whether the robot can move on the ceiling behind a general house. The experiment was conducted at the house of the housing exhibition hall under the cooperation of the house maker.

Fig. 4.42 shows the entrance to the ceiling space. The robot accessed the ceiling from this door.

Figure 4.42 Entrance to the ceiling space

Fig. 4.43 shows WAMOT in the ceiling. Since many insulation materials are laid on the back of the general ceiling in addition to the obstacle of the bar, the robot needs to move on this rough terrain. The robot is attached to a lifeline, so that the robot can be rescued in case of emergency.

Figure 4.43 WAMOT in the ceiling

As a result, it was confirmed that the robot can move on the insulation without problems and has the ability to climb over the ducts and beams. The insulation covered on the ceiling was supposed to be soft and difficult to move, but the robot could move even in such a soft environment.

4.4.4 Discussion

4.4.4.1 Teleoperation system

Since the transmitter used in the teleoperation system is also used in the radio control, operation was easy. In addition, communication lag is small, and the burden of operation can be reduced. Since the ease of teleoperation largely depends on the users, the author feels that it will be necessary to make specifications that can be freely selected between the method by the transmitter used this time and the method by the smartphone developed by the monitoring system.

Among the cameras with two attached to the robot, the image of the camera attached behind the robot in the direction of travel was easier to use for teleoperation. Since the robot itself is not reflected in the angle of view of the front camera, it is difficult to grasp the distance between the obstacles and the robot. On the other hands, since the robot itself was reflected in the angle of view behind the camera, it became easier to understand the relative positional relation with the surrounding environment.

In the actual experiment on the ceiling, there was a ceiling board between robot and transmitter, but communication was successful. It was also possible to install a fixed camera at the entrance to the ceiling and operate the robot from that image. When assuming actual operation, it is possible to put a camera and an access point at the entrance of the ceiling.

4.4.4.2 Demonstrations

It was confirmed that the robot had a sufficient locomotion performance in the simulated environment of the ceiling around which the cables were stretched. In addition, it was confirmed that, it has a high locomotion performance to move over a soft surface and cope with obstacles such as ducts and beams in the actual ceiling. This shows that the mechanical design proposed in the research is effective and it was possible to apply even on such rough terrain.

Since the robot was a lightweight design, it was confirmed that the robot is operated without destroying a thin plate in the ceiling. Also, because the robot is lightweight, it was easy to carry the robot into the ceiling. Since there are few robots with high mobility with lightweight design like WAMOT, the proposed design can be significantly differentiated from other robots in the field operated this time. In the future, the author plans to further lighter weight and improve the problems in actual operation.

The ceiling is harsh environments such as narrow, unable to move heavy objects, and difficult to cope with many obstacles. Therefore, it becomes difficult for humans to enter and work. In such a harsh environment, the advantages of robots working on behalf of human beings are great. In the future, robots that can be used in these environments are expected to spread.

Chapter 5: Discussion

5.1 Chapter introduction

Overall discussion of this study is described in this chapter. First, the author explains the originality and impact of this thesis. Next, the author discusses the effectiveness and validity of the proposed methods for improving locomotion performance of the mobile robots from the viewpoints of both robotics and application side. Some limitations are also explained for future works.

5.2 Originality and impact

5.2.1 Two actuators mechanism

As shown in the differences from other rough terrain mobile robots in Chapter 1, the robot proposed in this research is novel in that it is driven with only two motors. The mechanism driven by only two motors and its effectiveness are introduced in Chapter 2, which is advantageous in terms of cost, weight, energy consumption and ease of control. This research is intended to solve research subjects such as difficulty in rough terrain movement if the number of actuators is small, which gives an impact on the common sense of robot development.

5.2.1.1 Novel structure

By limiting the number of actuators, the idea of a novel wheel and shell shape were proposed. A lot of conventional studies seem to focus on constructing a drive unit that can operate complicatedly and studying optimal control methods of a large number of actuators to deal with rough terrain. In this study, details of the shape of a robot, which is not usually noticed, was examined by limiting the number of actuators. This study showed that the shapes of wheels and a shell have a large influence on the locomotion performance outdoors, and a method of designing the details shape was proposed. The author hopes that many robot's developers will have the opportunity to review the shape of the robot to be used outdoors by my proposals.

5.2.1.2 Light weight and compact design

Saving weight and compact design of the robot are considered to be the best advantage of the simple structure using two motor mechanism. This enables various applications as in the application example introduced in chapter 4 and increase the usability. In the case of this study, it is expected that the developed robot will be used for applications such as inspection as an infrastructure in tunnels as well as inspections on the ceiling as additional application. In addition, there are cases where size and weight have a large advantage in monetary terms like the moon rover. From these situations, the author thinks that small and lightweight originality greatly contributes to the spread of robots. The author thinks that this is one example where the originality part of this research has an impact on society.

Reducing the size and weight of the robot does not only expands the range of use, but also has the advantage of reducing the burden on the user, and it is possible to reduce the load of transporting the robot to the target environment. This also can be stated the fact that it was able to reduce the user's burden when carrying it to each outdoor experiment. In the case of WAMOT, it was possible to store it in a small carrying case, and it was possible to carry it to various environments using a car or a public transportation system. In addition to this advantage, it is also possible to reduce the environmental load caused by the own weight and the size of the robot when using the robot with the natural environment. This is extremely small compared with the environmental burden given by humans, which is one factor that increases the significance of using robots.

5.2.1.3 Comparing to the other related works

When compared to the other related works, there are few cases where locomotion performance in rough terrain can be realized with only two actuators. The author compared the developed robot with robots close to the developed robot that can be moved on rough terrain which has already been commercialized. Table 5.1 shows the comparison of small and practical robots.

Table 5.1 Comparison of small and practical robots

	 Moogle (Daiwa House)	 Fistlook (iRobot)	 Jaguar-4x4-wheel (Dr Robot	 WAMOT (This study)
Applications	Underfloor inspection	Military reconnaissance	Hoby	Environmental Monitoring
Actuators	3	3	4	2
Size [mm]	495x280x280	254x229x102	570x530x255	360x250x200
Weight [kg]	11.5	2.3	20.0	5.0
Climbing step ability [mm/mm(x-z plan)]	0.30 (150 [mm])	0.69 (170 [mm])	0.27 (155 [mm])	0.58 (150 [mm])

Moogle [5.1] that is developed by Daiwa House is the underfloor inspection robots and the robot have the high locomotion performance to cope with the obstacles such as concrete blocks under the floor. When the robot climbs up the high step, the arm different from the crawler used for normal movement applies force to the surface behind the robot so that the area of the supporting polygon is kept large and the stability during climbing is increased. This is an operation that is performed because it is difficult to climb a high step with only two motors used for locomotion.

Fristlook [5.2] that is developed by iRobot is the military reconnaissance robots and the robot also have high locomotion performance while the size and the weight of the robot are small. The robot could move on uneven surfaces such as rabble and the robot are very sturdy so that the robot can survive a 15 foot drop onto concrete. When the robot climbs up the high step, the arm different from the crawler is also used as the same mechanism as Moogle, this can enable to climb the step up to 170 [mm] height.

Jaguar-4x4-wheel [5.3] that is developed by Dr Robot is hobby use and the robot could move on rough terrain. Since the robot has 4 actuated powerful wheels, the robot could move on the surface very fast (Max. 11 [km/h]). The robot also could climb the step up to 155 [mm] using its large tires that can handle rough terrain. However, considering the size of the robot, the performance to climbing the step is not so high, so it can be seen that it is about 1/2 of the performance compared with the developed robot by dimensionlessized numerical value by the size of the robot.

Many robots that have been put into practical use for rough terrain movements by using three or more actuators so far, thus realizing high locomotion performance by increasing the number of actuators. However, as the number of actuator increases, it is necessary to control advanced timing to control the robot's motion, which seems to make it difficult to automate the robot. Robots that require high rhythm patterns and timings may cause trouble in outdoor environments where it is difficult to predict the surface, and adaptability to the environment is low.

It became possible to have a robot with high locomotion performance as same as with three or more actuators. I think that the difference in this design has a big influence on the control of the robot.

5.2.2 Internal sensors control

As shown in the differences from other rough terrain mobile robots in Chapter 1, the robot proposed in this study is also novel in that it is controlled mainly by internal sensors. The proposed control does not use the geometry sensors such as cameras and laser in terms of saving computational cost and power consumption, though almost mobile robot studies use this sensor for control and navigating the robot.

5.2.2.1 High versatility

By only using the internal sensors for control, the versatility of the robot is increasing. Especially for the small mobile robot like a WAMOT, the influence from the outside condition becomes very large. The posture of the robot greatly changes even with small steps, and obstacles around the grass and the like cause great influence on the vision of the robot as noise. It also generally consumes large burden to the processing the sensing data from the outside due to the noise influence by particles such as sand and dust or weather condition such as rain and sunlight. However, a control using only the internal sensor is proposed in this research, and it is characterized by being hardly influenced by outside. Since the GNSS used as the sensor on the outside can be mounted inside the shell of the robot, the sensor itself does not come in contact with the outside, and stable sensor processing can be performed. For these reasons, it might be judged that adaptation is possible for any outdoor robot, even if the robot in an extreme environment, the range of use can be said wide.

One of the features is that the size of each sensor is small, since only simple sensors are used. For example, the method of estimating the hardness of the surface in the environmental recognition in Chapter 3 measures the current applied to the motor, and the size of the sensor is very small enough to be mounted on the motor controller. As a previous study, a method to estimate the hardness of the surface using a 6-axis force sensor has been proposed. However, in the case of this sensor, it is considered difficult to adapt it to a compact mobile robot because of the problem that the size and location of the sensor itself is difficult. The proposed method solves this problem and there is a possibility that the robot can have the same function, though measurement accuracy might be considered to be a problem. Therefore, the authors think that this control technology can be applied to other small robots, and the impact is large in that sense.

It is also important that the sensor being used is a general-purpose sensor which is built into a robot. Many mobile robots in recent years use the motors as actuators, and in many cases, encoders and current measuring devices mount as standard for controlling them. In addition, the IMU for measuring the posture of the robot is also a general sensor widely used in recent years, and its sensor processing technique is also spreading. GNSS is common for robots that use outdoors and is used to express its own position with world coordinates. Their generality also can be understood from the fact that these sensors are equipped as standard on modern smart phones. The authors think that the control method proposed in this thesis is already available on many other robots because the method uses only these general sensors.

5.2.2.2 Comparing to other related works

The control design is so simple than rhythmic patterned control such as a central pattern generator (CPG) [5.4-6]. Many biomimetic robots generate stable movement by generating rhythmic movement patterns. Conversely, if there is no rhythmic pattern, it is difficult for the robot to move stably, it is especially difficult to go through uneven terrain. The proposed control design doesn't need to advanced control thanks to the mechanical design, though control of rhythmic patterns may improve mobility performance and efficiency.

The control design is also simpler than the way of Simultaneous Localization and Mapping (SLAM) using cameras or laser range finders [5.7,8]. Many robots get detailed information on the surroundings for movement and move while grasping the positional relationship with them in detail. Conversely, if the robot cannot grasp the detailed positional relationship with the obstacle, it is easy for the robot to fall into the immovable state and it is difficult to move continuously. Since the control design proposed this time is very simple, it is a robust system that can be moved even if detailed position cannot be grasped. Addition to this, the control design is robust hard to depend on weather and environment thought low accuracy of localization and environmental recognition might sometimes become a problem. The author thinks that the proposed control is suitable for long-term operation without requiring high precision.

5.3 Effectiveness and validity

5.3.1 Monitoring system

5.3.1.1 Possibility for contributing to monitoring

The system can survey flexible without human labor load and the risk of entering into the dangerous area. With the proposed a novel monitoring method, it will be possible to monitor large-scale in detail. As introduced in Chapter 4, the robot has the potential to perform various tasks on behalf of human beings. Since it is difficult for the current robot technology to exceed the ability of a human, in many cases it has more time than the time when a human work. However, the robot has the ability to correctly repeat the decided work without getting tired. This means that it is possible to work continuously including nighttime if solving the problem of energy supply can be solved, and in some cases, it can exceed the human workload. The authors hope that by the development of robot technology, the time will come when the robots will work efficiently on behalf of human beings, such as hard labor in harsh environments that humans do not like.

5.3.1.2 Able to reduce the burden on the environment

A trace where the robot travels does not damage to the environment so much than that of humans do thanks to light weight. Surveys that many people enter may cause great damage to the nature. This is because the weight of a human being is about 60 [kg], and when a large number of people are involved, surrounding food adds unexpected power in usual natural. On the other hand, the developed robot has a weight of about 5 [kg], which is much smaller than the load given by a human. As a result of discussion with Prof. Koizumi in Waseda University, if the load is as large as the robot developed, it can be regenerated by natural automatic healing ability.

5.3.2 Locomotion performance

5.3.2.1 Validity of the performance of the experiments

The robot developed in this proposal can be summarized that the shape of the wheel and the shape of the shell had a major influence on the locomotion performance as hardware. This can be said that the so-called compatibility; the way the robot is in contact with the solid parts in the outside world, has a great influence. Especially, as the rigidity of the individual is higher, the influence is considered to be greater.

Stones, rubble, fallen trees have high rigidity on the road surface that was experimented this time. Since correspondence to these obstacles can mainly be expressed by exchanging forces between the driving part and the surface, it can be considered that the shape of the wheel has the greatest influence on the locomotion performance. Two-wheel models are proposed in this thesis and the effectiveness of these wheels is described by using a general step model and a general straight-line slope model. The locomotion performance has been discussed based on models with these ideal shapes, however, there is no such ideal shaped surface in actual unprecedented grounds. Therefore, it is important to operate the robot in a real environment to think about compatibility with the road surface, and selectively use the wheels according to the usage environment.

Resistance to robots by high grasses with relatively low rigidity can be considered as the next major influencing factor. Since contact between these obstacles and the robot is mainly on the shell of the robot, it is considered that the change in the shell shape of the robot affected the locomotion ability. However, when considering the influence of these grasses, it is necessary to consider the density and the characteristics as the material. When the grass density increases, it behaves similarly to obstacles with high rigidity, such as trees and stones. Also, if the robot gives a force in the direction to pull out the grass from the root instead of the direction in which the grass bends, a very strong resistance is generated. This phenomenon occurs more frequently when the grass is entangled on the shafts of the robot, therefore, further improvements in structure and control are expected to make it difficult for the grass to get entangled.

5.3.2.2 Relationship between mechanical and control design

Simple mechanical design greatly contributes to become the control algorithm simple. In this study, the control algorithm was significantly simplified by limiting the number of actuators of the robot to be only two. Also, by proposing a novel locomotion mechanism based on the principle of movement of living organisms, stable movement became possible without requiring complicated control that required conventional rhythms. In addition, by giving a target to the mechanical design of the robot, it was possible to reduce the control pattern to be considered. It is confirmed that the mechanical design has a great influence on the control like these phenomena.

The author feels that the control algorithms heavily depend on the robot's body. And, the findings obtained this time is consistent with the idea in the book "How the Body Shapes the Way We Think: A New View of Intelligence" by Rolf Pfeifer [5.9]. In this book, as the concept of the new intelligence, the body has been proposed to be a priority than thinking. In general, it is recognized that the body moves after thinking is done. Therefore, this concept is sometimes understood to be wrong. However, it can be understood from this study that the factor that the body has a big influence on the thinking. Knowledge by robots sometimes helps elucidate the principle of human beings.

5.2.2.3 The possibility to apply to other robots

The mechanical design and control design proposed in this study are able to increase the locomotion performance. The author thinks that this design can be applied to other robots.

The proposed method is very simple, and there are many parts common to other robots. For example, it is necessary for the mobile robot outdoors to think about the interaction between the rough terrain and the robot during the locomotion, and the model proposed this time can be used when understanding the phenomenon and designing the details of the robot. Regarding control design as well, since the proposed method uses only the sensors normally installed in the robot, it can be used by many other robots. This proposal relates to the basic part of the mobile robot, and in that sense, it can be said that it is a technology with high general versatility. The authors hope that the findings obtained in this study will be used by many researchers.

5.4 Limitation

5.4.1 Model improvements

5.4.1.1 Static model

In this thesis, it is characterized that it uses a static model for representing a locomotion performance of the robot. Thus, there is a feature that is easy to understand the phenomenon represents using geometric and statics point of view. This is made considering that the movement of the robot is not so large, and it is assumed that the element of the motion of the robot can be neglected as the range of the error. However, in order to understand the phenomena more precisely or when the movement of the robot become large like a situation that the robot speed increases, it is conceivable that elements of the robot's motion have a great influence on its movement performance. It is necessary to the introduction of the dynamics in such cases.

As a result of refraining from introducing dynamics, there is also a problem that the robot cannot overcome a step beyond its own height. In this thesis, it has been assumed that the robot does not need to cope with such a large step. However, if extensive investigations are considered in the future, further movement to the z direction method may be necessary. In order to solve this problem, additional mechanisms such as jumping with elements of spring and flighting with multi rotors are required.

5.4.1.2 2D-modeled locomotion performance

3D-modeled locomotion performance is needed for further mobility analysis. Assuming that it moves on a soft surface such as sandy or snowy, it is assumed that a large stress is applied to the ground because the area of the robot's wheel and the ground is small. Therefore, if the robot dugs the ground and the shell of the robot is mounted on the surface, the robot may be considered to be immovable condition. In order to avoid such a situation, it is necessary to design the width of the wheel of the robot widely and reduce the stress applied to the surface. However, since it is predicted that the weight increase and the turning performance will be deteriorated if the lateral width is made too large, it is necessary to obtain the optimum value using the 3D model.

In order to consider the ability of turning, a 3D model is required. In the 2D model, as the longitudinal direction of the robot becomes longer, the performance of climbing the slope and the step is increasing, though the weight increases depending on the size of the robot. However, as the length in the longitudinal direction increases, more power is required for turning. This is due to the fact that the moment increases as the point where the robot contacts the surface during rotation is away from the center of rotation. When considering other various abilities, a 3D model is required, and further optimization is required according to the target environment.

5.4.2 Limit on energy efficiency

In this thesis, a simple control system using an internal sensor that does not use the geometry sensors is proposed and the robot could autonomous movement in extreme environment such as a forest. In this system, a method using environment data acquired by humans before the operation and data based on the experience of the robot has been proposed as a method for increasing the movement efficiency. This is a methodology for assuming that the targeted environmental monitoring is to move repeatedly in the same place for long term. However, in the case of monitoring in an environment where human cannot enter or where the robot does not pass through the same place for exploratory use, problems may occur in the energy efficiency of the proposed method.

5.4.2.1 The place where humans cannot enter in

In the case where human cannot enter in, the method of using the robot's movement experience is applied. However, the energy efficiency in movement is considered to be low in the situation before learning, and the risk of the robot becoming immovable is increased. Even in the case where environmental information is acquired by humans before the operation in an environment where human can enter, there is a possibility that a heavy burden on human become a problem. As a method to solve these problems, the research group to which the author belongs has been studying a method of acquiring environmental information by remote controlled UAV in before the operation.

5.4.2.2 A single investigation

In the case of the robot does not pass through the same place such as exploratory applications, it is difficult to directly increase the energy efficiency of the movement data accumulated by the robot, and the path planning based on the movement data of the robot cannot be applied. In addition, the energy efficiency in movement might be inferior in the case of using the geometry information acquired by the robot. Regarding efficiency, it greatly affects the mobile environment.

For example, in the case of in a complicated environment, there is a possibility that movement using the geometry information can lower energy consumption If there are technologies that can be recognized even in complex environments. On the other hand, in an environment that is not complicated, the method that does not use the geometry information may possibly be better in terms of overall energy efficiency. The authors think that it is important to select these methods according to the usage environment.

5.4.3 Limit of application range

5.4.3.1 Limit due to characteristics of robot

As the concept design of the developed robot, it is assumed to perform monitoring in large-scale and long-term operation. This is an idea so as to realize the monitoring by having multiple robots even if the performance of each robot is not so high, and it is not intended to adapt to the scene of rapid information collection such as at the time of disaster. When using a robot for quick and urgent tasks, it is desirable to have a high-performance robot without limiting the number of actuators and with high computing and power capacity than the one proposed in this thesis.

In this thesis, the locomotion performance of the robot is evaluated for the purpose of monitoring only, and that of for outdoor mobile robot with some work does not necessarily apply to this. For example, in the case where the work arm is mounted on a robot or a robot that carries objects, the stability may be a one of the most important evaluating items of the locomotion performance. In addition, since the work speed of the robot is not included in the evaluation item in this thesis, the robot is basically stationary when measuring the environment in order to prevent noise of the sensor. However, the work speed is sometimes required in some applications, and the speed of movement also needs to be evaluated in addition to stability during movement. These items are not mentioned in this thesis, and in that sense, it can be said that there is a limit range of application. Regarding these evaluation items, they are introduced in automobile engineering and National Institute of Standards and Technology (NIST).

5.4.3.2 Limit for harsher environment

It is difficult to investigate areas where the radiation level is extremely high, while radiation monitoring is introduced as an application example. The developed robot has not been subjected to radiation protection yet. There is a possibility that an abnormality will occur in the electronic board causing the robot to stop when entering a building inside a nuclear power plant. To solve this problem, it is necessary to remodel each electronic component so as to correspond to radiation or to use a radiation shielding sheet for the structural design of the robot.

The hardware is also needed for improvement for harsher environments, such as radiation hardening of the electronics and preventing a change of temperature in the robot. For example, it has been reported that a robot that conducts an investigation in a building of a nuclear power plant in Fukushima where a nuclear accident occurred stops the robot due to a high radiation dose.
Temperature control for protecting electronic parts is required because the temperature tolerance of electronic parts that can be mounted on robots used in outer space is also decided. In order to deal with this, it is necessary to shut off heat transferring between the inside and the outside of the robot, and it is necessary to devise measures such as installing a heater inside and keeping it at a certain temperature or higher.

Chapter 6: Conclusion

6.1 Chapter introduction

Conclusion and future work are described in this chapter. The author summarizes the overall contents of this thesis and organize the main points of this study. And, the author summarizes the issues considered as extensions of this study and shows the future direction of the study.

6.2 Conclusion

My general conclusion is that the locomotion performance of mobile robot on rough terrain could be increased by the both side approach of designing mechanical and control with the concept of simple design and low power consumption. The methods of increasing the performance are proposed and the effectiveness and validity of the methods were evaluated by each experiment.

Novel mechanical designs using two motors and novel control designs using internal sensors are proposed. These novel proposals not only contribute to develop my long-term goal of developing monitoring system using mobile robots, but also contribute to the other applications. This is the impact of its originality and it has been shown that small size and light weight are useful for various applications.

6.3 Future works

The author proposes a novel idea of monitoring system using mobile robot. This idea can be used not only for monitoring on the ground introduced in this thesis, but also for extensive monitoring such as water, land, sky, and space. Figure 6.1 shows an image and load map of developing huge monitoring cloud. The author believes that it is possible to acquire information on all environments by various monitoring robots, and that an era in which a huge database can be constructed will come in the future. This huge database, monitoring cloud, will maintain the environment, detect of abnormality and explore resources. In order to construct this huge monitoring cloud, two aspects of technological development, expand the robot's range of action and to cooperate with multiple robots become important.

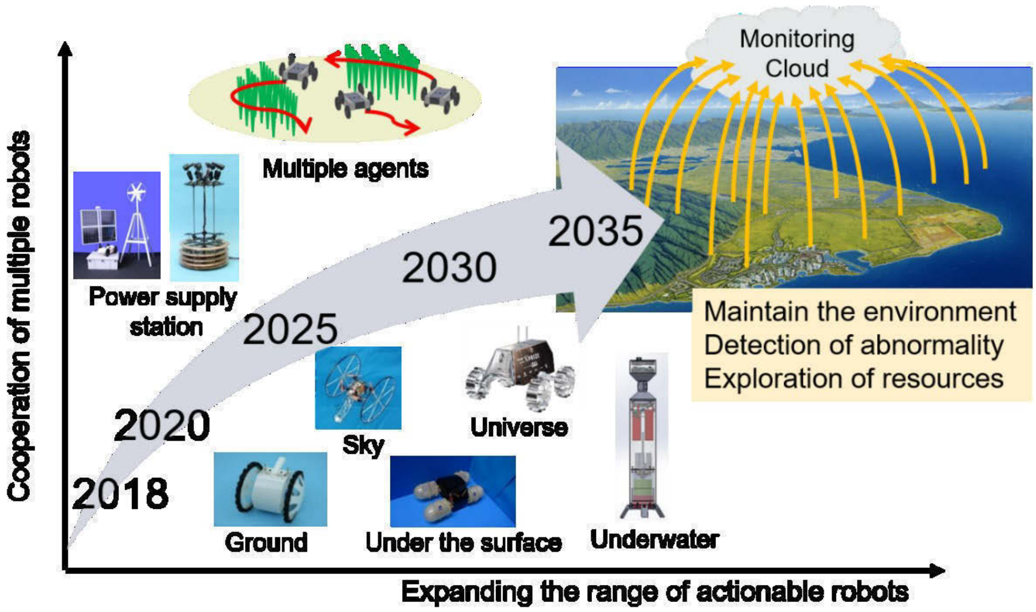

Figure 6.1 Future prospects: Developing huge monitoring cloud

6.3.1 Expanding the range of actionable robots

The robot proposed in this study has been developed focusing on moving in the forest environment. In the future, development of the other robots is expected for further adaptation to the environment.

As the authors explained in Chapter 5, there is a big restriction in vertical movement. In order to solve this problem, additional mechanisms such as jumping with elements of spring and flighting with multi rotors are required. As new robots shown in the appendix, having the jumping function with elements of spring and flighting function with multi rotors are considered to be solve this problem. The range on the ground that can be observed will be expanded by the developments.

Although the developed robot is waterproof, but this is just a specification to be able to endure the rain breeze on the ground. In order for the robot to enter the water, it is necessary to develop a further waterproofing and a locomotion mechanism suitable for the environment. Addition to this, in order for the robot to move stably on a soft surface such as sand, it is necessary not to design only the x-z plane but a design considering the lateral direction of the robot. By these measures, it becomes possible to move into the ocean or the seabed, and furthermore, it is possible to monitor the space like the moon over the atmosphere.

6.3.2 Cooperation of multiple robots

By considering the operation of multiple units, a large-scale and long-term monitoring can be approached to realize.

The energy management is needed in order to realize continuous monitoring. Development of the power supply station becomes important in considering the energy of the robot. Some of the consideration of development of power supply station is described in the appendix.

It is also necessary to consider the task schedule of multiple robots. Each robot is required to perform optimum work while recognizing each other's situation and some calculations are needed to guide optimal behavior. In this study’s proposal, it is assumed that these complex calculations are performed not in the robot but in the server. Moreover, it is necessary to develop a large-scale and robust network in order to construct these systems.

References

Chapter 1

[1.1] Central Disaster Management Council, "Report of the Committee for Technical Investigation on Countermeasures for Earthquakes and Tsunamis Based on the Lessons Learned from the "2011 off the Pacific coast of Tohoku Earthquake"", Cabinet Office, Government of Japan, 2011.

[1.2] Investigation Committee on the Accident at Fukushima Nuclear Power Stations of Tokyo Electric Power Company, "Executive Summary of the Final Report", 2012.

[1.3] Industrial Machinery Division Ministry of Economy, Trade and Industry, "Trends in the Market for the Robot Industry in 2012", 2012.

[1.4] New Energy and Industrial Technology Development Organization (NEDO), "2014 White paper on Robotization of Industry, Business and Our Life", 2014.

[1.5] Rachel Carson, "Silent Spring", Mariner Books; Reprint, 1994.

[1.6] Intergovernmental Panel on Climate Change (IPCC), "Climate change 2013: The physical science basis," Cambridge University Press, 2013.

[1.7] K. R. Miller, et al., "Conserving the world's biological diversity," International Union for Conservation of Nature and Natural Resources, 1990.

[1.8] P. W. Birnie et al.," International Law and the Environment". 2009.

[1.9] Bogue, Robert. "Robots for monitoring the environment. " Industrial Robot: An International Journal 38.6 (2011): 560-566.

[1.10] P. W. Taylor, Respect for Nature: A Theory of Environmental Ethics, Princeton University Press, 2011.

[1.11] L. M. Jenny and V. Mark, "Gains in native species promote biotic homogenization over four decades in a human-dominated landscape," J. Ecol., vol. 101, pp. 1542–1551, 2013.

[1.12] Ministry of Agriculture, Forestry and Fisheries, "Crop Damage by Wild Birds and Animals", The 88th statistical yearbook of Ministry of Agriculture, Forestry and Fisheries, http://www.maff.go.jp/e/data/stat/88th/index.html, 2013.

[1.13] Onoyama K., et al., “Data Analysis of Deer-Train Collisions in Eastern Hokkaido, Japan”. In: Data Science, Classification, and Related Methods. Studies in Classification, Data Analysis, and Knowledge Organizatio, Springer, 1998.

[1.14] A. Soga, et al., “The relationship between spatial distribution of sika deer–train collisions and sika deer movement in Japan”, Human–Wildlife Interactions, Vol.9, pp.198–210, 2015.

[1.15] Brian F. Wakeling, et al., “Mule deer and movement barriers”, 2015.

[1.16] Cabinet Office, Government of Japan, “Disaster Management in Japan”, Director general for disaster management, 2015.

[1.17] Ministry of Land, Infrastructure, Transport and Tourism (MLIT), The maintenance of national road network in Japan.

[1.18] Ministry of Land, Infrastructure, Transport and Tourism (MLIT) of Japan, “Sasago Tunnel Ceiling Collapse on the Chuo Expressway on the Chuo Expressway (Sequence of Events and Countermeasures)”,

[1.19] Fukushima Prefecture, Fukushima Prefecture Radioactivity measurement map, http://fukushima-radioactivity.jp/pc/ (2017.9.15 accessed)

[1.20] Shizuoka Prefecture, Forest resource monitoring survey, http://www.pref.shizuoka.jp/sangyou/sa-610/monitoring.html

[1.21] Fukushima Prefectural Government, “Survey from vehicle, Instrument and method for measuring radiation, Radiation levels in the prefecture” http://www.pref.fukushima.lg.jp/site/portal-english/en02-01.html (2017.10.29 Accessed)

[1.22] M. Dunbabin and L. Marques, "Robots for Environmental Monitoring: Significant Advancements and Applications," in IEEE Robotics & Automation Magazine, vol. 19, no. 1, pp. 24-39, 2012.

[1.23] I. Vasilescu, et al., “Data collection, storage, and retrieval with an underwater sensor network,” Proc. 3rd Int. Conf. Embedded Networked Sensor Systems, SenSys. New York: ACM, 2005, pp. 154–1652, 2005.

[1.24] D. Bhadauria, et al., “A robotic sensor network for monitoring carp in Minnesota lakes,” in Proc. IEEE Int. Conf. Robotics and Automation (ICRA), pp. 3837–3842, 2010.

[1.25] O. Pizarro, et al., “Large area 3D reconstruction from underwater surveys” in Proc. IEEE/MTS OCEANS Conf. Exhibition, Kobe, Japan, vol. 2, pp. 678–687, 2004.

[1.26] P. Tokekar, et al., “Active target localization for bearing based robotic telemetry,” in Proc. IEEE/RSJ Int. Conf. Intelligent Robots and Systems, pp. 488–493, 2011.

[1.27] M. Dunbabin, et al., “Data muling over underwater wireless sensor networks using an autonomous underwater vehicle,” in Proc. IEEE Int. Conf. Robotics and Automation, ICRA, pp. 2091–2098, 2006.

[1.28] V. Hombal, et al., “Multiscale adaptive sampling in environmental robotics,” in Proc. IEEE Conf. Multisensor Fusion and Integration for Intelligent Systems, pp. 80–87, 2010.

[1.29] P. Borgstrom, et al., “Field-tests of a redundantly actuated cable-driven robot for environmental sampling applications,” in Proc. IEEE Int. Conf. Automation Science and Engineering, pp. 615–620, 2009.

[1.30] D. Yoerger, et al., “Fine-scale three-dimensional mapping of a deep-sea hydrothermal vent site using the Jason ROV system,” Int. J. Robot. Res., vol. 19, no. 11, pp. 1000–1014, 2000.

[1.31] B. Zhang and G. Sukhatme, “Adaptive sampling for estimating a scalar field using a robotic boat and a sensor network,” in Proc. IEEE Int. Conf. Robotics and Automation, pp. 3673–3680, 2007.

[1.32] M. Dunbabin and P. Corke, “A framework for marine sensor network and autonomous vehicle interaction,” in Proc. OCEANS, Sydney, pp. 1–7, 2010.

[1.33] R. N. Smith, et al., “USC CINAPS builds bridges: observing and monitoring the southern California bight,” IEEE Robot. Automat. Mag, vol. 17, no. 1, pp. 20–30, 2010.

[1.34] G. S. Sukhatme, et al., “Design and development of a wireless robotic networked aquatic microbial observing system,” Environ. Eng. Sci., vol. 24, no. 2, pp. 205–215, 2007.

[1.35] S. Barkby, et al., “An efficient approach to bathymetric SLAM,” in Proc. IEEE/RSJ Int. Conf. Intelligent Robots and Systems, pp. 219–224, 2009.

[1.36] S. Williams, et al., “Surveying nocturnal cuttlefish camouflage behavior using an AUV,” in Proc. IEEE Int. Conf. Robotics and Automation, ICRA, pp. 214–219, 2009.

[1.37] S. Williams, et al., “Repeated AUV surveying of urchin barrens in North Eastern Tasmania,” in Proc. IEEE Int. Conf. Robotics and Automation (ICRA), pp. 293–299, 2010.

[1.38] W. Li, J. Farrell, et al., “Moth-inspired chemical plume tracing on an autonomous underwater vehicle,” IEEE Trans. Robot, vol. 22, no. 2, pp. 292–307, 2006.

[1.39] R. Camilli, et al., “Integrating in-situ chemical sampling with AUV control systems,” in Proc. MTTS/IEEE TECHNO-OCEAN, vol. 1, pp. 101–109, 2004.

[1.40] D. Kruger, et al., "Optimal AUV path planning for extended missions in complex, fast-flowing estuarine environments," in Proc. IEEE Int. Conf. Robotics and Automation, pp. 4265–4270, 2007.

[1.41] G. A. Hollinger, et al., "Autonomous data collection from underwater sensor networks using acoustic communication," in Proc. IEEE/RSJ Int. Conf. Intelligent Robots and Systems, pp. 3564–3570, 2011.

[1.42] P. Rynne and K. von Ellenrieder, "Development and preliminary experimental validation of a wind-and solar-powered autonomous surface vehicle," IEEE J. Ocean. Eng., vol. 35, no. 4, pp. 971–983, 2010.

[1.43] P. Wadhams, et al., "A new view of the underside of arctic sea ice," Geophys. Res. Lett., vol. 33, no. 4, pp. 1–5, 2006.

[1.44] M. A. Tivey, et al., "Thickness of a submarine lava flow determined from near-bottom magnetic field mapping by autonomous underwater vehicle," Geophys. Res. Lett., vol. 25, no. 6, pp. 805–808, 1998.

[1.45] J. Gould, et al., "Argo profiling floats bring new era of in situ ocean observations," Eos Trans. AGU, vol. 85, no. 19, p. 179, 190–191, 2004.

[1.46] R. Smith, et al., "Cooperative multi-AUV tracking of phytoplankton blooms based on ocean model predictions," in Proc. MTS/IEEE OCEANS, pp. 1–10, 2010.

[1.47] E. Fiorelli, et al., "Multi-AUV control and adaptive sampling in Monterey Bay," in Proc. IEEE/OES Autonomous Underwater Vehicles, pp. 134–147, 2004.

[1.48] P. Bhatta, et al., "Coordination of underwater glider fleet for adaptive sampling," in Proc. Int. Workshop Underwater Robotics, pp. 61–69, 2005.

[1.49] D. Paley, et al., "Cooperative control for ocean sampling: The glider coordinated control system," IEEE Trans. Control Syst. Technol, vol. 16, no. 4, pp. 735–744, 2008.

[1.50] N. Leonard, et al., "Coordinated control of an underwater glider fleet in an adaptive ocean sampling field experiment in Monterey Bay," J. Field Robot., vol. 27, no. 6, pp. 718–740, 2010.

[1.51] M. Moline, et al., "Optical delineation of benthic habitat using an autonomous underwater vehicle," J. Field Robotics, vol. 24, no. 6, pp. 461–472, 2007.

[1.52] N. Barrett, et al., "AUV benthic habitat mapping in South Eastern Tasmania," in Proc. 7th Int. Conf. Field and Service Robots, July 2009, pp. 1–10.

[1.53] S. B. Williams, et al., "Autonomous underwater vehicle-assisted surveying of drowned reefs on the shelf edge of the Great Barrier Reef, Australia," J. Field Robot, vol. 27, no. 5, pp. 675–697, 2010.

[1.54] C. Carmell and D. Stilwell, "A comparison of two approaches for adaptive sampling of environmental processes using autonomous underwater vehicles," in Proc. MTS/IEEE OCEANS, pp. 1514–1521, 2005.

[1.55] M. Jakuba and D. Yoerger, "Autonomous search for hydrothermal vent fields with occupancy grid maps," in Proc. ACRA, pp. 1–10, 2008.

[1.56] M. Dunbabin and A. Grinham, "Experimental evaluation of an autonomous surface vehicle for water quality and greenhouse gas emission monitoring," in Proc. IEEE Int. Conf. Robotics and Automation (ICRA), pp. 5268–5274, 2010.

[1.57] R. Smith, et al., "Autonomous underwater vehicle trajectory design coupled with predictive ocean models: A case study," in Proc. IEEE Int. Conf. Robotics and Automation (ICRA), pp. 4770– 4777, 2010.

[1.58] J. Witt and M. Dunbabin, "Go with the flow: Optimal AUV path planning in coastal environments," in Proc. Australasian Conf. Robotics and Automation, pp. 1–9, 2008.

[1.59] L. Whitcomb, et al., "Navigation and control of the Nereus hybrid underwater vehicle for global ocean science to 10,903 m depth: Preliminary results," in Proc. IEEE Int. Conf. Robotics and Automation, pp. 594–600, 2010.

[1.60] R. Smith, et al., "Cooperative multi-AUV tracking of phytoplankton blooms based on ocean model predictions," in Proc. MTS/IEEE OCEANS, pp. 1–10, 2010.

[1.61] D. C. Webb, P. J. Simonetti, and C. P. Jones, "SLOCUM: An underwater glider propelled by environmental energy," IEEE J. Ocean. Eng., vol. 26, no. 4, pp. 447–452, 2001.

[1.62] B. Allen, et al., "REMUS: A small low cost AUV: System description, field trials, performance results," in Proc. MTS/IEEE OCEANS, pp. 994–1000, 1997.

[1.63] G. Griffiths, et al., "Towards environmental monitoring with the Autosub autonomous underwater vehicle," in Proc. Int. Symp. Underwater Technology, pp. 121–125, 1998.

[1.64] J. Manley and S. Willcox, "The wave glider: A persistent platform for ocean science," in Proc. OCEANS, Sydney, pp. 1–5, 2010.

[1.65] A. Jensen, et al., "AggieAir — a low-cost autonomous multispectral remote sensing platform: New developments and applications," in Proc. IEEE Int. Geoscience and Remote Sensing Symposium (IGARSS), pp. IV-995–IV-998, 2009.

[1.66] S. Nebikera, et al., "A lightweight multispectral sensor for micro UAV—Opportunities for very high resolution airborne remote sensing," Int. Archiv. Photogram., Remote Sens. Spatial Inform. Sci, vol. 37, no. B1, pp. 1193–2000, 2008.

[1.67] A. Rango, et al., “Using unmanned aerial vehicles for rangelands: Current applications and future potentials,” Environ. Pract, vol. 8, no. 3, pp. 159–168, 2006.

[1.68] A. Watts, et al., “Small unmanned aircraft systems for low-altitude aerial surveys,” J. Wildlife Manage, vol. 74, no. 7, pp. 1614–1619, 2010.

[1.69] A. H. Goktogan, et al., “A rotary-wing unmanned air vehicle for aquatic weed surveillance and management,” J. Intell. Robot. Syst, vol. 57, no. 1, pp. 467–484, 2010.

[1.70] M. Rahimi, et al., “Adaptive sampling for environmental field estimation using robotic sensors,” in Proc. IEEE/RSJ Int. Conf. Intelligent Robots and Systems, (IROS), pp. 3692–3698, 2005.

[1.71] M. Rahimi, et al., “Adaptive sampling for environmental robotics,” in Proc. IEEE Int. Conf. Robotics and Automation, ICRA, vol. 4, pp. 3537–3544, 2004.

[1.72] A. Lucieer, et al., “Using an unmanned aerial vehicle (UAV) for ultra-high resolution mapping of Antarctic moss beds,” in Proc. Aust. Conf. Remote Sensing and Photogrammetry, pp. 1–12, 2010.

[1.73] J. Berni, et al., “Thermal and narrowband multispectral remote sensing for vegetation monitoring from an unmanned aerial vehicle,” IEEE Trans. Geosci. Remote Sens, vol. 47, no. 3, pp. 722–738, 2009.

[1.74] L. Techy, et al., “Coordinated aerobiological sampling of a plant pathogen in the lower atmosphere using two autonomous unmanned aerial vehicles,” J. Field Robot, vol. 27, no. 3, pp. 335–343, 2010.

[1.75] L. Merino, et al., “A cooperative perception system for multiple UAVs: Application to automatic detection of forest fires,” J. Field Robot., vol. 23, no. 3, pp. 165–184, 2006.

[1.76] L. Techy, et al., “UAV coordination on convex curves in wind: An environmental sampling application,” in Proc. European Control Conf., pp. 4967–4972, 2009.

[1.77] A. Ollero, et al., “Multiple eyes in the skies: Architecture and perception issues in the COMETS unmanned air vehicles project,” IEEE Robot. Automat. Mag., vol. 12, no. 2, pp. 46–57, 2005.

[1.78] F. Korner, et al., “Autonomous airborne wildlife tracking using radio signal strength,” in Proc. IEEE/RSJ Int. Conf. Intelligent Robots and Systems (IROS), pp. 107–112, 2010.

[1.79] A. Elfes, et al., “A semi-autonomous robotic airship for environmental monitoring missions,” in Proc. IEEE Int. Conf. Robotics and Automation, vol. 4, pp. 3449–3455, 1998.

[1.80] N. Tahir and G. Brooker, "Feasibility of UAV based optical tracker for tracking Australian plague locust," in Proc. Australasian Conf. Robotics and Automation (ACRA), pp. 1–10, 2009.

[1.81] S. Teh, et al., "Experiments in integrating autonomous uninhabited aerial vehicles (UAVs) and wireless sensor networks," in Proc. Aust. Conf. Robotics and Automation, pp. 1–10, 2008.

[1.82] J. Cobano, et al., "Data retrieving from heterogeneous wireless sensor network nodes using UAVs," J. Intell. Robot. Syst., vol. 60, no. 1, pp. 133–151, 2010.

[1.83] P. Lin and C. Lee, "The eyewall-penetration reconnaissance observation of typhoon longwang (2005) with unmanned aerial vehicle, aerosonde," J. Atmos. Ocean. Tech., vol. 25, no. 1, pp. 15–25, 2008.

[1.84] H. Choi and J. How, "Coordinated targeting of mobile sensor networks for ensemble forecast improvement," IEEE Sensors J, vol. 11, no. 3, pp. 621–633, 2011.

[1.85] M. Bryson, et al., "Airborne vision based mapping and classification of large farmland environments," J. Field Robot., vol. 27, no. 5, pp. 632–655, 2010.

[1.86] M. Wolf, et al., "Probabilistic motion planning of balloons in strong, uncertain wind fields," in Proc. IEEE Int. Conf. Robotics and Automation (ICRA), pp. 1123–1129, 2010.

[1.87] A. Klesh and P. Kabamba, "Solar-powered aircraft: Energy-optimal path planning and perpetual endurance," J. Guid., Contr. Dynam, vol. 32, no. 4, pp. 1320–1329, 2009.

[1.88] G. Holland, et al., "The aerosonde robotic aircraft: A new paradigm for environmental observations," Bull. Amer. Meteorol. Soc., vol. 82, no. 5, pp. 889–901, 2001.

[1.89] A. Noth, et al., "Flying solo and solar to mars," IEEE Robot. Automat. Mag, vol. 13, no. 3, pp. 44–52, 2006.

[1.90] M. Reggente, et al., "The DustBot system: Using mobile robots to monitor pollution in pedestrian area," Chem. Eng., vol. 23, pp. 273–278, 2010.

[1.91] L. Marques, et al. "Environmental monitoring with mobile robots," in Proc. IEEE/RSJ Int. Conf. Intelligent Robots and Systems, pp. 3624–3629, 2005.

[1.92] L. Marques, et al., "Olfaction-based mobile robot navigation," Thin Solid Films, vol. 418, no. 1, pp. 51–58, 2002.

[1.93] R. Shah, et al., "Data mules: Modeling and analysis of a three-tier architecture for sparse sensor networks," Ad Hoc Netw, vol. 1, no. 2-3, pp. 215–233, 2003.

[1.94] O. Tekdas, et al., “Using mobile robots to harvest data from sensor fields,” IEEE Wireless Commun., vol. 16, no. 1, pp. 22–28, 2009.

[1.95] D. R. Thompson and D. Wettergreen, “Intelligent maps for autonomous kilometer-scale science survey,” in Proc. Int. Symp. Artificial Intelligence, Robotics and Automation in Space, pp. 1–8, 2008.

[1.96] D. Bhadauria, et al., “Robotic data mules for collecting data over sparse sensor fields,” J. Field Robot, vol. 28, no. 3, pp. 388–404, 2011.

[1.97] J. Bares and D. Wettergreen, “Dante II: Technical description, results, and lessons learned,” Int. J. Robot. Res, vol. 18, no. 7, pp. 621– 649, 1999.

[1.98] G. Astuti, et al., “An overview of the volcan project: An UAS for exploration of volcanic environments,” J. Intell. Robot. Syst., vol. 54, no. 1-3, pp. 471–494, 2009.

[1.99] D. Bapna, et al., “The Atacama desert trek: Outcomes,” in Proc. IEEE Int. Conf. Robotics and Automation, pp. 597–604, 1998.

[1.100] 谷和男，”移動ロボットの分類”，ロボット工学ハンドブック，社団法人日本ロボット学会，pp321-322, 1990.

[1.101] Bruzzone, L. and Quaglia, G. “Review article: locomotion systems for ground mobile robots in unstructured environments”, Mechanical Sience, Vol. 3, Issue 2, pp. 49-62, 2012.

[1.102] X. Meng, et al., “A review of quadruped robots and environment perception”, Proc. 35th Chinese Control Conference (CCC), pp. 6350-6356, 2016.

[1.103] R.S. Mosher, Test and evaluation of a versatile walking truck, in Proceedings of Off-road Mobility Research Symposium, pp.359-379, 1968.

[1.104] R.B. McGhee, Some finite state aspects of legged locomotion, Mathematical Biosciences, Vol.2, No.1, pp.67-84, 1968.

[1.105] R.B. McGhee, and A.A. Frank, On the stability properties of quadruped creeping gaits, Mathematical Biosciences, Vol. 3, pp.331-351, 1968.

[1.106] M. Buehler, R. Playter, and M. Raibert, Robots step outside, in International Symposium on Adaptive Motion of Animals & Machines, 2005: 1-4

[1.107] M. Raibert, et al, “Bigdog, the rough-terrain quadruped robot”, in Proc. the 17th IFAC World Congress, Volume 41, Issue 2, pp. 10823-10825, 2008

[1.108] D. Wooden, et al, “Autonomous navigation for BigDog”, Proc. 2010 IEEE International Conference on Robotics and Automation, pp. 4736-4741, 2010.

[1.109] S. Hirose, and K. Kato, “Study on quadruped walking robot in Tokyo Institute of Technology-past, present and future”, in IEEE International Conference on Robotics and Automation, pp. 414-419, 2000.

[1.110] K. Arikawa, and S. Hirose, "Development of quadruped walking robot TITAN-VIII", in Proc. the IEEE/RSJ International Conference on Intelligent Robots and Systems, pp. 208-214, 1996.

[1.111] H. Komatsu, et al, "Development of Quadruped Walking Robot TITAN-XII and Basic Consideration about Mechanics of Large Obstacle Climbing", in The 2nd IFToMM Asian Conference on Mechanism and Machine Science, 2012.

[1.112] S. Hirose, et al, "TITAN VII: Quadruped walking and manipulating robot on a steep slope", in Proc. the IEEE International Conference on Robotics and Automation, pp. 494-500, 1997.

[1.113] R. Hodoshima, et al., "Development of TITAN XI: a quadruped walking robot to work on slopes", in IEEE/RSJ International Conference on Intelligent Robots and Systems, pp. 792-797, 2004.

[1.114] R. Hodoshima, et al, "Development of a quadruped walking robot to work on steep slopes, TITAN XI (walking motion with compensation for compliance)", in IEEE/RSJ International Conference on Intelligent Robots and Systems, pp. 2067-2072, 2005.

[1.115] K. Kato, and S. Hirose, "Development of the quadruped walking robot," TITAN-IX", in Proceedings of the 26th Annual Conference of the IEEE Industrial Electronics Society, pp. 40-45, 2000.

[1.116] K. Kato, and S. Hirose, "Development of the quadruped walking robot, TITAN-IX—mechanical design concept and application for the humanitarian de-mining robot", Advanced Robotics, Vol. 15 No.2, pp. 191-204, 2001.

[1.117] B. Jakimovski, Biologically inspired approaches for locomotion, anomaly detection and reconfiguration for walking robots. Berlin: Springer, 2011.

[1.118] M. Zak, et al, "Overview of bio-inspired control mechanisms for hexapod robot," Proc. 15th International Conference on Intelligent Systems Design and Applications (ISDA), Marrakech, pp. 160-165, 2015.

[1.119] Klinker S., et al., "Destination Moon and beyond for the Micro rover Nanokhod," Proc. DGLR international Symposium to Moon and byound, 2007.

[1.120] K. Nagatani et al., "Redesign of rescue mobile robot Quince," 2011 IEEE International Symposium on Safety, Security, and Rescue Robotics, pp. 13-18, 2011.

[1.121] R. Eric, et al., "Quince : A Collaborative Mobile Robotic Platform for Rescue Robots Research and Development". the Abstracts of the international conference on advanced mechatronics, pp. 225-230, 2010.

[1.122] Miller. D. P., et al "A.: Experiments with a Long-Range Planetary Rover", Proc. the International Symposium on Artificial Intelligence, Robotics and Automation in Space, 2003.

[1.123] T. Kubotam, "Japanese lunar robotics exploration by co-operation with lander and rover", Journal of Earth System Science, Vol. 114, Issue 6, pp. 777–785, 2005.

[1.124] R. Lindemann and C. Voorhees "Mars exploration rover mobility assembly design, test, and performance", Proc. the 2005 IEEE Conference on Systems, Man and Cybernetics, pp. 450–455, 2005.

[1.125] T. Thueer, et al., "CRAB-Exploration rover with advanced obstacle negotiation capabilities", Proc. the 9th ESA Workshop on Advanced Space Technologies for Robotics and Automation, 2006.

[1.126] T. Thueer, et al, "Comprehensive Locomotion Performance Evaluation of All-Terrain Robots", Proc. the IEEE/RSJ International Conference on Intelligent Robots and Systems, 2006.

[1.127] Shimon Y. Nof, "Handbook of Industrial Robotics, 2nd Edition", Wiley, 1999.

[1.128] Eisen, et al., "Sojourner Mars Rover Thermal Performance," SAE Technical Paper 981685, 1998.

[1.129] Rover Team, "Characterization of the Martian Surface Desposits by the Mars Pathfinder Rover, Sojourner", Science Vol. 278 (5344), pp1765-1768, 1997.

[1.130] G. A. Bekey, "Robot Locomotion: An Overview" in Autonomous Robots (Japanese Edition), Chaper 7, pp.169-223, 2007.

[1.131] R. Volpe et al., ""Rockys 7: a next generation Mars rover prototype", Advanced Robotics, Vol. 11, No, 4, pp.341-358, 1997.

[1.132] K. Iagnemma, et al., "Control of Roboticic Vehicles with Actively Articulated Suspensions in Rough Terrain", Autonomous Robots 14, pp.5-16, 2003.

[1.133] S. D. Herbert, et al, "Loper: A quadruped-hybrid stair climbing robot," in Proc. 2008 IEEE International Conference on Robotics and Automation, pp. 799-804, 2008.

[1.134] K. Nagatani, et al., "Development and Field Test of Teleoperated Mobile Robots for Active Volcano Observation", in Proc. 2014 IEEE/RSJ International Conference on Inteligent Robots and Systems (IROS), pp. 1932-1937, Sep. 2014.

[1.135] A. C. Smith et al, "The motion of a finite-width rimless wheel in 3D", in Proc. 1998 IEEE International Conference on Robotics & Automation, pp. 2345-2350, May 1998.

[1.136] K. Shankar et al, “Motion Planning and Control for a Tethered, Rimless Wheel Dif-ferential Drive Vehicle”, in Proc. 2013 IEEE/RSJ International Conference on In-telligent Robots and Systems (IROS), pp. 4829-4836, Nov. 2013.

[1.137] H. Yamada and S. Hirose, “Study of Active Cord Mechanism -Approximations to Continuous Curves of a Multi-joint Body-”, 日本ロボット学会誌, Vol.26, No.1, pp.110-120, 2008.

[1.138] S. Chiaverini, et al, “Kinematically Reducdant Manupulators” Springer Handbook of Robotics, Part B, Chapter 11, pp.245-268, 2008.

[1.139] H. Durrant-Whyte and T. Bailey, "Simultaneous localization and mapping: part I," in IEEE Robotics & Automation Magazine, vol. 13, no. 2, pp. 99-110, 2006.

[1.140] B. J. Guerreiro, et al, "Sensor-based simultaneous localization and mapping — Part II: Online inertial map and trajectory estimation," 2012 American Control Conference (ACC), pp. 6334-6339, 2012.

[1.141] D. P. Romero-Martí, et al., “Navigation and path planning using reinforcement learning for a Roomba robot”, Proc. 2016 XVIII Congreso Mexicano de Robotica, pp. 1-5. 2016.

[1.142] N. Tan, et al., “Robot ergonomics: A case study of chair design for Roomba”, Proc. 24th IEEE International Symposium on Robot and Human Interactive Communication (RO-MAN), pp. 246-251, 2015.

[1.143] E. Ruiz, et al., “Development of a Control Platform for the Mobile Robot Roomba Using ROS and a Kinect Sensor”, Proc. 2013 Latin American Robotics Symposium and Competition, pp. 55-60, 2013.

[1.144] D. Rea, J. E. Young and P. Irani, “The Roomba mood ring: An ambient-display robot”, Proc. 7th ACM/IEEE International Conference on Human-Robot Interaction (HRI), pp. 217-218, 2012.

[1.145] B. Tribelhorn and Z. Dodds, “Evaluating the Roomba: A low-cost, ubiquitous platform for robotics research and education”, Proc. 2007 IEEE International Conference on Robotics and Automation, pp. 1393-1399, 2007.

[1.146] J. L. Jones, “Robots at the tipping point: the road to iRobot Roomba”, in IEEE Robotics & Automation Magazine, vol. 13, no. 1, pp. 76-78, 2006.

[1.147] R. Allen, et al, “The Range Beacon Placement Problem for Robot Navigation”, Proc. 2014 Canadian Conference on Computer and Robot Vision, pp. 151-158, 2014.

[1.148] TrossenRobotics home page, on line available, http://www.trossenrobotics.com/phantomx-ax-hexapod.aspx. 2015.

[1.149] P. Arena, P. Furia, L. Patané and M. Pollino, "Fly-inspired sensory feedback in a reaction-diffusion neural system for locomotion control in a hexapod robot," 2015 International Joint Conference on Neural Networks (IJCNN), Killarney, 2015, pp. 1-8.

[1.150] G. Best, et al., "Terrain Classification Using a Hexapod Robot", Proc. Australasian Conference on Robotics and Automation, 2013.

[1.151] N. Kottege, et al., "Energetics-informed hexapod gait transitions across terrains", Proc. 2015 IEEE International Conference on Robotics and Automation (ICRA), , pp. 5140-5147, 2015.

[1.152] M. Hörger, et al, "Real-Time Stabilisation for Hexapod Robots," in Experimental Robotics, Springer Tracts in Advanced Robotics, vol 109. Springer, pp.729-744, 2015.

[1.153] J. Mrva and J. Faigl, "Tactile sensing with servo drives feedback only for blind hexapod walking robot", Proc. 10th International Workshop on Robot Motion and Control (RoMoCo), pp. 240-245, 2015.

[1.154] M. Mori and S. Hirose, "Three-dimensional serpentine motion and lateral rolling by active cord mechanism ACM-R3", Proc. IEEE/RSJ International Conference on Intelligent Robots and Systems, pp. 829-834 vol.1, 2002.

[1.155] M. Mori and S. Hirose, "Development of active cord mechanism ACM-R3 with agile 3D mobility", Proc. 2001 IEEE/RSJ International Conference on Intelligent Robots and Systems, pp. 1552-1557 vol.3, 2001.

[1.156] M. Mori and S. Hirose, "Locomotion of 3D Snake-Like Robots – Shifting and Rolling Control of Active Cord Mechanism ACM-R3-", JRM, Vol.18, No.5, pp. 521-528, 2006.

[1.157] S. Hirose, E. F. Fukushima, "Snakes and Strings: New Robotic Components for Rescue Operations", in The International Journal of Robotics Research, Vol. 23, Issue 4-5, pp. 341-349, 2004.

[1.158] S. Hirose and H. Yamada, "Snake-like robots [Tutorial]", in IEEE Robotics & Automation Magazine, vol. 16, no. 1, pp. 88-98, 2009.

[1.159] S. Hirose and M. Mori, "Biologically Inspired Snake-like Robots", 2004 IEEE International Conference on Robotics and Biomimetics, pp. 1-7, 2004.

[1.160] F. Matsuno and K. Suenaga, "Control of redundant 3D snake robot based on kinematic model", Proc. 2003 IEEE International Conference on Robotics and Automation, pp. 2061-2066 vol.2, 2003.

[1.161] CERES Continuous Environmental Radioactive Emission Surveyor, http://www.isc.meiji.ac.jp/~amslab/ceres/index.html, (2018.01.01 Accessed)

Chapter 2

[2.1] K. Tanaka, et al., “Hardware and control design considerations for a monitoring system of autonomous mobile robots in extreme environment”, Proc. 2017 IEEE International Conference on Advanced Intelligent Mechatronics (AIM), pp. 1412-1417, 2017.

[2.2] K. Tanaka et al., “The effect of the phase difference on the climbing ability of notched wheel”, Proc. 19th International Conference on Climbing and Walking Robot, World Scientific, pp. 514-522, 2016.

[2.3] K. Tanaka, et al., “A Study of Wheel Shape for Increasing Climbing Ability of Slopes and Steps”, Proc. 21st CISM IFToMM Symposium on Robot Design, Dynamics and Control, Springer, pp.55-72, 2016.

[2.4] K. Tanaka, et al., “A Novel Approach to Increase the Locomotion Performance of Mobile Robots in Fields with Tall Grasses”, IEEE Robotics and Automation Letters (RA-L), Volume 1, Issue 1, pp.122-129, 2016.

[2.5] D. Kuroiwa, H. Ishii, K. Tanaka, et al., “A Study on Effects of Outer Shape of Mobile Robot on Locomotive Performance in Grass Field”, Proc. 6th International Conference on Advanced Mechatronics (ICAM), pp. 161-162, 2015.

[2.6] K. Tanaka, et al., “Mechanical design of a mobile robot with elliptic legs for environmental monitoring”, Proc. 2014 IFToMM Asian Conference on Mechanism and Machine Science (Asian MMS), 2014.

[2.7] 石井裕之, 田中克明, 他, “Development of mobile robot with specially designed wheels 特殊形状車輪を有する屋外移動ロボットの開発”, Proc. 21st Jc-IFToMM Symposium, pp. 1-8, 2015.

[2.8] 黒岩大輔，他，“自律移動型環境モニタリングロボットの開発 第 2 報: 自重を利用して障害物を排除しつつ前進する外装の設計”，第 32 回日本ロボット学会学術講演会予稿集，3Q1-02，pp. 1-4，2014.

[2.9] 田中克明，他，“Development of mobile robot with elliptic legs for outdoor locomotion 楕円型脚を有する屋外移動ロボットの開発”，Proc. 19th Jc-IFToMM Symposium, pp. 1-4, 2014.

[2.10] 谷和男，”移動ロボットの分類”，ロボット工学ハンドブック，社団法人日本ロボット学会，pp321-322, 1990.

[2.11] Bruzzone, L. and Quaglia, G. “Review article: locomotion systems for ground mobile robots in unstructured environments”, Mechanical Science, Vol. 3, Issue 2, pp. 49-62, 2012.

[2.12] U. Saranli, et al., “RHex: A simple and highly mobile hexapod robot,” Int. J. Robot. Res., vol. 20, no. 7, pp. 616–631, 2001.

[2.13] A. Greenfield, et al, “Solving models of controlled dynamic planar rigid-body systems with frictional contact. International Journal of Robotics Research”. Vol. 2, No. 11, pp.911-931, 2005.

[2.14] U. Saranli, et al., “Model-based dynamic self-righting maneuvers for a hexapedal robot”. International Journal of Robotics Research, Vol. 23 No.9, pp. 903-918, 2004.

[2.15] R. Altendorfer, et al., “RHex: A biologically inspired hexapod runner. Autonomous Robots”, Vol. 11 No.3, pp.207-213, 2001.

[2.16] R. Altendorfer, et al., “Evidence for spring loaded inverted pendulum running in a hexapod robot”. In D. Rus and S. Singh, editors, Experimental Robotics VII, Lecture Notes in Control and Information Sciences, chapter 5, pp. 291-302. Springer, 2000.

[2.17] U. Saranli, et al., “Multi-point contact models for dynamic self-righting of a hexapod robot”. Proc. the Sixth International Workshop on the Algorithmic Foundations of Robotics, pp. 75-90, 2004.

[2.18] U. Saranli and D. E. Koditschek. “Template based control of hexapedal running”. Proc. the IEEE International Conference on Robotics and Automation, pp. 1374-1379, 2003.

[2.19] U. Saranli and D. E. Koditschek. “Back flips with a hexapedal robot”. Proc. the IEEE International Conference on Robotics and Automation, Vol. 3, pp. 2209-2215, 2002.

[2.20] H. Komsuoglu, et al., “Proprioception based behavioral advances in a hexapod robot”. In International Conference on Robotics and Automation, Vol. 4, pp. 3650-3655, 2001.

[2.21] M. Buehler, et al. “Dynamic locomotion with four and six legged robots”. Proc. the International Symposium on Adaptive Motion of Animals and Machines, 2000.

[2.22] U. Saranli, et al., “Design, modeling and preliminary control of a compliant hexapod robot”. Proc. the IEEE International Conference on Robotics and Automation, Vol. 3, pp. 2589-96, 2000.

[2.23] U. Saranli, et al., “Toward the control of a multi-jointed, monoped runner”. Proc. of the IEEE International Conference on Robotics and Automation, Vol. 3, pp. 2676-82, 1998.

[2.24] M. Buehler, “Dynamic Locomotion and Energetics of RHex, a Six-Legged Robot”. The Physiologist, Vol. 45 No. 4, pp. 340, 2002.

[2.25] M. Buehler. “Dynamic Locomotion with One, Four and Six-Legged Robots”. Journal of the Robotics Society of Japan, Vol. 20, No.3, pp.15-20, 2002.

[2.26] D. Campbell and M. Buehler. “Preliminary Bounding Experiments in a Dynamic Hexapod”. In Bruno Siciliano and Paolo Dario, editors, Experimental Robotics VIII, p. 612-621, Springer-Verlag, 2003.

[2.27] N. Neville, M. Buehler. “Towards Bipedal Running of a Six Legged Robot”. Proc. the 12th Yale Workshop on Adaptive and Learning Systems, 2003.

[2.28] D. McMordie, et al., “Towards a Dynamic Actuator Model for a Hexapod Robot”. Proc. the 2003 IEEE Int. Conf. on Robotics and Automation, 2003.

[2.29] D. Campbell, M. Buehler. “Stair Descent in the Simple Hexapod 'RHex'”. Proc. the 2003 IEEE Int. Conf. on Robotics and Automation, 2003.

[2.30] E. Z. Moore, et al., “Reliable Stair Climbing in the Simple Hexapod 'RHex'”, Proc. 2002 IEEE Int. Conf. on Robotics and Automation, Vol 3, pp 2222-2227, 2002.

[2.31] M. Buehler. “RePaC design and control: Cheap and fast autonomous runners”. Proc. the 4th Int. Conf. on Climbing and Walking Robots, 2001.

[2.32] D. McMordie and M. Buehler. “Towards Pronking with a Hexapod Robot”. Proc. the 4th Int. Conf. on Climbing and Walking Robots, 2001.

[2.33] E.Z. Moore and M. Buehler. “Stable Stair Climbing in a Simple Hexapod”. Proc. the 4th Int. Conf. on Climbing and Walking Robots, 2001.

[2.34] P.-C. Lin, et al., “Sensor Data Fusion for Body State Estimation for a Hexapod Robot with Dynamical Gaits”. In Proc. IEEE Int. Conf. Robotics and Automation, pp4744-4749, 2005.

[2.35] S. Skaff, et al., “A Context-Based State Estimation Technique for Hybrid Systems”. In Proc. IEEE Int. Conf. Robotics and Automation, pp3935-3940, 2005.

[2.36] P.-C. Lin, et al., “Toward a 6 DOF Body State Estimator for a Hexapod Robot with Dynamical Gaits”. In IEEE/RSJ International Conference on Intelligent Robots and Systems, pp2265-2270, 2004.

[2.37] P.-C. Lin, et al., “Legged Odometry from Body Pose in a Hexapod Robot”. In IFRR 9th International Symposium on Experimental Robotics, 2004.

[2.38] P.-C. Lin, et al., “A Leg Configuration Sensory System for Dynamical Body State Estimates in a Hexapod Robot”. In Proc. IEEE Int. Conf. Robotics and Automation, pp1391-1396, 2003.

[2.39] S. Skaff, et al., “Inertial navigation and visual line following for a dynamical hexapod robot”. In Proc. of 2003 IEEE/RSJ International Conference on Intelligent Robots and Systems, Vol 2, pp808-1813, 2003.

[2.40] S. D. Herbert, et al, “Loper: A quadruped-hybrid stair climbing robot,” in Proc. 2008 IEEE International Conference on Robotics and Automation, pp. 799-804, 2008.

[2.41] K. Nagatani, et al., “Development and Field Test of Teleoperated Mobile Robots for Active Volcano Observation”, in Proc. 2014 IEEE/RSJ International Conference on Inteligent Robots and Systems (IROS), pp. 1932-1937, Sep. 2014.

[2.42] A. C. Smith et al, “The motion of a finite-width rimless wheel in 3D”, in Proc. 1998 IEEE International Conference on Robotics & Automation, pp. 2345-2350, May 1998.

[2.43] Macedo, Jose, Roberto Manduchi, and Larry Matthies. “Ladar-based discrimination of grass from obstacles for autonomous navigation.” Springer Berlin Heidelberg, 2001.

[2.44] Bellutta, Paolo, et al., “Terrain perception for DEMO III,” Intelligent Vehicles Symposium, 2000. IV 2000. Proceedings of the IEEE. IEEE, 2000.

[2.45] Kim, Dongshin, et al., “Traversability classification using unsupervised on-line visual learning for outdoor robot navigation,” Robotics and Automation, 2006. ICRA 2006. Proceedings 2006 IEEE International Conference on. IEEE, 2006.

[2.46] Kato, Keisuke, and Shigeo Hirose, “Development of the quadruped walking robot, TITAN-IX—mechanical design concept and application for the humanitarian de-mining robot,” Advanced Robotics 15.2, 2001, pp. 191-204.

[2.47] Fukushima, Edwardo F., Noriyuki Kitamura, and Shigeo Hirose, “Development of tethered autonomous mobile robot systems for field works,” Advanced robotics 15.4, 2001, pp. 481-496.

[2.48] Iwano, Yuki, and Atsunari Kobayashi. “Development of a trimmer-type mowing robot.” Advanced Mechatronic Systems (ICAMechS), 2012 International Conference on. IEEE, 2012.

[2.49] Yamada, Yasuhiro, et al. “Mechanical Weeding Using a Paddy Field Mobile Robot for Paddy Quality Improvement.” Towards Autonomous Robotic Systems. Springer Berlin Heidelberg, 2014. pp. 185-189.

[2.50] C. Li, A. O. Pullin, D. W. Haldane, H. K. Lam, R. S. Fearing, and R. J. Full, “Terradynamically streamlined shapes in animals and robots enhance traversability through densely cluttered terrain,” Bioinspiration Biomimetics, vol. 10, no. 4, p. 046003, Jun. 2015.

[2.51] S. J. Jones, “Ships in ice – A review,” Proc. 25th Symp. on Nav. Hydrodyn. St. John’s, Newfoundland and Labrador, Canada, Aug. 2004.

[2.52] L. W. Ferris, “The proportions and form of icebreakers,” in Proc. Spring Meeting St. Lawrence Seaway, Jun. 1959, pp. 6–25.

[2.53] Runeberg, R. “On steamers for winter navigation and icebreaking,” Proc. Inst. Civil Eng., vol. 97, pt. III, 1889, pp. 277–301.

[2.54] K. D. Park and H. S. Kim, “Study on the ship ice resistance estimation using empirical formulas,” Proc. ASME 2014 33rd Int. Conf. Ocean, Offshore and Arctic Eng., OMAE2014-23971, Jun. 2014.

[2.55] Shimansky, Y.A., "conditional standards of ice qualities of a ship", New York: Engineering Consulting and Translation Center, 1938

Chapter 3

[3.1] K. Tanaka, et al., "A study on path planning for small mobile robot to move in forest area", Proc. 2017 IEEE International conference on robotics and biomimetics (ROBIO), 2017.

[3.2] K. Tanaka, et al., "A study on path planning for small mobile robot to move in forest area", Proc. 2017 IEEE International Conference on Advanced Intelligent Mechatronics (AIM), pp. 1412-1417, 2017.

[3.3] K. Tanaka, et al., "Novel Method of Estimating Surface Condition for Tiny Mobile Robot to Improve Locomotion Performance", Proc. 2015 IEEE/RSJ International Conference on Intelligent Robots and Systems (IROS), pp. 6515-6520, 2015.

[3.4] K. Tanaka, et al., "Design of Operating Software and Electrical System of Mobile Robot for Environmental Monitoring", Proc. 2014 IEEE International Conference on Robotics and Biomimetics (ROBIO), p1763-1768, 2014.

[3.5] 田中克明，他，"自律移動型環境モニタリングロボットの開発 第 8 報：走行データを利用したコストマップ生成"，第 34 回日本ロボット学会学術講演会予稿集，1H1-01，pp. 1-4，2017.

[3.6] 田中克明，他，"自律移動型環境モニタリングロボットの開発 第 6 報：森林内での経路計画の検討"，第 34 回日本ロボット学会学術講演会, 3C1-02，pp. 1-4，2016.

[3.7] 田中克明，他，"自律移動型環境モニタリングロボットの開発 第 3 報: 安価なセンサの組み合わせによる自律走行", 第32回日本ロボット学会学術講演会予稿集, 3Q1-03，pp. 1-4，2014.

[3.8] 田中克明，他，自律移動型環境モニタリングロボットの開発 第 1 報: 運用・電気系システムの設計と実装，第 31 回日本ロボット学会学術講演会予稿集，1H3-04，pp. 1-4，2013.

[3.9] Misono, Yusuke, et al. "Development of laser rangefinder-based SLAM algorithm for mobile robot navigation." SICE, 2007 Annual Conference. IEEE, 2007.

[3.10] Malartre, Florent, et al. "Real-time dense digital elevation map estimation using laserscanner and camera slam process." Control Automation Robotics & Vision (ICARCV), 2010 11th International Conference on. IEEE, 2010.

[3.11] Yokozuka, Masashi, et al. "Robotic wheelchair with autonomous traveling capability for transportation assistance in an urban environment." Intelligent Robots and Systems (IROS), 2012 IEEE/RSJ International Conference on. IEEE, 2012.

[3.12] Brand, Christoph, et al. "Stereo-vision based obstacle mapping for indoor/outdoor SLAM." Intelligent Robots and Systems (IROS 2014), 2014 IEEE/RSJ International Conference on. IEEE, 2014.

[3.13] Motte, Isabelle, and Guy Campion. "A slow manifold approach for the control of mobile robots not satisfying the kinematic constraints." IEEE Transactions on Robotics and Automation 16.6 (2000): 875-880.

[3.14] Sidek, Naim, and Nilanjan Sarkar. "Dynamic modeling and control of nonholonomic mobile robot with lateral slip." Systems, 2008. ICONS 08. Third International Conference on. IEEE, 2008.

[3.15] Hashimoto, Kenji, et al. "Realization of biped walking on soft ground with stabilization control based on gait analysis." Intelligent Robots and Systems (IROS), 2012 IEEE/RSJ International Conference on. IEEE, 2012.

[3.16] Iagnemma, Karl, and Steven Dubowsky. "Mobile robot rough-terrain control (RTC) for planetary exploration." Proceedings of the 26th ASME Biennial Mechanisms and Robotics Conference, DETC. Vol. 2000. 2000.

[3.17] 谷和男，”移動ロボットの分類”，ロボット工学ハンドブック，社団法人日本ロボット学会，pp321-322, 1990.

[3.18] Hyunjin Kang, “Study on Biped Walking Robot Adaptable to Various Road Profiles”, Ph.D. thesis in Waseda University, Waseda University Repository, 2013.

[3.19] Kawai, S., et al. "A method to distinguish road surface conditions for car-mounted camera images at night-time." ITS Telecommunications (ITST), 2012 12th International Conference on. IEEE, 2012.

[3.20] Deng, Weiwen, and Qingrong Zhao. "Road surface condition identification based on statistical pattern recognition method." Intelligent Transportation Systems, 2009. ITSC'09. 12th International IEEE Conference on. IEEE, 2009.

[3.21] Lin, Paul P., Maosheng Ye, and Kuo-Ming Lee. "Intelligent observer-based road surface condition detection and identification." Systems, Man and Cybernetics, 2008. SMC 2008. IEEE International Conference on. IEEE, 2008.

[3.22] Ishigami, Genya, et al. "Terramechanics - based model for steering maneuver of planetary exploration rovers on loose soil." Journal of Field robotics 24.3 (2007): 233-250.

[3.23] Hashimoto, Kenji, et al. "New foot system adaptable to convex and concave surface." Robotics and Automation, 2007 IEEE International Conference on. IEEE, 2007.

[3.24] Brooks, et al.:"A robust layered control system for a mobile robot.", IEEE Journal of 2.1: 14-23, 1986.

[3.25] Payton, David. :"An architecture for reflexive autonomous vehicle control.", Proceedings. IEEE International Conference on. Vol. 3. IEEE, 1986.

[3.26] Connell, et al.:"SSS: A hybrid architecture applied to robot navigation.", Proceedings. IEEE International Conference on. IEEE, 1992.

[3.27] S. A. Restrepo, et al., "Path planning applied to the mobile robot GBOT", Proc. 2012 XVII Symposium of Image and Artificial Vision (STSIVA), pp. 281-288, 2012.

[3.28] D. Amorim, et al., "A physics-based optimization approach for path planning on rough terrains," Proc. 12th International conference on informatics in control, Automation and robotics (ICINCO), pp. 259-266, 2015.

[3.29] T. Ohki, et al., "Path planning for mobile robot on rough terrain based on sparse transition cost propagation in extended elevation maps", Proc. 2013 IEEE International conference on mechatoronics and automation, pp.495-499, 2013.

[3.30] W. Ali, et al., "Visual Tree Detection for Autonomous Navigation in Forest Environment," in *Proc. IEEE Intelligent Vehicles Symposium*, pp560-565, 2008.

[3.31] P. Fleischmann, et al., "An Adaptive Detection Approach for Autonomous Forest Path Following using Stereo Vision," in *Proc. 14th International Conference on Control, Automation, Robotics & Vision*, Su41.1, 2016.

[3.32] D. Wooden, et al., "Autonomous Navigation for BigDog," in *Proc. 2010 IEEE International Conference on Robotics and Automation*, pp.4736-4741, 2010.

[3.33] J. A. Bagnell, et al., "Learning for Autonomous Navigation," *IEEE Robotics & Automation Magazine*, vol. 17, no. 2, pp. 74-84, 2010.

[3.34] K. Alonzo, et al., "Toward reliable off road autonomous vehicles operating in challenging environments," *The International Journal of Robotics Research*, Vol.25, no. 5-6, pp. 449-483, 2006.

[3.35] J. Alberts, et al., "Autonomous Navigation of an Unmanned Ground Vehicle in Unstructured Forest Terrain," in *Proc. 2008 ECSIS Symposium on Learning and Adaptive Behaviors for Robotic Systems (LAB-RS)*, pp. 103-108, 2008.

[3.36] L. Murphy, et al., "Creating and using probabilistic costmaps from vehicle experience," Proc. 2012 IEEE/RSJ International Conference on Intelligent Robots and Systems, pp. 4689-4694, 2012.

[3.37] S. Martin and P. Corke, "Long-term exploration & tours for energy constrained robots with online proprioceptive traversability estimation," 2014 IEEE International Conference on Robotics and Automation (ICRA), Hong Kong, pp. 5778-5785, 2014.

[3.38] H. Jun, et al., "The influence of the sigmoid function parameters on the speed of backpropagation learning" in Proc. International Workshop on Artificial Neural Networks, 1995.

[3.39] J. Yao, et al., "Path Planning for Virtual Human Motion Using Improved A* Algorithm", in Proc. 2010 Seventh International Conference on Information Technology: New Generations (ITNG), pp. 1154-1158, 2010.

Chapter 4

[4.1] K. Tanaka, et al., "Design of Operating Software and Electrical System of Mobile Robot for Environmental Monitoring", *Proc. 2014 IEEE International Conference on Robotics and Biomimetics (ROBIO)*, p1763-1768, 2014.

[4.2] K. Tanaka, et al., "A novel method of ecosystem management using multiple mobile robots", 第 64 回日本生態学会大会, K02-04, 2017.

[4.3] 石井裕之，田中克明，他，"Development of a mobile robot with 3D scanner for monitoring of forests 自走式 3 次元森林計測ロボットの開発"，Proc. 2016 JSME Conference on Robotics and Mechatronics, 2A2-06b4, pp. 1-4, 2016.

[4.4] 石井裕之，他，"自走式 3 次元トンネル計測ロボットシステムの開発　模擬トンネルにおける現場実証の報告"，第 33 回日本ロボット学会学術講演会予稿集，3K1-01，pp. 1-4，2015.

[4.5] 石井裕之，他，"Development of mobile robot with 3D scanner for disasters in tunnel

[4.6] -System configuration and verification experiment-自走式 3 次元トンネル計測ロボットシステムの開発-システム構成および実証実験-"，Proc. 2015 JSME Conference on Robotics and Mechatronics, 2P1-O08, pp. 1-2, 2015.

[4.7] 石井裕之，田中克明，他，"自律移動型環境モニタリングロボットの農林業への応用"，第 18 回 計測自動制御学会システムインテグレーション部門講演会予稿集，3C4-1，pp. 1-5，2014.

[4.8] 田中克明，他，"自律移動型環境モニタリングロボットの開発　第 1 報: 運用・電気系システムの設計と実装"，第 31 回日本ロボット学会学術講演会予稿集，1H3-04，pp. 1-4，2013.

[4.9] M. Dunbabin and L. Marques, "Robots for environmental monitoring: Significant advancements and applications," in IEEE Robot. Autom. Mag., vol. 19, no. 1, pp. 24–39, 2012.

[4.10] M. Dunbabin, et al. "A framework for marine sensor net- work and autonomous vehicle interaction," in Proc. OCEANS, Sydney, May 2010, pp. 1–7.

[4.11] R. N. Smith, J. Das, et al. “USC CINAPS builds bridges: observing and monitoring the southern California bight,” IEEE Robot. Automat. Mag, vol. 17, no. 1, pp. 20–30, 2010
[4.12] N. Yoshida and J. Kanda, “Tracking the Fukushima radionuclides,” Science, vol. 336, no. 6085, pp. 1115–1116, 2012.
[4.13] Y. Agarwal, et al., “Wireless wakeups revisited: energy management for VoIP over wi-fi smartphones,” in Proc. 5th Int. Conf. Mobile Systems, Applications and Services, ACM, 2007.
[4.14] Juang, Shih-Yao, and Jih-Gau Juang. “Real-time indoor surveillance based on smartphone and mobile robot. ” Industrial Informatics (INDIN), 2012 10th IEEE International Conference on. IEEE, 2012.
[4.15] Kim, Yeon-Gyun, et al. “Smartphone-controlled user calling system for a mobile robot. ” Robotics (ISR), 2013 44th International Symposium on. IEEE, 2013.
[4.16] N. D. Lane, et al., “A survey of mobile phone sensing,” in IEEE Commun. Mag., vol. 8, no. 9, pp. 140–150, 2010.
[4.17] Ministry of the Environment Government of Japan, “Guidelines for Method of Measurement of Radioactive Concentration (Tentative Translation),” Chapter 2, 2013.
[4.18] AdIn Research, Inc., http://www.adin.co.jp/, (2018.01.06 accessed)
[4.19] 近藤修平，他，“ICP を応用した傾斜地三次元立木マップの構築”，第 12 回公益法人計測自動制御学会システムインテグレーション部門 講演会，2011
[4.20] 国土交通省,「次世代社会インフラ用ロボット技 術・ロボットシステム (公募)」 https://www.mlit.go.jp/sogoseisaku/constplan/sosei_constplan_fr_000023.html (2018.01.06 accessed)
[4.21] Okochi Laboratory, https://www.okochi-waseda.com/ (2018.01.06 accessed)
[4.22] 金野俊太郎，大河内博，勝見尚也，緒方裕子，片岡淳，岸本彩，岩本康弘，反町篤行，床次眞司（2017）福島県の里山における植物，土壌，底砂中放射性セシウムの長期変動，分析化学，66，163-174.
[4.23] 黒島碩人，緒方裕子，大河内博，床次眞司，反町篤行，細田正洋 (2014) 福島県浪江町の里山に大気沈着した放射性セシウムの森林内分布と挙動，大気環境学会誌，49，93-100.
[4.24] 名古屋俊士，香村一夫，大河内博 (2012) 東日本大震災と環境汚染（分担）「放出された放射性物質のゆくえ―福島第一原発事故の環境影響」,早稲田大学ブックレット, p.75-105.
[4.25] The Point Cloud Library, http://pointclouds.org/ (2018.01.06 accessed)
[4.26] 川道美枝子，他 “京都市内でのハクビシン (Paguma larvata) の社寺等への出没動向”，京都歴史災害研究，第 16 号，pp11-15，2015.

[4.27] Osaka Prefectural Institute of Public Health, Osaka, “Notes on the fauna in the nests of rats with faunistic constitution and quantitative observation of them”, Medical Entomology and Zoology, Vol. 10, No. 3 pp. 176-178, 1959.

[4.28] 阿部學, “鳥類用巣箱の哺乳類による評価”, Honyurui Kagaku (Mammalian Science), Vol. 29 (1989) No. 1, pp.37-48, 1989.

[4.29] K. Fujimoto, et al., “Ecological studies on ixodid ticks : 1. Ixodid ticks on vegetations and wild animals at the low mountain zone lying south-western part of Saitama Prefecture”, Medical Entomology and Zoology, Vol. 37, No. 4 pp. 325-331, 1986.

[4.30] S. Yamamoto, et al., “Scabies in wild raccoon dogs, Nyctereutes procyonoides at the Tomioka-Kanra district in Gunma Prefecture, Japan”, Medical Entomology and Zoology, Vol. 49, No. 3, pp. 217-222, 1998.

[4.31] M. Nakao and N. Takada, “Survey of tick fauna in the Kyushu mainland, Japan”, Medical Entomology and Zoology, Vol. 48, No. 1, pp. 39-44, 1997.

Chapter 5

[5.1] 狭小空間点検ロボット, moogle モーグル, http://www.daiwahouse.co.jp/robot/moogle/, (2018.01.07 Accessed)

[5.2] iRobot 110 FirstLook Robot, http://www.army-technology.com/projects/irobot-110-firstlook-robot/, (2018.01.07 Accessed)

[5.3] Jaguare-4x4 wheel specification, http://jaguar.drrobot.com/specification_4x4w.asp, (2018.01.07 Accessed)

[5.4] C. Liu, et al., “CPG-Inspired Workspace Trajectory Generation and Adaptive Locomotion Control for Quadruped Robots”, in IEEE Transactions on Systems, Man, and Cybernetics, Part B (Cybernetics), vol. 41, no. 3, pp. 867-880, 2011.

[5.5] J. Yu, et al., “A Survey on CPG-Inspired Control Models and System Implementation”, in IEEE Transactions on Neural Networks and Learning Systems, vol. 25, no. 3, pp. 441-456, 2014.

[5.6] J. Or and A. Takanishi, “A biologically inspired CPG-ZMP control system for the real-time balance of a single-legged belly dancing robot”, 2004 IEEE/RSJ International Conference on Intelligent Robots and Systems (IROS), vol.1, pp. 931-936, 2004.

[5.7] H. Durrant-Whyte and T. Bailey, "Simultaneous localization and mapping: part I," in IEEE Robotics & Automation Magazine, vol. 13, no. 2, pp. 99-110, 2006.

[5.8] B. J. Guerreiro, et al, "Sensor-based simultaneous localization and mapping — Part II: Online inertial map and trajectory estimation," 2012 American Control Conference (ACC), pp. 6334-6339, 2012.

[5.9] Pfeifer, Rolf, and Josh Bongard. "How the body shapes the way we think: a new view of intelligence", MIT press, 2006.

Research achievements

By Type	Theme	Journal name	Date & year of publication	Name of authors inc. yourself
a. Academic papers				
○ 1	A study on path planning for small mobile robot to move in forest area	*Proc. 2017 IEEE International conference on robotics and biomimetics (ROBIO)*	December 2017	<u>Katsuaki Tanaka</u> Yuya Okamoto Hiroyuki Ishii Daisuke Kuroiwa Hiroya Yokoyama Sho Inoue Satoshi Okabayashi Qing Shi Yusuke Sugahara Atsuo Takanishi
2	Development of Cylindrical Cam Shape to Improve Efficiency of Jumping Function of Mobile Robot	*Proc. 2017 IEEE International conference on robotics and biomimetics (ROBIO)*	December 2017 (掲載決定)	Sho Inoue <u>Katsuaki Tanaka</u> Yuya Okamoto Hiroyuki Ishii Daisuke Kuroiwa Hiroya Yokoyama Satoshi Okabayashi Qing Shi Yusuke Sugahara Atsuo Takanishi
3	A design of a small mobile robot with a hybrid locomotion mechanism of wheels and multi-rotors	*Proc. 2017 IEEE International Conference on Mechatronics and Automation (ICMA)*, pp. 1503-1508	August 2017	<u>Katsuaki Tanaka</u>, Di Zhang, Sho Inoue, Ritaro Kasai, Hiroya Yokoyama, Koki Shindo, Ko Matsuhiro, Shigeaki Marumoto, Hiroyuki Ishii, Atsuo Takanishi

By Type	Theme	Journal name	Date & year of publication	Name of authors inc. yourself
a. Academic papers				
○ 4	Hardware and control design considerations for a monitoring system of autonomous mobile robots in extreme environment	*Proc. 2017 IEEE International Conference on Advanced Intelligent Mechatronics (AIM)*, pp. 1412-1417	July 2017	Katsuaki Tanaka, Yuya Okamoto, Hiroyuki Ishii, Daisuke Kuroiwa, Junko Mitsuzuka, Hiroya Yokoyama, Sho Inoue, Qing Shi, Satoshi Okabayashi, Yusuke Sugahara, Atsuo Takanishi
5	aMUSSELs: Diving and anchoring in a new bio-inspired under-actuated robot class for long-term environmental exploration and monitoring	*Proc. 18th Towards Autonomous Robotic Systems (TAROS) Conference,* Springer, pp. 300-314	July 2017	Elisa Donati, Godfried J. van Vuuren, Donato Romano, Katsuaki Tanaka, Thomas Schmickl, Cesare Stefanini
6	Novel Extendable Arm Structure Using Convex Tapes for Improving Strength of Pipe on Tiny Mobile Robots	*Proc. IEEE International Conference on Robotics and Biomimetics*, pp. 637-642	December 2016	Katsuaki Tanaka, Hiroya Yoyokama, Hiroyuki Ishii, Sho Inoue, Qing Shi, Satoshi Okabayashi, Yusuke Sugahara, Atsuo Takanishi
○ 7	The effect of the phase difference on the climbing ability of notched wheel	*Proc. 19th International Conference on Climbing and Walking Robot*, World Scientific, pp. 514-522	September 2016	Katsuaki Tanaka, Hiroyuki Ishii, Daisuke Endo, Junko Mitsuzuka, Satoshi Okabayashi, Qing Shi, Yusuke Sugahara, Atsuo Takanishi

By Type	Theme	Journal name	Date & year of publication	Name of authors inc. yourself
a. Academic papers				
8	A mobile robot plays with a rat	*Proc. 38th Annual International Conference of the IEEE Engineering in Medicine and Biology Society (EMBC)*,	August 2016	Hiroyuki Ishii, Qing Shi, Yusuke Sugahara, Katsuaki Tanaka, Hikaru Sugita, Satoshi Okabayashi, Atsuo Takanishi
○ 9	A Study of Wheel Shape for Increasing Climbing Ability of Slopes and Steps	*Proc. 21st CISM IFToMM Symposium on Robot Design, Dynamics and Control, Springer*, pp.55-72	Jun 2016	Katsuaki Tanaka, Hiroyuki Ishii, Daiki Endo, Junko Mitsuzuka, Daisuke Kuroiwa, Yuya Okamoto, Yusaku Miura, Qing Shi, Satoshi Okabayashi, Yusuke Sugahara, Atsuo Takanishi
○ 10	A Novel Approach to Increase the Locomotion Performance of Mobile Robots in Fields with Tall Grasses	*IEEE Robotics and Automation Letters (RA-L)*, Volume 1, Issue 1, pp.122-129	January 2016	Katsuaki Tanaka, Hiroyuki Ishii, Daisuke Kuroiwa, Yuya Okamoto, Eric Mossor, Hikaru Sugita, Qing Shi, Satoshi Okabayashi, Yusuke Sugahara, Atsuo Takanishi
11	A Study on Effects of Outer Shape of Mobile Robot on Locomotive Performance in Grass Field	*Proc. 6th International Conference on Advanced Mechatronics (ICAM)*, pp. 161-162.	December 2015	Daisuke Kuroiwa, Hiroyuki Ishii, Katsuaki Tanaka, Yuya Okamoto, Qing Shi, Hikaru Sugita, Eric Mossor, Satoshi Okabayashi, Yusuke Sugahara, Atsuo Takanishi

By Type	Theme	Journal name	Date & year of publication	Name of authors inc. yourself
a. Academic papers				
12	Development of Battery Charging System Using Wireless Power Transmission for Outdoor Mobile Robots	*Proc. 6th International Conference on Advanced Mechatronics (ICAM)*, pp.110-111	December 2015	Yuya Okamoto, Hiroyuki Ishii, Katsuaki Tanaka, Daisuke Kuroiwa, Qing Shi, Hikaru Sugita, Eric Mossor, Satoshi Okabayashi, Yusuke Sugahara, Atsuo Takanishi
○ 13	Novel Method of Estimating Surface Condition for Tiny Mobile Robot to Improve Locomotion Performance	*Proc. 2015 IEEE/RSJ International Conference on Intelligent Robots and Systems (IROS)*, pp. 6515-6520	October 2015	Katsuaki Tanaka, Hiroyuki Ishii, Yuya Okamoto, Daisuke Kuroiwa, Yusaku Miura, Daiki Endo, Junko Mitsuzuka, Qing Shi, Satoshi Okabayashi, Yusuke Sugahara, Atsuo Takanishi
14	Behavior modulation of rats to a robotic rat in multi-rat interaction	*2015 IOP PublishingBioinspiration & Biomimetics*, Volume 10, Number 5	September 2015	Qing Shi, Hiroyuki Ishii, Katsuaki Tanaka, Yusuke Sugahara, Atso Takanishi, Satoshi Okabayashi, Qiang Huang Toshio Fukuda
○ 15	Design of Operating Software and Electrical System of Mobile Robot for Environmental Monitoring	*Proc. 2014 IEEE International Conference on Robotics and Biomimetics (ROBIO)*, p1763-1768	December 2014	Kaitsuaki Tanaka, Hiroyuki Ishii, Shinichiro Kinoshita, Qing Shi, Hikaru Sugita, Satoshi Okabayashi, Yusuke Sugahara, Atsuo Takanishi

By Type	Theme	Journal name	Date & year of publication	Name of authors inc. yourself
a. Academic papers				
○ 16	Mechanical design of a mobile robot with elliptic legs for environmental monitoring	*Proc. 2014 IFToMM Asian Conference on Mechanism and Machine Science (Asian MMS)*	July 2014	Katsuaki Tanaka, Hiroyuki Ishii, Shinichiro Kinoshita, Qing Shi, Hikaru Sugita, Satoshi Okabayashi, Yusuke Sugahara, Atsuo Takanishi
c. Lectures				
1	A Study on increasing locomotion efficiency of mobile robot on rough terrain -Costmap generation by Visual Information from UAV- 不整地移動ロボットの移動効率上に関する研究 -UAV からの視覚情報を利用したコストマップ生成-	*第18回 計測自動制御学会システムインテグレーション部門講演会予稿集*	December 2017	鐘 婷婷, 田中 克明, 小嶋 博, 松広 航, 木田 和紀, 井上 翔宇, 岡林 誠士, 菅原 雄介, 石井 裕之, 高西 淳夫
2	自律移動型環境モニタリングロボットの開発 第 8 報：走行データを利用したコストマップ生成	*第34回日本ロボット学会学術講演会予稿集,* 1H1-01, pp. 1-4	September 2017	田中克明 呉成偉 木田和紀 小嶋博 石青 岡林誠士 菅原雄介 石井裕之 高西淳夫
3	自律移動型環境モニタリングロボットの開発 第 7 報：自律的・高効率給電に向けた充電ステーションの設計・製作	*第34回日本ロボット学会学術講演会予稿集,* 2E1-01, pp. 1-4	September 2017	木田和紀 田中克明 フローリアン・マーシアン 呉成偉 庄司暁 井上翔宇 横山裕也 小嶋博 岡林誠士 菅原雄介 石井裕之 高西淳夫

By Type	Theme	Journal name	Date & year of publication	Name of authors inc. yourself
c. Lectures				
4	小型移動ロボットの跳躍機能の効率化に向けた円筒カム形状の検討 A study on an effective shape of the cylindrical cam for jumping of tiny mobile robot	*Proc. 23rd Jc-IFToMM Symoposium*, pp. 38-45	Jun 2017	田中克明, 井上翔宇, 横山裕也, 岡林誠士, 石青, 菅原雄介, 石井裕之, 高西淳夫
5	A novel method of ecosystem management using multiple mobile robots	*第 64 回日本生態学会大会*, K02-04	March 2017	Katsuaki Tanaka, Hiroyuki Ishii, Satoshi Okabayashi, Qing Shi, Yusuke Sugahara, Atsuo Takanishi
6	自律移動型環境モニタリングロボットの開発 第 6 報：森林内での経路計画の検討	*第 34 回日本ロボット学会学術講演会*, 3C1-02, pp. 1-4	September 2016	田中克明, 岡本侑也, 黒岩大典, 井上翔宇, 横山裕也, 石青, 岡林誠士, 菅原雄介, 石井裕之, 高西淳夫
7	自律移動型環境モニタリングロボットの開発 第 5 報：センサ昇降用の伸縮式アームの開発	*第 34 回日本ロボット学会学術講演会*, 3C1-01, pp. 1-4	September 2016	横山裕也, 田中克明, 黒岩大典, 岡本侑也, 井上翔宇, 岡林誠士, 菅原雄介, 高西淳夫
8	屋外環境にて走行・跳躍を行う小型モニタリングロボットの開発	*第 34 回日本ロボット学会学術講演会*, 1D1-06, pp. 1-4	September 2016	井上翔宇, 田中克明, 横山裕也, 三塚純子, 岡本侑也, 黒岩大典, 岡林誠士, 菅原雄介, 石井裕之, 高西淳夫

By Type	Theme	Journal name	Date & year of publication	Name of authors inc. yourself
c. Lectures				
9	小型移動ロボットの遊びがラットにもたらす効果の検討	*第34回日本ロボット学会学術講演会予稿集*, 1G2-07, pp. 1-4	September 2016	石井裕之, 田中克明, 石青, 高西淳夫
10	A Novel Approach to Increase the Locomotion Performance of Mobile Robots in Fields with Tall Grasses	*2016 IEEE International Conference on Robotics and Automation (ICRA)*	May 2016	Katsuaki Tanaka, Hiroyuki Ishii, Daisuke Kuroiwa, Yuya Okamoto, Eric Mossor, Hikaru Sugita, Qing Shi, Satoshi Okabayashi, Yusuke Sugahara, Atsuo Takanishi
11	A Study of Notched Wheel Shape on Tiny Mobile Robot 小型移動ロボットの切り掛け車輪形状に関する検討	*Proc. 2016 JSME Conference on Robotics and Mechatronics*, 2A2-06b4, pp. 1-4	June 2016	田中克明, 横山裕也, 石井裕之, 遠藤大輔, 石青, 岡林誠士, 菅原雄介, 高西淳夫
12	Development of a mobile robot with 3D scanner for monitoring of forests 自走式3次元森林計測ロボットの開発	*Proc. 2016 JSME Conference on Robotics and Mechatronics*, 2A2-06b4, pp. 1-4	June 2016	石井裕之, 田中克明, 菅原雄介, 望月寿彦, 塩沢恵子, 佐々木浩二, 緒方裕子, 大河内博, 高西淳夫
13	Mechanical Design of the Small Amphibious Mobile Robot for Environmental Monitoring 環境モニタリングのための小型水陸両用移動ロボットの機体設計	*日本機械学会関東支部総会講演会 2016*, OS1218, pp. 1-2	March 2016	塩田勇也, 石神知哉, 秋山勇人, 菅原雄介, 本田康裕, 遠藤央, 柿崎隆夫, 田中克明, 石井裕之, 高西 淳夫

By Type	Theme	Journal name	Date & year of publication	Name of authors inc. yourself
c. Lectures				
14	自律移動型環境モニタリングロボットの開発 第4報：路面環境の認識とそれに合わせた走行制御法の検討	*第33回日本ロボット学会学術講演会予稿集*, 2C2-04, pp. 1-4	September 2015	田中克明, 石井裕之, 遠藤大輝, 三塚純子, 三浦祐作, 黒岩大典, 岡本侑也, 石青, 岡林誠士, 菅原雄介, 高西淳夫
15	自走式3次元トンネル計測ロボットシステムの開発 模擬トンネルにおける現場実証の報告	*第33回日本ロボット学会学術講演会予稿集*, 3K1-01, pp. 1-4	September 2015	石井裕之, 望月寿彦, 塩沢恵子, 佐々木浩二, 田中克明, 岡本侑也, 黒岩大典, 菅原雄介, 高西淳夫
16	ホビー用小型移動ロボットのモデリングと屋外での運動性能向上に関する検討	*第33回日本ロボット学会学術講演会予稿集*, 3K2-06, pp. 1-4	September 2015	三塚純子, 石井裕之, 三浦祐作, 田中克明, 遠藤大輝, 岡本侑也, 黒岩大典, 石青, 岡林誠士, 菅原雄介, 高西淳夫
17	Development of mobile robot with specially designed wheels 特殊形状車輪を有する屋外移動ロボットの開発	*Proc. 21st Jc-IFToMM Symposium*, pp. 1-8	July 2015	石井裕之, 田中克明, 遠藤大輝, 岡本侑也, 黒岩大典, 菅原雄介, 高西淳夫

By Type	Theme	Journal name	Date & year of publication	Name of authors inc. yourself
c. Lectures				
18	Development of mobile robot with 3D scanner for disasters in tunnel -System configuration and verification experiment- 自走式3次元トンネル計測ロボットシステムの開発 -システム構成および実証実験-	*Proc. 2015 JSME Conference on Robotics and Mechatronics*, 2P1-O08, pp. 1-2	May 2015	石井裕之, 望月寿彦, 塩沢恵子, 佐々木浩二, 田中克明, 岡本侑也, 黒岩大典, 菅原雄介, 高西淳夫
19	Mechanical design of the small land mobile robot for environmental monitoring 環境モニタリングのための小型陸上移動ロボットの機体設計	*Proc. 2015 JSME Conference on Robotics and Mechatronics*, 1P2-G02, pp. 1-4	May 2015	塚原裕基, 松井康郎, 塩田勇也, 上田チエミ, 菅原雄介, 遠藤央, 柿崎隆夫, 田中克明, 石井裕之, 高西淳夫
20	自律移動型環境モニタリングロボットの農林業への応用	*第18回 計測自動制御学会システムインテグレーション部門講演会予稿集*, *3C4-1*, pp. 1-5	December 2014	石井裕之, 田中克明, 菅原雄介, 高西淳夫
21	自律移動型環境モニタリングロボットの開発 第 3 報: 安価なセンサの組み合わせによる自律走行	*第32回日本ロボット学会学術講演会予稿集*, 3Q1-03, pp. 1-4	September 2014	田中克明, モサ— エリック 石井裕之, 岡本侑也, 黒岩大典, 杉田光, 石青, 岡林誠士, 菅原雄介, 高西淳夫

By Type	Theme	Journal name	Date & year of publication	Name of authors inc. yourself
c. Lectures				
22	自律移動型環境モニタリングロボットの開発 第 2 報: 自重を利用して障害物を排除しつつ前進する外装の設計	*第 32 回日本ロボット学会学術講演会予稿集*, 3Q1-02, pp. 1-4	September 2014	黒岩大典, 石井裕之, 岡本侑也, 石青, 杉田光, モサー エリック, 田中克明, 岡林誠士, 菅原雄介, 高西淳夫
23	ワイヤレス給電システムを用いた自律移動型屋外作業用ロボットへのエネルギ供給システムの構築	*第 32 回日本ロボット学会学術講演会予稿集*, 3Q1-01, pp. 1-4	September 2014	岡本侑也, 石井裕之, 黒岩大典, 石青, 杉田光, モサー エリック, 田中克明, 岡林誠士, 菅原雄介, 高西淳夫
24	小型移動ロボットと遊びを通したラットの鬱状態の改善	*第 32 回日本ロボット学会学術講演会予稿集*, 1O3-03, pp. 1-4	September 2014	石井裕之, 杉田光, 石青, 田中克明, 黒岩大典, 岡本侑也, 岡林誠士, 菅原雄介, 高西淳夫
25	自律移動型環境モニタリングロボットの開発 第 1 報: 運用・電気系システムの設計と実装	*第 31 回日本ロボット学会学術講演会予稿集*, 1H3-04, pp. 1-4	September 2013	田中克明, 石井裕之, 木下新一, 石青, 杉田光, 岡林誠士, 菅原雄介, 高西淳夫
26	Development of mobile robot with elliptic legs for outdoor locomotion 楕円型脚を有する屋外移動ロボットの開発	*Proc. 19th Jc-IFToMM Symposium*, pp. 1-4	May 2014	田中克明, 石井裕之, 菅原雄介, 石青, 岡林誠士, 木下新一, 杉田光, 高西淳夫

By Type	Theme	Journal name	Date & year of publication	Name of authors inc. yourself
e. Others (Patents)				
1	路面状況認識装置、そのプログラム、及び移動体システム	特願 2015-169850	August 2015	
(Awards)				
2	Second prize	Project MARS - Education League JP-, HP Mars Home Planet	December 2017	
3	Finalist, Young Investigator Fund Best Paper Award	23th symposium on Japanese Council of IFToMM	March 2018	
4	Best Award, ESJ64 English Presentation Award	The ecological society of Japan	March 2016	
5	Finalist, Program for Leading Graduate Schools The First Business Plan Competition	Program for Leading Graduate School	September 2015	
6	2015 IEEE RAS Travel Award	IEEE Robot and Automation Society	February 2014.	
7	Excellence Prize	Mini-Conference in Monash University		